DOCTORAL THESIS

Co-Design of Wireless Networked Control Systems: Model-based Architecture and Joint Optimization

Kanwal Ashraf

Co-Design of Wireless Networked Control Systems: Model-based Architecture and Joint Optimization

KANWAL ASHRAF

TALLINN UNIVERSITY OF TECHNOLOGY
School of Information Technologies
Thomas Johann Seebeck Department of Electronics

The dissertation was accepted for the defence of the degree of Doctor of Philosophy (Information and Communication Technology) on 17 May 2024

Supervisor: Professor Yannick Le Moullec,
Thomas Johann Department of Electronics, School of Information Technologies
Tallinn University of Technology
Tallinn, Estonia

Co-supervisor: Dr. Tamas Pardy,
Department of Chemistry and Biotechnology, School of Science
Tallinn University of Technology
Tallinn, Estonia

Opponents: Professor Guy Gogniat,
Lab-STICC Laboratory CNRS UMR 6285
Université Bretagne Sud
Lorient, France

Professor Maurizio Magarini,
Department of Electronics, Information and Bioengineering
Politecnico di Milano
Milan, Italy

Defence of the thesis: 17 June 2024, Tallinn

Declaration:
Hereby I declare that this doctoral thesis, my original investigation and achievement, submitted for the doctoral degree at Tallinn University of Technology, has not been submitted for any academic degree elsewhere.

Kanwal Ashraf

_____
signature

Juhtmevabade võrgustatud juhtimissüsteemide koosdisain: mudelipõhine arhitektuur ja ühisoptimeerimine

KANWAL ASHRAF

**TAL
TECH**
KIRJASTUS

Contents

List of Publications

The present Ph.D. thesis is based on the following publications that are referred to in the text by Roman numbers.

  I (ETIS 3.1) **K. Ashraf**, Y. Le Moullec, T. Pardy and T. Rang, "Model-based System Architecture for Event-triggered Wireless Control of Bio-analytical Devices," 2021 24th Euromicro Conference on Digital System Design (DSD), 2021, pp. 465-471, DOI: `https://doi.org/10.1109/DSD53832.2021.00076.`[1]

  II (ETIS 1.1) **K. Ashraf**, Y. Le Moullec, T. Pardy and T. Rang, "Design of Cyber Bio-Analytical Physical Systems: Formal Methods, Architectures, and Multi-System Interaction Strategies," Microprocessors and Microsystems, Vol. 97, Issue C, pp. 104780, 2023, DOI: `https://doi.org/10.1016/j.micpro.2023.104780.`

  III (ETIS 1.1) **K. Ashraf**, Y. Le Moullec, T. Pardy and T. Rang, "Joint Optimization via Deep Reinforcement Learning in Wireless Networked Controlled Systems," IEEE Access, Vol. 10, pp. 67152 - 67167, 2022, DOI: `https://doi.org/10.1109/ACCESS.2022.3185244`

  V (ETIS 5.2[2]) **K. Ashraf**, Y. Le Moullec, T. Pardy and T. Rang, "Decentralized Distributed Data Structure for Bioanalytical Laboratory Setups," 8th ACM WomENcourage Conference, 2021, `https://womencourage.acm.org/2021/wp-content/uploads/2021/07/59_extendedabstract.pdf`

  VI (ETIS 1.1) R. Jõemaa, N. Gyimah, **K. Ashraf**, K. Pärnamets, A. Zaft, O. Scheler, T. Rang and T. Pardy, "CogniFlow-Drop: Integrated modular system for automated generation of droplets in microfluidic applications", IEEE Access, Vol. 11, pp. 104905 - 104929, 2023, DOI: `https://doi.org/10.1109/ACCESS.2023.3316726`

Paper under review

Future Publication IV (ETIS 3.1) **K. Ashraf**, Y. Le Moullec, T. Pardy and T. Rang, "Co-Design of a Wireless Networked Control System for Reliability and Resource-Efficiency", *under revision, to be re-submitted to Baltic Electronics Conference 2024 (BEC2024)*.

Patent Application

Future Publication VII (Patent application) Owner: Tallinn University of Technology ; Inventors: **K. Ashraf**, K. Pärnamets, R. Jõemaa, N. Gyimah, T. Pardy, "Integrated modular system for automated generation of droplets in microfluidic applications and method thereto"; Priority number: EE P202300024; Priority date: 20.09.2023.

Note: the patent application is not included in appendix because it is under evaluation.

---

[1]This paper received the Euromicro DSD 2021 Special Session Best Paper Award
[2]Extended abstract + poster

Author's Contributions to the Publications

I   In Publication 1, I am the main author: I proposed the model-based system architecture, I proposed the extension of the timed automata for the use case, I simulated and verified the use case by means of the UPPAAL software, and I wrote the manuscript. I revised the manuscript, taking my supervisors' feedback into account.

II In Publication 2, I am the main author: I extended the concepts presented in the publication 1 by introducing multi-system interaction concepts, I ran the simulations using UPPAAL Stratego, and I wrote the manuscript. I revised the manuscript, taking my supervisors' feedback into account.

III In Publication 3, I am the main author: I formulated the objective function, I proposed the model-free solution (using reinforcement learning), I ran the network simulations using OMNet++, compared the proposed RL model with non-learning techniques, and I wrote the manuscript. I revised the manuscript, taking my supervisors' feedback in account.

IV In Future Publication IV, I am the main author: I proposed the resource allocation and wireless networked control system reliability mechanism and the method for modifying the control strategy via variable inter-packet gap. I proposed the RL-based strategy that ensured effective control and efficient resource allocation in the presence of moderate to high packet loss. I ran the simulations and revised the paper based on my supervisors' feedback.

V   In Publication V, I am the main author: I proposed the physical, conceptual, and logical data flow models using SAP PowerDesigner, and I wrote the manuscript. I revised the manuscript, taking my supervisors' feedback into account.

VI In Publication VI, I am the third author: I designed and implemented a communication infrastructure for the cogni-Flow module to ensure that all subscribers get the necessary data with a maximum delay of 100 ms. I co-wrote the manuscript and revised it, taking my supervisors' and co-authors' feedback into account.

VII In Future Publication VII (patent application) , I am one of the inventors: I proposed the data and wireless communication framework for the invention.
Note: the patent application is not included in appendix because it is under evaluation.

Abbreviations

6LowPAN	IPv6 over Low-Power Wireless Personal Area Networks
ANT+	Adaptive Network Topology
CPS	Cyber Physical System
C51	Categorical DQN (Q-learning algorithm, based on DQN)
CBPS	Cyber Bioanalytical Physical System
CBPS	Cyber Biological and Physical System
CPMS	Cyber Physical Microfluidic System
CPBS	Cyber Physical Biochemical System
D7A	DASH7 Alliance Protocol
DQN	Deep Q Networks
DDQN	Double Deep Q Networks
DL	Deep Learning
DRL	Deep Reinforcement Learning
E2E	End-to-End
eCAL	enhanced Communication Abstraction Layer
GUI	Graphical User Interface
IIoT	Industrial Internet of Things
IMC	Internal Model Control
IPG	Inter-Packet Gap
IrDa	Infrared Data Association
LSTM	Long Short-Term Memory
LQR	Linear Quadratic Regulator
MAC	Media Access Control
MBSE	Model-Based System Engineering
MoC	Model of Computation
MPC	Model Predictive Control
NLP	Natural Language Processing
PER	Packet Error Rate
PPO	Proximal Policy Optimization
PID	Proportional–Integral–Derivative
POC	Point of Care
POCT	Point of Care Testing
PV	Process Variable
QoC	Quality of Control
QoS	Quality of Service
RL	Reinforcement Learning
SP	Set Point
UI	User Interface
URLLC	Ultra-Reliable Low Latency Communications
WBANs	Wireless Body Area Networks
WiFi	Wireless Fidelity
WirelessHART	Wireless Highway Addressable Remote Transducer Protocol
WNCS	Wireless Networked Controlled System
Z-wave	Zensys Wave

List of Figures

List of Tables

1 Introduction

Cyber-physical systems (CPSs) [1, 2] are conceptual frameworks that integrate computation, networking, and physical operations. These systems comprise networked embedded devices, including controllers, sensors, and actuators, which collectively perceive, monitor, and regulate their physical environment. Recently, there has been an increase in the deployment of the wireless networked control system (WNCS) paradigm which is a type of CPS that specifically uses wireless communication to interconnect sensors, actuators, and controllers in dynamic physical systems [3, 4, 5]. CPSs and WNCSs are of growing interest for both academia and industry. This significant growth can be mainly attributed to the essential role that CPSs and WNCSs play in various applications under the umbrella of the Industrial Internet of Things (IIoT), including industrial automation, autonomous vehicles, predictive maintenance, aerospace, healthcare, and others [6, 7].

In essence, WNCS systems are geographically distributed control systems consisting of wirelessly networked sensors and actuators, and a central or decentralized controller [3]. Unlike a communication system focused on reliable or efficient data delivery, a WNCS is geared towards specific goals, emphasizing the need for optimal control performance within the constraints of communication, computation, and control resources [4]. Such systems typically operate in a closed-loop mode, where the controller continuously monitors the system's states and adjusts its operating parameters according to the network and control constraints. WNCSs offer many benefits as compared to wired systems, including higher flexibility, lower cost, etc. Indeed, WNCSs are more flexible and easier to install and deploy, especially in locations where space is limited or where a wired installation is not desirable or not even feasible; WCNSs can be installed in almost any location, making them highly adaptable to a variety of industrial and non-industrial environments. Another advantage of WCNSs is their potential for cost savings, as they do not require as much expensive equipment and extensive labor as wired systems usually do [3].

However, WNCSs also face many challenges, such as delays (including control, computation, and communication), packet losses, interference, resource constraints, and security issues, which require novel and efficient solutions that can jointly design and optimize their communication and control mechanisms [8, 9]. In fact, WNCSs are highly dependent on reliable, dynamic, and secure wireless communication between the sensor, controller, and actuator. As communication and control are interdependent, a co-design of both these aspects is essential in WNCSs to accomplish optimal control performance. This presents new design challenges for control-performance driven communications, as opposed to the more conventional rate-focused approaches.

To fulfill the requirements of both CPSs and WNCSs, one must address the system's attributes, i.e. topology, adaptability, functionality, reliability, and resource efficiency during the design process. The design process includes modeling and analysis of the system in such a way that it does fulfill the criteria to operate in the real world [10].

The modeling must address both the functional properties (i.e. what the system shall do) and non-functional properties (how/under which conditions or constraints) of the system, which can significantly impact the behavior and performance of systems communicating with each other under time constraints [11, 12, 13]. How well such properties can be captured and assessed depends highly on the method used i) to model the system, i.e. model(s) of computation (Moc), language, tools[3], and ii) to test that

---

[3]Examples of MoC, language, and tool used in this thesis are extended timed automata, Python, and Uppaal, respectively.

system with use cases. Modeling a system does require knowledge about its dynamics. However, WNCSs and CPSs may have varied requirements depending on the use case. This leads to the need to propose model-based and model-free reinforcement learning (RL)[4] approaches for the subjected system, as discussed in the following.

Model-based wireless control of the system would require to formulate exact dynamics of the system and then use those dynamics to incorporate during the design of controller so that the control can perform optimally. However, the wireless network itself comes with many uncertainties, so the controller faces more challenges in addition to what it is expected the system would exhibit. This means that the design of the controller must include the network uncertainties as well, in order to reach optimal performance, which requires not only model-based approaches but also model-free approaches.

The wireless network models, i.e. Markov chains, generative flow Markov chains, or hidden Markov chains, use statistical distribution to handle different network states. However, in reality, wireless networks are far too complex [14] to be simplified with some probability distribution or some static number. Moreover, different wireless technologies handle the scheduling, delay distribution, and resource allocation differently depending upon the priority of the user (in QoS management). Factors such as interference, user mobility, and network load add more complexity to the model, thus simplified models or distribution dependent models are not enough. The use of ML based models allow to simulate complex network model where the system could handle unpredicted states well.

1.1 Overview of the Main Use Case

The majority of the work in this Ph.D. thesis considers a use case example that falls under the healthcare domain, as introduced below. On the other hand, Contribution IV (Chapter 5) considers a use case example that falls under the industrial robot domain, which is introduced separately in Chapter 5.

For the past few years, CPSs and WNCSs have played a significant role in the healthcare sector, leading to both centralized and decentralized flows of information in the Point-of-Care (PoC) paradigm. The use of these concepts is expanding towards POC diagnostics ([15]) and research efforts are ongoing towards implementing POC diagnostic processes using Lab-on-chip (LoC) principles and devices.

Bioanalytics and diagnostics can now be performed at the time and place of patient care thanks to POC devices [16, 17, 18]. By 2028, the market size for point-of-care testing (POCT) is projected to reach 81.37 billion US dollars [19]. Such a number clearly illustrates the growing demand and potential of POC and POCT for improving healthcare delivery and outcomes; however, achieving such promises still requires research and development efforts in terms of new or improved technologies.

POC devices based on microfluidics are low-cost, easy-to-use, and fast sample-to-answer outcomes for non-technical operators, and are growing in relevance in the clinical diagnostic industry [20]. Complex analyzes, such as multiplexed DNA testing, are made possible by technological progress, which opens the door to innovation but also comes with many challenges [21].

Microfluidics [22, 23, 24] is a key enabler of POC and POCT; microfluidics refers to both the science and technology of manipulating small amounts of fluids, typically in the

---

[4]RL is a type of Machine Learning (ML) algorithms.

range of μL to pL, that circulate in micro-channels with sizes ranging from ten to hundreds of μm. This is a multidisciplinary field that combines different disciplines, such as molecular analysis and molecular biology, biodefence, microelectronics, and the design and fabrication of miniaturized devices comprising of micro-channels and chambers.

Microfluidics has contributed significantly to the technological advancement of POC devices, hereby enabling automation in the pharmaceutical and diagnostic fields thanks to the use of small reagent volume, increased particle monodispersity with uniform drug composition, and efficient evaluation methods for drug testing [25, 26, 27]. Indeed,

- the use of a small volume of reagent (a few μL) reduces the cost, waste, and sample consumption of the tests, as well as the risk of contamination and cross-reaction;

- increased particle monodispersity with a uniform drug composition improves the quality, stability, and efficacy of drug delivery systems. A microfluidic POC device can produce nanoparticles with precise size, shape, and surface properties for targeted drug delivery;

- efficient drug testing evaluation methods allow for rapid and accurate detection of biomarkers, pathogens, and drug resistance. Some microfluidic POC devices can perform nucleic acid amplification and detection with high sensitivity and specificity in less than an hour.

While the above leads us to the motivation of taking POC diagnostic as a use case of CPS/WNCS, it should be kept in mind that the work is also applicable to other types of use cases; indeed, the proposed modeling and analysis techniques are based on both general requirements and use case requirements.

The motivation to choose POC diagnostics not only depends upon the value that WNCSs or CPSs based diagnostics system (i.e. reliable, cost-effective and robust diagnostics) will bring to the health care sector, but it also is based on various components of the diagnostic system which are used in various other applications. For example, fluidic pumps are also used in the food industry, water quality analysis, mixing, packaging, and many more applications other than biotech. Using a pump as a use case helps check performance under the constraints of a specific system, i.e. fluidic pumps, but the work proposed in this thesis can be applied to other systems too.

1.2 Design and Implementation of WNCSs Devices

As mentioned earlier, the design of WNCSs must meet several requirements, i.e. reliability, resource efficiency, and robustness before the system is set in use for real-life scenarios. Thus, the process of designing must follow the required steps as below, which helps analyze the system in detail.

- Identify Critical Interacting Variables: This includes delay (control, communication), packet loss, energy consumption, and scheduling. Defining a communication and control architecture helps recognizing the flow of information between different field and essential components of the system.
  The bounds on delay, control errors, synchronization errors, and packet loss help achieving a specific QoS and QoC by the system.

- Analyze and Design the Control System: Defining reliability[5], scalability[6], robust control[7], and communication[8] requirements by taking into account effect of interacting variables (factors that influence the behavior and performance of the system, e.g. inputs, outputs, processes, parameters, and environment). They can be complex, non-linear, time-varying, and interdependent, making it difficult to model and predict their impact on control system performance.

- Adjust Control and Communication Parameters: A trade-off between reliability, scalability and resource allocation is needed because these objectives are often conflicting, meaning that improving one objective may degrade another. Defining efficient communication and control resource allocation to deal with the number and type of devices, the data rate and latency, the power consumption and battery life, and the environmental conditions and interference In addition to achieving specific QoS and QoC, the resource allocation under a defined reliability bound helps system achieve a specific performance with minimum resources.

- Review the Wireless Network Control System design requirements and specifications.

Modeling plays a key role in all of the above mentioned steps. It helps testing the proposed framework under the system requirements.

In relation to the use cases and the publications, there are no predefined quantified (performance) requirements based on existing standards; thus, the work is exploratory and the goal is to find the minimum or maximum performance indicators values. As a baseline, some bounds on delay, power, bit rate, channel capacity, velocity, flow rate, angle and transmission and reception time were introduced (see Table 1[9] and Table 2 for Publications I, II, and Publications III, Future IV, and VI, respectively.)

The bounds (Table 1, Table 2) introduced were helpful in identifying if the designed algorithms supported the system achieve performance within the design requirements.

---

[5] Ability to function correctly, consistently under normal and abnormal conditions.

[6] Ability to handle increasing or decreasing demands without compromising quality of service.

[7] Ability to maintain stability and performance in the presence of uncertainties and disturbances.

[8] Ability to exchange information and coordinate actions with other systems or components.

[9] $tx1\_min, tx2\_min, tx3\_min$ corresponds to lower bounds on transmission time for network unit, $tx1\_max, tx2\_max, tx3\_max$ corresponds to upper bounds on transmission time for network unit, $tc1\_max, tc2\_max, tc3\_max$ corresponds to upper bounds on transmission time for control unit, $tc1\_min, tc2\_min, tc3\_min$ corresponds to lower bounds on transmission time for network unit, e corresponds to exponential rate for each state, $tp1\_min, tp2\_min, tp3\_min$ corresponds to guard for communication of device 1, device 2, and device 3, $tp1\_max, tp2\_max, tp3\_max$ corresponds to synchronization for communication of device 1, device 2, and device 3.

Parameter	tp1_min tp1_max	tp2_min tp2_max	tp3_min tp3_max	tc1_min tc1_max	tc2_min tc2_max	tc3_min tc3_max	Delay (Stringent Delay Strategy)	(e)
Value (bounds)	20 40	50 100	100 300	24 50	54 110	104 310	100 ms	(3)
Parameter	tx1_min tx1_max	rx1_min rx1_min	tx2_min tx2_max	rx2_min rx2_max	tx3_min tx3_max	rx3_min rx3_max	Delay (Lenient Delay Strategy)	
Value (bounds)	5 2	45 22	5.00 2	105 52	5 2	305 302	200 ms	

Table 1: Bounds on different variables for Publications I, II. See footnote[9] on previous page for definitions of tp's and tx's.

Parameters	Values (bounds)
E2E Delay (for Control Applications)	200 ms
Bit Rate (Control Application)	800 Kbps
Bit Rate (Background Application)	33.3 Mbps
Channel Capacity (Max)	54 Mbps
Flow Rate	8$-$10 uL
Power (min)	95mW
Velocity (max)	0.5 cm/s
Angle	85$-$9 degrees
E2E Delay (for receiving)	100 ms (Publication VI)

Table 2: Bounds on different variables for Publication III, IV, VI

1.3 Problem Statement, Research Hypothesis and Research Questions

The analysis of existing design approaches reveals that they are not able to cope with all the critical interacting variables (e.g. delay, packet less, synchronization errors, etc.) in the co-design approach for WNCSs, or do not even follow a co-design approach but rather an interactive design. In line with this, several critical research gaps should be addressed, including providing better support to analyze the system at early design stages, i.e. improving the existing architectures, integrating model-free and model-based frameworks for analyzing and verifying that the system meets its requirements, reliability, scalability and robustness requirements of the devices at both model level, design level, as well as on the benchmarking level.

To ensure that system meets the optimal control and communication requirements, 1) it is needed to improve existing architectures so that they can well align with system requirements, 2) Additionally, in order for a system to satisfy specific QoS and QoC requirements, algorithms that aid in increasing the level of wireless automation of devices must be developed and evaluated.

One of the key issues with the previously proposed architectures in the scientific literature is their inefficiency for defining the non-functional properties of the devices. In addition, the problem could become more complex if one lacks the model of the device itself.

The research hypothesis of this Ph.D. is defined as: "The integration of model-based and model-free design methodologies to implement a high-level of automation in WNCS for complex analytical workflow (exemplified on a point-of-care diagnostic application) can help meet the reliability, scalability, and robustness requirements."
This lead to the formulation of the following research questions:

- **RQ1:** For the purpose of automating complex processes involving bio-analytical instruments, how can the principles of WNCSs (as a type of CPS) and the principles of biological processes be integrated and applied together?

- **RQ2:** What is the impact of decentralized versus centralized system communication architectures on the device's overall performance in terms of scalability, Quality of Service (QoS) and Quality of Control (QoC)?

- **RQ3:** How can Quality of Control (QoC) and Quality of Service (QoS) be improved in WNCSs?

  - How to achieve reliability by compensating network delay, control delays, packet loss, high traffic?
  - How can robustness of overall system be achieved in terms of bandwidth, power, and self-adaptive configuration?

To address the aforementioned research questions, a comprehensive analysis of the existing architecture for communication and control of devices was conducted (see Section 2). Model-based versus model-free approaches for WNCSs involve a delicate balance. Using conventional optimization techniques for resource allocation in model-free system design may be challenging, as the physical dynamics of the system are unknown and the nature of the wireless communication network may be non-deterministic. The use of appropriate wireless communication technology is determined by the device's time constraints, power constraints, computation constraints, and range constraints. These constraints ensure that the system meets both functional and non-functional properties during the early design phases. The next section summarizes the contributions provided in this Ph.D. work.

1.4 Thesis Contributions

In Publication I, **"Model-based System Architecture for Event-triggered Wireless Control of Bio-analytical Devices," 2021 24th Euromicro Conference on Digital System Design (DSD) (ETIS 3.1)**, the main contributions are:

- The novel model-based system architecture concept for event-triggered wireless control of bio-analytical CPSs using extended timed automata.

- The specification and verification of the proposed system concept using extended timed-automata in UPPAAL, for a droplet flow cytometer for antibiotic susceptibility testing of the bacteria use case.

In Publication II, **"Design of Cyber Bio-Analytical Physical Systems**: **Formal Methods, Architectures, and Multi-System Interaction Strategies", Microprocessors and Microsystems, Vol. 97, Issue C, pp. 104780, 2023** (extended version of Publication I), the main contribution, in addition to the one mentioned for the DSD2021 conference paper, is:

- To analyze the interaction of several devices, we evaluated the system's trade-off by means of UPPAAL to choose between centralized and decentralized communication architectures under known and unknown traffic patterns.

Centralized CPS control [28] may become inefficient when dealing with multi-system interaction [29, 30] because the systems are distributed across a large area and the overall computational complexity may increase significantly. Therefore, a decentralized and distributed approach to network control is preferable. UPPAAL Stratego is used to analyze strategies for achieving specific delays and bandwidth consumption while preventing packet loss during network congestion. The results indicate that under strict delay constraints and high traffic, the use case system chooses the decentralized strategy over the centralized strategy, whereas in scenarios with low traffic, the centralized strategy is more effective at ensuring the reliable operation of systems.

In Publication III, **"Joint Optimization via Deep Reinforcement Learning in Wireless Networked Controlled Systems," IEEE Access, Vol. 10, pp. 67152 - 67167, 2022**, the contributions are:

- The proposed joint optimization of WNCSs using a co-design approach. The aim is to analyze the benefit of using a model-free RL in stochastic systems as compared to classical and modern control methods.

- To analyze the problem in depth, classical optimization theory is used to formulate the problem. The objective of the problem is defined as the minimization of control errors under network constraints, as well as errors introduced via the used reinforcement Q-learning technique.

- The problem is extended for the application of droplet generation using a stepper motor where the flow rate is controlled by motor operation. To estimate the control delays as close as possible to reality, we performed the benchmarking of Raspberry Pi which is used as a central control unit of fluidic pumps in our laboratory setups. The wireless control of the pump is obtained via WiFi and network uncertainties were mimicked using the OMNet++ simulation tool.

The control performance of the system without network effect in the reward function (Scenario 1) was good with the C51 algorithm; when including OMNet++-based network effect in the reward function (Scenario 2), all three algorithms (C51, DQN, DDQN) achieved the best performance with an exponential reward function, and only C51 with a linear reward function. C51 and DDQN performed well in Scenario 3, but DQN did not converge.

In Future Publication IV, **Co-Design of a Wireless Networked Control System for Reliability and Resource-Efficiency", to be re-submitted to Baltic Electronics Conference 2024 (BEC2024)**, the main contributions are:

- This work aims to maximize control-communication reliability and resource efficiency across the control and communication layers by using RL techniques. Resource optimization in both control and communication layer is achieved by controlling Inter−Packet Gap (IPG).

- The main contribution of this study is in its holistic optimization approach, which addresses the challenges pertaining to the reliability of control communication and the efficiency of resource utilization concurrently. Indeed, by integrating RL techniques, the suggested methodology offers a holistic approach that considers the interplay between both levels.

- In contrast to traditional techniques, this work uses simulation-based scenarios to validate the suggested method. The validation method used in this study offers a more thorough and practical assessment of the suggested optimization procedure, as opposed to the prevailing mostly analytical methodologies seen in previous research.

In Publication V, **"Decentralized Distributed Data Structure for Bioanalytical Laboratory Setups," 8th ACM WomENcourage Conference, 2021, (extended abstract+poster, ETIS 5.1)**, the main contributions are:

- The main structure for data communication. The communication-based data flow structure is decentralized and supports different devices in a bioanalytical laboratory unit.

- The conceptual, logical, and physical data flow models for bio-analytical laboratory setup.

This system model worked as expected when subjected to the specified constraints. In addition to this, the case study demonstrates the implications of formal techniques for the design and verification of wireless automation of high-throughput laboratory setups in Model-Based System Engineering (MBSE).
The results showed that the system favours the decentralised technique when there are strong latency limitations and heavy traffic, but it is more reliable in low-traffic conditions when the centralised strategy is used. The minimal delay between two systems is 125 ms to prevent excessive traffic, 129 ms (centralised), and 87 ms (decentralised).

In Publication VI **"CogniFlow-Drop: Integrated Modular System for Automated Generation of Droplets in Microfluidic Applications," in IEEE Access, vol. 11, pp. 104905-104929, 2023, doi: 10.1109/ACCESS.2023.3316726**, as part of the overall CogniFlow-Drop system, an additional contribution is:

- The suggested development of a wireless communication-based automation system that operates in an event-triggered way, utilizing pre-defined data structures in a publisher-subscriber configuration.

- The same is also included in Future Publication VII (patent application) **"Integrated modular system for automated generation of droplets in microfluidic applications and method thereto"; Priority number: EE P202300024; Priority date: 20.09.2023.**

Table 3 shows the mapping between the contributions, chapters, publications, and RQs of this thesis.

	Chapter and Publication(s)	RQ1 (Integration of bioanalytical system and WNCSs)	RQ2 (decentralized vs. centralized system communication)	RQ3 (Improving QoC and QoS in WNCSs)
Contribution 1 (Model-based system architecture for event-triggered wireless control)	Chapter 3, Publications I and II	✓	✓	
Contribution 2 (Joint optimization of WNCSs using co-design)	Chapter 4, Publication III			✓
Contribution 3 (Method for control-communication reliability and resource efficiency)	Chapter 5, Future Publication IV			✓
Contribution 4 (Decentralized communication-based data flow structure)	Chapter 6, Publications V, VI		✓	
Contribution 5 (Wireless communication-based automation system)	Chapter 6, Publications V and VI, Future Publication VII	✓	✓	

Table 3: Mapping between the contributions, chapters, publications and RQs of this thesis

1.5 Thesis Organization

This thesis is organized as follows:

- Chapter 1 (this chapter) provides fundamental principles of wireless networked controlled systems, which are crucial for comprehending their functionality and applications. This chapter additionally presents the problem statement, research hypothesis, and research question that will be examined and discussed throughout the thesis. Furthermore, it emphasizes the thesis's contributions in terms of improving knowledge in the domain of wireless networked controlled systems. Ultimately, the chapter offers a well-defined structure of the thesis, offering the reader a concise outline of what to anticipate in the next chapters.

- Chapter 2 begins with a brief summary of control systems and then provides an overview of the existing research in several areas encompassing wireless control system design, design of CPSs, wireless communication and its use in point-of-care devices, RL, the comparison between model-based and model-free RL, and MBSE. Note: the more specific state of the art related to the individual contributions are presented in the following respective chapters.

- Chapter 3 discusses the utilization of MBSE methods in designing Cyber-Physical Systems (CPSs). The work specifically focuses on the definition of a model-based system architecture and on the deployment of POC devices to demonstrate the significance of formal approaches in modeling, verifying, and validating these systems. The proposed strategies aim to achieve particular delays and bandwidth usage while reducing packet loss under network congestion, and are then compared. The results demonstrated that the system prefers the decentralised strategy when strict latency constraints and high traffic are present, whereas it is more reliable in low-traffic scenarios when the centralised strategy is implemented. The minimum delay between two systems is 125 ms (avoiding excessive traffic), 129 ms (centralised), and 87 ms (decentralised).

- Chapter 4 introduces the design of an optimal control system that addresses uncertainties in network conditions. It also provides an algorithm that enables the control system to function effectively even in poor network conditions. The method considers multiple parameters, including delay, packet loss, and bandwidth limitations. The chapter also assesses the effectiveness of the proposed algorithm, showcasing its ability to improve the performance of control systems even in the presence of variable levels of network unpredictability.

- Chapter 5 introduces resource allocation techniques and explores the importance of reliable control performance in WNCSs. The chapter focuses on the challenges encountered in achieving reliable control performance in WNCSs, specifically addressing problems associated with packet losses and latency. The chapter explores the utilization of reinforcement learning (RL) strategies to guarantee reliable control performance in these systems. The chapter illustrates the application of inverted pendulum simulation to showcase the effectiveness of the suggested methodology.

- In Chapter 6, the distribution and flow of data for WNCSs are discussed, along with guidelines for the development of user interfaces for software that interacts with these systems in the context of point-of-care applications.

- Chapter 7 provides a summary of the main contributions, presents the conclusion of the thesis, and emphasizes future work.

The framework for the Ph.D. thesis (including contributions denoted by Cx with green font) is shown in Fig. 1.
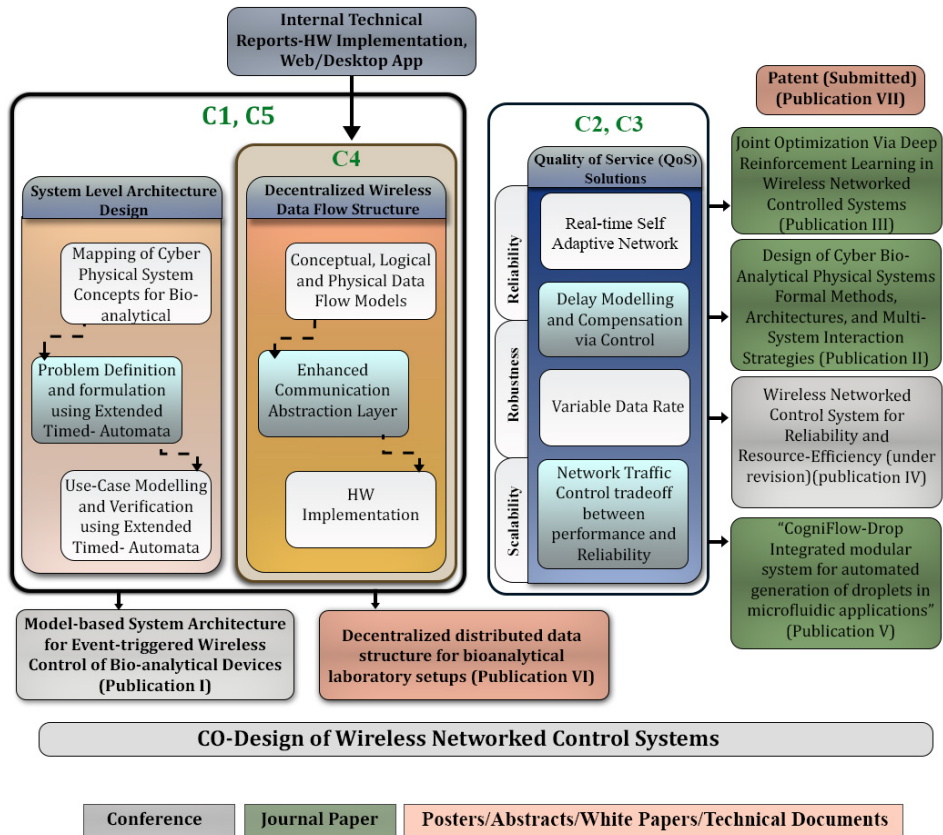
Figure 1: Framework for the Ph.D. thesis. The contributions are denoted by Cx with green font.

2 Some Background on Co-design and Models for Wireless Network Controlled Systems

To gain insights into WNCSs and achieve the goals of this Ph.D., a study of the scientific literature was carried out on WNCSs, CPSs, MBSE, wireless communication and modeling for POC devices, as well as on ML in WNCSs and their comparison with classical control.

*While the following sections present an general overview of the above-listed topics, **it is important to highlight that the specific state of the art for each contribution of this thesis is summarized later in its own chapter**. The current chapter provides the essential background required to develop an understanding towards achieving the Ph.D. objective. The contributions of the cited works are summarized individually in the next sections; on the other hand, their limitations and the research gaps are summarized collectively at the end of the chapter.*

2.1 Brief Summary of Control Systems

Control systems are used in a wide range of applications, including transportation, production, manufacturing, and many more, such as WNCSs introduced in the previous chapter. As mentioned earlier, controlled systems usually comprise of sensors, actuators, and of the actual controller(s), where the goal of control is to maintain a stable behavior of the actuators, possibly based on sensor inputs [31]. Control systems can be divided into several categories depending upon i) the absence or presence of feedback, i.e. open-loop and closed-loop control, ii) upon the behavior of the system, i.e. linear or non-linear, and iii) upon the type of time-domain representation and analysis, i.e. continuous time or discrete time [32, 33]. These three aspects are briefly discussed in what follows.

Fig. 2 illustrates the difference between open-loop and closed-loop control. An open-loop control system requires no feedback from the system's response to the controller's input, i.e. the control action does not depend on the process output (also known as the controlled process variable). Open-loop control is utilized in a variety of applications, e.g. a stepper motor that moves a specific distance with each pulse received. To position it, the necessary pulse count is simply applied to the motor input. While creating such control systems is simple, the operation is not effective for systems with a low tolerance for error.

In order to achieve e.g. higher accuracy or when dealing with systems that have a restricted range of output, it is crucial for the controller to consider the system's response in relation to its input. Such a closed-loop (feedback) mechanism allows the system to adjust its controller output (input for the system/actuator) in response to e.g. changes in external variables, such as temperature fluctuations, that may cause abnormal operation. As a counter-part to the stepper motor example mentioned above, a servo motor is an example of a closed-loop controlled system, i.e. it operates by receiving the initial and target positions and calculates the error or difference between the two and operates the motor until the error is minimized.

Moreover, the categorization of control systems can also be based on the system behavior, i.e. either linear or non-linear. The behavior of a linear system is deterministic and can be modeled using simple equations [34]. In contrast, a non-linear control system exhibits complex behavior, and the output patterns of the system are often unpredictable, or sometimes even extremely unpredictable. In the context of linear systems, the system is typically expressed using state-space equations, and the process
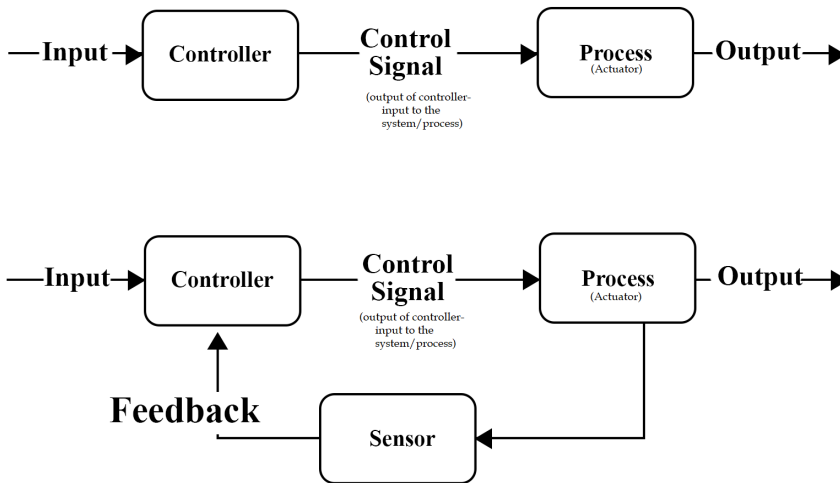
Figure 2: Illustration of control systems in the absence of feedback (top: open-loop control) or in the presence of feedback (bottom: closed-loop control)

of analyzing stability is rather straightforward [35]. The controller design is not highly complex, and a straightforward implementation of e.g. Proportional–Integral–Derivative (PID), Internal Model Control (IMC), or Smith Predictor is sufficient to achieve a stable response [36].

Conversely, in the case of non-linear systems, their behavior is too complex to be described by simple state-space equations. To analyze stability, it is necessary to linearize the system [37]. In the case of non-linear systems, it is nowadays common to design a controller using RL or other methods of machine learning in order to achieve a stable operation of the system [38].

Finally, the control can also be categorized as continuous time or discrete time (Fig. 3) based on how the evolution of variables over time is modeled. The primary distinction between these two is the time-sampling of the input and output. Continuous time systems work continuously without intervals (or infinitesimally small intervals), while discrete time systems function at fixed intervals [39] (e.g. by acquiring values of an analog signal at constant or variable rate via sampling, or if the process is inherently discrete time). continuous time control often utilizes proportional or integral or derivative based control, or in combination as in PID. On the other hand, discrete time control often operates based on sequences or difference equations [40]. It is possible to design a discrete time controller for a continuous time system [39] and vice versa.
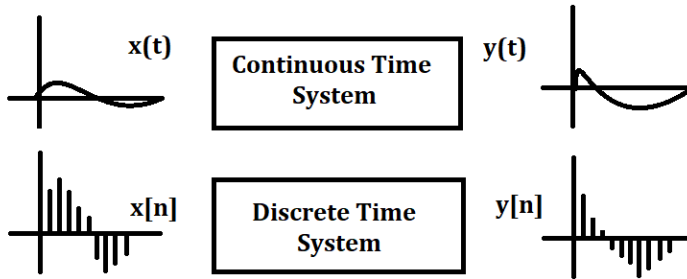
Figure 3: Illustration of continuous time control and discrete time control. Top: control input (x(t)) and response (y(t)) for a continuous time control system. Bottom: control input (x[n]) and response (y[t]) for a discrete time control system.

In the rest of this thesis, control is characterized as i) closed-loop control, ii) non-linear, and iii) discrete time.

It should also be noted that in control theory, "optimal control" refers to the process of finding a control law that minimizes a certain cost function for a dynamic system. However, the term "optimal" in "optimal control" does not guarantee that the control strategy is always the best because in practical applications there are trade-offs between achieving optimality and other aspects such as real-time implementation constraints. This thesis focuses on the optimal control of a system by addressing a joint-optimization problem (control and wireless communication) which is in nature a non-convex problem. The objective is to achieve a certain level of performance, described as the system requirements, by minimising several factors such as steady state control error, bandwidth consumption, power consumption, packet loss, and latency etc., while ensuring quality of control (QoC) and quality of service (QoS).

2.2 Co-design in Wireless Networked Control Systems

As previously stated, WNCSs are decentralized systems comprising controllers, actuators, and sensors that can communicate wirelessly. This enables WNCSs to be used in a variety of fields, including automotive, smart buildings, industrial automation, and robotics, among others. Several co-design frameworks have been developed to address the challenges experienced by WNCSs. These frameworks have focused on either optimizing i) control parameters (such as sampling time, stability, or routing), ii) network parameters (including delays, packet loss, and jitter), or both i) and ii).

The optimization of either control parameters based on networked conditions, or vice versa, falls under the category of cross-layer design [41, 42] (Left-hand side of Fig. 4), whereas co-design aims to optimize both control and network parameters together for the system to reach optimal performance (Right-hand side of Fig. 4).
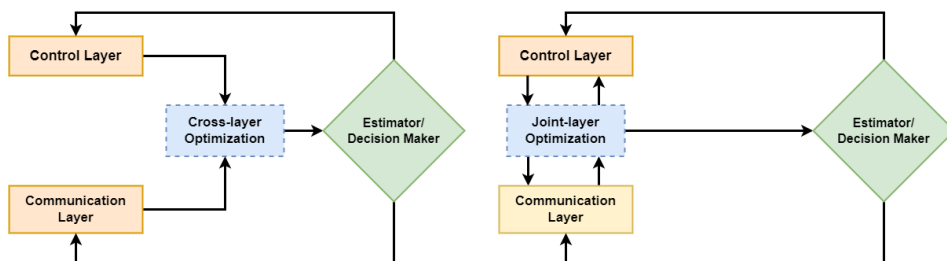
Figure 4: The two main categories of design frameworks for WNCSs. Left: cross-layer design (optimizes either control parameters based on networked conditions or vice versa; the optimizer does not make joint optimization of different parameters). Right: Co-design (optimizes both control and network parameters together).

Co-design strategies falling under the right-hand side of Fig. 4 and developed specifically for WNCS are also helpful for the design of CPS in general because nowadays the physical, network, and application layers of WNCSs are also core components of many CPSs. The main challenge in designing CPSs and thus WNCSs is the limitations of modeling frameworks in their representation and simulation of unpredictability, continuum, and determinism [43]. There is a strong need to focus on modeling and analyzing the system so that it can integrate interaction between the control and communication domains in a unified way. The designed system should be able to address the complexity added to the system as a result of interaction between the domains e.g. delays, losses, computation, resource allocation and scalability. Reliability and the trade-off between control and communication objectives must be properly addressed to achieve optimal performance [3].

2.2.1 Cross-Layer and co-design of Wireless Network Controlled Systems

In [42], a cross-layer design framework is proposed for systems with energy limitations, where control system optimization is performed by imposing constraints on wireless networks. This helped achieve control level optimization for an inverted pendulum application; results show how the stability, performance, computation time, energy consumption, and transmission delay are affected by different control and communication strategies, and that there is a trade-off between stability and performance, and between energy efficiency and performance.

In [44], a cross-layer design methodology is proposed to address periodic traffic

timeliness and optimize channel utilization by adjusting the sampling rate between the controller and sensor in a WNCS. Their proposed method can adjust the sampling period to achieve the best control performance and meet the time constraint in WNCSs and it can use the channel more efficiently and reduce the useless data as compared to non cross-layer methods.

The work [41] optimizes control performance as a function of controller design and network parameters using cross-layer design framework where multiple control loops are present in the system. The paper explores controller design with dropped packets, demonstrating the separation of estimation and control under network assumptions and also discusses wireless network design, highlighting implicit tradeoffs between network throughput, time delay, and packet loss probability. A cross-layer design framework for networked control applications is proposed and validated on a double inverted pendulum system.

[45] also uses a cross-layer design strategy where control architecture optimizes communication cost while maintaining control performance. The paper introduces a control architecture integrating Low-power wireless bus and rate adaptation and self-triggered control strategies. It presents optimal rate selection algorithms, novel network adaptation mechanisms and explores the tradeoff between communication cost and control performance. Results show that rate adaptation and self-triggered control offer advantages in control performance and energy efficiency (e.g. up-to 47% energy savings for comparable control mean average error as compared to traditional control systems at fixed sampling rates).

Work [46] focuses on security in WNCS and investigates the resilient control problem for a class of WNCS under a denial-of-service (DoS) attack, adopting a cross-layer view and obtaining Nash power strategies and optimal control strategy in the the delta-domain [10] in the cyber- and physical-layer, respectively, to bring the control performance to the desired security level by dynamically manipulating the cyber-layer pricing parameters.

At the time of writing this thesis, work [47] recently (February 2024) proposed a Deep Reinforcement Learning (DRL)-based algorithm for estimating-controlling-scheduling co-design of a model-unknown non-linear Wireless-networked control system (WNCS) over wireless fading channels with model-free and model-based data, as well as with the awareness of the sensor's Age-of-Information (AoI) states and dynamic channel states. Experiments show significant performance gains, e.g. up-to 72% – 99% performance improvement over the baseline Scheduler-Reward.

The work [48] presents a methodology for the joint design of control and communication for WNCSs using a combination of simulation and optimization approaches. In addition, the same work analyzed how the choice of control algorithms and communication protocols affects the stability and performance of the WNCS.

[49] proposes a co-design framework for wireless system identification in WNCSs, which optimizes the wireless resource allocation while ensuring the identification accuracy under confidence level. Two design problems are solved for maximizing the throughput or minimizing the power consumption and deriving the minimum number of data samples for identification, by using Lagrangian method, Hungarian algorithm, and finite-time identification theory for exploiting the relationship between the power consumption and channel allocation given the finite-time wireless system identification

---

[10]Delta-domain: mathematical domain used to model and analyze discrete time systems, such as CPSs, based on the delta operator (difference operator that relates the current and the next values of a signal). Advantages over the traditional z-domain include better numerical stability, easier implementation, and closer resemblance to the continuous time domain

performance requirement, leading to up-to 26.4% energy savings.

[50] reviews the communication–control co-design methods for wireless networked automation systems and analyzes the correlations between control and communication systems, in particular i) control optimization problems with communication constraints and ii) communication optimization problem with control constraints, and highlights that the scientific literature lacks in works that combine the control and communication requirements as objectives. The paper also proposes a co-design model for cloud control of AGVs in future factories; results show that communication–control co-design can lower the coding rate requirements and wireless resources consumption, and improve the probability of system instability and the number of admissible AGVs. The results also highlight that the control system is more stable when sampling time increases (from 1 to 5 ms in the use case), but becomes more unstable past a certain point (from 6 ms in the use case).

A review was also conducted around model-based and model-free design approaches, different control and co-design methodologies [51, 52] and the integration of CPSs concepts in the devices, which are presented later in the respective chapters of the thesis.

2.2.2 Wireless Communication Technologies for Point of Care Devices

In the initial phase of this Ph.D. thesis, a literature review was conducted to analyze the state-of-the-art in the field of wireless communication for POC devices. A systematic literature review (Appendix 5, not published) helped to identify the dominant communication methods and technologies used in POC devices. A period of 6 years (2015-2020)'s research documents (i.e. papers, books, tutorials, etc.) were analyzed; the documents were narrowed down to 39 items for comparative analysis. The final selection of documents included 16 items for long-range and 23 for short-range wireless communication technologies.

The research [53] shows the use of Zigbee for portable surface stress biosensor test system due to its low-cost and low-power. NFC is found to be useful for several health sector applications especially in health management systems for medical data acquisition, disease diagnostics, and patient care [54, 55]. Recently, several research efforts have been carried out to use NFC in self-diagnostics devices. Due to higher data rates, the Bluetooth has been shown to be beneficial in the transfer of medical data and records in many present health care devices. The paper [56] deliberates the use of Bluetooth as a wireless communication tool for paper-based Point-of-Care testing (POCT) device for the detection of neuron-specific enolase.

Several research efforts [57, 58] show the use of Wi-Fi as a powerful connectivity tool for e-health applications. The major focus of these researches is to use Wi-Fi as a connectivity tool; however, performance evaluation of Wi-Fi itself is not performed. The research [59] gave a state-of-the-art overview of UWB use for Wireless Body Area Networks (WBANs) and challenges associated with its implementation in health care devices. ANT+ [60] is an ultra-low-power, short-range and scalable wireless network protocol used mainly for wearable devices. Other short-range wireless technologies 6LowPAN [60], Z-wave [60], WirelessHART [61, 60], DASH7 [62, 63, 60] and IrDa [60] can also be used in health care devices for patient monitoring applications [64, 65]. However, the research does not show the use of these technologies in POC medical devices.

The research [66] show the use of LoRaWAN for e-health applications and evaluate the performance of the communication protocol for different indoor scenarios. The

research [67] show the use of NB-IoT for drug infusion control, the introduction of an edge computing layer was proposed to reduce the major challenge of NB-IoT which is latency. The studies [68, 69, 70] propose the use of SigFox for personalized health-care devices. LTE-CAT-M1 [69] and Wi-SUN [71] are other low-power long-range communication methods considered as a viable wireless communication tool for health care applications. Although for POC monitoring devices the use of wireless communication technology is identified as broad whereas for POC diagnostic devices, its use is only restricted to few well-known wireless communication technologies, i.e. Bluetooth and RFID due to limited research in the field.

In addition to the above review, some selected works illustrating the current advances in the field of health care regarding the use of wireless communication were also analyzed. [72] emphasizes the significant impact of 5G technology on healthcare and wearable devices, highlighting its potential to improve patient monitoring, illness prevention, and specialist care accessibility. Furthermore, [73] examines the wireless technologies used in Wireless Body Area Networks (WBANs), explores their medical uses, and addresses the obstacles and potential advancements in the sector. Another article [74] outlines current and upcoming trends in POC technology, including technologies that have been approved or cleared by the Food and Drug Administration or are in the research phase. The paper discusses the potential clinical applications of developing technologies such as wearables, noninvasive testing, mass spectrometry, and digital microfluidics, focusing on strategies beyond technical proof of concept for clinical implementation and impact.

2.3 Model-based and ML based Design in Wireless Network Controlled Systems

The work presented in [75] presents several structures and control methods developed to enhance the efficiency of Networked Control Systems (NCS) using Model-Based Networked Control Systems (MB-NCS) methodologies, emphasizing the significance of model-based system engineering in NCSs, to achieve lower data transmission rates and generate appropriate control inputs.

A discrete Markov switching system model [76] is developed for WNCSs by integrating the 802.11 protocol and a novel scheduling method. This model represents packet drop sequences as states of a Markov chain to enable the creation of a variable controller using linear matrix inequalities (LMIs) in Matlab. It considers both known and unknown dropout probabilities and is validated through simulation.

The research presented in [77] integrates gain scheduling and time-delay system modeling to reduce communication consumption while maintaining control performance by employing a less conservative self-triggered method for scheduling and operating a WNCS on an IEEE 802.15.4 network.

In [78], a novel model-dependent scheduling (MDS) approach is presented for networked control systems that accommodate disturbances, time-delays, and medium access constraints. In order to improve system stability, the approach considers both constant and random time-delays while choosing states. Additionally, in order to handle system disturbance and uncertainty, it integrates a co-design technique based on switched systems and a robust H-infinity. Their proposed MDS has better stability compared to maximum error first and try once discard (MEF-TOD). MDS needs less switches as it uses the error between the ideal dynamic and the real system; the states scheduled in each sampling period are the optimal ones making MDS more stable.

The research presented in [79] proposes a new method for allocating radio resources

in proactive vehicular networks, utilizing a "generalized closed-loop" model and DRL, where data transmission success rate is the reliability indicator. The method uses radio resource utilization information from the vehicle's past uplink; vehicles use local or global data transmission experience to select the best quality radio resource; DRL is based on the latest resource utilization information (RRUI) of vehicle and resource occupancy information. The simulations demonstrate that the method attains a data transmission success rate of over 98% when the resource load rate approaches 40%.

2.4 Model-based Design methods for Point of Care Devices

This section encompasses topics of model-based design for POC devices.

The review [80] emphasizes the importance of wearable sensors in POCT, discussing their design, types, and recent advancements in non-invasive biomarker measurements. It also covers challenges and future possibilities, such as integrating with the IoT for self-healthcare.

The research presented in[81] explores the application of MBSE, and customized object-oriented systems engineering method modeling, focusing on problem, context, technical requirements, logical, and physical levels, for constructing bioanalytical devices, facilitating interdisciplinary cooperation among biochemical processes, software, hardware, and mechanics. The paper also stresses that the transformation of product lifecycle processes from document-centric to MBSE will provide a competitive advantage.

In order to enable automation in the healthcare industry, numerous architectures and models integrating CPSs concepts with medical devices have been proposed in recent years [82, 83]. However, such integration with bio-analytical devices is still new, under-researched, and there are very few works proposing an architecture and model for the design of these devices. The works [84, 85] inspired model-based system design methodology in bio-analytical and diagnostic devices and SysML modeling of the system. Using SysML, it is possible to model system behavior; however, non-functional properties, which are essential for the synchronized operation of the system under constraints, cannot be fully accounted for using this method.

Increasingly, bioanalytical devices integrate the concepts and features of wireless-enabled CPS, which can help improve efficient laboratory control. In this context, a Cyber Bioanalytical Physical System (CBPS)[11] integrates physical and biological processes with computation and communication domains, enabling efficient remote operation of the processes. Synchronization between devices in a CBPS ensures stability and reliability [90]. Fault tolerance and delay requirements [91, 92] limit system performance (as in URLLC) [93]. Delays introduced by control systems, such as computation and prediction delays, and wireless network uncertainties, such as queuing, transmission, and backhaul delays, affect these factors [91, 92]. It is important to consider the design of WNCS (as a sub-domain of CPS) as a co-design problem rather than an interactive design in which one design lies on top of the other. Co-designing WNCSs can improve application control and information distribution.

---

[11]Related but not necessarily identical concepts are also referred to as e.g. medical cyber physical systems (MCPS) [86], cyber physical microfluidic chip (CPMC) [87], cyber physical microfluidic system (CPMS) [88], cyber biological and physical system (CBPS) [89], or cyber physical biochemical system (CPBS) [84]

2.5 Model-free and Model-based Machine Learning

Model-based ML methods [94] predict outcomes by constructing a model of the environment, while model-free ML algorithms [95] learn from experience without relying on an environment model. Linear Regression and Decision Trees are examples of model-based ML methods, while Q-Learning, Deep Q-Network (DQN), and PPO are examples of model-free ML techniques. Model-based procedures are less accurate but require fewer samples, whereas model-free methods are more reliable and consistent, but require more data samples. Table 4 summarizes the key differences between model-free and model-based ML techniques, extracted from the scientific literature.

Property	Model-free	Model-based
Complexity [96]	Simple as it learns from experience	More complex due to need of building and maintaining the environment model
Computation [97]	As no model is used, its computationally less expensive	As it requires building and maintaining model of environment, its computationally expensive
Accuracy [98]	depends upon experiences	depends upon model updates
Adaptibility [96]	Adapts by learning through new experience	Requires model updates
Sample efficiency [96]	Less sample efficient	more simple efficient

Table 4: Comparison of essential properties of model-free ML and model-based ML

In addition to the above, different applications of ML require a thorough examination of ML techniques to determine whether a model-based or model-free approach is appropriate.

Several works incorporating ML in the design of WNCSs or CPSs can be found in the scientific literature. A concise selection thereof is highlighted in what follows. The editorial presented in [99] highlights the potential of Deep Learning (DL) to enhance the utilization of limited spectrum resources in wireless communications for CPS, how it can also be used to understand normal and abnormal behavior in CPS components and devices, and how DL methods are crucial in predicting new attacks, often mutations of previous ones, by learning from existing examples.

The research presented in [100] proposes employing RL to determine when smart sensors in a wireless network should analyze measurements, considering the balance between latency and accuracy as well as resource limitations, with a focus on optimizing the latency-accuracy trade-off. Numerical simulations on smart sensing for the Internet of Drones show that the proposed Q-learning-based learned policy can outperform conventional design choices but also static policies.

The work [101] discusses the potential of unsupervised explainable ML in CPSs. It reviews existing work in ML, presents initial requirements for explainable unsupervised ML for CPS, and proposes a Self-Organizing Maps-based explainable clustering method that generates global and local explanations using feature perturbation techniques. The results show that the proposed method identifies key features for decision-making in Self-organizing Maps and that it is a strong candidate for explainable unsupervised machine learning, compared to current methods.

2.6 Summary of the Background on the Co-design and modeling of WNCS

The above general background overview, as well as the specific state of the art presented in the next chapters, show that significant progress has been achieved in the design methods of WNCSs. However, there still exist limitations and research gaps. The research on the novel model-based system architecture for event-triggered wireless control lacks an understanding of its dynamic adaptability in response to fluctuating network conditions; it is needed to explore how the system can autonomously switch between centralized and decentralized strategies in scenarios including varying levels of network congestion and traffic. Adaptability and robustness of joint optimization of WNCSs using a co-design approach in dynamic and uncertain network environments is also under-researched; further exploration is needed to understand performance in such scenarios. Adaptability and scalability for maximizing control-communication reliability and resource efficiency lacks an understanding of its evaluation by e.g. simulations, beyond purely analytical studies. Moreover, practical implementation and optimization of decentralized communication-based data flow structures on use cases of bioanalytical systems are scarce, particularly in terms of accommodating various devices and establishing conceptual, logical, and physical data flow models, as well as in the implications of formal techniques for designing and verifying such use cases with Model-Based System Engineering (MBSE).

This chapter has presented an overview of some essential background related to the Ph.D. sub-topics and highlighted general limitations and research gaps.

As mentioned at the beginning of this chapter, the specific state of the art for each contribution of this thesis is presented in its own chapter. The next chapters present the individual contributions of the Ph.D. thesis, including their respective overviews of the corresponding state of the art.

3 Model-based System Architecture for Wireless Networked Control Systems

This chapter discusses the need for model-based system design in WNCSs and suitable approaches for achieving optimal control at early design stages. The chapter is based on the following publications:

Publication 1: K. Ashraf, Y. Le Moullec, T. Pardy and T. Rang, "Model-based System Architecture for Event-triggered Wireless Control of Bio-analytical Devices," 2021 24th Euromicro Conference on Digital System Design (DSD), 2021, pp. 465-471, `https://doi.org/10.1109/DSD53832.2021.00076`

Publication 2: K. Ashraf, Y. Le Moullec, T. Pardy and T. Rang, Design of Cyber Bio-Analytical Physical Systems: Formal Methods, Architectures, and Multi-System Interaction Strategies, Microprocessors and Microsystems, Vol. 97, Issue C, pp. 104780, 2023, DOI: `https://doi.org/10.1016/j.micpro.2023.104780`

The reader is encouraged to look at the above papers (provided in appendix) for additional details and results.

The integration of CPS concepts into bio-analytical devices aims to enhance device automation and diagnostic capabilities. This contribution explores:

- A model-based system architecture that builds upon an extended timed automata-based formal technique. In contrast to prior research that utilizes models focused in SysML or UML, the proposed strategy allows the wireless control of bio-analytical devices through the utilization of a formal methodology.

- Model-Based System Engineering (MBSE) implications of formal techniques for the design and verification of wireless automation of high-throughput laboratory setup. A case study named "A droplet flow cytometer for testing bacteria's susceptibility to antibiotics" was modeled and analyzed using the formal method.

- A trade-off between centralized and decentralized information flow strategies to improve system performance in the context of delay and bandwidth constraints. UPPAAL Stratego is used to analyze strategies for achieving specific delays and bandwidth consumption while minimizing packet loss during network congestion.

Fig. 5 provides a graphical abstract of the contribution on model-based system architecture for WNCs. The key elements of the figure are discussed below and in Publications I and II.

Integration of the principles of WNCSs (as a type of CPS) and the principles of biological processes into bio-analytical devices is highly desirable to enable device automation as well as to improve diagnostic and analytical capabilities. The results indicate that when dealing with strict delay constraint and heavy congestion, the use case system opts for the decentralized technique instead of the centralized option. In situations with minimal traffic, the centralized solution demonstrates greater effectiveness in maintaining the reliable functioning of systems.

The demand for automation in laboratory-based biochemical analysis and portable fast diagnostic equipment has witnessed a substantial increase in recent years, owing to the global spread of numerous diseases. The surge in demand may be attributed mostly
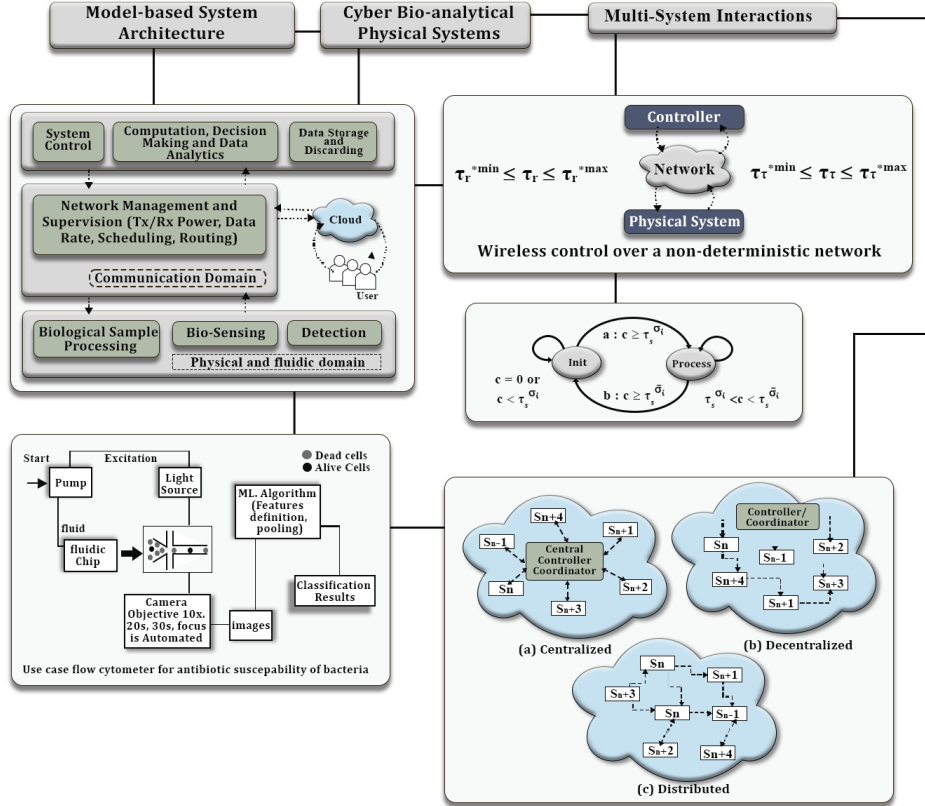
Figure 5: Graphical abstract of the contribution on model-based system architecture for WNCs. The key elements of the figure are discussed below and in Publications I and II.

to the imperative to enhance medication research, analysis, testing, and rapid diagnostic techniques [102, 103, 104]. Nevertheless, there exist multiple challenges linked to the accomplishment of this automation, and the complexity of the problem has been well defined in our prior research [105, 106], i.e. automation of chip design, sensor technology, light source, and fabrication processes.

The integration of CPS concepts with microfluidic and biochemical domains is being undertaken to facilitate automation in the field of bioanalytics. CPSs are designed to combine physical and computational capabilities over a communication network. These systems also incorporate user feedback by utilizing cloud-based technologies. In the early phases of design, it is crucial to take into account both functional and non-functional aspects in order to guarantee reliable and efficient automated functioning within real-world limitations. Several architectures and models have been proposed for incorporating CPS concepts with medical devices [107, 108], but research on the integration of CPS concepts with bioanalytical devices remains limited. There also exists the well-defined ISO/IEEE 11073 set of standards for health informatics, including POC medical device service-oriented communication [109]. However, the same is not true for CPBS or CBPS.

Language	Complexity	Expressiveness	Analyzability
Petri−nets [110]	Simple but does not handle continuous behavior and complexity increases with increasing clocks [111]	good for modeling concurrency, synchronization, and distributed systems but less effective for continuous dynamics [112]	excellent for concurrent behavior analysis and deadlock detection. [111]
TimedAutomata	Less complex than hybrid automata [113]	Expressive for systems with strict time requirements [114]	well suited for verifying temporal aspects in real-time systems [113]
HybridAutomata [115]	Complexity increases with more clocks or mixed behaviors	Highly expressive for mixed behaviors (Continuous & Discrete)	Challenging for systems with large number of clocks and mixed behavior
Pi-Calculus [116]	Complex communication mechanisms and high concurrency make scenarios challenging	good expressiveness in modeling concurrent and distributed systems with complex communication patterns	Challenging for complex systems

Table 5: Formal modeling Languages

Very few works [84, 117] using SysML or UML based modeling language proposed a CPS based architecture for diagnostic devices. In [118], a comprehensive analysis of modeling languages and techniques is presented, along with a list of their limitations. In addition to emphasizing modeling requirements, this work discusses the significance of addressing the functional and non-functional properties of CPS to ensure the device operates correctly. It is possible to model system behavior using SysML; however, as mentioned earlier in this paper, non-functional properties are required for the synchronized operation of the system under constraints and cannot be thoroughly addressed using this method. Moreover, as the number of interconnected systems increases, so do the variables used to account for this interaction, necessitating a more streamlined and trustworthy modeling strategy which leads to formal methods based approaches. Table 5 shows a comparison different formal methods for modeling system based on complexity, analyzability and expressiveness.

The selection of the timed-automata modeling language is based on a comparative analysis of many elements of modeling languages and the stringent timing demands of control systems. Timed automata are a sub-class of hybrid automata with a finite number of resettable real-valued timers. Timed automata can be used to characterize both functional and non-functional aspects of real-time systems, such as timing behavior. Timed automata, unlike straightforward finite state machines, have time constraints [114].

3.1 Wireless Event-Triggered Control

Wireless event-triggered control [119] is an approach that aims to optimize network traffic by selectively transmitting data solely when significant events occur. This strategy effectively reduces the cost of communication and decreases energy consumption in comparison with time-triggered control, which involves frequent data transfer. The technology provides rapid control responses with minimal delay, enabling adaptable control approaches in various fields such as robotics, autonomous systems, and industrial automation. Furthermore, it enhances the longevity of battery life for sensors and IoT devices that rely on batteries for power.

Nevertheless, the system encounters various limits, including but not limited to the detection of events that may not be accurately identified, issues related to the stability of the network, challenges in scaling the system to handle increasing demands, concerns regarding security measures, complexities associated with the system's design and implementation, as well as limitations imposed by available resources.

In systems where there are stringent resource requirements, wireless event-triggered control is given priority over time-triggered control [3]. In the context of bio-analytical systems, data transfer can be facilitated by event-based mechanisms. However, in order to ensure that the developed system adheres to the maximum allowable delay, a modeling language based on timed automata is used. This ensures the synchronization of several systems and prevents the occurrence of deadlocks.
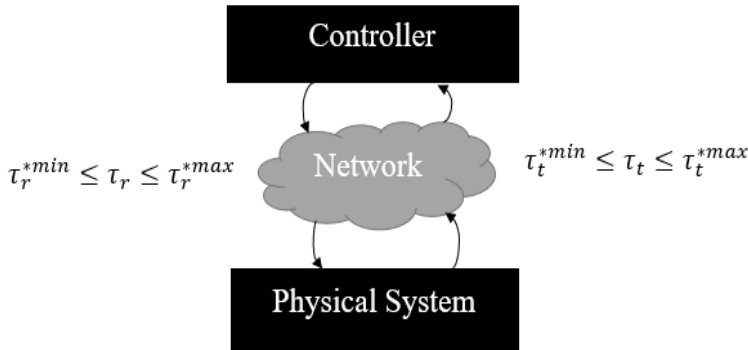
Figure 6: Wireless control over a non-deterministic network, where τ_t^{*min}, τ_r^{*min}, τ_t^{*max}, τ_r^{*max} are the minimum and maximum times for a sample to be transmitted and received, respectively.

It was supposed that every bio-analytical system functioned as a Linear Time Invariant (LTI) system. In the scenario where the network is non-deterministic, meaning that the time taken by each sample to reach its destination is unknown, there exists a delay associated with the transmission of each sample, denoted as τ_t, as well as a delay associated with the reception of each sample, denoted as τ_r. Furthermore, the minimum times required for the sample to be transferred and received are denoted as τ_t^{*min} and τ_r^{*min}, respectively. Similarly, the maximum times required for the sample to be transmitted and received are denoted as τ_t^{*max} and τ_r^{*max}, respectively, as seen in Fig. 6. When dealing with multiple systems interacting with each other over wireless network the scabaility and reliability are major network design performance benchmarking tools.

The major network architecture to achieve scalability are centralized, decentralized and distributed. Fig. 7 shows an overview of generalized centralized, decentralized, and distributed system architectures. The increasing number of devices poses a challenge to
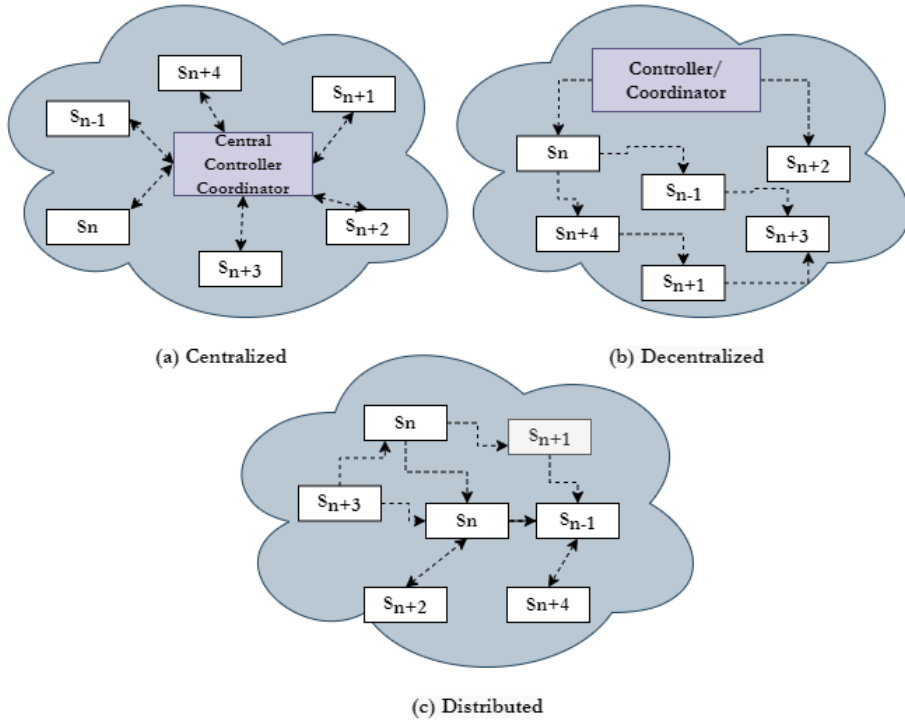
Figure 7: (a) Centralized, (b) Decentralized, (c) Distributed System Architecture for information control and transmission.

the interaction among multiple systems [29, 30]. A centralized control approach for Cyber-Physical Systems (CPS) [28] may become inefficient in such scenarios, as the systems are often distributed across space and the overall computational complexity could experience a significant increase. Moreover, a distributed or decentralized CPS architecture [120] is preferable when network resources are scarce, such as when bandwidth is limited or time-delay restrictions are stringent. When deciding between a centralized control strategy and a decentralized or distributed control approach, there is always a trade-off.

If the number of systems interacting with each other is smaller than the upper bound on network constraints like as bandwidth and power, a centralized control and communication method would be preferable than a distributed one, where information flow could experience significant delays. Consequently, there arises a necessity for conducting a comprehensive examination of network designs in order to assess their scalability and maintain their reliability while operating under the limitations of bandwidth and latency requirements.

In order to evaluate the most appropriate strategy, a methodology based on Stochastic Timed Automata (STA) was used. Uppaal Stratego [121], a tool for optimizing, simulating, and exploring strategies in pricing strategic timed games, was used to simulate the strategy. The results and further details of the approach are presented a bit later under Section 3.3.

3.2 Modeling Framework and Case Study

The preliminary definitions of hybrid and timed automata for the use case under study, as well as their parallel construction, are provided in Table 6.

Both hybrid and timed automata derive their semantics from two rules: discrete rule for discrete state transitions and continuous time rule for continuous time steps. In the case of parallel compositions involving n systems, denoted as $T_1, T_2, ..., T_n$, the discrete transitions between the edges of two consecutive systems, T_i and T_{i+1}, can be categorized into two types: "Rule Synchronization" and "Rule Non-Synchronization".

The process of bacterial antibiotic susceptibility analysis is facilitated by a droplet-based flow cytometer, which operates by producing sizable droplets that encompass bacteria, reagents, and antibiotics. The droplets are subjected to incubation, and subsequently, images are acquired using a high-speed camera. These images are then identified utilizing a Machine Learning algorithm. The susceptibility of bacteria to various antibiotic concentrations is determined by the ratio between dead and living cells. In a laboratory setting, it is possible for these devices to be situated at a considerable distance from one another and establish communication over a wireless network. The primary sub-blocks of the droplet flow cytometer under consideration for the examination of bacterial antibiotic susceptibility are depicted in Fig. 8.
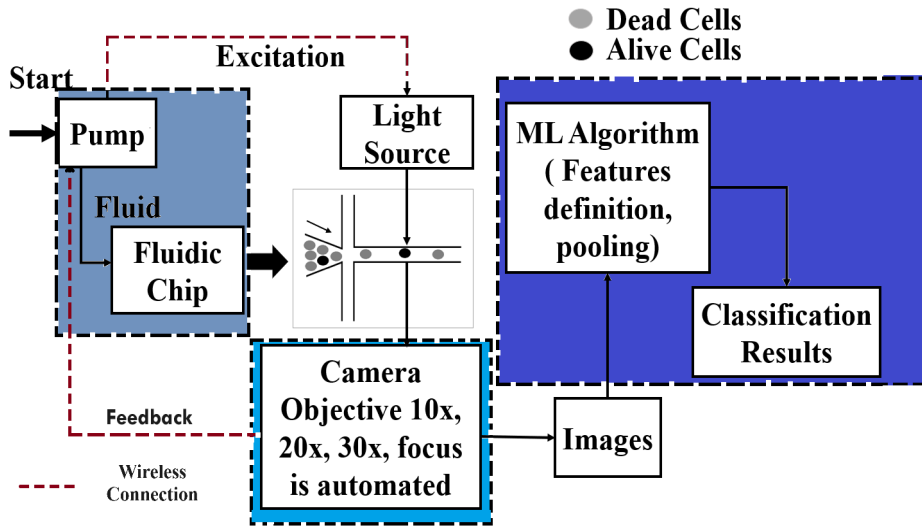
Figure 8: Use case: flow cytometer for antibiotic susceptibility of bacteria, where the main building blocks are the droplet generation unit (pump, fluidic chip), imaging unit/sensing unit (light source, camera), and detection unit (ML algorithm, classification results). Here control is applied to the fluid flow to create droplets of certain size while the output of the wireless camera provides a feedback to the pump for optimizing the parameters of the flow mechanism. The pump control unit also sends control instructions to the light source. The detection unit can be implemented on board with the sensing unit, or it could be remote (wirelessly connected).

The droplet flow cytometer system comprises three primary components: the Droplet Generation Unit, the Imaging Unit/Sensing Unit, and the Detection Unit. The control unit of each sub-block is connected to the central controller by a wireless communication network. The droplet production unit uses a pump for fluid volume regulation and a microfluidic chip for the purpose of initialization. The imaging unit usess a light source and a high-speed intelligent camera to acquire images at different

Automata	Definition	Rules
Hybrid Automata	**Definition 1** A hybrid automaton is a tuple H = (L, Var, g, Γ, Edge, Act, Inv, Init) where: $L \rightarrow$ Set of locations, States $\Sigma = L \times V$, V: set of all valuations v, where $v : Var \rightarrow \mathbb{R}$ $Var \rightarrow$ Real-Valued Variables, $L \rightarrow 2^{Var}$ $g \rightarrow$ Conditional/Guard function $\Gamma \rightarrow$ Set of Labels $Inv \rightarrow$ Invariant function, $Inv(l) \subseteq V, l \in L$ $Act \rightarrow$ functions consists of set of activities, $f : \mathbb{R}_{\geq 0} \rightarrow V$ $Edge \rightarrow$ Set of transitions, $Edge \subseteq L \times \Gamma \times g(Var) \times 2^{Var} \times L$ $Init \rightarrow$ Initial Location, $Init \subseteq L$	**Discrete Rule** The discrete rule governing transitions between states is written as $(l, v) \xrightarrow{a} (l', v')$ for $(l, a, (v, v'), l') \in Edge$ and invariant $v' \in Inv(l')$ must hold. On the other hand, the time rule governing the time can pass in the current location and the variable related to the location can evolve given that $f \in Act$ such that $f(0) = v, f(t) = v'$. **continuous time Rule** The continuous time rule is given by $(l, v) \xrightarrow{a} (l, v')$ for $f[(0,t)] \in Inv(l)$ and t is strictly positive.
Timed Automata	**Definition 2** A timed automaton is a tuple $T = (L, \Gamma, Edge, C, Inv, Init)$ where: $L \rightarrow$ Set of locations, States $\Sigma = L \times V$, V: set of all valuations v, where $v : Var \rightarrow \mathbb{R}$ $C \rightarrow$ Set of real-valued clocks $\Gamma \rightarrow$ Set of Labels $Inv \rightarrow$ function that assigns set of invariants to locations based on Clock Constraints (CC), $L \rightarrow CC(C)$ $Edge \rightarrow$ Set of transitions, $Edge \subseteq L \times CC(C) \times \Gamma \times 2^C \times L$ $Init \rightarrow$ Set of Initial States, $Init \subseteq L$	The semantics for timed-automata are given for the discrete rule and continuous rule: **Discrete Rule** $$(l, v) \xrightarrow{a} (l', v') : (l, a, (g, C), l') \in Edge$$ $$, v \models g, v' = reset(C) \quad v, v' \models Inv(l') \qquad (1)$$ where g is the guard. **continuous time Rule** $$(l, v) \xrightarrow{t} (l, v') : t \in \mathbb{R}_{\geq 0}, v' \models Inv(l), v' = v + t \qquad (2)$$
Parallel Composition	**Definition 3** The parallel timed automata composition $T_1 \parallel T_2 ... \parallel T_n$ of n systems such that $T_1 = (L_1, \Gamma_1, Edge_1, C_1, Inv_1, Init_1), T_2 = (L_2, \Gamma_2, Edge_2, C_2, Inv_2, Init_2), ..., T_n = (L_n, \Gamma_n, Edge_n, C_n, Inv_n, Init_n)$, and such that clocks and states are pairwise disjoint, is given by: • $L = L_1 \times L_2 \times ... \times L_n$ • $C = C_1 \times C_2 ... \times C_n$ • $\Gamma = \Gamma_1 \times \Gamma_2 ... \times \Gamma_n$ • $Inv(l_1, l_2) = Inv_1(l_1) \wedge Inv_2(l_2), ..., Inv(l_{n-1}, l_n) = Inv_{n-1}(l_{n-1}) \wedge Inv_n(l_n)$ for all $(l_1, l_2, ... l_n) \in L$ • $Init = \{((l_1, l_2, ... l_n), v) \in \Sigma | (l_1, v) \in Init_1 \wedge (l_2, v) \in Init_2, ... \wedge (l_n, v) \in Init_n\}$	**Rule Synch :** $$\frac{(l_i, a, (g_i, C_i), l_i') \in Edge_i, (l_{i+1}, a, (g_{i+1}, C_{i+1}), l_{i+1}') \in Edge_{i+1}}{((l_i, l_{i+1}), a, (g_i \wedge g_{i+1}, C_i \times C_{i+1}), (l_i', l_{i+1}')) \in Edge} \quad (3)$$ **Rule Non−Synch$_i$:** $$\frac{(l_i, a, (g, C), l_i') \in Edge_i, a \notin \Gamma_{i+1}}{((l_i, l_{i+1}), a, (g, C), (l_i', l_{i+1})) \in Edge_i} \quad (4)$$ **Rule Non−Synch$_{i+1}$:** $$\frac{(l_{i+1}, a, (g, C), l_{i+1}') \in Edge_{i+1}, a \notin \Gamma_i}{((l_i, l_{i+1}), a, (g, C), (l_i, l_{i+1}')) \in Edge} \quad (5)$$
Extended Timed Automata	**Definition 4** Extended timed automata is a tuple $T = (L, \Gamma, Edge, C, Var, Chan, Inv, Init, P)$ Where $L \rightarrow$ Set of locations, States $\Sigma = Loc \times V$, V: set of all valuations v, where $v : Var \rightarrow \mathbb{R}$ $C \rightarrow$ Set of real-valued clocks $Var \rightarrow$ Set of non-clock real-valued local variables $Chan \rightarrow$ Set of non-clock shared variables $\Gamma \rightarrow$ Set of Labels $Inv \rightarrow$ function that assigns a set of invariants to locations based on Clock Constraints (CC), local variables constraints $\Phi(Var)$ and set of shared channel variables $\varphi(Chan)$, $L \rightarrow CC(C) \wedge \Phi(Var) \wedge \varphi(Chan)$ $Edge \rightarrow$ Set of transitions, $Edge \subseteq L \times CC(C) \times \Phi(Var) \times \varphi(Chan) \times \Gamma \times 2^C \times 2^{Var} \times 2^{Chan} \times L$ $Init \rightarrow$ Set of Initial States, $Init \subseteq L$ $P \rightarrow$ Assigns user−defined exponential delay rate (e) to each location, $L \rightarrow e(P)$, The exponential rate P defines an exponential distribution to leave each state under unbounded delays.	Extended Timed Automata follow the same rules as Timed Automata's discrete and continuous rules.

Table 6: Definitions and Rules for Hybrid Automata, Timed Automata, Parallel Composition, and Extended Timed Automata

frame rates and resolutions. The detecting unit usess a microcontroller for the purpose of image classification through the utilization of machine learning methods, namely deep learning techniques including artificial neural networks. The central controller initiates the activation of individual sub-units in a predetermined sequence using a wireless communication network, and subsequently enters a state of sleep or low power consumption, until a trigger command is received. The scheduling of networks is based on priorities, where non-deterministic networks have a designated period for the reception and transmission of commands. The wireless control of these devices is represented using boolean variables, channels, and clock variables.

To ensure a system satisfies requirements like time restrictions, synchronization, and deadlocks, model verification is essential. The UPPAAL tool is used to verify and check systems under probabilistic, limited, and unbounded delay distributions. For simplicity and major focus of our work we have only discussed network unit in detail here. For network unit in droplet flow cytometer, the main states are: $DG\_sending$, $Im\_sending$, $DT\_sending$, $wait\_DG$, $wait\_Im$, $wait\_DT$, and ACK_DG, ACK_Im, ACK_DT. In addition to clocks, defined transmission variables (guards) like $tx1\_max$ ($DG\_sending$), $tx2\_max$ ($Im\_Sending$), and $tx3\_max$ ($DT\_Sending$) also impose bounds on the state transition in network unit. Based on exponential delay model for the network, Fig. 9 shows the UPPAAL based network model.
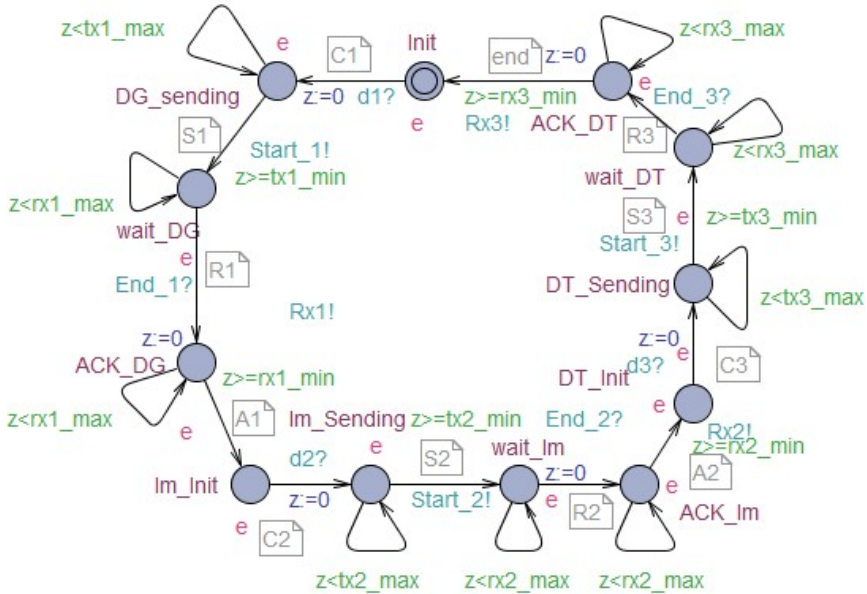
Figure 9: Network unit for droplet flow cytometer, where the main states are: $DG\_/Im\_/DT\_sending$, $wait\_DG/\_Im/\_DT$, and $ACK\_DG/\_Im/\_DT$.

In any system, the discrete probability option for every path might help in estimating the latency. For every path, a study of costs and reachability times could also be carried out. The formal verification demonstrated that the device operated in the correct sequence and at the appropriate time, and that the modeled use case did not violate any time constraints. Fig. 10 shows an example of the network model with discrete probabilities defined for delayed and non-delayed paths.

State transitions, probability density distributions, and probability comparisons of states at different intervals could all be validated with the query-based verification method as in table 7.
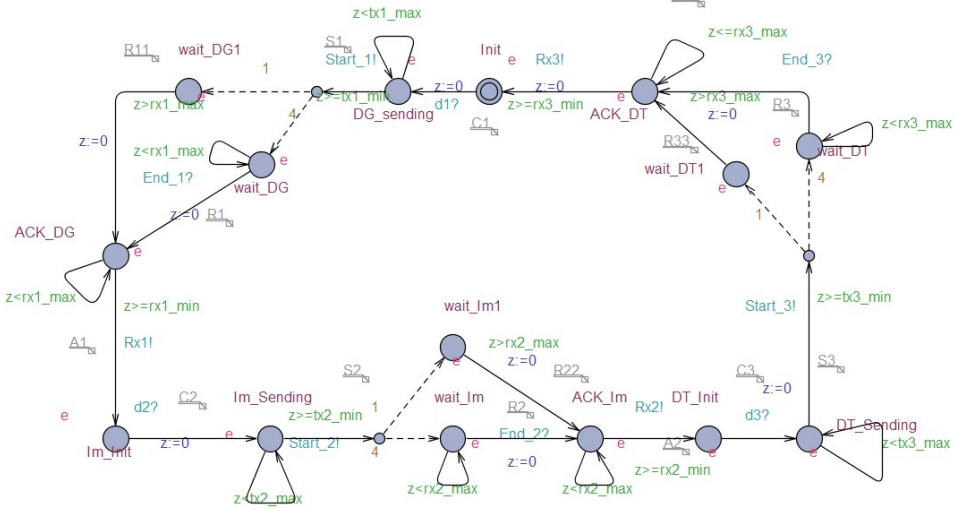
Figure 10: Network unit with discrete probabilistic non-delayed and delayed paths (1/4, 4/5)

Table 7: Verification Queries

Queries	Properties
$E <>$ *Communication.wait and* $z \geq tx1\_max$	Delay
$A[]!$(*Communication.Sending* $\&\&$ *Bio_Chip_control.Rate_Definition*)	Synchronization
$A[]$*Communication.wait imply* $z \geq tx1\_min$	Reset
simulate$[<= 300]$Network.ACK_DG, Control. *Droplet_Generation, Imaging.Process_D*2	Simulation
$Pr[=<100](<>$ Network.DG_sending$) >= Pr[<= 100]$	Probability
$(<>$ *Control.Imaging*$)$	Comparison

3.3 Scalability vs. Reliability and Key Results

By their very nature, CBPS are real-time distributed systems that rely on several devices interacting with one another in cooperative and competitive ways to maximize performance [122, 123]. This necessitates an analysis of the scalability and reliability of the network of these devices. As mentioned earlier we used UPPAAL stratego to model network architectures to make sure the system follows reliability requirements when scaling the network. In the context of the use case, we developed a model to represent the interaction between two systems.

This model considers three possible scenarios for information flow between the systems: centralized, decentralized, and network traffic aware (state able to decided the best information flow architecture under network load). Additionally, the model allows the system to make a decision between the centralized and decentralized approaches.

Expanding upon the concept of centralized and decentralized architecture, wherein a coordinator assumes the responsibility of overseeing all or a subset of nodes, it becomes possible to regulate the transmission of information across various nodes (see Fig. 7).

In both centralized and decentralized control, network traffic is an unmanageable variable. By incorporating knowledge of the traffic load into the system, we may effectively determine the most suitable approach for managing information flow in order to optimize the utilization of network resources while adhering to specified delay limitations.
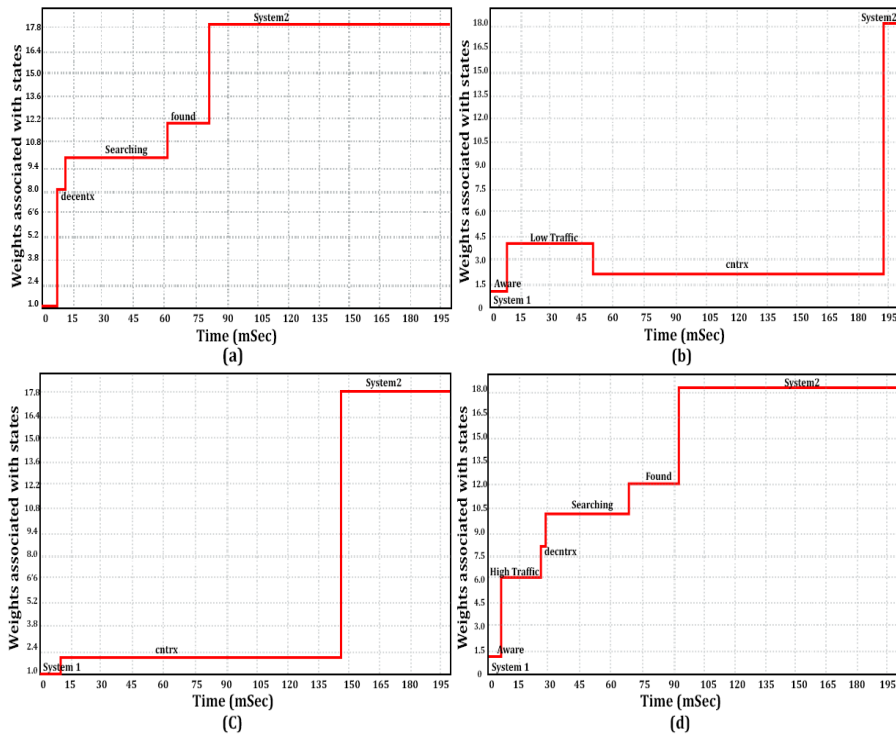
Figure 11: UPPAAL Strategies (a): Decentralized Information Flow (System1→decntrx→Searching→found→System2); (b): Traffic Aware Information Flow (System1→Aware→LowTraffic→cntrx→System2); (c): Centralized Information Flow (System1→cntrx→System2); (d): Traffic Aware Information Flow (System1→Aware→HighTraffic→decntrx→Searching→found→System2).

This study examined the selection of architectural design for facilitating the transmission of information between System 1 and System 2, considering both controlled and uncontrollable stages. The probability of achieving a delay that is less than $150ms$ is estimated to be 0.76, with a 95% confidence interval. The average bandwidth use is around 1700 kilobits per second (kbps) with a 95% confidence interval. The study examined four distinct approaches for selecting among decentralized, centralized, and traffic-aware communication methods.

The initial technique attempted to deal with delay constraints in order to mitigate instances of heavy network congestion and facilitate the transmission of information.

The second technique prioritized the reduction of transmission latency to a minimum.

The third technique successfully identified a compromise between minimizing latency through either decentralized or centralized design, while also mitigating the occurrence of heavy network traffic situations.

The fourth technique was designed to minimize the utilization of network resources, specifically bandwidth, while also minimizing delay, irrespective of the underlying network architecture.

The simulation findings indicate that the most appropriate approach for the utilized use case is to choose for a centralized design, as it ensures reduced delay and reliable communication. The average estimated bandwidth consumption is 960 kilobits per second (kbps), while the average delay estimate is 109 milliseconds (ms), both with a 95% confidence interval. The multi-system interaction example showed how this model can be utilized in Model-based System Engineering (MBSE).

3.4 Conclusion on Model-based System Architecture for Wireless Networked Control Systems

This study introduced a novel model-based system architecture for modeling bio-analytical cyber-physical systems (CPSs) with constraints, utilizing extended timed-automation, and incorporating wireless network communication; the novelty is in the utilization of a formal methodology (contrary to prior research that utilizes models focused in SysML or UML). A timed strategic methodology was used to provide a comprehensive assessment of the constraints related to latency and bandwidth. The primary objective was to provide and demonstrate a formal model-based architecture for bio-analytical devices, with the longer-term aim of promoting the adoption of formal techniques in the field of bio-analytical devices in subsequent research efforts.

In order to illustrate the practical implementation of the suggested methodology, a use case was studied, simulated, and validated using the UPPAAL tool. The scope of the study was expanded to include multi-system interaction through the utilization of timed stochastic automata, which were assessed using UPPAAL Stratego. The findings indicate that the centralized communication architecture yielded a minimum delay of 129 ms from system1 to system2. In contrast, the decentralized architecture resulted in a lower delay of 87 ms. Additionally, when high-traffic circumstances were circumvented, the delay was reduced to 125 ms.

This chapter focused on the performance of centralized and decentralized communication architectures, and it was and found that the decentralized one had lower delay under normal and high-traffic conditions. The next chapter deals with how network uncertainties affect the control performance and the complexity of the optimization problem stemming from the complex nature of the wireless network.

4 Optimal Control under Network Uncertainties using Machine Learning

This chapter discusses the network uncertainties affecting the control performance and the complexity of the optimization problem due to the complex nature of the wireless network. The chapter is based on the following publication:

Publication 3: K. Ashraf, Y. Le Moullec, T. Pardy and T. Rang, Joint Optimization via Deep Reinforcement Learning in Wireless Networked Controlled Systems, IEEE ACCESS, 2022.

The reader is encouraged to look at the above paper (provided in appendix) for additional details and results.

This chapter highlights the key elements from the above publication, namely:

- The comprehensive analysis of the current obstacles encountered in the design of efficient WNCSs and explores the potential of DRL in mitigating these challenges.

- The novel co-design methodology that improves the system's overall performance by effectively resolving network uncertainties such as latency and fluctuating throughput, thereby enabling the system to achieve optimal control performance.

- The in-depth examination of how DRL algorithms may effectively optimize the trade-off between communication resources and control performance in WNCS.

The novelty of this contribution is in the DRL-based co-design approach for joint-optimization of WNCS; unlike traditional control methods that requires a-prior knowledge of the systems dynamics, the model-free approach can adapt to stochastic behavior applications.

Fig. 12 provides a graphical abstract of the contribution on optimal control under network uncertainties using machine learning. The key elements of the figure are discussed below and/or in Publication III.

The objective of the work is to evaluate the advantages of employing model-free reinforcement learning (RL) in stochastic systems, in comparison to both traditional and contemporary control techniques. The problem is expanded to encompass the application of droplet creation utilizing a stepper motor (inside each of the pumps, while all four pumps are working at the same time), and the resolution is assessed within the context of three distinct network scenarios (as shown in the left hand side of Fig. 12).

Simulation of network uncertainty is conducted, and a comparative analysis of several RL techniques is performed. The utilization of a deep Q-learning algorithm is used in order to address and minimize overestimation errors. The efficacy and effectiveness of these approaches are then assessed and compared to alternative model-free reinforcement learning algorithms.

The C51 reinforcement learning algorithm incorporates an experience replay buffer, serving as an intermediary approach between offline and online algorithms. This inclusion facilitates accelerated convergence in comparison to the DQN and DDQN algorithms. The evaluation of RL algorithms entails the examination of several measures, including average reward, convergence speed, and stability.

Furthermore, an examination is conducted to assess the influence of various network characteristics and configurations on the performance of the algorithms, with the aim of acquiring a more profound comprehension of their efficacy in practical situations.
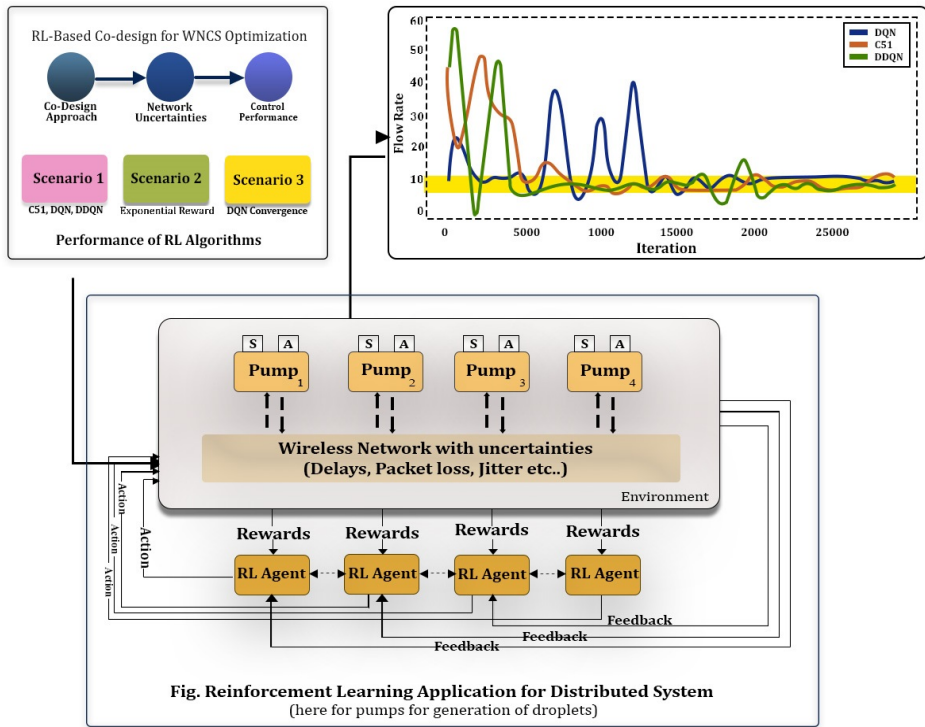
Figure 12: Graphical abstract of the contribution on optimal control under network uncertainties using RL

Moreover, the C51 algorithm integrates a distributional methodology, enabling a more precise depiction of the uncertainty associated with the estimation of values. This phenomenon has the potential to enhance the investigation and use of the surrounding environment, hence yielding superior performance in comparison to conventional Q-learning algorithms. Achieving the ideal equilibrium between observation size and performance is crucial in order to effectively use the advantages offered by the C51 algorithm.

The application of predictive control to any given system is commonly perceived as an optimization problem, wherein the objective is to solve for an optimal control strategy over a specified control horizon, taking into account the dynamics of the system. In contrast, RL is predicated upon the interaction between one or more agents and an environment. The primary objective of RL is for the agent to learn the policy by leveraging input from the environment. This knowledge acquisition process is achieved through a combination of exploration and exploitation strategies, with the ultimate aim of solving an optimization issue [124].

Table 8 presents a concise comparison between RL (both model-based and model-free), Model Predictive Control (MPC), and Linear Quadratic Regulator (LQR). MPC has been shown to exhibit similar performance to RL algorithms in the context of convex problems ([125]). However, in the case of WNCS, where the network problem may possess non-deterministic or non-convex characteristics, MPC control is not capable of efficiently solving the problem ([126]; also refer to Table 8).

Table 8: Comparison of RL vs. Contemporary Control Methods

Methods	Complexity	Adaptability	Problem Convexity	Model Requirement	Robustness	Convergence Time	High-dimensional data handling
Reinforcement Learning (Model-based)	Low (Online), High (Offline) [127, 128]	High [129, 130]	Not required [130]	Yes [130]	Low [131, 130]	Low-to-Medium[1] [127]	Good [132]
Reinforcement Learning (Model-free)	Low (Online), High (Offline) [127, 128]	High [129, 130]	Not required [130]	No [130]	Low [131, 130]	Low-to-Medium[1] [127]	Good [132]
Model Predictive Control (MPC)	High (Online), Low (Offline) [127, 128]	Low [130]	Required [130]	Yes [130]	High [130]	Medium-to-High[1] [127]	Moderate [132]
Linear Quadratic Regulator (LQR)	Low [133]	Low [134]	Required[2] [135]	Yes	Moderate [134]	Low[3] [136]	Moderate

[1] Depends upon dimensional complexity
[2] RL can help handling model-free cases
[3] Linear Convergence

4.1 Model-free Value-based vs. Policy-based RL Algorithms

In the field of RL, an agent acquires knowledge of the policy or valuation function by considering the dynamics of the system. This entails either being provided with a model of the environment or learning the model via the use of available data or actual implementation [137, 138, 139]. RL methods can be categorized as either model-based or model-free. Model-free algorithms can play a significant role in real-world scenarios when the system model is absent or where it is not feasible to provide a proof for a particular action. The model-free RL algorithms may be further categorized into policy-based or value-based learning strategies ([140],[141]).

For example, in the context of autonomous driving, the precise modeling of intricate dynamics inherent in real-world traffic settings poses a significant challenge. In instances of this nature, model-free reinforcement learning (RL) algorithms may be used to acquire optimum policies by direct learning from trial and error experiences. This enables the vehicle to travel in a secure and efficient manner, without dependence on a pre-established system model.

Table 9 shows the major comparison between Policy-based, value-based and hybrid RL algorithms in terms of function, key algorithms, strenghts, drawbacks and examples.

In this work, our main focus was to highlight the use of value-based model-free algorithms in WNCSs. The algorithms chosen in this work are extensions of simple Q-learning algorithms, specifically DQN, DDQN and C51 also known as categorical DQN. The only difference between simple Q-learning and DQN [142] is that the agent in DQN is based on neural networks rather than a simple Q-table. Although providing only the bounds or rules for the environment should be sufficient for these algorithms, we evaluated them to observe their responses when subjected to deterministic data.

Characteristics	Policy-based RL	Value-based RL	Hybrid RL
Function	Policy optimization [143]	Value-function estimation [143]	hybrid (Policy based optimization using a value function or vice versa) [144, 145]
Key Algorithms	REINFORCE, PPO,TRPO,A2C, DDPG [146]	DQN, DDQN, C51, Q-Learning, Dueling DQN, SARSA [146]	Hy-Q [147], TASAC [148]
Strengths	Continuous Action Space, Stochastic and Non-Differentiable Policies	Discrete Actions, High-Dimensional State Spaces	Improved Stability, Sample Efficiency, handling both continuous and discrete space [149]
Drawbacks	Frequently Require Extensive Computation, Vulnerable to Local Optimally, and Sensitive to Initial Policies	Difficulties with Continuous Actions, High Learning Variability, May Lead to Sub-optimal Policies	Complexity, Computational Resources, Local Optima, limited Interpret-ability
Examples	Autonomous Driving [150]	Chess, Clinics [151]	Robotics and Autonomous Control [149] , Natural Language Processing (NLP)

Table 9: Policy vs. Value-based & Hybrid Model-free Algorithms (Items without references: knowledge consolidated from multiple sources)

4.2 Proposed Co-Design Methodology for Control Performance under Network Uncertainties

The system under consideration is a centralized, distributed event-triggered system that operates across a shared communication network. This system is susceptible to many uncertainties in the network, such as random delays, variable sampling time, packet losses, and packet reordering. The primary aim of the designed learning algorithm is to mitigate control errors and additional disturbances while taking into account network disturbances, with the ultimate goal of achieving optimal control performance by closely following the reference trajectory. The goal is to maximize Quality of Service (QoS) and Quality of Control (QoC), which is achieved by minimizing synchronization and control errors, and is expressed as follows:

$$max(QoS \ and \ QoC)$$

Which is based on minimization of control errors e_c^i and noise $w(t)$ for i^{th} system.

$$minf(e_c^i, w(t))$$

The cost function for Mean-square control error is given by:

$$J_c^e = \mathbb{E}[\sum_{j=1,i\neq j}^{N} (y_r(t) - y_i(t))^T (y_r(t) - y_i(t))] \tag{6}$$

where $y_r(t)$ is the reference output (or set point). Based on constraints and optimization goal, the overall objective with the constraints is given as below:

$$\min_{\substack{d_q,d_p,d_t \\ C_{max},j=1,N,i\neq j}} (\mathbb{E}[\sum_{j=1,i\neq j}^{N} (y_r(t) - y_i(t))^T (y_r(t) - y_i(t))]) \tag{7}$$

$$\text{s.t. } d_t + d_p + d_q \leq D_{max} \tag{7a}$$

$$\sum_{i=1}^{N} B_i \ log_2(1 + \frac{P_t}{B_i\sigma^2} z_t) \leq C_{max} \tag{7b}$$

$$N \leq N_{max} \tag{7c}$$

$$\delta(\sigma_i) \geq 0, \delta(\sigma_i) \in \{0,1\} \tag{7d}$$

$$\mathbb{E}[\vartheta)] + e^s \leq \varepsilon_{max} \tag{7e}$$

$$\mathbb{E}[\vartheta] \leq \gamma c; c = \varepsilon\frac{n-1}{n+1} \tag{7f}$$

$$e^s = \mathbb{E}[\sum_{j=1,i\neq j}^{N} K_{ij}(y_j(t) - y_i(t))] \tag{7g}$$

The overall delay reduction in a WNCS ensures stability by reducing the sum of transmission, processing, and queuing delays, which are random and can be modeled as Markov chains (constrained by Equation 7a). An inverse correlation may be observed between the transmission delay and the effective bandwidth of a network, which ultimately imposes a limitation on the queuing delay. However, in the context of non-deterministic networks, it may not be necessary to utilize delay models that specify an upper limit on the end-to-end delay and channel capacity through the independent adjustment of various delay factors. To gain a more comprehensive understanding of the correlation between latency and the number of devices, the use of the co-design strategy provides optimum control performance within the limitations of wireless networks when contrasted with the interactive design approach. The issue is defined within the framework of traditional optimization theory and exhibits a significant degree of non-determinism, characterized by an uncertain quantity of devices.

The proposed approach entails the computation of the upper limit of devices that can be accommodated within the constraints of channel capacity, delays, and errors (synchronization). A reward is assigned as a function of the output response in order to attain optimal control performance. In order to guarantee dependability, it is imperative to adhere to the channel capacity limitation, which imposes a restriction on the maximum quantity of devices engaged in communication. The restrictions labeled as Equations 7a, 7b, and 7c are presumed to adhere to an upper limit of reliability denoted as κ_{opt}. This ensures that the system achieves the lowest possible latency and errors while operating within the limitations imposed by the channel capacity.

The restriction denoted by Equation 7g is applicable in the context of multi-agent interaction. In order to streamline the problem to a single agent scenario, we have omitted the constraint from Equation 7g.

4.2.1 Proposed Algorithm, Simulation and Results

In order to accurately assess the performance in a realistic setting, we acquired the network and control settings for the pump utilized in our laboratory, shown in Fig. 13.
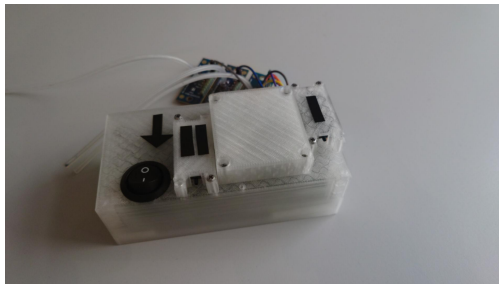
Figure 13: Our compact, portable, dual−channel piezoelectric pressure generator (i.e. pump) for droplet microfluidics application. Note that this is a complete wireless control system unit integrating sensing, actuation, and control.

The details of the setup are provided in Publication 3. The objective of the network simulations was to ascertain the End-to-End (E2E) latency for control and background traffic applications. The network was emulated utilizing the 802.11e standard ([152]), with Quality of Service (QoS) service both enabled and deactivated. The Media Access Control (MAC) uses a prioritized distributed channel access mechanism to minimize delay in applications that are sensitive to delay. The network setup included several components, including controllers, servers, configurators, access points, and radio media. The proposed approach, see **Algorithm 1**, summarizes the method used to solve the problem.

Three different scenarios were used to achieve the RL control of a pump in the presence of network uncertainty. In Scenario 1, OMNet++ was used to simulate network uncertainties, i.e. delay and bandwidth utilization. Binary search was used to estimate the optimal number of devices to meet latency and bandwidth restrictions for reliable performance. Scenario 2 utilized OMNET++ latency and network statistics as control factors in the RL environment design and dynamic parameters in the reward function to maximize algorithm performance during network uncertainty. In Scenario 3, network uncertainties were random variables in the RL reward function. Finally, convergence was used to compare the DQN, DDQN, C51, and Long Short-Term Memory (LSTM) RL algorithms (Table 10).

To reduce complexity, it was assumed that the agents operate independently, and the problem was solved for a single agent interacting with an environment containing other agents. The reward function was modified to incorporate the impact of latency and bandwidth usage by introducing a reliability component, denoted ρ that was assigned a probability value ranging from 0 to 1. The agent was trained using three algorithms: DQN, DDQN, and C51 and the results were compared. The C51 algorithm demonstrated superior performance, exhibiting greater stability in average returns. The results indicated that the C51 algorithm exhibited superior performance compared to both DDQN and DQN with linear rewards. In the context of random network scenarios, it was shown that both C51 and DDQN exhibited favorable performance; however, DQN failed to converge. This implies that the DQN may not be ideal for situations with significant network traffic, despite its good performance in terms of average reward when applied to a single agent.

Algorithms	Covariance	Pearson's Correlation	Spearman's Correlation
Test Data Input([10,6,6,10,6,10,6,6,6,6,10,6,6,6,10,6,6,6,6,6,6,5,6,6,6,8,6,6,6])			
DQN (Scenario1)	0.39	0.05	0.076
DQN (Scenario2)	-3.69	-0.19	-0.17
DQN (Scenario3)	0.12	0.008	-0.03
DDQN (Scenario1)	0.59	0.02	0.07
DDQN (Scenario2)	-0.57	-0.03	0.43
DDQN (Scenario3)	1.80	0.1	0.04
C51 (Scenario2)	8.49	0.61	0.45
C51 (Scenario1)	1.73	0.26	-0.07
C51 (Scenario3)	-0.4	-0.91	-0.09
Test Data Input ([10,6,6,10,6,10,6,6,8,6,10,6,6,6,10,6,6,6,8,9,10,10,8,10,6,10,8,6,10,6])			
DQN (Scenario1)	-0.22	-0.02	0.19
DQN (Scenario2)	-6.5	-0.29	0.03
DQN (Scenario3)	1.47	0.08	0.04
DDQN (Scenario1)	3.07	0.11	0.20
DDQN (Scenario2)	1.32	0.06	0.20
DDQN (Scenario3)	4.38	0.21	0.20
C51 (Scenario1)	-0.8	-0.61	-0.11
C51 (Scenario2)	6.04	0.36	0.39
C51 (Scenario3)	0.11	0.04	0.04
LSTM with RNN with OMNet++ Simulation Data			
LSTM (Prediction on Test Data)	0.031	0.22	-0.35

Table 10: Performance Evaluation of Reinforcement Learning Algorithms Results

---

Algorithm 1 Proposed Algorithm to solve the co-design problem

---

Require: End to End Delay, $d^p, d^t, d^q, N, B_{max}$,
  bit-rate, power, sensitivity, Signal-to-Noise Ratio
  (SNIR) threshold and trigger coefficient
Ensure: $\min(J_c^e)$
  $N \leftarrow n$
  Step1: Determine Channel capacity for each user
  Step2: Determine Delay for each user
  Step3: Determine maximum number of allowable Users
  while $N \leq N_{max}$ and $C \leq C_{max}$ **do**
    if $y_{ref} - y_i$ is positive **then**
      $r \Leftarrow r + 1$
      $y_{ref} \Leftarrow y_i$ ▷ Dynamic Reference Change
    else if $y_{ref} - y_i$ is negative **then**
      $r \Leftarrow r - 1$
    else if $y_{ref} - y_i$ is zero **then**
      $y_{ref} \Leftarrow y_i$
    end if
  end while

The flow rate variation achieved after 30000 iterations, using network simulations in the reward function, is depicted in Fig. 14; the data presented in this figure clearly demonstrates that the DQN algorithm (blue curve) requires more time to reach a stable response in terms of flow rate (at approximately 14000 iterations). In contrast, both the DDQN (green curve) and C51 (orange curve) algorithms exhibit relatively faster attainments of a stable responses (at approximately 4500 and 7000 iterations, respectively). However, C51 maintains the stability and DDQN shows some minor unstable behavior at later iterations.
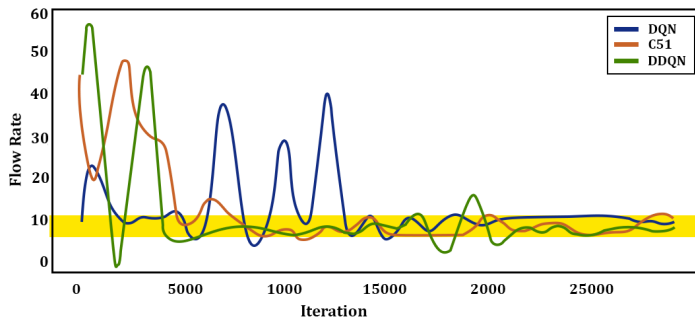
Figure 14: Flow rate prediction under network constraints using OMNet++ network simulation data. The yellow line highlights the convergence of the methods.

The goal was to optimize mean-square error over the time for the flow rate. The settling time is observed for different algorithms where Process Variable (PV) reaches the Setting Point (SP). An additional viewpoint to consider is to the analysis of the function played by the experience replay buffer. The performance of the C51 method was evaluated in Scenario 2, employing various batch sizes for the retention of past observations. Increasing batch size increases early average rewards, whereas decreasing batch size decreases cumulative rewards. The simulation findings indicate that C51 has outstanding results even in the presence of random network circumstances, hence confirming the reliability of employing model-free reinforcement learning (RL) methodologies. The scalability of a system is limited by network restrictions, and the inclusion of network effects in reward functions aids in the acquisition of knowledge about dynamic network circumstances.

4.3 Conclusion on Optimal Control under Network Uncertainties using Machine Learning

The study summarized in this chapter primarily focused on the novel co-design approach for the joint-optimization of wireless networked controlled systems, employing model-free RL. In contrast to traditional control methods that rely on a-priori knowledge of the systems dynamics, model-free RL can adapt to stochastic behavior applications; the emphasis was on the significance of wireless network restrictions, in conjunction with control system constraints, in order to get an optimal level of system performance. The study extensively examined several facets of the issue within the framework of optimization theory and presented a compelling case for the adoption of RL over traditional and robust control approaches, highlighting several motivating

considerations. The theory was applied in a practical scenario where a double emulsion droplet creation unit was utilized as a use case. To accomplish control performance under defined restrictions, the DQN, DDQN, and C51 algorithms were used. The algorithm C51 demonstrated superior performance compared to other algorithms, mostly attributed to its ability to effectively solve multi-modal problems.

The findings also demonstrated the significance of the reward function in influencing the learning process of the agent. It was observed that meticulous design of the reward function has the potential to enhance the agent's performance. As of now, our research does not address the dependability concerns arising from the implementation of event-triggered control in order to enhance efficiency. The objective in future research is to investigate a compromise between enhanced performance and reliability in diverse network circumstances through the utilization of hybrid control methodologies. Furthermore, the investigation of power limits has not been thoroughly examined and remains an area for future research.

In this chapter, the focus was on optimal control under network uncertainties by means of RL using value-based algorithms and their comparison with traditional optimization methods. In the next chapter, the focus is placed on optimal resource consumption in WNCSs and how ML compares with traditional resource allocation methods.

5 Optimal Resource Consumption in Wireless Networked Control Systems using Machine Learning

This chapter is based on the following paper:

Future Publication IV: K. Ashraf, Y. Le Moullec, T. Pardy and T. Rang, "Co-Design of a Wireless Networked Control System for Reliability and Resource-Efficiency", under revision, to be re-submitted.

The reader is encouraged to look at the above paper (provided in appendix) for additional details and results.

This chapter discusses the importance of optimal resource consumption in wireless networked controlled systems and the role ML plays as compared to traditional resource allocation methods. The novelty is in the optimization of the the the inter-packet gap (IPG) on the wireless communication layer which makes the system more resource-efficient via policy switching (from reliable time-triggered control to either energy-efficient time-triggered control or event-triggered control).

5.1 Traditional Resource Allocation Methods

Optimal resource consumption is a critical factor to benchmark the performance of WNCSs. For a system to perform certain control tasks while maintaining a specified QoS the division or allocation of transmit power is a challenging task. The amount of power available to the device affects both device performance and battery life. In traditional power resource allocation methods, the power allocation among devices is based on either a constant, proportional, or max-min fairness policy. In these policies, the aim is to make sure the devices meet the minimum requirement for control and communication while consuming the complete available power resources.

Other resource allocation methods such as the water-fall algorithm are still used in practice to optimize power allocation in 5G channels due to their simplicity [153]. Traditional approaches also give us competition-based resource allocation as in game theory approaches [154]. The QoS-based optimization techniques, such as dynamic programming, search algorithms, genetic algorithms, and particle swarm optimization [155], aim to find an optimal resource allocation strategy that balances multiple factors, such as data rates, latency, reliability, and power consumption, to deliver the desired QoS levels.

These techniques typically adhere to a rule-based methodology [156] that may not be adaptable to extremely dynamic environments. These algorithms may not generalize well, and their actions are deterministic, which means they are based on predefined rules and the current state, and do not learn from previous experiences. These algorithms usually require a model of the system which is not an easy task to achieve in case of complex systems.

5.2 Reinforcement Learning based Resource Allocation Methods

RL algorithms acquire knowledge through interaction with the environment and experience. Through trial and error based on the rewards or penalties they receive for their actions, they determine the optimal resource allocation strategies. RL algorithms are highly generalizable and adaptable to a wide variety of network scenarios [157]. They

continuously update their policies based on new experiences, adapting them to environments that are constantly changing and dynamic. RL algorithms can be model-free (learning directly from experiences) or model-based (learning from an environment model). Model-free RL is more prevalent in complex or inadequately understood environments.

In complex and dynamic wireless networked systems where the optimal resource allocation strategy may not be known in advance, RL algorithms are ideally suited due to their ability to learn from experience, adapt through interactions, and generalize. The efficient power consumption in control system design as well as in wireless network design has been an important challenge since their beginning. As wireless communication technologies have been upgrading, the increasing complexity [158, 159] of these systems requires more adaptive and efficient resource allocation methods [160].

To achieve optimal performance, this Ph.D. thesis suggests that WNCSs can benefit from a co-design strategy based on reinforcement learning (RL) that simultaneously optimizes both network and control parameters. In particular, it is proposed that by optimizing the IPG on the wireless communication layer, it is possible to make the system more resource-efficient by allowing for a switch from a reliable time-triggered control policy to either an energy-efficient time-triggered control policy or an event-triggered control policy.

What follows presents the control of an inverted pendulum as an example.

5.2.1 Inverted Pendulum Control using RL-based Resource-Efficient Techniques over Wireless Networks

We use the control of an inverted pendulum to demonstrate the control of a system over a wireless network (industrial robotic mechanism using an inverted pendulum control system with tendons and a wireless network), as illustrated in Fig. 15.
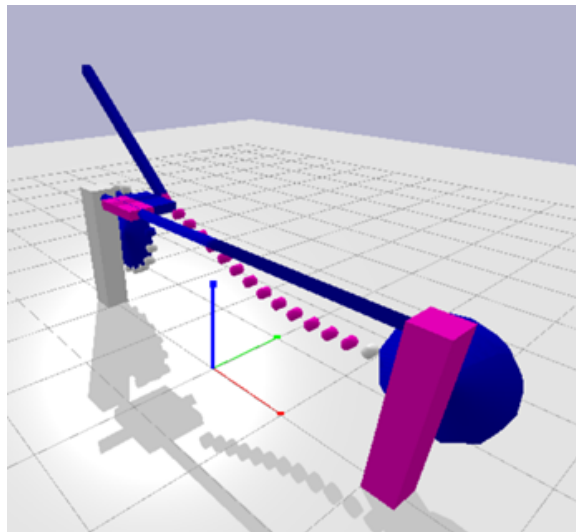
Figure 15: Inverted pendulum control via tendons using (Render Environment)

Such a control implementation is a paradigmatic instance of non-linear control. In addition, a simple pendulum control model can be simplified to a linear model for smaller variations, despite the non-linear relationship between gravity and angular

position. It is impossible to linearize the model of an inverted pendulum because of the intricate interaction between the rotational velocity and the applied force [161]. The concept of this example of an optimal resource consumption in WNCSs using ML is shown in Fig. 16.

We find that inverted pendulum control is particularly well-suited to our purposes because even the smallest uncertainties introduced by a wireless network would severely degrade the control performance, making it extremely challenging to achieve control stability if adequate precautions are not taken.
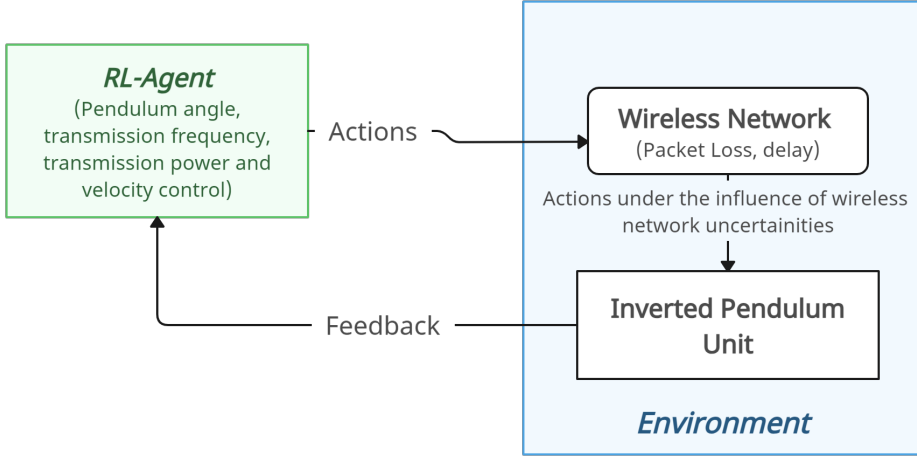
Figure 16: Illustration of the concept

An analytical formulation of the problem was performed as a first step in the analysis and solution of the problem in both the theoretical and simulation dimensions. The defined problem was then implemented in a simulation setting where the proposed RL-based technique was utilized to assess how the network limitations affected the performance of a tendon-controlled inverted pendulum.

Consequently, the Max-Min optimization theory was used to formulate the objective of reaching a trade-off between reliability and resource efficiency within acceptable performance limits. To maximize reliability, the control error should be the minimum possible, although, on the control side, this depends on the control methodology used. However, in a networked controlled system, the packet loss (p) and the packet error rate (per) would also significantly affect reliability. The Max-Min problem for joint optimization of reliability (γ_{cc}) and resource efficiency (r_{cons}) for both the control and communication side is formulated as below:

$$Q_{opt_{obj}} = max(\gamma_{cc}) + min(r_{cons}) \tag{8a}$$

$$max(\gamma_{rel}) = min \sum_{i=1}^{n}(y_{ref} - yi) + min \sum_{i=1}^{n} p_L^* \tag{8b}$$

$$min(r_{cons}) = min \sum_{i=1}^{n} P_{cons} \tag{8c}$$

$$\text{s.t.} \quad d_{overall} \le d_{max} \tag{8d}$$

$$per \le per^* \tag{8e}$$
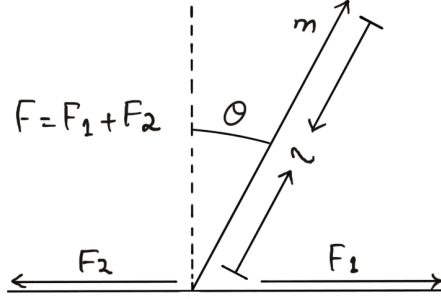
Figure 17: Illustration of the Motion of an Inverted Pendulum

The power consumed (P_{cons}) is a function of information transmission frequency (i_{tf}) and the power used to transmit it (P_t), so Equation 10 can be written as:

$$P_{cons} = f(i_{tf}, P_t) \tag{9}$$

Additionally,

$$i_{tf} = f(C_{meth}, IPG, N) \tag{10}$$

where C_{meth} denotes event-triggered or time-triggered control, IPG indicates inter-packet gap, and N represents devices. The greater the delay between packets, the more efficiently the system uses its resources; however, the receiver system may start to assume packet loss after a certain time period if the delay goes above certain threshold. Furthermore, the network may get congested if packets are transmitted too quickly (lower inter-packet interval), leading to increased delays, resource use, and dependability. We postulate that there must be a way to regulate the system to compensate for packet loss and delays between individual packets in order to maximize efficiency. From Lagrange's equation of motion, we can construct the two equations of motion for the inverted pendulum shown in Fig. 17. The reaction force (N) [162] acting on the free body diagram of the inverted pendulum can be derived as:

$$N = m\ddot{x} + ml\ddot{\theta}\cos\theta - ml\dot{\theta}^2\sin(\theta) \tag{11}$$

where l is the length of the pendulum, m is its mass, $theta$ is its vertical angle, and x is its current location. Calculating the total perpendicular forces is required to determine the second equation of motion of this system. Resolving the system along this axis greatly simplifies the underlying mathematics. The equation obtained should be as follows:

$$(I + ml^2)\ddot{\theta} + mgl\sin\theta = -ml\ddot{x}\sin\theta \tag{12}$$

where I is the moment of inertia of the pendulum.

5.2.2 Proposed Algorithm, Simulation & Results
Two distinct algorithms were formulated with the objective of facilitating the training of RL agents. Each respective strategy was purposefully developed to address the impact of network effects on both actions and states. The current methodology aims to assess the possible ramifications of network uncertainty on the behaviors and states of agents, acknowledging that the unpredictability of networks might have a significant influence on several aspects of the learning process. The inclusion of uncertainty in the

decision-making process of the agent holds the potential to augment the overall results of the learning process.

Algorithm 2

The algorithm 2 (corresponding to Algorithm 1 in Future Publication IV) explores the following criteria in the training process:

- The benefits of incorporating uncertainty in decision-making for an agent's learning process

- Exploring the role of uncertainty in improving the adaptability and flexibility of an agent's actions.

- Investigating how uncertainty can lead to more robust and resilient learning outcomes for agents.

- Examining the challenges associated with implementing uncertainty-based decision-making in intelligent systems.

- Discussing potential applications and implications of incorporating uncertainty into the learning process of AI agents across various domains.

Algorithm 3

In contrast, Algorithm 3 (corresponding to Algorithm 2 in Future Publication IV) takes a more conservative track, with the goal of avoiding the introduction of new options under bad channel circumstances and safeguarding the current state in the case of network failure. This broad variety of options is especially important for managing devices over wireless networks.

The difficulty of wireless communication can be proactively addressed by including perturbations in the state to accommodate for missing or delayed inputs (Algorithm 3). The fundamental goal of this strategic choice is to improve the agent's ability to adapt and perform well in situations when changes in network dynamics may present difficulties in maintaining smooth control. This probability distribution ensures that the time intervals between consecutive packets are evenly distributed. By utilizing a uniformly distributed inter-packet gap probability, the simulation accurately represents real-world wireless channel behavior.

The study uses a Python-based gym library to simulate an industrial robotic mechanism using an inverted pendulum control system with tendons and a wireless network. The control side uses Proximal Policy Optimization (PPO) for stability and handling continuous state spaces. The wireless channel function simulates packet loss, delay, and transmission gaps, achieving desired stability in congestion and resource-efficient techniques. The control-communication reliability is calculated over 100 episodes, and the reward is calculated over 1000 iterations/steps. The proposed approach is compared to PID control, highlighting the importance of RL for optimal performance in a wireless network.

Algorithm 2 Proposed algorithm to solve the co-design problem with network uncertainties introduced in actions

---

Require: End to End Delay, d^p, d^t, d^q, N, t (transmission frequency), power consumption (transmission), Signal-to-Noise Ratio, action with max reward (a_{rmax}), the minimum required power to transmit P_{min}, previous state $state_{next}$ (velocity, angle), current state $state$, reward as a result of agent's current action $reward_{step}$, agent's action during learning a_{step}, delay introduced due to inter-packet gap (d_{IPG}), state corresponding to action leading to max reward ($state_{a_{max}}$), packet loss (p_L)
Ensure: $max(\gamma_{cc}) + min(r_{cons})$
   $N \leftarrow n$
   while $per \leq per^*$ and $d_{overall} \leq d_{max}$ and $i \leq$ max_iterations **do**
      $i+=i$
      if $i\%t = 0$ **then**
         $IPG \leftarrow$ True or $P_L \leftarrow$ True
         $P_t \leftarrow P_{min}$
         $state \leftarrow state_{a_{rmax}}$
         $reward \leftarrow reward_{max} \mapsto a_{rmax}$
         $d_{overall} += d_{IPG}$
      else
         $IPG \leftarrow$ False and $P_L \leftarrow$ False
         $P_t \leftarrow P_{max}$
         $state_{next} \leftarrow state$
         $reward \leftarrow reward_{step} \mapsto a_{step}$
      end if
      if p_L or IPG **then**
         $r_{total} += reward_{prev}$
      end if
      if $!p\_L$ and $!IPG$ **then**
         $r_{total} += reward$
         $reward_{prev} \leftarrow reward$
      end if
   end while

Algorithm 3 Proposed algorithm to solve the co-design problem with network uncertainties introduced in Agent's state

---

Require: End to End Delay, d^p, d^t, d^q, N, t (transmission frequency), power consumption (transmission), Signal-to-Noise Ratio, action with max reward (a_{rmax}), the minimum required power to transmit P_{min}, previous state $state_{next}$ (velocity, angle), current state $state$, reward as a result of agent's current action $reward_{step}$, agent's action during learning a_{step}, total reward r_{total}, previous reward $reward_{prev}$, packet loss (p_L), delay introduced due to inter-packet gap (d_{IPG})

Ensure: $max(\gamma_{cc}) + min(r_{cons})$

    $N \leftarrow n$

    while $per \leq per^*$ and $d_{overall} \leq d_{max}$ and $i \leq$ max_iterations **do**

        i+=i

        if $i\%t = 0$ **then**

            $IPG \leftarrow$ True or $P_L \leftarrow$ True

            $P_t \leftarrow P_{min}$

            $state \leftarrow state_{prev}$

            $reward \leftarrow -1$

            $d_{overall} += d_{IPG}$

        else

            $IPG \leftarrow$ False and $P_L \leftarrow$ False

            $P_t \leftarrow P_{max}$

            $state_{next} \leftarrow state$

            $reward \leftarrow reward_{step} \mapsto a_{step}$

        end if

        if p_L or IPG **then**

            $r_{total} += reward_{prev}$

        end if

        if $!p\_L$ and $! IPG$ **then**

            $r_{total} += reward$

            $reward_{prev} \leftarrow reward$

        end if

    end while

5.2.3 Results

The results demonstrated that the PID-based control of the pendulum did not stabilize when subjected to packet loss, even though the previous control input was maintained to enhance stability. The simulation included network dependability characteristics such as packet loss, packet error rate, and delay to model uncertainties in wireless networks. The control input was relayed across a network experiencing a 15% packet loss rate. The use of only packet loss resulted in the lack of stabilisation in the pendulum control system. In order to improve control stability, the previous input was sustained (see Fig. 18) to be used in situations when there is ambiguity or loss in the wireless network. Nevertheless, the control system based on the PID algorithm failed to achieve stability.

Over the course of 100 episodes and 1000 iterations, the RL agent was used to simulate a pendulum by adjusting its position. After 20-25 episodes of training, the agent exhibited fewer fluctuations and more stable control performance. During training, the agent stabilized angle and velocity parameters and compensated for packet loss disturbances. Network disruptions based on packet loss were utilized to train the RL agent. Changes in reward during training, such as the introduction of noise to system, can be compensated by the agent within the same range of episodes (refer to Fig. 19 and Fig. 20).

The performance of the RL algorithm is evaluated based on the system's state and actions that cause packet loss in order to establish stability in the presence of diverse packet losses or inter-packet gaps.
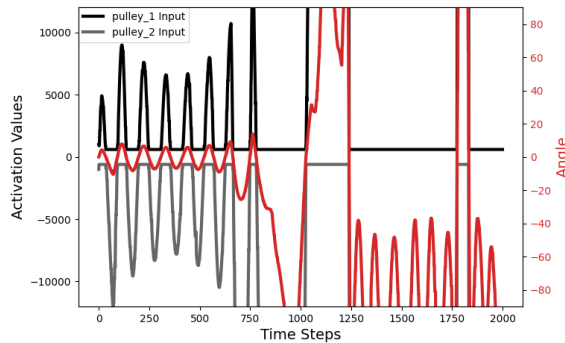
Figure 18: Inverted pendulum control via tendons using PID under network uncertainties, i.e. 15% packet loss
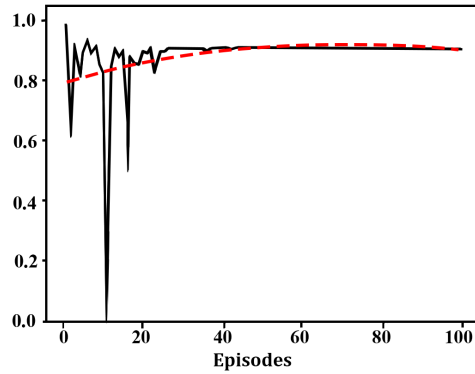
Figure 19: Reward in the inverted pendulum control via tendons using RL control under the effect of random noise
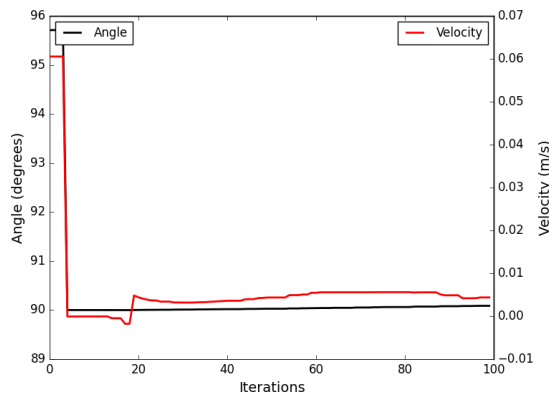
Figure 20: Inverted pendulum control via tendons using RL control (angle and velocity) under the effect of random noise

To evaluate stability under various conditions, network uncertainties were incorporated. Introducing uncertainties in actions could improve learning results, as the agent can learn even if some actions are noisy or lost due to poor network conditions. Including network degradation in the agent's state could enhance performance, particularly for wireless network control. The system's stability relies on the reward function's ability to incorporate the previous state. A buffer of length 10 was used to retain the previous state and reward.

The reinforcement learning-based method adapts to control disturbances caused by system-added noise and wireless network interference. The stability of a system is enhanced in scenarios without uncertainty or high uncertainty rates. The reinforcement learning-based method allows the agent to adapt to control disturbances induced by system-added noise and wireless network interference. The system exhibits satisfactory performance in the presence of packet loss or inter-packet gap.

The results show that power consumption decreases from 100 mW during continuous transmission to 95 mW (see Fig. 22) when transitioning from an increased inter-packet gap, resulting in packet loss.

Q-learning was also used to study pendulum behavior with fixed and uniform delays and gap probability, but the agent failed to learn during training (see Fig. 21).

This showed the comparison between policy versus value-based learning RL algorithms; further details of the results are presented in the submitted article (Future Publication IV).
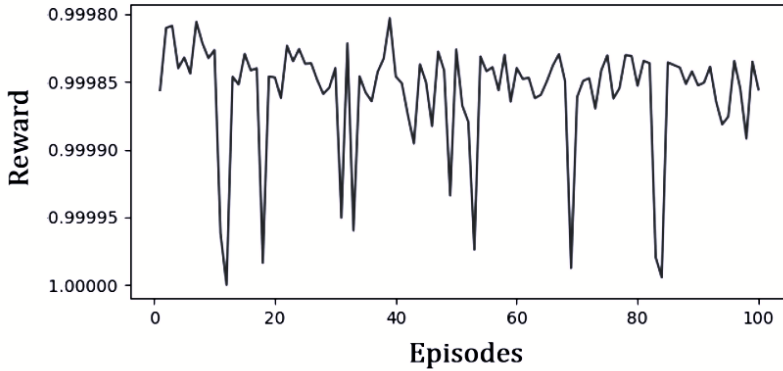
Figure 21: Inverted pendulum control via tendons using RL control (Q-learning) under the effect of uniform network loss
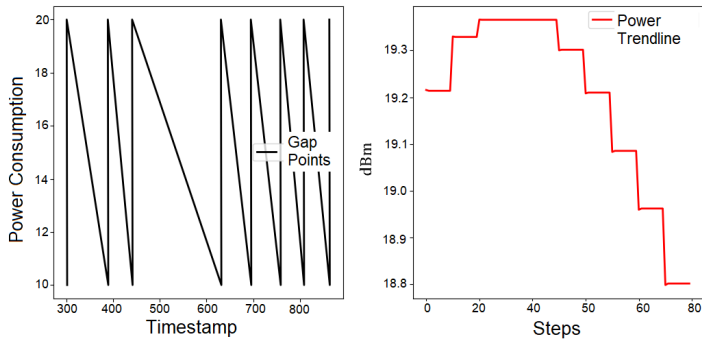
Figure 22: Power consumption (dBm) vs. IPG for RL-based control of inverted pendulum over wireless network

63

The CPU time utilized by various functions during the training process was evaluated using the Pybullet profiler (refer to Table 11). "CPU total" sums the CPU time required to call and execute a function, "#of calls" indicates the number of times a function is invoked.

The algorithm described as "model_inference" is utilized to generate predictions. For multiplying matrices, "matmul" and "mm" are utilized. "linear" refers to the neural network operation that is linear in nature. "Zeros" denotes a tensor comprised solely of zeros. "t" and "transpose" denote the transpose operation, respectively. When "Unsqueeze" is applied to a tensor, its dimension increases. The "to-textunderscore copy" function duplicates a tensor. By using "Squeezetextunderscore," a tensor's dimension is decreased.

After 100 episodes, the model interference algorithm maintained the highest average self-CPU % at nearly 40%.

Table 11: CPU time consumption for training code (Single Episode)

Function	Self CPU%	Self CPU time	CPU total time	Time avg.	#of Calls
model_inference	36.55%	575.000 μs	1.469 ms	1.469 ms	1
aten::matmul	8.33%	131.000 μs	385.000 μs	192.500 μs	2
aten::mm	7.31%	115.000 μs	121.000 μs	60.500 μs	2
aten::linear	5.47%	86.000 μs	648.000 μs	324.000 μs	2
aten::zeros	4.96%	78.000 μs	104.000 μs	104.000 μs	1
aten::t	4.83%	76.000 μs	138.000 μs	69.000 μs	2
aten::unsqueeze	4.58%	72.000 μs	81.000 μs	40.500 μs	2
aten::_to_copy	3.81%	60.000 μs	96.000 μs	96.000 μs	1
aten::transpose	3.05%	48.000 μs	62.000 μs	31.000 μs	2
aten::squeeze_	2.99%	47.000 μs	52.000 μs	26.000 μs	2

5.2.4 Additional results using advanced control method

To put the above into perspective, this section presents some additional results obtained with another advanced control method, namely MPC.

MPC is a method used to optimize control actions within a limited time frame, taking into account system constraints [163]. Nevertheless, because of its complexity, dynamics, constraints, high processing cost, and lack of robustness, MPC might not be appropriate for operating an inverted pendulum system with tendons. However, to investigate this claim, Equation 12 was used as a reference for modelling the inverted pendulum and the MPC-based controller.

$$\dot{\theta} = \frac{d}{dt}\theta, \;\; \ddot{\theta} = \frac{u - mg\sin(\theta)}{ml^2}$$

Here u is the applied torque, m is the mass, $\ddot{\theta}$ is the angular acceleration, and l is the length of the pendulum. We linearize the inverted pendulum model, where a simple mass-spring-damper system is used as a model. Based on the current state and the control input, future states are predicted; the pendulum initial angle is set to 45 degrees, the MPC horizon is set to 10, the initial tendon tension (control input) is set to 0.1, whereas the reference angle is set to 90 degrees.

The cost function is defined as per (13):

$$J(u) = (u - u_{\text{ref}})^T \cdot (u - u_{\text{ref}}) \tag{13}$$

where u_{ref} is the reference value of the applied torque u.

The state's cost is $Q = np.diag([100, 1])$, indicating that the cost function weights the first state (the pendulum angle) 100 times more than the second state (angular velocity). To maintain stability and avoid falling, this prioritizes keeping the pendulum angle close to the reference. $R = np.diag([0.1])$ indicates that the cost function weighs the control input 0.1 times more than the state. This allows for more aggressive control actions while minimizing control effort, thus reducing actuator wear. The length of the pendulum is set to 1 m, the mass to 1 kg, and gravity to 9.8 m/s.

Even after repeated attempts at adjusting the values of R and Q, the system remained unstable, as can be seen in Figure 23. This validates our earlier argument that the inverted pendulum model is non-linear and that attempting to convert it to linear may aid in understanding and controlling the system using advanced control methods, but would not produce adequate results.

The next attempt was to use a *non-linear* model and design the MPC controller accordingly. By tuning the parameters a little bit for the non-linear model, the system reached a stable response in 5000 iterations, as can be seen in Figure 24 (Figure shows time vs state).
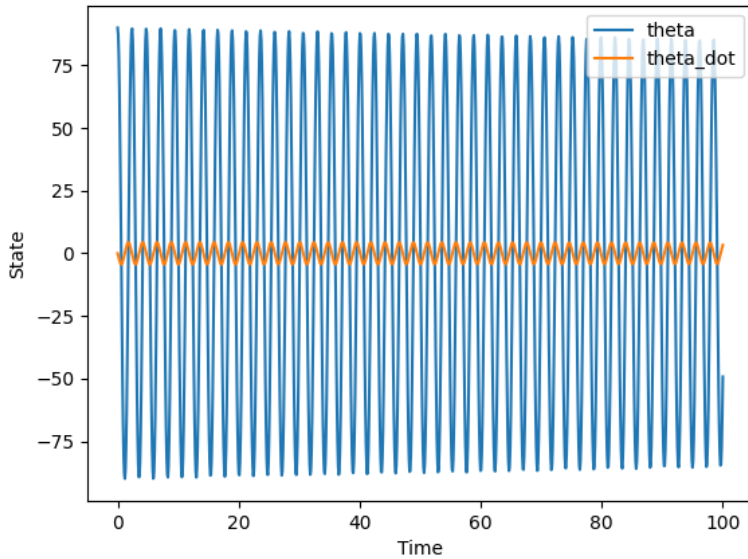
Figure 23: Inverted pendulum control via MPC for the linearized model. With the linearized model, the system remains unstable.
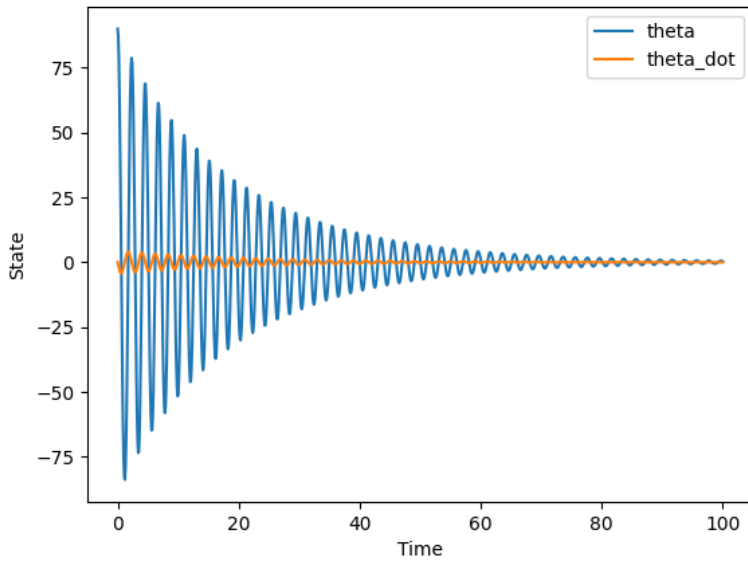

Figure 24: Inverted pendulum control via MPC for the non-linear model. With this linear model, the system stabilizes. (Non Linear Model)

As an initial step to add disturbance to system, a Gaussian disturbance was introduced to the control input with 0 mean and 0.1 standard deviation; the system was still able to maintain a stable response. Subsequently, we started introducing some packet losses and delays into the control input of the system. The system was able to sustain control performance despite these packet losses or delays by maintaining past input in case of such occurrences. Note that this was achieved by a simple implementation of packet loss probability and delay modelling, which is not very realistic.

Therefore, in order to accurately simulate real-life packet loss and delay scenarios, we included a uniform disturbance with a standard deviation of 0.1 into the control system's input. This approach is more realistic and accounts for the fact that actual packet loss and delay situations may be far more severe than basic probabilities and delays. However, on this occasion, the controller was unable to reach the specified output and the system ran out of memory (the system used for simulations had 32 GB of installed RAM and was equipped with an i7-1065G7 CPU running at a frequency of 1.30 GHz to 1.50 GHz).

5.3 Conclusion on Optimal Resource Consumption in Wireless Networked Control Systems using ML

The research presented in this chapter suggests that co-designing wireless control systems simultaneously at network and control layers offers advantages over interactive design. Factors such as latency, packet loss, and control strategy must be considered for reliable and resource-efficient co-design. The proposed RL-based approach is novel as it optimizes the IPG, enhancing resource efficiency through policy switching from reliable time-triggered control to energy-efficient time-triggered control or event-triggered control. This makes it immune to network packet loss and compensates for network fluctuations. On the contrary, the MPC-based approach did not yield results when subjected to realistic packet losses and delays.

Balancing reliability, efficiency, and performance is crucial for optimal performance , which can be achieved with the proposed RL-based approach). However, training the agent is time-consuming and may not reach stability if insufficient data is provided. Future improvements should focus on the quantity and quality data. The deeper analysis of the code showed a maximum of 40% CPU consumption for each function with the proposed RL-based approach.

This chapter has presented this thesis' contribution to optimal resource consumption in WNCSs using ML. The next chapter focuses on data distribution in WNCSs.

6 Data Distribution in Wireless Networked Control Systems

This chapter is based on the following two publications and one future publication:

Publication V: K. Ashraf, Y. Le Moullec, T. Pardy and T. Rang, "Decentralized Distributed Data Structure for Bioanalytical Laboratory Setups," 8th ACM WomENcourage Conference, 2021, `https://womencourage.acm.org/2021/wp-content/uploads/2021/07/59_extendedabstract.pdf`

Publication VI: R. Jõemaa, N. Gyimah, K. Ashraf, K. Pärnamets, A. Zaft, O. Scheler, T. Rang and T. Pardy, "CogniFlow-Drop: Integrated modular system for automated generation of droplets in microfluidic applications" IEEE Access, Vol. 11, pp. 104905 - 104929, 2023, DOI: `https://doi.org/10.1109/ACCESS.2023.3316726`

Patent Application - Owner: Tallinn University of Technology ; Inventors: K. Ashraf, K. Pärnamets, R. Jõemaa, N. Gyimah, T. Pardy, "Integrated modular system for automated generation of droplets in microfluidic applications and method thereto"; Priority number: EE P202300024; Priority date: 20.09.2023.
Note: the patent application is not included in appendix because it is under evaluation.

The reader is encouraged to look at the above papers (provided in appendix) for additional details and results.

The consideration of data and information flow is of the utmost significance in the design of bioanalytical devices. This chapter presents the following:

- A data distribution structure for bio-analytical laboratories based on a decentralized publish-subscribe model.

- The main structure for data communication and the conceptual, logical, and physical data flow models.

- Data Communication and User-interface design.

The novelty of this work lies in i) how it allows integrating various domains (computational, communication, and application-specific) via a decentralized data-centric communication architecture, and ii) how the structured data serialization (along with metadata) using Google's Protobuf enables the number and type of devices in the network to be extended without making major changes to the data structures, and iii) how inter-host communication via enhanced Communication Abstraction Layer (eCAL) supports low latency communication with fair reliability.

Fig. 25 provides a graphical abstract of the contribution on data distribution in WNCSs. The key elements of the figure are discussed below and in Publications V, VI, and patent application (Future Publication VII).
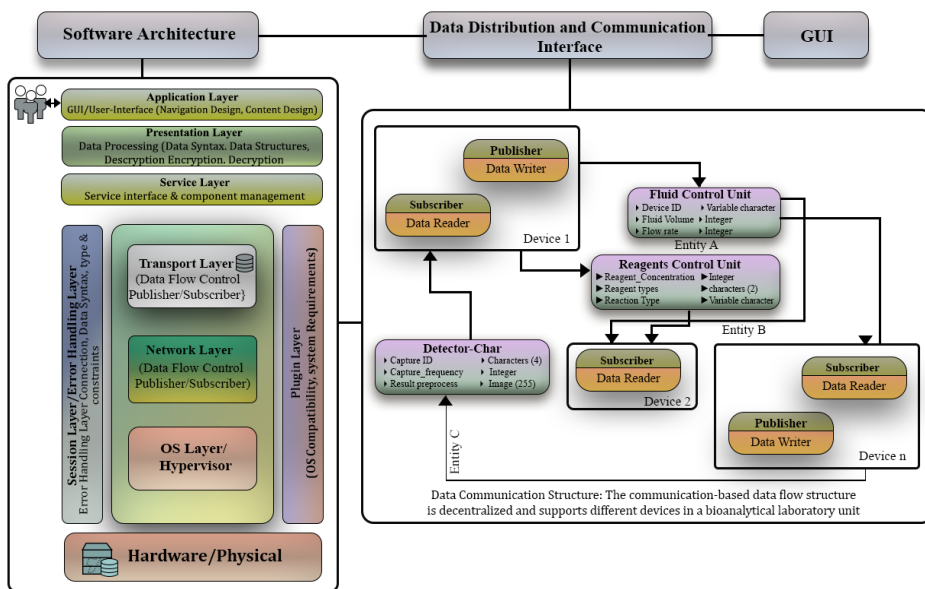
Figure 25: Graphical abstract of the contribution on data distribution in WNCSs

6.1 Data Distribution Architecture

This study proposes a decentralized publish-subscribe paradigm for bio-analytical labs, with an emphasis on data distribution and communication structures. The primary framework for data communication and flow models is established, with the objective of achieving scalable and resilient communication among laboratory units.

There are two main architecture for information flow : client−server [164, 165] and publisher-subscriber [166]. Table 12 shows the comparison between these architecture to pin point major differences in terms of communication, data flow, decoupling, scalability and message delivery.

According to [167], the efficiency of real-time data transfer can be enhanced by utilizing a publisher-subscriber architecture, as opposed to a client-server architecture. The objective of this work is to include multiple domains, including computing, communication, fluidic, and biochemical, into a bioanalytical laboratory establishing that enables high-throughput analysis.

This is achieved by the implementation of a decentralized communication architecture as mentioned in Publication 2. The proposed technique has the potential for enhanced versatility across a range of applications, in contrast to the existing client-based architectures commonly used in biochemical and bioanalytical laboratories.

The use of the data structure would facilitate the integration of numerous domains across several applications, hence augmenting the efficiency and efficacy of information distribution and administration.

Feature	Client—Server	publisher—subscriber
Communication-model [110]	Simple but does not handle continuous behavior and complexity increases with increasing clocks [111]	good for modeling concurrency, synchronization, and distributed systems but less effective for continuous dynamics [112]
Information Flow	Less complex than hybrid automata [113]	Expressive for systems with strict time requirements [114]
Message delivery[115]	Complexity increases with more clocks or mixed behaviors	Highly expressive for mixed behaviors (Continuous & Discrete)
Pi-Calculus [116]	Complex communication mechanisms and high concurrency make scenarios challenging	Good expressiveness in modeling concurrent and distributed systems with complex communication patterns

The data flow structure proposed for bio-analytical laboratories uses the publish-subscribe model, see Fig. 26, wherein entities and tasks are distributed across distinct devices. Every device is assigned to a certain entity and either subscribes to or publishes data to that entity, adhering to specific Quality of Service requirements. This arrangement facilitates decentralized data flow among the devices.
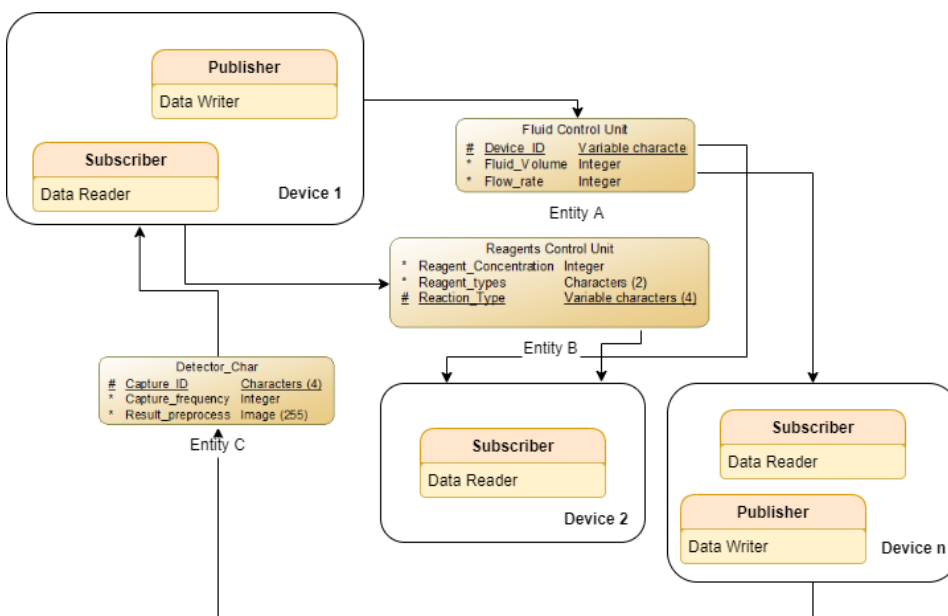
Figure 26: Main structure for data communication with a publish-subscribe model. The communication-based data flow structure is decentralized and supports different devices in a bioanalytical laboratory unit.

The investigation focused on a bio-analytical laboratory setup comprising three distinct units: the Biological Sample Processing Unit, the Computational Unit, and the Sensing Unit. SAP PowerDesigner is utilized for the creation of conceptual, logical, and physical data flow models pertaining to individual units. The conceptual model delineates the interconnections of information flow between various entities, incorporating attribute definitions and employing many-to-many interactions. The logical data flow model is an extension of the conceptual model. The physical data model offers a comprehensive examination of database entities and tables, facilitating the translation of the conceptual model into tangible components required for the practical development and execution of a system.

6.2 User−Interface Design

The software architecture for the CPBS should facilitate the management of both functional and non-functional attributes of devices via a unified publisher-subscriber interface. The major requirements encompass several aspects such as information communication, data handling, process management, scheduling, operating system capabilities, and user interface. The objective is to enhance the usability of hardware interfaces with both human users and other interconnected devices.
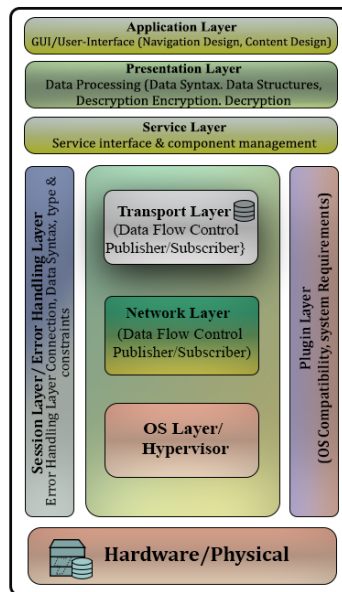
Figure 27: Proposed Layered Software Architecture for CPBS. The architecture considers the principles of service-oriented software architecture, three-tier architecture OSI model, and Cisco's OSI model for cloud computing.

The proposed multi-layer software architecture combines service-oriented, three-tier architecture OSI model, and Cisco's OSI model for cloud computing 27. It consists of a presentation layer, service layer, plugin layer, session layer, transport layer, and network layer. The presentation layer manages user input and control actions, while the service layer manages service components and interfaces. The low-level layers include hardware/physical and OS layers for managing hardware resources. Considering

a thorough analysis of software design, the practical execution of the project ensured the feasibility of inter-host communication.

The structured data was serialized, including metadata, via Google's Protobuf serialization standard. By applying this approach, the capacity to expand the quantity and variety of devices inside the network can be enhanced with minimal modifications to the data structures. An enhanced Communication Abstraction Layer (eCAL) was implemented to facilitate communication. The data rate achieved using eCAL was dependent upon the payload, whereas the utilized data-centric communication architecture facilitated low latency communication with a reasonable level of reliability.

Fig. 28 illustrates the comprehensive data transfer method. After establishing a secure connection, the data transfer occurs through an intermediate layer that requires data serialization. The user sends and receives required data using graphical user interface.
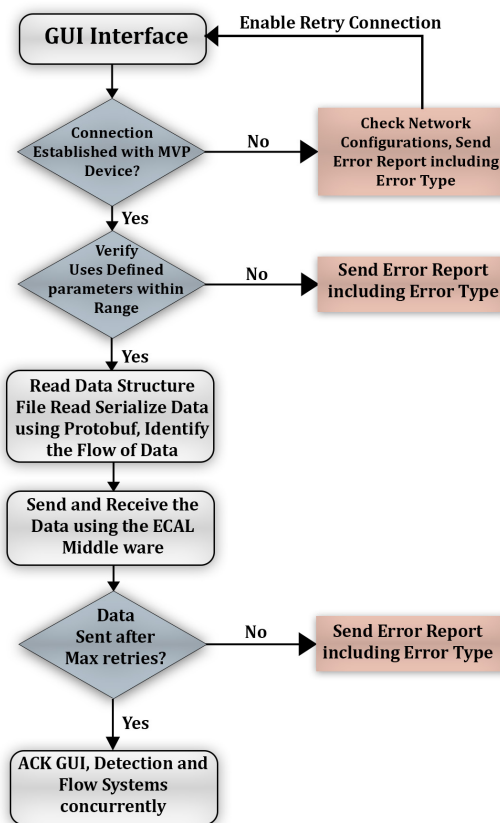
Figure 28: Implementation of the communication interface, data transmission, reception, verification, and a Graphical User Interface for accessibility.

The CogniFlow-Drop prototype can be operated through the graphical user interface (GUI) by specifying parameters for droplet creation rate and size and transmitting them using the provided task-specific buttons. In the event that the selected parameters did not fall within the permissible limits or were of an incorrect kind, an error message was displayed, prompting the user to make the necessary modifications. The provided parameters underwent serialization through a specific protocol and were thereafter

transmitted to the recipient device in the format of messages. Unless specifically stopped from the graphical user interface (GUI), tasks were automatically stopped on the controlling device upon completion.

To assess the effectiveness of the designed communication and graphical user interface, the CogniFlow-Drop device was effectively connected to a laptop using a Wi-Fi hotspot. This connection facilitated the seamless transmission and reception of message packets at regular intervals of 100 milliseconds. The functional tests encompassed many procedures, namely setup calibration, droplet formation, size and rate target series tests, and the introduction of artificial delay through the user interface (UI).

This chapter has presented main structure for data communication and user interface design for bio-analytical devices. The chapter also summarized software architecture necessary for CPBS and co-design in general. The next chapter concludes this Ph.D. thesis by summarizing the problem and the work that has been conducted, the main results and key findings, and also suggests possible directions for future work.

7 Conclusion and Future Work

To conclude this thesis, this chapter firstly provides a summary of the topic, RQs, and contributions made in this thesis. Secondly, the chapter outlines some possible research perspectives.

7.1 Summary

This Ph.D. thesis investigated challenges pertaining to the design of WNCS, in particular 1) managing uncertainties, i.e. delays, packet losses, and synchronization errors in the wireless channel while at the same time guaranteeing the reliability, scalability, and resilience of the system, as well as 2) dealing with the rising complexity of designing WNCSs when the model of the devices and/or their environments is unknown or only partially known.

Against this backdrop, the following specific RQs were formulated:

- **RQ1:** For the purpose of automating complex processes involving bio-analytical instruments, how can the principles of WNCSs (as a type of CPS) and the principles of biological processes be integrated and applied together?

- **RQ2:** What is the impact of decentralized versus centralized system communication architectures on the device's overall performance in terms of scalability and reliability?

- **RQ3:** How can Quality of Control (QoC) and Quality of Service (QoS) be improved in WNCSs?

  - How to achieve reliability by compensating network delay, control delays, packet loss, high traffic?
  - How can robustness of overall system be achieved in terms of bandwidth, power, and self-adaptive configuration?

To answer those RQs, this Ph.D. thesis revolved around the co-design principles for designing WNCSs. In particular, it proposed models and methods for the co-design of communication and control, strategies for adaptive and robust control, and it also explored the suitability and significance of model-based and model-free design methods for achieving reliability, resource efficiency, and scalability.

In line with the above RQs, the contributions made in this Ph.D. thesis are summarized as follows:

- Contributing towards RQ1 and RQ2, this thesis proposed a novel model-based system architecture for event-triggered wireless control with extended timed automata in WNCS. The contribution also proposed and compared strategies to achieve specific delays and bandwidth consumption while preventing packet loss during network congestion. A droplet flow cytometer was used as a WNCS use case.

  Results indicate that under strict delay constraints and high network traffic, the decentralized strategy is favored over the centralized strategy. Conversely, in low-traffic scenarios, the centralized strategy proves more effective in ensuring reliable system operation. The minimum delay between two systems is 129 ms (centralized), 87 ms (decentralized), and 125 ms (in scenarios avoiding high traffic). This contribution was described in Chapter 3 and Publications I and II.

- Then, contributing towards RQ2, this thesis proposed a novel joint optimization method for WNCSs, following the co-design principle. It applies classical optimization theory to minimize control errors under network constraints and errors introduced by the reinforcement Q-learning technique. The problem was extended and applied to a droplet generation system. Control performance was evaluated for three algorithms (C51, DQN, DDQN) and three scenarios (both without and with network effects in the reward function, as well as with network uncertainties with random variables in the RL reward function).

  Results indicate that the C51 algorithm outperforms the other algorithms, which is primarily due to its effectiveness in solving multi-modal problems. This contribution was presented in Chapter 4 and Publication III.

- Next, as a contribution to RQ3, the thesis introduced a novel method to maximize control-communication reliability and resource efficiency across the control and communication layers by regulating the IPG. The proposed method integrates RL techniques to concurrently address control communication reliability and resource utilization efficiency. Unlike previous research in the field that primarily relies on analytical methods, the simulation-based validation method used in the contribution offers a more comprehensive and practical assessment of the optimization procedure. A co-design reinforcement learning (RL)-based control method is applied to successfully solve the multi-objective problem.

  Simulation results illustrate that the proposed method effectively maintains or enhances control performance, even in the presence of packet losses. The proposed RL-based method shows an average decrease in transmission power of up to 10% and exhibits resilience to network packet loss, a common issue in older control systems that may significantly degrade performance. This contribution was presented in Chapter 5 and Publications IV.

- In addition to the above contribution to RQ2, the thesis also proposed and developed a novel decentralized communication-based data flow structure to support various connected devices, applied in a bioanalytical laboratory case study. This structure encompasses the conceptual, logical, and physical data flow models.

  The case study confirms that the proposed system model worked as expected when subjected to the specified constraints; it also highlights the implications of formal techniques (synchronization etc.) in designing and verifying wireless automation of high-throughput laboratory setups in MBSE. This contribution was presented in Chapter 6 and Publications V and VI, and Future Publication VII.

- Lastly, another contribution supporting RQ1 and RQ2 is the developed wireless communication -driven automation system that operates based on event triggers, making use of predefined data structures in a publisher-subscriber setup. This contribution was presented as part of Chapter 6 and Publications V and VI, and Future Publication VII.

7.2 Perspectives

In addition to the contributions presented in this thesis, several opportunities for future research have been identified, as briefly outlined in what follows.

- The joint design of communication and control modules presented in this thesis contributes to improving the communication and control performance of WNCSs; the work also considered the issue of random effects in communication. However, in some scenarios, the communication channel could also be highly dynamic. Addressing such dynamics could be carried out by combining communication theory and a data-driven approach where ML algorithms are used for predicting communication channel dynamics in WNCS. This could be built on work such as the knowledge-driven machine learning model for channel estimation and GAN-LSTM based AI framework for wireless channel prediction proposed in [168].

- Another aspect to be further researched is the increasing requirements of information timeliness. While such requirements were not extremely demanding in the use cases studied in this thesis, there are more and more use cases of WNCSs that must meet (ultra-) low-latency requirements for fast decision-making and prompt actuations and reactions in industrial processes or safety-critical applications. For such cases, information timeliness must be systematically integrated in the co-design of communication.

  This could build upon works such as incorporating Age of Information [47] as previously discussed in Chapter 2, or Haxhibeqiri [169] and Nikhileswar [170] that explore the integration of Time-Sensitive Networking (TSN) with wireless technologies such as Wi-Fi 6/6E and 5G to achieve deterministic communication and reliability, or Lu [171] that proposes a non-collision theory-based deterministic scheduling method for ultralow latency communication in edge-enabled Industrial Internet of Things, or Popovski [172] that introduces a statistical framework for timing requirements in wireless communication systems, which includes both latency and information freshness.

- Looking further ahead, the shift towards semantic communication in networked systems is considered to be a crucial factor in meeting future service requirements; this approach, which focuses on the importance of information, requires the development of advanced semantic metrics and optimal sampling theories, but also requires a unified framework for semantic communication research from a metric perspective [173].

  The increasing role of AI in communication technologies further emphasizes the importance of semantic communication [174]. Integrating semantic communication in WNCS could build upon e.g. [175] that focuses on semantics and task-oriented scheduling for networked control systems and the development of a contention-free algorithm and a new metric for wireless resource scheduling, or on [176] that evaluates the performance of transport layer protocols and introduces a semantic-aware policy.

- Finally, the issue of security was deliberately not included in the scope of this Ph.D. work. Nevertheless, it is necessary to safeguard WNCSs against potential cyber-threats that may compromise availability (correct operations' readiness), reliability (correct service's continuity), safety (no severe impact on the user(s) and the environment), integrity (no improper system alteration or data breaches).

The principle of cyber-physical co-design for security is a natural research direction candidate to build upon the work presented in this thesis as it would allow exploring co-design approaches that integrate cybersecurity considerations into the early stages of WNCS development, ensuring that security is an inherent aspect of the system's architecture and operation.

This could build upon or integrate, for example, joint Nash power strategies and optimal control strategy at the cyber-layer and physical-layer to bring the control performance to the desired security level by dynamically manipulating the cyber-layer pricing parameters [46], or the dual security control framework and Takagi-Sugeno fuzzy model using time-delay system theory combined with a robust observer and a co-design method to estimate and regulate the state and fault, to optimize the control and communication [177].

Security-by-design could also be investigated to the design of WNCSs by applying security principles and best practices throughout the system development life cycle, and using security testing and evaluation methods to ensure the security quality of the system. This would require a co-engineering approach that involves both safety and security teams and uses a common framework and methodology to harmonize the other design goals and that of safety and security.

References

[1] G. Siddesh, G. Deka, K. Srinivasa, and L. Patnaik, eds., *Cyber Physical Systems: A Computational Perspective (1st ed.)*. Chapman and Hall/CRC, 11 2015.

[2] P. Marwedel, T. Mitra, M. Grimheden, and H. Andrade, "Survey on education for cyber-physical systems," *IEEE Design Test*, vol. PP, pp. 1–1, 07 2020.

[3] P. Park, S. Coleri Ergen, C. Fischione, C. Lu, and K. H. Johansson, "Wireless network design for control systems: A survey," *IEEE Communications Surveys Tutorials*, vol. 20, no. 2, pp. 978–1013, 2018.

[4] Y. Wang, S. Wu, C. Lei, J. Jiao, and Q. Zhang, "A review on wireless networked control system: The communication perspective," *IEEE Internet of Things Journal*, vol. 11, no. 5, pp. 7499–7524, 2024.

[5] M. S. Mahmoud, "Wireless networked control system design: An overview," in *2014 IEEE 23rd International Symposium on Industrial Electronics (ISIE)*, pp. 2335–2340, 2014.

[6] B. Pradhan, S. Bhattacharyya, and K. Pal, "Iot-based applications in healthcare devices," *Journal of Healthcare Engineering*, vol. 2021, pp. 1–18, 03 2021.

[7] T. Primya, G. Kanagaraj, and G. Subashini, "An overview with current advances in industrial internet of things (iiot)," in *International Conference on Communication, Circuits, and Systems*, (Singapore), pp. 89–97, Springer Singapore, 2021.

[8] W. Liu, G. Nair, Y. Li, D. Nesic, B. Vucetic, and H. V. Poor, "On the latency, rate, and reliability tradeoff in wireless networked control systems for iiot," *IEEE Internet of Things Journal*, vol. 8, no. 2, pp. 723–733, 2021.

[9] C. Pillajo and R. Hincapié, "Stochastic control for a wireless network control system (wncs)," in *2020 IEEE ANDESCON*, pp. 1–6, 2020.

[10] M. Schranz, W. Elmenreich, and M. Rappaport, *Designing Cyber-physical Systems with Evolutionary Algorithms*, pp. 111–135. Cham: Springer International Publishing, 2018.

[11] V. Chiprianov, K. Falkner, L. Gallon, and M. Munier, "Towards modelling and analysing non-functional properties of systems of systems," in *2014 9th International Conference on System of Systems Engineering (SOSE)*, pp. 289–294, 2014.

[12] D. Lohmann, W. Schroder-Preikschat, and O. Spinczyk, "Functional and non-functional properties in a family of embedded operating systems," in *10th IEEE International Workshop on Object-Oriented Real-Time Dependable Systems*, pp. 413–420, 2005.

[13] S. Preuße and H.-M. Hanisch, "Verifying functional and non-functional properties of manufacturing control systems," in *2011 3rd International Workshop on Dependable Control of Discrete Systems*, pp. 41–46, 2011.

[14] A. Ulusoy, A. Onat, and O. Gurbuz, "Wireless model based predictive networked control system," *IFAC Proceedings Volumes*, vol. 42, no. 3, pp. 40–47, 2009. 8th IFAC Conference on Fieldbuses and Networks in Industrial and Embedded Systems.

[15] J. A. Stankovic, "Research directions for cyber physical systems in wireless and mobile healthcare," *ACM Trans. Cyber-Phys. Syst.*, vol. 1, nov 2016.

[16] W. Zhang, S. Guo, W. S. Pereira Carvalho, Y. Jiang, and M. J. Serpe, "Portable point-of-care diagnostic devices," in *Analytical Methods*, vol. 8, pp. 7847–7867, Royal Society of Chemistry, nov 2016.

[17] M. Zarei, "Portable biosensing devices for point-of-care diagnostics: Recent developments and applications," in *TrAC - Trends in Analytical Chemistry*, vol. 91, pp. 26–41, Elsevier B.V., jun 2017.

[18] A. St John and C. P. Price, "Existing and Emerging Technologies for Point-of-Care Testing.," *The Clinical biochemist. Reviews*, vol. 35, pp. 155–67, aug 2014.

[19] Grand View Research, "Point Of Care Diagnostics Market Size, Share Trends Analysis Report By Product (Infectious Diseases, Glucose Testing, Cardiac Markers), By End-use (Clinics, Home, Hospitals), By Region, And Segment Forecasts, 2024 - 2030 ." `https://www.fortunebusinessinsights.com/industry-reports/point-of-care-diagnostics-market-101072`, 2024.

[20] T. Nguyen, V. A. Chidambara, S. Z. Andreasen, M. Golabi, V. N. Huynh, Q. T. Linh, D. D. Bang, and A. Wolff, "Point-of-care devices for pathogen detections: The three most important factors to realise towards commercialization," in *TrAC Trends in Analytical Chemistry*, vol. 131, p. 116004, Elsevier B.V., 2020.

[21] S. B. Haga, "Challenges of development and implementation of point of care pharmacogenetic testing," *Expert Review of Molecular Diagnostics*, vol. 16, pp. 949–960, sep 2016.

[22] W. Li, H. Xi, and S. H. Tan, eds., *Insights and Advancements in Microfluidics*. MDPI, 2018.

[23] W. C. Tian and E. Finehout, *Microfluidics for biological applications*. Springer US, 2009.

[24] "Point of Care [POC] Diagnostics Market Size, Trends | Report 2029." `https://www.fortunebusinessinsights.com/industry-reports/point-of-care-diagnostics-market-101072`, 2021.

[25] W. Postek, P. Gargulinski, O. Scheler, T. S. Kaminski, and P. Garstecki, "Microfluidic screening of antibiotic susceptibility at a single-cell level shows the inoculum effect of cefotaxime on: E. coli," *Lab on a Chip*, vol. 18, no. 23, pp. 3668–3677, 2018.

[26] T. S. Kaminski, O. Scheler, and P. Garstecki, "Droplet microfluidics for microbiology: Techniques, applications and challenges," *Lab on a Chip*, vol. 16, no. 12, pp. 2168–2187, 2016.

[27] O. Scheler, K. Makuch, P. R. Debski, M. Horka, A. Ruszczak, N. Pacocha, K. Sozański, O. P. Smolander, W. Postek, and P. Garstecki, "Droplet-based digital antibiotic susceptibility screen reveals single-cell clonal heteroresistance in an isogenic bacterial population," *Scientific Reports*, vol. 10, no. 1, pp. 1–8, 2020.

[28] E. Sultanovs and A. Romanovs, "Centralized healthcare cyber-physical system's data analysis module development," *2016 IEEE 4th Workshop on Advances in Information, Electronic and Electrical Engineering, AIEEE 2016 - Proceedings*, no. November 2016, pp. 1–4, 2017.

[29] D. Calvaresi, M. Marinoni, A. Sturm, M. Schumacher, and G. Buttazzo, "The challenge of real-time multi-agent systems for enabling iot and cps," in *WI '17: Proceedings of the International Conference on Web Intelligence*, pp. 356–364, 08 2017.

[30] A. Ali, "Towards the design of cyber-physical system via multi-agent system technology," *International Journal of Scientific and Engineering Research*, vol. 7, 10 2016.

[31] S. Sy, N. Sy, and M. Zainon, *Control Systems Engineering*. Penerbit Universiti Teknikal Malaysia Melaka, 2010.

[32] N. Nise, *Control Systems Engineering*. Wiley, 2020.

[33] J. T. Tou, *Digital and sampled-data control systems*. McGraw-Hill New-York, 1959.

[34] Y. Bavafa-Toosi, "4 - time response," in *Introduction to Linear Control Systems* (Y. Bavafa-Toosi, ed.), pp. 333–436, Academic Press, 2019.

[35] Y. Bavafa-Toosi, "8 - nichols-krohn-manger-hall chart," in *Introduction to Linear Control Systems* (Y. Bavafa-Toosi, ed.), pp. 701–741, Academic Press, 2019.

[36] Y. Bavafa-Toosi, "9 - frequency domain synthesis and design," in *Introduction to Linear Control Systems* (Y. Bavafa-Toosi, ed.), pp. 743–844, Academic Press, 2019.

[37] K. Tahboub, "Control of a class of nonlinear systems via linear controllers with application to robots," in *1995 IEEE International Conference on Systems, Man and Cybernetics. Intelligent Systems for the 21st Century*, vol. 5, pp. 4428–4433 vol.5, 1995.

[38] S. F. Kamarulzaman, T. Shibuya, and S. Yasunobu, "A learning-based non-linear control system with constraint consideration," in *SICE Annual Conference 2011*, pp. 2474–2479, 2011.

[39] M. J. Błachuta, "Continuous-time design of discrete-time control systems," in *1997 European Control Conference (ECC)*, pp. 1981–1986, 1997.

[40] C. Johnson, "A general theory of "discrete/continuous" type discrete-time control for linear dynamical systems," in *Proceedings of Thirtieth Southeastern Symposium on System Theory*, pp. 56–61, 1998.

[41] X. Liu and A. Goldsmith, "Cross-layer design of control over wireless networks," in *Advances in Control, Communication Networks, and Transportation Systems: In Honor of Pravin Varaiya* (E. H. Abed, ed.), (Boston, MA), pp. 111–136, Birkhäuser Boston, 2005.

[42] A. Chamaken, L. Litz, M. Kraemer, and R. Gotzhein, "Cross-layer design of wireless networked control systems with energy limitations," in *2009 European Control Conference (ECC)*, pp. 2325–2330, 08 2009.

[43] E. A. Lee, "Fundamental limits of cyber-physical systems modeling," *ACM Trans. Cyber-Phys. Syst.*, vol. 1, nov 2016.

[44] Y.-L. Chen, "Cross-layer design and optimization for wireless networked control systems," Master's thesis, Queensland University of Technology, 2012.

[45] Y. Ma, C. Lu, and Y. Wang, "Efficient holistic control: Self-awareness across controllers and wireless networks," *ACM Trans. Cyber-Phys. Syst.*, vol. 4, jun 2020.

[46] Y. Yuan, H. Yuan, D. W. C. Ho, and L. Guo, "Resilient control of wireless networked control system under denial-of-service attacks: A cross-layer design approach," *IEEE Transactions on Cybernetics*, vol. 50, no. 1, pp. 48–60, 2020.

[47] Z. Zhao, W. Liu, D. E. Quevedo, Y. Li, and B. Vucetic, "Deep learning for wireless-networked systems: A joint estimation-control–scheduling approach," *IEEE Internet of Things Journal*, vol. 11, no. 3, pp. 4535–4550, 2024.

[48] A. Chamaken and L. Litz, "Joint design of control and communication in wireless networked control systems: A case study," in *Proceedings of the 2010 American Control Conference*, pp. 1835–1840, 2010.

[49] Z. Han, X. Li, Z. Zhou, K. Huang, Y. Gong, and Q. Zhang, "Wireless communication and control co-design for system identification," *IEEE Transactions on Wireless Communications*, pp. 1–1, 2023.

[50] Y. Qiao, Y. Fu, and M. Yuan, "Communication–control co-design in wireless networks: A cloud control agv example," *IEEE Internet of Things Journal*, vol. 10, no. 3, pp. 2346–2359, 2023.

[51] P. Martí, J. Yépez, M. Velasco, R. Villà, and J. M. Fuertes, "Managing quality-of-control in network-based control systems by controller and message scheduling co-design," *IEEE Transactions on Industrial Electronics*, vol. 51, no. 6, pp. 1159–1167, 2004.

[52] H. Benítez-Pérez, J. L. Ortega-Arjona, P. E. Méndez-Monroy, E. Rubio-Acosta, and O. A. Esquivel-Flores, "Control Strategies and Co-Design of Networked Control Systems - Considering Time Delay Effects," in *Modeling and Optimization in Science and Technologies (MOST)*, vol. 13, 2019.

[53] S. Sang, X. Fan, X. Tang, T. Wang, and A. Jian, "Portable surface stress biosensor test system based on ZigBee technology for health care," *Biotechnology & Biotechnological Equipment*, vol. 29, no. 4, pp. 798–804, 2015.

[54] P. R. Chopade, P. Deshmukh, K. Kamble, and D. Nazarkar, "NFC Based Health Care System," in *International Journal of Innovative Science, Engineering Technology*, vol. 3, pp. 414–419, 2016.

[55] M. Zulqarnain, S. Stanzione, G. Rathinavel, S. Smout, M. Willegems, K. Myny, and E. Cantatore, "A flexible ECG patch compatible with NFC RF communication," *Nature Partner Journals - npj Flexible Electronics*, vol. 4, no. 1, pp. 1–9, 2020.

[56] Y. Fan, J. Liu, Y. Wang, J. Luo, H. Xu, S. Xu, and X. Cai, "A wireless point-of-care testing system for the detection of neuron-specific enolase with microfluidic paper-based analytical devices," *Biosensors and Bioelectronics*, vol. 95, no. April, pp. 60–66, 2017.

[57] L. J. V. Escobar and S. A. Salinas, "E-Health prototype system for cardiac telemonitoring," *Proceedings of the Annual International Conference of the IEEE Engineering in Medicine and Biology Society, EMBS*, vol. 2016-October, pp. 4399–4402, 2016.

[58] C. Zhao and X. Liu, "A portable paper-based microfluidic platform for multiplexed electrochemical detection of human immunodeficiency virus and hepatitis C virus antibodies in serum," *Biomicrofluidics*, vol. 10, p. 024119, mar 2016.

[59] I. Čuljak, Ž. L. Vasić, H. Mihaldinec, and H. Džapo, "Wireless body sensor communication systems based on UWB and IBC technologies: State-of-theart and open challenges," *Sensors (Switzerland)*, vol. 20, no. 12, pp. 1–32, 2020.

[60] A. Bensky, "Wireless personal area networks," in *Short-range Wireless Communication*, pp. 317–360, 2019.

[61] S. Han, J. Song, X. Zhu, A. K. Mok, D. Chen, M. Nixon, W. Pratt, and V. Gondhalekar, "Wi-HTest: compliance test suite for diagnosing devices in real-time WirelessHART™ mesh networks," *Wireless Networks*, vol. 21, pp. 1999–2018, aug 2015.

[62] A. Yearp, D. Newell, P. Davies, R. Wade, and R. Sahandi, "Wireless remote patient monitoring system: Effects of interference," in *2016 10th International Conference on Innovative Mobile and Internet Services in Ubiquitous Computing (IMIS)*, pp. 367–370, 2016.

[63] W. Ayoub, A. E. Samhat, F. Nouvel, M. Mroue, and J. C. Prévotet, "Internet of Mobile Things: Overview of LoRaWAN, DASH7, and NB-IoT in LPWANs Standards and Supported Mobility," *IEEE Communications Surveys and Tutorials*, vol. 21, no. 2, pp. 1561–1581, 2019.

[64] C. A. da Costa, C. F. Pasluosta, B. Eskofier, D. B. da Silva, and R. da Rosa Righi, "Internet of Health Things: Toward intelligent vital signs monitoring in hospital wards," in *Artificial Intelligence in Medicine*, vol. 89, pp. 61–69, Elsevier B.V., jul 2018.

[65] A. Yearp, D. Newell, P. Davies, R. Wade, and R. Sahandi, "Wireless remote patient monitoring system: Effects of interference," in *Proceedings - 2016 10th International Conference on Innovative Mobile and Internet Services in Ubiquitous Computing*, IMIS 2016, pp. 367–370, IEEE, dec 2016.

[66] M. T. Buyukakkaslar, M. A. Erturk, M. A. Aydin, and L. Vollero, "LoRaWAN as an e-Health Communication Technology," in *Proceedings - International Computer Software and Applications Conference*, vol. 2, pp. 310–313, IEEE Computer Society, sep 2017.

[67] H. Zhang, J. Li, B. Wen, Y. Xun, J. Liu, and S. Member, "Connecting Intelligent Things in Smart Hospitals Using NB-IoT," *IEEE Internet of Things Journal*, vol. 5, no. 3, pp. 1550–1560, 2018.

[68] M. Mayer and A. J. Baeumner, "A Megatrend Challenging Analytical Chemistry: Biosensor and Chemosensor Concepts Ready for the Internet of Things," *Chemical Reviews*, vol. 119, pp. 7996–8027, jul 2019.

[69] M. M. Alam, H. Malik, M. I. Khan, T. Pardy, A. Kuusik, and Y. Le Moullec, "A survey on the roles of communication technologies in IoT-Based personalized healthcare applications," *IEEE Access*, vol. 6, pp. 36611–36631, jul 2018.

[70] A. Ahad, M. Tahir, and K. L. A. Yau, "5G-based smart healthcare network: Architecture, taxonomy, challenges and future research directions," *IEEE Access*, vol. 7, pp. 100747–100762, 2019.

[71] T. Kato, "Standardization and Certification Process for "Wi-SUN" Wireless Communication Technology," *Anritsu Technical Review*, vol. 23, no. 1, pp. 22–33, 2015.

[72] D. H. Devi, K. Duraisamy, A. Armghan, M. Alsharari, K. Aliqab, V. Sorathiya, S. Das, and N. Rashid, "5g technology in healthcare and wearable devices: A review," *Sensors*, vol. 23, no. 5, 2023.

[73] H. Taleb, A. Nasser, A. Guillaume, N. Charara, and E. Cruz, "Wireless technologies, medical applications and future challenges in wban: a survey," *Wireless Networks*, vol. 27, 11 2021.

[74] P. Wang and L. J. Kricka, "Current and Emerging Trends in Point-of-Care Technology and Strategies for Clinical Validation and Implementation," *Clinical Chemistry*, vol. 64, pp. 1439–1452, 10 2018.

[75] E. García, P. J. Antsaklis, and L. A. Montestruque, "Model-based control of networked systems," in *Systems and Control: Foundations and Applications*, 2014.

[76] C. Hua and Y. Zheng, "Modeling and control for wireless networked control system," *International Journal of Automation and Computing*, vol. 8, pp. 357–363, 08 2011.

[77] Y.-B. Zhao, D. Xu, J. He, X. xi, and Y. Kang, "Model-based network scheduling and control for systems over the ieee 802.15.4 network," *Journal of Systems Science and Complexity*, vol. 34, pp. 1–17, 09 2020.

[78] S. Zhao and Y. Ji, "Model-dependent scheduling and h-infinity control co-design for networked control systems," *International Journal of Control, Automation and Systems*, vol. 19, 09 2020.

[79] X. Wang, Y. Wang, Q. Cui, K.-C. Chen, and W. Ni, "Machine learning enables radio resource allocation in the downlink of ultra-low latency vehicular networks," *IEEE Access*, vol. 10, pp. 44710–44723, 2022.

[80] D. Prakashan, R. P R, and S. Gandhi, "A systematic review on the advanced techniques of wearable point-of-care devices and their futuristic applications," *Diagnostics*, vol. 13, no. 5, 2023.

[81] E. Evin and Y. Uludağ, "Bioanalytical device design with model-based systems engineering tools," *IEEE Systems Journal*, vol. 14, no. 3, pp. 3139–3149, 2020.

[82] L. C. e Silva, M. B. Perkusich, F. M. Bublitz, H. O. de Almeida, and A. Perkusich, "A model-based architecture for testing medical cyber-physical systems," *Proceedings of the 29th Annual ACM Symposium on Applied Computing*, 2014.

[83] T. Li, F. Tan, Q. Wang, L. Bu, J.-N. Cao, and X. Liu, "From offline toward real time: A hybrid systems model checking and cps codesign approach for medical device plug-and-play collaborations," *Parallel and Distributed Systems, IEEE Transactions on*, vol. 25, 04 2012.

[84] E. Evin and Y. Uludağ, "Bioanalytical device design with model-based systems engineering tools," *IEEE Systems Journal*, vol. 14, no. 3, pp. 3139–3149, 2020.

[85] F. Patou, M. Dimaki, A. Maier, W. E. Svendsen, and J. Madsen, "Model-based systems engineering for life-sciences instrumentation development," *Systems Engineering*, vol. 22, no. 2, pp. 98–113, 2019.

[86] I. Lee, O. Sokolsky, S. Chen, J. Hatcliff, E. Jee, B. Kim, A. King, M. Mullen-Fortino, S. Park, A. Roederer, and K. K. Venkatasubramanian, "Challenges and research directions in medical cyber–physical systems," *Proceedings of the IEEE*, vol. 100, no. 1, pp. 75–90, 2012.

[87] Y. Luo, K. Chakrabarty, and T.-Y. Ho, *Hardware/Software Co-Design and Optimization for Cyberphysical Integration in Digital Microfluidic Biochips*. Switzerland: Springer Cham - Springer International Publishing Switzerland, 2016.

[88] J. Tang, M. Ibrahim, and K. Chakrabarty, "Randomized checkpoints: A practical defense for cyber-physical microfluidic systems," *IEEE Design Test*, vol. 36, no. 1, pp. 5–13, 2019.

[89] F. Patou, M. Dimaki, A. Maier, W. E. Svendsen, and J. Madsen, "Model-based systems engineering for life-sciences instrumentation development," *Systems Engineering*, vol. 22, no. 2, pp. 98–113, 2019.

[90] Q. Zhu and A. Sangiovanni-Vincentelli, "Codesign Methodologies and Tools for Cyber-Physical Systems," *Proceedings of the IEEE*, vol. 106, no. 9, pp. 1484–1500, 2018.

[91] S. K. Mazumder, ed., *Wireless networking based control*. Springer New York, NY, 2011.

[92] M. H. Mamduhi, D. Maity, S. Hirche, J. S. Baras, and K. H. Johansson, "Delay-sensitive Joint Optimal Control and Resource Management in Multi-loop Networked Control Systems," *IEEE Transactions on Control of Network Systems*, vol. 8, no. 3, pp. 1093–1106, 2021.

[93] B. Chang, "URLLC Design for Real-Time Control in Wireless Control Systems," *IEEE 5G World Forum, 5GWF 2018 - Conference Proceedings*, pp. 437–439, 2018.

[94] C. M. Bishop, "Model-based machine learning," *Philosophical transactions. Series A, Mathematical, physical, and engineering sciences*, vol. 371, 2013.

[95] A. Guez, M. Mirza, K. Gregor, R. Kabra, S. Racanière, T. Weber, D. Raposo, A. Santoro, L. Orseau, T. Eccles, G. Wayne, D. Silver, and T. Lillicrap, "An investigation of model-free planning," *Proceedings of the 36th International Conference on Machine Learning*, 2019.

[96] P. Swazinna, S. Udluft, D. Hein, and T. Runkler, "Comparing model-free and model-based algorithms for offline reinforcement learning," *IFAC-PapersOnLine*, vol. 55, no. 15, pp. 19–26, 2022. 6th IFAC Conference on Intelligent Control and Automation Sciences ICONS 2022.

[97] H. Zhu, B. Huang, and S. Russell, "On representation complexity of model-based and model-free reinforcement learning," *arxiv*, 2024.

[98] Y. Lei and A. Solway, "Conflict and competition between model-based and model-free control," *PLoS Computational Biology*, vol. 18, 2022.

[99] Y. Qian, "Deep learning for secure wireless communications in cyber physical systems," *IEEE Wireless Communications*, vol. 29, no. 2, pp. 2–3, 2022.

[100] L. Ballotta, G. Peserico, and F. Zanini, "A reinforcement learning approach to sensing design in resource-constrained wireless networked control systems," in *2022 IEEE 61st Conference on Decision and Control (CDC)*, IEEE, Dec. 2022.

[101] C. S. Wickramasinghe, K. Amarasinghe, D. L. Marino, C. Rieger, and M. Manic, "Explainable unsupervised machine learning for cyber-physical systems," *IEEE Access*, vol. 9, pp. 131824–131843, 2021.

[102] O. Scheler, K. Makuch, P. Debski, M. Horka, A. Ruszczak, N. Pacocha, K. Sozański, O.-P. Smolander, W. Postek, and P. Garstecki, "Droplet-based digital antibiotic susceptibility screen reveals single-cell clonal heteroresistance in an isogenic bacterial population," *Scientific Reports*, vol. 10, p. 3282, 02 2020.

[103] W. Li, H. Xi and S. H. Tan, "Insights and Advancements in Microfluidics," in *Micromachines*, MDPI, sep 2017.

[104] L. Brümmer, S. Katzenschlager, M. Gaeddert, C. Erdmann, S. Schmitz, M. Bota, M. Grilli, J. Larmann, M. Weigand, N. Pollock, A. Macé, S. Carmona, S. Ongarello, J. Sacks, and C. Denkinger, "Accuracy of novel antigen rapid diagnostics for sars-cov-2: A living systematic review and meta-analysis," *PLOS Medicine*, vol. 18, p. e1003735, 08 2021.

[105] N. Gyimah, O. Scheler, T. Rang, and T. Pardy, "Can 3d printing bring droplet microfluidics to every lab?—a systematic review," *Micromachines*, vol. 12, no. 3, 2021.

[106] K. Pärnamets, T. Pardy, A. Koel, T. Rang, O. Scheler, Y. Le Moullec, and F. Afrin, "Optical detection methods for high-throughput fluorescent droplet microflow cytometry," *Micromachines*, vol. 12, no. 3, 2021.

[107] L. C. Silva, M. Perkusich, F. M. Bublitz, H. O. Almeida, and A. Perkusich, "A model-based architecture for testing medical cyber-physical systems," in *Proceedings of the 29th Annual ACM Symposium on Applied Computing*, SAC '14, (New York, NY, USA), p. 25–30, Association for Computing Machinery, 2014.

[108] T. Li, F. Tan, Q. Wang, L. Bu, J.-N. Cao, and X. Liu, "From offline toward real-time: A hybrid systems model checking and cps co-design approach for medical device plug-and-play (mdpnp)," in *2012 IEEE/ACM Third International Conference on Cyber-Physical Systems*, pp. 13–22, IEEE, 2012.

[109] "Iso/iec/ieee international standard for health informatics–device interoperability–part 20701:point-of-care medical device communication–service oriented medical device exchange architecture and protocol binding," *ISO/IEEE 11073-20701:2020(E)*, pp. 1–48, 2020.

[110] G. Ausiello and L. Cabibbo, "Expressiveness and complexity of formal systems," in *Functional Models of Cognition: Self-Organizing Dynamics and Semantic Structures in Cognitive Systems* (A. Carsetti, ed.), pp. 103–120, Dordrecht: Springer Netherlands, 2000.

[111] T. Murata, "Petri nets: Properties, analysis and applications," *Proceedings of the IEEE*, vol. 77, no. 4, pp. 541–580, 1989.

[112] M. Diaz, "Application of petri nets to communication protocols," in *Petri Nets: Fundamental Models, Verification and Applications*, pp. 27 – 39, Wiley-ISTE, 01 2010.

[113] M. R. Hall and V. J. Benokraitis, "A mission planning architecture for an autonomous vehicle," in *Proceedings of the 1st International Conference on Industrial and Engineering Applications of Artificial Intelligence and Expert Systems, IEA/AIE 1988*, vol. 1, pp. 582–589, 1988.

[114] M. Mansouri-Samani, P. Mehlitz, C. Pasareanu, J. Penix, G. Brat, L. Markosian, O. O'Malley, T. Pressburger, and W. Visser, "Program model checking – a practitioner's guide," 01 2008. Technical Memorandum (TM) NASA/TM-2008-214577.

[115] T. A. Henzinger, P.-H. Ho, and H. Wong-Toi, "Hytech: A model checker for hybrid systems," in *Proceedings of the 9th International Conference on Computer Aided Verification*, CAV '97, (Berlin, Heidelberg), p. 460–463, Springer-Verlag, 1997.

[116] P. Baillot and A. Ghyselen, "Types for complexity of parallel computation in pi-calculus," *ACM Trans. Program. Lang. Syst.*, vol. 44, jul 2022.

[117] F. Patou, M. Dimaki, W. E. Svendsen, K. Kjægaard, and J. Madsen, "A smart mobile lab-on-chip-based medical diagnostics system architecture designed for evolvability," in *2015 Euromicro Conference on Digital System Design*, pp. 390–398, 2015.

[118] I. Graja, S. Kallel, N. Guermouche, S. Cheikhrouhou, and A. Hadj Kacem, "A comprehensive survey on modeling of cyber-physical systems," *Concurrency and Computation: Practice and Experience*, vol. 32, no. 15, p. e4850, 2020.

[119] X. Jin, A. Saifullah, C. Lu, and P. Zeng, "Real-time scheduling for event-triggered and time-triggered flows in industrial wireless sensor-actuator networks," in *IEEE INFOCOM 2019 - IEEE Conference on Computer Communications*, pp. 1684–1692, 2019.

[120] M. Mitici, J. Goseling, M. Graaf, and R. Boucherie, "Decentralized vs. centralized scheduling in wireless sensor networks for data fusion," *ICASSP, IEEE International Conference on Acoustics, Speech and Signal Processing - Proceedings*, pp. 5070–5074, 05 2014.

[121] A. David, P. G. Jensen, K. G. Larsen, M. Mikučionis, and J. H. Taankvist, "Uppaal stratego," in *Tools and Algorithms for the Construction and Analysis of Systems* (C. Baier and C. Tinelli, eds.), (Berlin, Heidelberg), pp. 206–211, Springer Berlin Heidelberg, 2015.

[122] T. Sanislav, S. Zeadally, G. Mois, and H. Fouchal, "Multi-agent architecture for reliable cyber-physical systems (cps)," in *2017 IEEE Symposium on Computers and Communications (ISCC)*, pp. 170–175, 2017.

[123] Q. Zhu, L. Bushnell, and T. Başar, *Resilient Distributed Control of Multi-agent Cyber-Physical Systems*, pp. 301–316. Heidelberg: Springer International Publishing, 2013.

[124] M. Yogeswaran and S. G. Ponnambalam, "Reinforcement learning: Exploration-exploitation dilemma in multi-agent foraging task," *Opsearch*, vol. 49, no. 3, pp. 223–236, 2012.

[125] S. Boyd and L. Vandenberghe, *Convex Optimization*. Cambridge University Press, 2004.

[126] C. She, R. Dong, Z. Gu, Z. Hou, Y. Li, W. Hardjawana, C. Yang, L. Song, and B. Vucetic, "Deep Learning for Ultra-Reliable and Low-Latency Communications in 6G Networks," *IEEE Network*, vol. 34, no. 5, pp. 219–225, 2020.

[127] S. Brandi, M. Fiorentini, and A. Capozzoli, "Comparison of online and offline deep reinforcement learning with model predictive control for thermal energy management," *Automation in Construction*, vol. 135, p. 104128, 03 2022.

[128] D. Ernst, M. Glavic, F. Capitanescu, and L. Wehenkel, "Model predictive control and reinforcement learning as two complementary frameworks," *Proceedings of the 13th IFAC Workshop on Control Applications of Optimisation*, 01 2006.

[129] S. Sendari, *Study on robustness and adaptability of genetic network programming with reinforcement learning for mobile robot*. PhD thesis, Waseda University, Japan, 2013.

[130] D. Görges, "Relations between model predictive control and reinforcement learning," *IFAC-PapersOnLine*, vol. 50, no. 1, pp. 4920–4928, 2017. 20th IFAC World Congress.

[131] S. Chen and Y. Li, "An overview of robust reinforcement learning," *2020 IEEE International Conference on Networking, Sensing and Control (ICNSC)*, pp. 1–6, 2020.

[132] Y. Lin, J. McPhee, and N. L. Azad, "Comparison of deep reinforcement learning and model predictive control for adaptive cruise control," *IEEE Transactions on Intelligent Vehicles*, vol. 6, no. 2, pp. 221–231, 2021.

[133] S. Dean, H. Mania, N. Matni, B. Recht, and S. Tu, "On the sample complexity of the linear quadratic regulator," *Foundations of Computational Mathematics*, vol. 20, 10 2017.

[134] A. A. Ghaffar and T. Richardson, "Model Reference Adaptive Control and LQR Control for Quadrotor with Parametric Uncertainties," *International Journal of Mechanical, Aerospace, Industrial, Mechatronic and Manufacturing Engineering*, vol. 9, no. 2, pp. 244–250, 2015.

[135] A. Scampicchio and G. Pillonetto, "A convex approach to robust lqr," in *2020 59th IEEE Conference on Decision and Control (CDC)*, pp. 3705–3710, 2020.

[136] H. Mohammadi, M. Soltanolkotabi, and M. R. Jovanović, "On the linear convergence of random search for discrete-time lqr," *IEEE Control Systems Letters*, vol. 5, no. 3, pp. 989–994, 2021.

[137] I. Clavera, J. Rothfuss, J. Schulman, Y. Fujita, T. Asfour, and P. Abbeel, "Model-based reinforcement learning via meta-policy optimization," in *Proceedings of The 2nd Conference on Robot Learning, PMLR 87:617-629*, 2018.

[138] V. Feinberg, A. Wan, I. Stoica, M. I. Jordan, J. E. Gonzalez, and S. Levine, "Model-based value estimation for efficient model-free reinforcement learning," in *Computing Research Repository (CoRR)*, 2018.

[139] D. Silver, T. Hubert, J. Schrittwieser, I. Antonoglou, M. Lai, A. Guez, M. Lanctot, L. Sifre, D. Kumaran, T. Graepel, T. Lillicrap, K. Simonyan, and D. Hassabis, "A general reinforcement learning algorithm that masters chess, shogi, and go through self-play," *Science*, vol. 362, no. 6419, pp. 1140–1144, 2018.

[140] A. Harvey, K. Laskey, and K.-C. Chang, "Machine learning applications for sensor tasking with non-linear filtering," 03 2021.

[141] C. Szepesvári, "Algorithms for reinforcement learning," *Synthesis Lectures on Artificial Intelligence and Machine Learning*, vol. 4, 01 2010.

[142] H. v. Hasselt, A. Guez, and D. Silver, "Deep reinforcement learning with double q-learning," in *Proceedings of the Thirtieth AAAI Conference on Artificial Intelligence*, AAAI'16, p. 2094–2100, AAAI Press, 2016.

[143] K. Sivamayil, E. Rajasekar, B. Aljafari, S. Nikolovski, S. Vairavasundaram, and I. Vairavasundaram, "A systematic study on reinforcement learning based applications," *Energies*, vol. 16, no. 3, 2023.

[144] Y. Wang, L. Dong, and C. Sun, "Cooperative control for multi-player pursuit-evasion games with reinforcement learning," *Neurocomputing*, vol. 412, pp. 101–114, 2020.

[145] Y. Wang, S. Fang, J. Hu, and D. Huang, "A novel active disturbance rejection control of pmsm based on deep reinforcement learning for more electric aircraft," *IEEE Transactions on Energy Conversion*, vol. 38, no. 2, pp. 1461–1470, 2023.

[146] D. D. Ningombam, "Deep reinforcement learning algorithms for machine-to-machine communications: A review," in *2022 13th International Conference on Computing Communication and Networking Technologies (ICCCNT)*, pp. 1–5, 2022.

[147] Y. Song, Y. Zhou, A. Sekhari, J. A. Bagnell, A. Krishnamurthy, and W. Sun, "Hybrid rl: Using both offline and online data can make rl efficient," 2023. arxiv / 11th International Conference on Learning Representations 2023 (ICLR 2023).

[148] T. Joshi, H. Kodamana, H. Kandath, and N. Kaisare, "Tasac: A twin-actor reinforcement learning framework with a stochastic policy with an application to batch process control," *Control Engineering Practice*, vol. 134, p. 105462, 2023.

[149] T. Haarnoja, A. Zhou, P. Abbeel, and S. Levine, "Soft actor-critic: Off-policy maximum entropy deep reinforcement learning with a stochastic actor," *International Conference on Machine Learning (ICML)*, 2018.

[150] P. Hart, L. Rychly, and A. Knoll, "Lane-merging using policy-based reinforcement learning and post-optimization," in *2019 IEEE Intelligent Transportation Systems Conference (ITSC)*, pp. 3176–3181, 2019.

[151] X. Wu, R. Li, Z. He, T. Yu, and C. Cheng, "A value-based deep reinforcement learning model with human expertise in optimal treatment of sepsis," *Nature Partners Jounal - npj Digital Medicine*, vol. 6, 02 2023.

[152] X. Xiao, "Chapter 13 - qos in wireless networks," in *Technical, Commercial and Regulatory Challenges of QoS* (X. Xiao, ed.), The Morgan Kaufmann Series in Networking, pp. 225–246, Boston: Morgan Kaufmann, 2008.

[153] S. Wei, Z. Zheng, and C. Wu, "Channel Power Allocation Optimization Based on Water-filling Algorithm in 5G," *Journal of Physics: Conference Series*, vol. 1871, no. 1, 2021.

[154] Z. Qu, Z. Qin, J. Wang, L. Luo, and Z. Wei, "A cooperative game theory approach to resource allocation in cognitive radio networks," in *2010 2nd IEEE International Conference on Information Management and Engineering*, pp. 90–93, 2010.

[155] G. Kang, J. Liu, M. Tang, and Y. Xu, "An effective dynamic web service selection strategy with global optimal qos based on particle swarm optimization algorithm," in *2012 IEEE 26th International Parallel and Distributed Processing Symposium Workshops PhD Forum*, pp. 2280–2285, 2012.

[156] S. Mallik and Z. Zhao, "Graph- and rule-based learning algorithms: a comprehensive review of their applications for cancer type classification and prognosis using genomic data," *Briefings in bioinformatics*, 2019.

[157] A. K. Shakya, G. Pillai, and S. Chakrabarty, "Reinforcement learning algorithms: A brief survey," *Expert Systems with Applications*, vol. 231, p. 120495, 2023.

[158] F. Salahdine, T. Han, and N. Zhang, "5g, 6g, and beyond: Recent advances and future challenges," *annals of telecommunications - annales des télécommunications*, pp. 1–21, 12 2022.

[159] M. Abusubaih, "Intelligent wireless networks: Challenges and future research topics," *Journal of Network and Systems Management*, vol. 30, 01 2022.

[160] N. K. Breesam, W. A. Al-Hussaibi, F. H. Ali, and I. M. Al-Musawi, "Efficient resource allocation for wireless-powered mimo-noma communications," *IEEE Access*, vol. 10, pp. 130302–130313, 2022.

[161] J. Zhang and Y. Zhang, "Optimal linear modeling and its applications on swing-up and stabilization control for rotary inverted pendulum," in *Proceedings of the 30th Chinese Control Conference*, pp. 493–500, 2011.

[162] L. B. Prasad, B. Tyagi, and H. O. Gupta, "Optimal control of nonlinear inverted pendulum system using PID controller and LQR: Performance analysis without and with disturbance input," *International Journal of Automation and Computing*, vol. 11, no. 6, pp. 661–670, 2014.

[163] M. Schwenzer, M. Ay, T. Bergs, and D. Abel, "Review on model predictive control: an engineering perspective," *The International Journal of Advanced Manufacturing Technology*, vol. 117, pp. 1–23, 11 2021.

[164] F. Tobagi and J. Long, "Client-server challenges for digital video," in *Digest of Papers COMPCON Spring 1992*, pp. 88–91, 1992.

[165] E. Drakopoulos and M. Merges, "Performance study of client-server storage systems," in *[1991] Digest of Papers Eleventh IEEE Symposium on Mass Storage Systems*, pp. 67–72, 1991.

[166] R. Rajkumar, M. Gagliardi, and L. Sha, "The real-time publisher/subscriber inter-process communication model for distributed real-time systems: design and implementation," in *Proceedings Real-Time Technology and Applications Symposium*, pp. 66–75, 1995.

[167] M. A. Mastouri and S. Hasnaoui, "Performance of a Publish/Subscribe Middleware for the Real Time Distributed Control systems," in *International Journal of Computer Science and Network Security*, 2007.

[168] D. Li, Y. Xu, M. Zhao, J. Zhu, and S. Zhang, "Knowledge-driven machine learning and applications in wireless communications," *IEEE Transactions on Cognitive Communications and Networking*, vol. 8, no. 2, pp. 454–467, 2022.

[169] J. Haxhibeqiri, P. A. Campos, I. Moerman, and J. Hoebeke, "Safety-related applications over wireless time-sensitive networks," in *IEEE 27th International Conference on Emerging Technologies and Factory Automation (ETFA)*, 2022.

[170] K. Nikhileswar, K. Prabhu, D. Cavalcanti, and A. Regev, "Time-sensitive networking over 5g for industrial control systems," in *2022 IEEE 27th International Conference on Emerging Technologies and Factory Automation (ETFA)*, p. 1–8, IEEE Press, 2022.

[171] Y. Lu, L. Yang, S. X. Yang, Q. Hua, A. K. Sangaiah, T. Guo, and K. Yu, "An intelligent deterministic scheduling method for ultralow latency communication in edge enabled industrial internet of things," *IEEE Transactions on Industrial Informatics*, vol. 19, no. 2, pp. 1756–1767, 2023.

[172] P. Popovski, F. Chiariotti, K. Huang, A. E. Kalør, M. Kountouris, N. Pappas, and B. Soret, "A perspective on time toward wireless 6g," *Proceedings of the IEEE*, vol. 110, no. 8, pp. 1116–1146, 2022.

[173] E. Uysal, O. Kaya, A. Ephremides, J. Gross, M. Codreanu, P. Popovski, M. Assaad, G. Liva, A. Munari, B. Soret, T. Soleymani, and K. H. Johansson, "Semantic communications in networked systems: A data significance perspective," *IEEE Network*, vol. 36, no. 4, pp. 233–240, 2022.

[174] X. Luo, H.-H. Chen, and Q. Guo, "Semantic communications: Overview, open issues, and future research directions," *IEEE Wireless Communications*, vol. 29, no. 1, pp. 210–219, 2022.

[175] O. Ayan, P. Kutsevol, H. Y. Özkan, and W. Kellerer, "Semantics- and task-oriented scheduling for networked control systems in practice," *IEEE Access*, vol. 10, pp. 115673–115690, 2022.

[176] P. Kutsevol, O. Ayan, and W. Kellerer, "Towards semantic-aware transport layer protocols: A control performance perspective," in *ICC 2023 - IEEE International Conference on Communications*, pp. 997–1002, 2023.

[177] L. Zhao and W. Li, "Co-design of dual security control and communication for nonlinear cps under dos attack," *IEEE Access*, vol. 8, pp. 19271–19285, 2020.

Acknowledgements

I also want to express my gratitude to my kind parents and my supportive husband. Their steadfast support, empathy, and belief in me have been important in my academic as well as professional achievements. Their persistent presence, affection, and support have provided me with stability and inspiration to surmount challenges and achieve my research goals.

Abstract

Co-Design of Wireless Networked Control Systems: Model-based Architecture and Joint Optimization

Wireless networked control systems (WNCS) combine wireless communication, compute, and control in a distributed topology. The potential applications of WNCSs may be found in a variety of fields under the umbrella of the Industrial Internet of Things (IIoT), including industrial automation, autonomous vehicles, healthcare, smart cities, etc. In contrast to conventional communication systems that prioritize data delivery, WNCSs aim for optimal control under resource constraints; they work in a closed-loop mode, where the controller adapts to the system and network conditions. This makes WNCSs well suited for building robust and efficient systems. However, designing WNCSs presents notable challenges, including managing uncertainties, delays, packet losses, and synchronization errors in the wireless channel, while at the same time guaranteeing the reliability, scalability, and resilience of the system. which calls for the co-design of communication and control. Moreover, the complexity of designing WNCSs rises when the model of the devices and/or their environments is unknown or only partially known, a common case in real-world situations. This calls for adaptive and robust control strategies that can learn from data and cope with uncertainties. This thesis revolves around a co-design framework for WNCSs and explores the suitability and significance of model-based and model-free design methods for achieving reliability, resource efficiency, and scalability.

The contributions are:

(i) A novel model-based system architecture for event-triggered wireless control with extended timed automata, and the specification and verification thereof. Strategies for achieving specific delays and bandwidth consumption while preventing packet loss during network congestion are proposed and compared. The results on a droplet flow cytometer use case indicate that under strict delay constraints and high traffic, the system chooses the decentralized strategy over the centralized strategy, whereas in scenarios with low traffic, the centralized strategy is more effective at ensuring the reliable operation of systems. The minimum delay between two systems is 129 ms (centralized), 87 ms (decentralized), and 125 ms (when avoiding high-traffic scenarios).

(ii) A novel joint optimization of WNCSs using a co-design approach. A classical optimization theory is used to minimize control errors under network constraints, as well as errors introduced by the used reinforcement Q-learning technique. The problem is extended and applied to a droplet generation system. Control performance is evaluated for three algorithms (C51, DQN, DDQN) and three scenarios (without and with network effects in the reward function, and with network uncertainties with random variables in the RL reward function). Results show that the C51 algorithm performs better than the two other algorithms, which is mostly attributed to its ability to effectively solve multi-modal problems.

(iii) A novel method aiming to maximize control-communication reliability and resource efficiency across the control and communication layers by controlling InterPacket Gap (IPG).

The proposed method addresses the reliability of control communication and the efficiency of resource utilization concurrently by integrating RL techniques. The validation method offers a more thorough and practical assessment of the suggested optimization procedure, as opposed to the prevailing primarily analytical methodologies

seen in previous research. The proposed approach successfully solves a multi-objective problem by using co-design reinforcement learning (RL)-based control method. Simulation results show that this method effectively maintains or improves control performance, even in the presence of packet losses. The proposed RL-based technique demonstrates an average decrease in transmission power of up to 10% and is resilient to network packet loss, a common issue in older control systems that may lead to significant performance degradation.

(iv) A novel decentralized communication-based data flow structure that supports different devices in a bioanalytical laboratory unit, including the conceptual, logical, and physical data flow models. The case study shows that the proposed system model worked as expected when subjected to the specified constraints and demonstrates the implications of formal techniques for the design and verification of wireless automation of high-throughput laboratory setups in Model-Based System Engineering (MBSE).

(v) an additional contribution is the suggested development of a wireless communication-based automation system that operates in an event-triggered way, utilizing pre-defined data structures in a publisher-subscriber configuration.

Kokkuvõte

Juhtmevabade võrgustatud juhtimissüsteemide koosdisain: mudelipõhine arhitektuur ja ühisoptimeerimine

Juhtmevaba võrgustikuga juhtimissüsteemid ("Wireless networked control systems" ehk WNCS) mis on ühendatud hajusas topoloogias ja sisaldavad kombinatsiooni juhtmevabast suhtlusest, arvutusvõimsusest ning juhtkontrollerist. WNCS-ide potentsiaalseid rakendusi võib leida mitmesugustes valdkondades mis on seotud tööstuslike asjade internetiga ("Industrial Internet of Things" ehk IIoT), sealhulgas tööstusautomaatika, autonoomsed sõidukid, tervishoid, nutikad linnad jne. Erinevalt tavapärastest sidesüsteemidest, mis eelistavad andmete edastamist, on WNCS-ide eesmärk optimaalne juhtimine ressursi piirangute korral. Nad töötavad suletud ahela režiimis, kus juhtkontroller kohandub süsteemi ja võrgu tingimustega.

See muudab WNCS-id sobivaks töökindlate ja tõhusate süsteemide ehitamiseks. Kuid WNCS-ide kavandamine esitab märkimisväärseid väljakutseid nagu võrgu ebakindluse, viivituste, andmepakettide kadumise ja sünkroniseerimisvigade haldamiseks juhtmevabas kanalis, tagades samal ajal süsteemi usaldusväärsuse, skaleeritavuse ja vastupidavuse. See nõuab side- ja juhtimissüsteemi ühiskavandamist.

Lisaks suureneb WNCS-ide kavandamise keerukus, kui seadmete ja/või nende keskkondade mudel on teadmata või ainult osaliselt teada, mis on reaalse maailma puhul tavapärane. See nõuab adaptiivseid ja vastupidavaid juhtimisstrateegiaid, mis suudavad õppida andmetest ja tulla toime tõrgete ja vigadega. See väitekiri keskendub WNCS-ide ühiskavandamise raamistikule ja uurib mudelpõhiste ja mudelivabade kavandamismeetodite sobivust ja tähtsust saavutamaks usaldusväärsust, ressursitõhusust ja skaleeritavust.

Panused on järgmised:

(i) Uus mudelpõhine süsteemi arhitektuur sündmuse-käivitatud juhtmevabaks juhtimiseks on laiendatud ajastatud automaadiga mis toetab nende spetsifitseerimist ja verifitseerimist. Pakutakse ja võrreldakse strateegiaid konkreetsete viivituste ja ribalaiuse tarbimise saavutamiseks, vältides samal ajal pakettide kadu võrgu läbilaskevõime ületamise korral. Tilgavoolu tsütomeetri uuringu tulemused näitavad, et ranged viivituspiirangud ja suure andmemahuga võrguliiklus sunnivad süsteemi valima detsentraliseeritud strateegia keskse strateegia asemel, samas kui madala andmemahuga võrgu stsenaariumides on keskne strateegia süsteemide usaldusväärse toimimise tagamisel tõhusam. Kahe süsteemi vaheline minimaalne viivitus on 129 ms (keskne), 87 ms (detsentraliseeritud) ja 125 ms (suure andmemahuga võrguliikluse vältimisel).

(ii) Uus ühine optimeerimine WNCS-ide jaoks, kasutab ühiskavandamise lähenemist. Klassikaline optimeerimisteooria on kasutusel süsteemi juhtimise vigade minimeerimiseks võrgupiirangute puhul, samuti vigade minimeerimiseks, mida kasutab kinnitusega õppe Q-õppe tehnika. Probleemi lahendust rakendatakse tilkade genereerimise süsteemile. Juhtkontrolleri tulemuslikkust hinnatakse kolme algoritmi (C51, DQN, DDQN) ja kolme stsenaariumi puhul (ilma ja võrgumõjudega preemiafunktsioonis ning võrgu ebakindlusega juhuslike muutujatega RL preemiafunktsioonis). Tulemused näitavad, et C51 algoritm toimib paremini kui kaks muud algoritmi, selle võimele tõhusalt lahendada mitmemoodilisi probleeme.

(iii) Uus meetod, mille eesmärk on maksimeerida juhtkontrolleri ja side usaldusväärsust ning ressursitõhusust läbi võrgu sidekihtide, kontrollides pakettidevahelist lünka ("InterPacket Gap" ehk IPG).

Pakutud meetod käsitleb juhtkontrolleri side usaldusväärsust ja ressursikasutuse tõhusust samaaegselt, integreerides RL-tehnikaid. Pakutud valideerimismeetod pakub põhjalikumat ja praktilisemat hinnangut optimeerimisprotseduurile, erinevalt varasemates uuringutes kasutatud peamiselt analüütilistest metoodidest. Pakutud lähenemisviis lahendab edukalt mitme eesmärgiga probleemi, kasutades kooskavandamise kinnitusega õppe (RL) masinõppe põhist juhtimismeetodit. Simulatsiooni tulemused näitavad, et see meetod säilitab või parandab tõhusalt juhtimissooritust isegi pakettide kadumise korral. Pakutud RL-põhine tehnika näitab kuni 10% keskmisest väiksemat edastusvõimsuse vajadust ja on vastupidav võrgu pakettide kadumisele, mis on tavaline probleem vanemates juhtimissüsteemides ja mis omakorda võib põhjustada olulist jõudluse langust.

(iv) Uus detsentraliseeritud sidepõhine andmevoo struktuur, mis toetab erinevaid seadmeid bioanalüütilises laboriüksuses, sealhulgas kontseptuaalseid, loogilisi ja füüsilisi andmevoo mudeleid. Juhtumiuuring näitab, et pakutud süsteemimudel töötas ootuspäraselt, kui seda rakendati määratud piirangutele, ja uuring demonstreerib formaalsete tehnikate mõju juhtmevaba automaatika kavandamisele ja kontrollimisele suure läbilaskevõimega laboriseadistustes mudelpõhises süsteemiinseneritöös ("Model-Based System Engineering" ehk MBSE).

(v) Lisapanusena on loodud pakkumine arendada juhtmevaba side põhine automaatikasüsteem, mis töötab sündmuse käivitatud viisil, kasutades eeldefineeritud andmestruktuure kirjastaja-tellijate konfiguratsioonis.

Appendix 1

Publication 1
K. Ashraf, Y. Le Moullec, T. Pardy and T. Rang, "Model-based System Architecture for Event-triggered Wireless Control of Bio-analytical Devices," 2021 24th Euromicro Conference on Digital System Design (DSD), 2021, pp. 465-471, https://doi.org/10.1109/DSD53832.2021.00076.

Model-based System Architecture for Event-triggered Wireless Control of Bio-analytical Devices

Kanwal Ashraf
Thomas Johann Seebeck Department of Electronics
Tallinn University of Technology
City, Country: Tallinn, Estonia
email address: kanwal.ashraf@taltech.ee

Yannick Le Moullec
Thomas Johann Seebeck Department of Electronics
Tallinn University of Technology
City, Country: Tallinn, Estonia
email address: yannick.lemoullec@taltech.ee

Tamás Pardy
Department of Chemistry and Biotechnology
& Thomas Johann Seebeck Department of Electronics
Tallinn University of Technology
City, Country: Tallinn, Estonia
email address: tamas.pardy@taltech.ee

Toomas Rang
Thomas Johann Seebeck Department of Electronics
Tallinn University of Technology
City, Country: Tallinn, Estonia
email address: toomas.rang@taltech.ee

Abstract—Bio-analytical devices have gained importance over the past few years because of their application in rapid diagnostics and biochemical analysis. The integration of the Cyber-Physical System (CPS) concept with bio-analytical devices is essential to enable automation of the device. Modeling of CPS-based bio-analytical devices can provide a deeper understanding of system behavior at early design stages and avoid costly iterations. In this paper, a model-based system architecture enabling wireless control of bio-analytical devices is proposed using the extended timed automata-based formal technique. Using this formal technique, a study case "A droplet flow cytometer for antibiotic susceptibility testing of bacteria" is modeled and verified using the UPPAAL tool. The synchronized operation of the modeled system under defined constraints was confirmed. In addition, the case study shows the implications of formal techniques for the design and verification of wireless automation of high-throughput laboratory setups in Model-Based System Engineering (MBSE).

Index Terms—Cyber-physical systems, Automata, Formal Verification, Biochemical analysis, Biological system modeling, Networked control systems

I. INTRODUCTION

The demand for automation in laboratory-based biochemical analysis and handheld rapid diagnostic devices has increased drastically over the past few years. The major factors affecting this increased demand are advancements in drug development, analysis, testing and rapid diagnostic methods [1], [2]. However, there are several challenges associated with achieving this automation and the problem complexity is well-defined in our previous works [3], [4].

To support automation in bio-analytics, the integration of Cyber-Physical System (CPS) concepts with the microfluidic and biochemical domains has become very topical. CPSs integrate physical and computational processing via a communication network [5], [6] and accounts for user feedback via the cloud. Besides, feedback is also provided from the control system to the physical processes over the communication channel and vice-versa [7]. CPSs have applications in several disciplines including healthcare, education, smart grid, automotive industry, etc. [8].

When designing a CPS, it is desirable to model the system for analyzing its behavior at the early design stage. The major properties that should be considered while designing CPSs include a range of functional and non-functional properties. Functional properties depict a particular behavior of the system, while non-functional properties include time-related properties, physical properties and behavioral properties. The reason to take these properties into account is to ensure a safe automated operation of the system. In [9], a comprehensive survey highlighting different modeling languages and techniques and what aspects each of them lacks has been provided.

To enable automation in the healthcare field, there have been several architectures and models proposed over the past few years which integrated the CPSs concepts with medical devices [10], [11]. However, such integration with bio-analytical devices is still new, under-researched, and there are very few works proposing an architecture and model for the design of these devices.

In [12], the authors proposed a modified schematic for bio-analytical devices by separating the fluidic and biochemical domains from physical processes in the CPSs architecture. Another research [13] proposed an evolvable system architecture

for lab-on-a-chip (LOC) devices. That work was extended to define platform-based design for LOC devices [14] and later a model-based system design framework was proposed for life science instruments [15]. The works [12], [15] motivated model-based system design methodology in bio-analytical and diagnostic devices and modeled the system using SysML. Using SysML it is possible to model system behavior but, as mentioned earlier in this paper, non-functional properties are essential for synchronized operation of the system under constraints; they cannot be completely handled with such an approach.

Moreover, neither of the aforementioned works focused on the communication domain of the device in detail. The introduction of wireless control in bio-analytical devices could help enable several features including scalability, robustness, and remote operation of these devices but will also introduce significant challenges. According to the authors' knowledge, despite its many features and advantages, wireless control of bio-analytical devices has not been investigated in depth. This paper seeks to address this research gap by providing a wireless control model for bio-analytical devices. Figure 1 depicts a simplified architecture concept for wireless control of a bio-analytical cyber-physical system also known as CBPS [15] and CPBS [12] by introducing the communication domain, in addition to the physical, fluidic and cyber domains. Here, the communication domain connects the cyber domain with the physical and fluidic domain and is assumed to deal with network management and supervision.
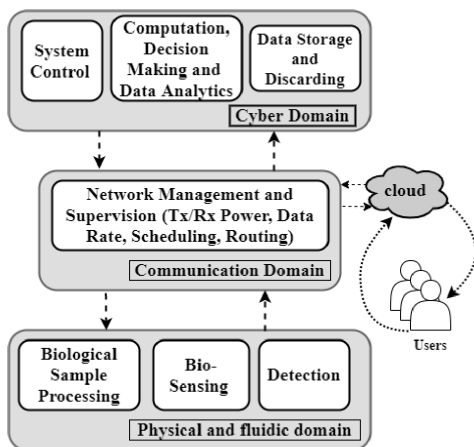

Fig. 1. Bio-analytical cyber physical system concept with cyber, communication, physical and fluidic domains

For considering the non-functional properties of the CPSs in modeling, the best method so far is to use formal techniques. Formal techniques use a mathematical approach to precisely define system behavior [9]. Some of the formal methods are Pi-calculus, Petri-net and Hybrid automata. Hybrid automata

[16], [17] is the most popular formal technique used in CPSs modeling because of its ability to model both the continuous and discrete behavior of the system. Timed automata, a sub-class of hybrid automata, are widely used for modeling a wide range of real-time systems as they can completely automate the verification and validation process, which is our main motivation.

The major contributions of this paper are as below:

- We propose a novel model-based system architecture concept for event-triggered wireless control of bio-analytical CPSs using extended timed automata.
- We specify and verify the proposed system concept using extended timed-automata in UPPAAL [18], for a droplet flow cytometer for antibiotic susceptibility testing of bacteria study case.

The event-trigger wireless control approach is employed to make the system resource-efficient. In addition to resource efficiency, the main idea behind modelling the system as event-triggered rather than time-triggered is due to fact that the biological processes are usually slow and could take minutes to hours to complete, whereas the communication is in the order of a few milliseconds. The non-functional properties, specifically time-dependent occurrence of different events in terms of synchronization for the whole system, is ensured. To the best of the authors' knowledge, this is the first work that models a bio-analytical system using a formal method and take wireless network constraints into account. The rest of the paper is organized as follows: Section II describes the preliminaries for the modeling framework, Section III discusses the problem formulation, Section IV presents the timed-automata based modeling for the case study, Section V discusses the model verification, and Section VI concludes the paper and provides some suggestions for future directions.

II. MODELING FRAMEWORK BASICS

Timed automata [19] are a sub-class of hybrid automata with a finite number of real-valued clocks which can be reset. As discussed earlier, the formal approach adopted in this work is based on timed automata; this section provides a few essential preliminary definitions of hybrid and timed automata.

Definition 1 A hybrid automaton is a tuple $H = (L, Var, g, \Gamma, Edge, Act, Inv, Init)$ where:

$L \rightarrow$ Set of locations, States $\Sigma = L \times V$, V: set of all valuations v, where $v : Var \rightarrow \mathbb{R}$

$Var \rightarrow$ Real-Valued Variables, $L \rightarrow 2^{Var}$

$g \rightarrow$ Conditional/Guard function

$\Gamma \rightarrow$ Set of Labels

$Inv \rightarrow$ Invariant function, $Inv(l) \subseteq V$, $l \in L$

$Act \rightarrow$ functions consists of set of activities, $f : \mathbb{R}_{\geq 0} \rightarrow V$

$Edge \rightarrow$ Set of transitions, $Edge \subseteq L \times \Gamma \times g(Var) \times 2^{Var} \times L$

$Init \rightarrow$ Initial Location, $Init \subseteq L$

The semantics of hybrid automata are based on two rules, discrete rule for discrete state transitions and continuous time

466

rule based on continuous time steps. The discrete rule governing transitions between states is written as $(l, v) \xrightarrow{a} (l', v')$ for $(l, a, (v, v'), l') \in Edge$ and invariant $v' \in Inv(l')$ must hold. On the other hand, the time rule governing: the time can pass in current location and the variable related to the location can evolve given that $f \in Act$ such that $f(0) = v, f(t) = v'$. The continuous time rule is given by $(l, v) \xrightarrow{a} (l, v')$ for $f[(0, t)] \in Inv(l)$ and t is strictly positive.

Definition 2 A timed automaton is a tuple $T = (L, \Gamma, Edge, C, Inv, Init)$ where:

$L \rightarrow$ Set of locations, States $\Sigma = L \times V$, V: set of all valuations v, where $v : Var \rightarrow \mathbb{R}$

$C \rightarrow$ Set of real-valued clocks

$\Gamma \rightarrow$ Set of Labels

$Inv \rightarrow$ function that assigns set of invariants to locations based on Clock Constraints (CC), $L \rightarrow CC(C)$

$Edge \rightarrow$ Set of transitions, $Edge \subseteq L \times CC(C) \times \Gamma \times 2^C \times L$

$Init \rightarrow$ Set of Initial States, $Init \subseteq L$

The semantics for timed-automata are given by:

Discrete Rule

$$(l, v) \xrightarrow{a} (l', v') : (l, a, (g, C), l') \in Edge$$
$$, v \models g, v' = reset(C) \ v, v' \models Inv(l') \quad (1)$$

where g is the guard.

Continuous Time Rule

$$(l, v) \xrightarrow{t} (l, v') : t \in \mathbb{R}_{\geq 0},$$
$$v' \models Inv(l), v' = v + t \quad (2)$$

Definition 3: Parallel composition The parallel timed automata composition $T_1 \parallel T_2 ... \parallel T_n$ of n systems such that $T_1 = (L_1, \Gamma_1, Edge_1, C_1, Inv_1, Init_1)$, $T_2 = (L_2, \Gamma_2, Edge_2, C_2, Inv_2, Init_2), ..., T_n = (L_n, \Gamma_n, Edge_n, C_n, Inv_n, Init_n)$, and such that clocks and states are pairwise disjoint, is given by:

- $L = L_1 \times L_2 \times ... \times L_n$
- $C = C_1 \times C_2 ... \times C_n$
- $\Gamma = \Gamma_1 \times \Gamma_2 ... \times \Gamma_n$
- $Inv(l_1, l_2) = Inv_1(l_1) \wedge Inv_2(l_2), ...,$
  $Inv(l_{n-1}, l_n) = Inv_{n-1}(l_{n-1}) \wedge Inv_n(l_n)$ for all $(l_1, l_2, ... l_n) \in L$
- $Init = \{((l_1, l_2, ... l_n), v) \in \Sigma | (l_1, v) \in Init_1 \wedge (l_2, v) \in Init_2, ... \wedge (l_n, v) \in Init_n\}$

For $i = 1, ..., n$ systems, the discrete transitions between the edges for two systems with automata T_i and T_{i+1} is given by $Rule\ Synchronization$ and $Rule\ Non-Synchronization$ i.e.:

Rule Synch :

$$\frac{(l_i, a, (g_i, C_i), l_i') \in Edge_i, (l_{i+1}, a, (g_{i+1}, C_{i+1}), l_{i+1}') \in Edge_{i+1}}{((l_i, l_{i+1}), a, (g_i \wedge g_{i+1}, C_i \times C_{i+1}), (l_i', l_{i+1}')) \in Edge} \quad (3)$$

Rule Non − Synch$_i$:

$$\frac{(l_i, a, (g, C), l_i') \in Edge_i, a \notin \Gamma_{i+1}}{((l_i, l_{i+1}), a, (g, C), (l_i', l_{i+1})) \in Edge_i} \quad (4)$$

Rule Non − Synch$_{i+1}$:

$$\frac{(l_{i+1}, a, (g, C), l_{i+1}') \in Edge_{i+1}, a \notin \Gamma_i}{((l_i, l_{i+1}), a, (g, C), (l_i, l_{i+1}')) \in Edge} \quad (5)$$

III. PROBLEM FORMULATION

In this section, essential concepts to obtain an event-triggered control for bio-analytical CPSs over the non-deterministic wireless network and the extension of timed-automata is provided.

A. Event-Triggered Control system with Non-deterministic Network

Assuming that each bio-analytical system acts as a Linear Time Invariant (LTI) system, we have the following equation:

$$\dot{\zeta}(t) = A\zeta(t) + Bx(t) . \quad (6)$$

where $\zeta(t)$ is the current state of the system, $\dot{\zeta}(t)$ is the next state of the system and $x(t)$ is the feedback for the system, depending upon controller gain K. Assuming the network is
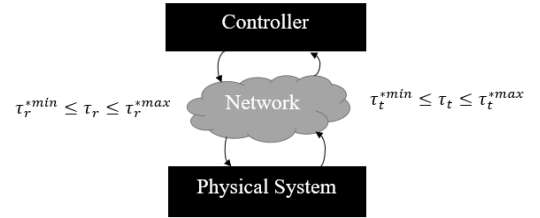

Fig. 2. Wireless control over a non-deterministic network

non-deterministic, i.e. the time taken by each sample to reach its destination is unknown, the delay associated with each sample to be transferred is τ_t and for reception is τ_r. Moreover, there exists minimum times $\tau_t^{*min}, \tau_r^{*min}$ and maximum times required $\tau_t^{*max}, \tau_r^{*max}$ for the sample to be transferred and received, respectively as depicted in figure 2. For a sequence of communication events τ_{ti} and τ_{ri} where $i \in \mathbb{N}$, the following assumption can be made:

$$\tau_t^{*min} \leq \tau_{ti+1} - \tau_{ti} \leq \tau_t^{*max}, \quad 0 < \tau_t^{*min} \leq \tau_t^{*max} \quad (7)$$

$$\tau_r^{*min} \leq \tau_{ri+1} - \tau_{ri} \leq \tau_r^{*max}, \quad 0 < \tau_r^{*min} \leq \tau_r^{*max} \quad (8)$$

To account for the network delays in more detail, one can refer to [20]. The feedback provided by the system to the controller will suffer delay based on the network delay [21]. Equation 9 reflects the controller feedback accounting for network delay.

$$v(t) = K\zeta(t) \quad t \in [t_k + \Delta, t_{k+1} + \Delta] \quad (9)$$

where Δ depends upon τ_r and τ_t. Hence, the difference between the sampled state and the current state is given by equation 10.

$$e(t) = \zeta(t_k) - \zeta(t) \quad t \in [t_k + \Delta, t_{k+1} + \Delta] \quad (10)$$

Employing the event triggered approach based on the same principle as mentioned in [22], the sampled trigger time rule is given by:

$$t_{k+1} = min\left\{t|t > t_k \quad : \quad |e(t)|^2 \geq \sigma|\zeta(t)|^2\right\} \qquad (11)$$

For sampled state x the inter-sample time is given by equation 12 based on trigger coefficient σ

$$\tau_\sigma = min\left\{t||e(t)|^2 \geq \sigma|\zeta(t)|^2 \quad : \quad \zeta(0) = x\right\} \qquad (12)$$

B. Timed Automata based Model for Non-Deterministic Wireless Communication

For the bio-analytical devices consisting of various subsystems, the proposed approach is to control each sub-unit using an event-triggered mechanism, while the network scheduling is priority based. For a simple use case, let σ_i be the trigger coefficient defined by event-triggered system control over non-deterministic channel for the ith single sub-system in the whole system, where $\sigma_i \in [0, \bar{\sigma}]$. The clock constraints (or guards) related to this sub-system are given by

$$\tau_s^{\sigma_i} \leq c \leq \tau_s^{\bar{\sigma}_i} \ . \qquad (13)$$

Assuming that the subsystem has only two states, i.e. Init and Process, the timed automata model of the sub-system can be written as:

- $L = \{Init, Process\}$
- $C = \{c\}$
- $\Gamma = \{a, b\}$
- $Edge = \{(Init, a, (c \geq \tau_s^{\sigma_i}, \{c\}), Process), (Process, b, (c \geq \tau_s^{\bar{\sigma}_i}, \{c\}), Init)\}$
- $Inv = \{Inv(Init) : c \leq \tau_s^{\sigma_i}, Inv(Process) : \tau_s^{\bar{\sigma}_i} < c < \tau_s^{\bar{\sigma}_i}\}$
- $Init = \{(Init, v_0) \text{ with } v_0(c) = 0\}$

The graphical representation of the sub-system is given in Figure 3. To include non-clock local and shared variables
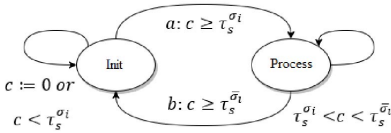

Fig. 3. State machine representation of event triggered control

(channels) and to model stochastic network behavior, we have extended the timed automata as below:

Definition 4 Extended timed automata is a tuple $T = (L, \Gamma, Edge, C, Var, Chan, Inv, Init, P)$ Where
$L \rightarrow$ Set of locations, States $\Sigma = Loc \times V$, V: set of all valuations v, where $v : Var \rightarrow \mathbb{R}$
$C \rightarrow$ Set of real-valued clocks
$Var \rightarrow$ Set of non-clock real valued local variables
$Chan \rightarrow$ Set of non-clock shared variables
$\Gamma \rightarrow$ Set of Labels

$Inv \rightarrow$ function that assigns set of invariants to locations based on Clock Constraints (CC), local variables constraints $\Phi(Var)$ and set of shared channel variables $\varphi(Chan)$, L $\rightarrow CC(C) \wedge \Phi(Var) \wedge \varphi(Chan)$
$Edge \rightarrow$ Set of transitions, $Edge \subseteq L \times CC(C) \times \Phi(Var) \times \varphi(Chan) \times \Gamma \times 2^C \times 2^{Var} \times 2^{Chan} \times L$
$Init \rightarrow$ Set of Initial States, $Init \subseteq L$
$P \rightarrow$ Assigns user-defined exponential delay rate (e) to each location, $L \rightarrow e(P)$
where the exponential rate P defines an exponential distribution to leave each state under unbounded delays. The extended model is well-suited to control parameters like volume, flow-rate and synchronization between the devices.

IV. CASE-STUDY: BIO-ANALYTICAL DEVICES

The basic working principle of a droplet-based flow cytometer for the analysis of bacterial antibiotic susceptibility is based on droplet generation on a large scale, where each droplet encapsulates a single cell or small population of bacteria, reagents and antibiotics [1]. The generated droplets are then incubated to allow bacteria to grow or die depending upon their resilience against the specific concentration of the antibiotic. After the incubation, several images are captured using a high-speed camera. The camera images are then classified using a Machine Learning (ML) algorithm where dead and alive cells are identified. Depending upon the ratio of dead or live cells, the bacterial susceptibility against a specific concentration of the antibiotic can be determined. Figure 4 shows the major sub-blocks of the considered droplet flow cytometer for the analysis of the antibiotic susceptibility of bacteria.

Fig. 4. Use case: flow cytometer for antibiotic susceptibility of bacteria

Based on the major building blocks of the droplet flow cytometer, the system can be divided into three major units, i.e. the Droplet Generation Unit, Imaging Unit/Sensing Unit and Detection Unit. Each of the sub-block has a control unit which is connected to the central controller over a wireless communication network. A brief description of each sub-unit and wireless control unit is given below.

A. Droplet-Generation Unit

The droplet generation unit consists of a pump for controlling pre-processed (incubated) fluids volume at a specific rate

468

for a specified duration and a microfluidic chip. The droplet generation starts with an initialization command to the pump with a defined flow rate and duration. The central controller communicates over the network for initialization and goes to the sleep mode until it is not triggered by the sub-unit with an acknowledgement about its task completion.

B. Imaging Unit

The imaging unit consists of a light source and a high-speed smart camera unit which is capable of capturing images at a variable frame rate (FR). The imaging unit is also able to adjust the resolution and Depth of Field (DoF). The control of the imaging unit activates via central controller at a specified FR, resolution and DoF which is adjustable by the smart camera unit depending on the required image quality.

C. Detection Unit

The detection unit consists of a micro-controller able to classify the images using machine learning. The used ML algorithm could be based on deep learning using artificial neural networks where a trained classifier can classify images depending upon their features.

D. Wireless Control Unit

Upon instantiating, the central controller activates each sub-unit in a specified order over a wireless communication network and goes to sleep or low power mode unless a trigger command is received to acknowledge the task completion by the sub-units. As mentioned earlier in section III-B the network scheduling is priority-based and there is a specified duration for a non-deterministic network to receive and send the commands, both to the controller as well as to the sub-units. The path or run time transitions for the modeled wireless control of these devices are based on Boolean variables/channels, as well as clock variables. They are given as:

Controller Run Time Transitions

$$Initialization \xrightarrow{\text{d1:U1,Chan}} Droplet\_Generation$$
$$\xrightarrow{\text{y:Init2,C}} : Init\_U2 \xrightarrow{\text{d2:U2,Chan}} Imaging, ...$$
$$Detection \xrightarrow{\text{y:finish,C}} Initialization$$

with invariants as below:

$$Inv = \{Inv(Droplet\_Generation) : y{<}tc1\_max,$$
$$Inv(Imaging) : y{<}tc2\_max,$$
$$Inv(Detecion) : y{<}tc3\_max\}$$

Network Run Time Transitions

$$Init \xrightarrow{\text{d1:C1,Chan}} DG\_sending$$
$$\xrightarrow{\text{z:S1,C}} : wait\_DG \xrightarrow{\text{End\_1:R1,Chan}} ACK\_DG, ...$$
$$ACK\_DT \xrightarrow{\text{Rx3:end,Chan}} Init$$

with invariants as below:

$$Inv = \{Inv(DG\_sending) : z{<}tx1\_max,$$
$$Inv(wait\_DG) : z{<}rx1\_max, Inv(ACK\_DG) : z{<}$$
$$rx1\_max, Inv(Im\_Sending) : z{<}tx2\_maxInv(wait\_Im) :$$
$$z{<}rx2\_max, Inv(ACK\_Im) : z{<}rx2\_max, Inv(DT\_$$
$$Sending) : z{<}tx3\_maxInv(wait\_DT) : z{<}rx3\_max,$$
$$Inv(ACK\_DT) : z{<}rx3\_max\}$$

The run time transitions for other sub-units and their parallel composition can be formulated based on the same principles as mentioned here and in Section III.

V. VERIFICATION WITH UPPAAL

Model verification is essential to ensure that the designed system meets all the specifications e.g. time constraints, synchronization and is deadlock-free. For model checking and verification, we used UPPAAL. UPPAAL is a model checking, verification and validation tool [18]. During verification, the system was analyzed under bounded, unbounded and probabilistic delay distribution using Stochastic Model Checking (SMC). Figures 5 and 6 show the Control and Network models executed in UPPAAL for generic subsystems with no specific functionality defined. Each of the sub-systems was then further
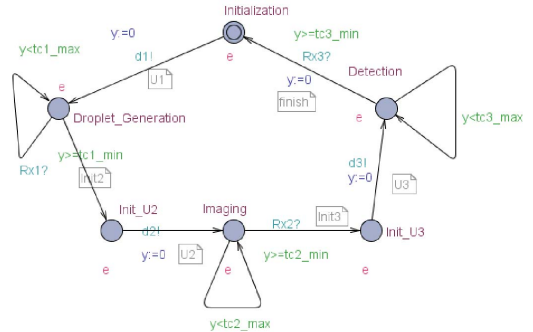
Fig. 5. Control unit for droplet flow cytometer

modeled in depth. Figure 7 shows the detection unit model; for conciseness, the other sub-system models can be found at url: https://github.com/KanwalAshraf/UPPAAL_Models.git.

In addition to the use of the UPPAAL simulator, the models have been further verified using different queries based on the language reference guide of UPPAAL. Examples of some of the queries used for system verification is given in Table I.

Using the query-based verification system, state transitions, probability density distribution and probability comparison of states at different intervals could be verified.

Figure 8 shows the state transition within a bounded time interval; here, the synchronization between different states of the controller, network and sub-unit can be visualized. In addition to exponential delay distribution, the network

469

Fig. 6.   Network unit for droplet flow cytometer

Fig. 7.   Detector unit for droplet flow cytometer

model could also have discrete probabilistic delay defined for different paths in the model.

Figure 9 shows an example of the network model with a discrete probability defined for delayed and non-delayed paths. Figure 10 shows the probability density distribution for ACK_DG state for time lower than (blue bars) and higher

Fig. 8.   Network control model simulation: state transition within a bounded interval

Fig. 9.   Network unit with discrete probabilistic delays

than (orange bars) $rx1\_max$ threshold, with confidence 0.95, for the model depicted in Figure 9. Here the discrete probabilistic choices (1/5, 4/5) associated with the paths increases the probability density associated with $z > rx1\_max$. The discrete probabilistic choice for each path could help in the estimation of the delay in any system. Additionally, the cost and reachability time analysis could also be performed for each path. The formal verification showed that the modeled use case did not violate time constraints and that the device

TABLE I
VERIFICATION QUERIES

Queries	Properties
E $<>$ Communication.wait and $z \geq tx1\_max$	Delay
A[]!(Communication.Sending&& Bio_Chip_control.Rate_Definition)	Synchronization
A[]Communication.wait imply $z \geq$ tx1_min	Reset
simulate[$< = 300$]Network.ACK_DG, Control. Droplet_Generation, Imaging.Process_D2	Simulation
Pr[=<100J($<>$ Network.DG_sending) $>$ $= Pr[<= 100]($<>$ Control.Imaging$)$	Probability Comparison

Fig. 10.   Probability density distribution for the network unit

470

operation was executed in order and synchronized.

VI. CONCLUSION

In this paper, an extended timed-automaton based formal technique was presented for modeling bio-analytical CPSs taking into account control over a wireless network with constraints. The main aim was to provide a formal model-based architecture for bio-analytical devices to motivate the further application of formal techniques in bio-analytical devices. To depict the application of the proposed technique, a case study was modeled and verified using UPPAAL. The use of this model is promising when dealing with large laboratory setups and diagnostic systems and can be used in Model-based System Engineering Methodology (MBSE). The introduction of wireless connectivity will enable the connection of different units in a high-throughput laboratory setup without any physical connection between sub-units and event-triggered control will make the system resource-efficient. The verification helped to analyze the system under bounded, unbounded and probabilistic delay distribution. For future work, there are several issues to consider, including non-deterministic behavior of the device at different user inputs, fault detection of sub-units as well as other network issues including network failure.

REFERENCES

[1] Scheler, O., Makuch, K., Debski, P.R. et al. Droplet-based digital antibiotic susceptibility screen reveals single-cell clonal heteroresistance in an isogenic bacterial population. Sci Rep 10, 3282 (2020), doi: 10.1038/s41598-020-60381-z.

[2] W. Li, H. Xi, and S. H. Tan, Insights and Advancements in Microfluidics. 2018.

[3] Gyimah, Nafisat; Scheler, Ott; Rang, Toomas; Pardy, Tamas (2021). Can 3D Printing Bring Droplet Microfluidics to Every Lab? —A Systematic Review. Micromachines, 12 (3), 339. DOI: 10.3390 / mi12030339 .

[4] Pärnamets, K .; Pardy, T .; Koel, A .; Rang, To .; Scheler, O .; Le Moullec, Y .; Afrin, F. (2021). Optical Detection Methods for High-Throughput Fluorescent Droplet Microflow Cytometry. Micromachines, 12. DOI: 10.3390 / mi12030345 .

[5] R. Crowder, "Cyber Physical systems and security," in Electric Drives and Electromechanical Systems, Elsevier, 2019, pp. 271–289.

[6] K. D. Kim and P. R. Kumar, "Cyber-physical systems: A perspective at the centennial," in Proceedings of the IEEE, May 2012, vol. 100, no. SPL CONTENT, pp. 1287–1308, doi: 10.1109/JPROC.2012.2189792.

[7] H. Li, Communications for Control in Cyber Physical Systems. Elsevier, 2016.

[12] E. Evin and Y. Uluda, "Bioanalytical Device Design with Model-Based Systems Engineering Tools," IEEE Syst. J., vol. 14, no. 3, pp. 3139–3149, 2020, doi: 10.1109/JSYST.2020.2993377.

[8] H. Chen, "Applications of Cyber-Physical System: A Literature Review," J. Ind. Integr. Manag., vol. 02, no. 03, p. 1750012, 2017, doi: 10.1142/s2424862217500129.

[9] I. Graja, S. Kallel, N. Guermouche, S. Cheikhrouhou, and A. Hadj Kacem, "A comprehensive survey on modeling of cyber-physical systems," Concurr. Comput. , vol. 32, no. 15, pp. 1–18, 2020, doi: 10.1002/cpe.4850.

[10] L. C. Silva, M. Perkusich, F. M. Bublitz, H. O. Almeida, and A. Perkusich, "A model-based architecture for testing medical Cyber-Physical Systems," Proc. ACM Symp. Appl. Comput., no. March, pp. 25–30, 2014, doi: 10.1145/2554850.2555028.

[11] T. Li, F. Tan, Q. Wang, L. Bu, J. Cao and X. Liu, "From Offline toward Real-Time: A Hybrid Systems Model Checking and CPS Co-design Approach for Medical Device Plug-and-Play (MDPnP)," 2012 IEEE/ACM Third International Conference on Cyber-Physical Systems, Beijing, China, 2012, pp. 13-22, doi: 10.1109/ICCPS.2012.10.

[13] F. Patou, M. Dimaki, W. E. Svendsen, K. Kjaegaard, and J. Madsen, "A smart mobile lab-on-chip-based medical diagnostics system architecture designed for evolvability," Proc. - 18th Euromicro Conf. Digit. Syst. Des. DSD 2015, no. August, pp. 390–398, 2015, doi: 10.1109/DSD.2015.11.

[14] F. Patou, F. AlZahra'a Alatraktchi, C. Kjægaard, M. Dimaki, J. Madsen, and W. Svendsen, "Evolvable Smartphone-Based Platforms for Point-of-Care In-Vitro Diagnostics Applications," Diagnostics, vol. 6, no. 3, p. 33, 2016, doi: 10.3390/diagnostics6030033.

[15] F. Patou, M. Dimaki, A. Maier, W. E. Svendsen, and J. Madsen, "Model-based systems engineering for life-sciences instrumentation development," Syst. Eng., vol. 22, no. 2, pp. 98–113, 2019, doi: 10.1002/sys.21429.

[16] S. Geng, J. Peng, and P. Li, "Modeling and verification of cyber-physical systems under uncertainty," ICNC-FSKD 2017 - 13th Int. Conf. Nat. Comput. Fuzzy Syst. Knowl. Discov., no. 3, pp. 1491–1496, 2018, doi: 10.1109/FSKD.2017.8392986.

[17] F. Tan, Y. Wang, Q. Wang, L. Bu, R. Zheng, and N. Suri, "Guaranteeing Proper-Temporal-Embedding safety rules in wireless CPS: A hybrid formal modeling approach," Proc. Int. Conf. Dependable Syst. Networks, 2013, doi: 10.1109/DSN.2013.6575357.

[18] J. Bengtsson, K. Larsen, F. Larsson, P. Pettersson, and W. Yi, "UPPAAL-a tool suite for automatic verification of real-time systems," in Lecture Notes in Computer Science (including subseries Lecture Notes in Artificial Intelligence and Lecture Notes in Bioinformatics), Oct. 1996, vol. 1066, pp. 232–243, doi: 10.1007/BFb0020949.

[19] R. Alur and D. L. Dill, "A theory of timed automata," Theor. Comput. Sci., vol. 126, no. 2, pp. 183–235, 1994, doi: 10.1016/0304-3975(94)90010-8.

[20] M. S. Mahmoud and M. M. Hamdan, "Fundamental issues in networked control systems," IEEE/CAA J. Autom. Sin., vol. 5, no. 5, pp. 902–922, 2018, doi: 10.1109/JAS.2018.7511162.

[21] R. G. Sanfelice, "Networked hybrid dynamical systems: Models, specifications, and tools," in Lecture Notes in Control and Information Sciences, vol. 475, Springer Verlag, 2018, pp. 325–356.

[22] P. Tallapragada and N. Chopra, "Event- Triggered dynamic output feedback control of LTI systems over sensor-controller-actuator networks," Proc. IEEE Conf. Decis. Control, pp. 4625–4630, 2013, doi: 10.1109/CDC.2013.6760613.

Appendix 2

Publication 2
K. Ashraf, Y. Le Moullec, T. Pardy and T. Rang, "Design of Cyber Bio-Analytical Physical Systems: Formal Methods, Architectures, and Multi-System Interaction Strategies", Microprocessors and Microsystems, Volume 97, Issue C, pp. 104780, 2023.

Design of Cyber Bio-Analytical Physical Systems: Formal Methods, Architectures, and Multi-System Interaction Strategies

Kanwal Ashraf[a,*], Yannick Le Moullec[a], Tamás Pardy[a,b], Toomas Rang[a,b]

[a]*Thomas Johann Seebeck Department of Electronics, Tallinn University of Technology, Tallinn, Estonia*
[b]*Department of Chemistry and Biotechnology, Tallinn University of Technology, Tallinn, Estonia*

Abstract

Integration of the Cyber-Physical System (CPS) concept with bio-analytical devices is highly desirable to enable device automation as well as to improve diagnostic and analytical capabilities. By modeling CPS-based bio-analytical devices, where the model serves as the foundation for the system design, a thorough evaluation of the system behavior can be provided early in the design process, avoiding costly iterations. On the other hand, this modeling must address the interaction of different entities, the dynamic behavior of the system, as well as the non-functional properties that are essential for the device to function properly.

This paper presents a model-based system architecture that builds upon an extended timed automata-based formal technique that enables the wireless control of bio-analytical devices, in contrast to previous works which build upon SysML or UML based Models. Using this formal approach, a study case "A droplet flow cytometer for antibiotic susceptibility testing of bacteria" is modeled and verified using the UPPAAL tool which shows the implications of formal techniques for the design and verification of wireless automation of high-throughput laboratory setups in Model-Based System Engineering (MBSE). Moreover, the paper extends the above aspects by adding the possibility to model multi-system interaction, which we use to analyze the trade-off between centralized and decentralized information flow strategies for better system performance under delay and bandwidth constraints. UPPAAL Stratego is used to analyze strategies for achieving specific delays and bandwidth consumption while avoiding packet losses in the event of network congestion. The results show that under strict delay constraints and high traffic, the use-case system selects the decentralized strategy over the centralized strategy, whereas in low traffic scenarios, the centralized strategy is more effective to ensure the reliable operation of systems.

Keywords:
Cyber Bio-analytical Physical Systems (CBPSs), Wireless Networked Control Systems, Formal Methods, Formal Verification, Biochemical analysis, Biological system modeling.

1. Introduction

Due to the global spread of various epidemics, there has been a significant increase in the demand for automation in laboratory-based biochemical analysis and handheld rapid diagnostic devices over the past few years. The primary factors driving this increased demand are the need to advance drug development, analysis, testing, and rapid diagnostic methods (1; 2; 3). However, there are several challenges associated with

achieving this automation and the problem complexity is well-defined in our previous works (4; 5).

To support automation in bio-analytics, the integration of Cyber-Physical System (CPS) concepts with the microfluidic and biochemical domains has become very topical. CPSs integrate physical and computational processing via a communication network (6; 7) and accounts for user feedback via the cloud. Besides, feedback is also provided from the control system to the physical processes over the communication channel and vice-versa (8), this feedback is important to obtain a robust and reliable performance of the system under dynamic changes.

When designing a CPS, it is desirable to model the system for analyzing its behavior at the early design stage because the systems are usually complex. The essential points that should be considered while designing CPSs include a range of functional and non-functional properties. Functional properties depict a particular behavior of the system, while non-functional

---

*Corresponding Author
Email addresses: `Kanwal.Ashraf@taltech.ee` (Kanwal Ashraf), `yannick.lemoullec@taltech.ee` (Yannick Le Moullec), `tamas.pardy@taltech.ee` (Tamás Pardy), `toomas.rang@taltech.ee` (Toomas Rang)
URL: `www.taltech.ee` (Kanwal Ashraf), `www.taltech.ee` (Yannick Le Moullec), `www.taltech.ee` (Tamás Pardy), `www.taltech.ee` (Toomas Rang)

properties include time-related properties, physical properties and behavioral properties. The reason to take these properties into account is to ensure a safe automated operation of the system under practical constraints.

To enable automation in the healthcare field, there have been several architectures and models proposed over the past few years which integrated the CPSs concepts with medical devices. The integration of CPSs concepts with bio-analytical devices is still new, under-researched, and there are very few works proposing an architecture and model for the design of these devices.

In (9), the authors proposed a modified schematic for bio-analytical devices by separating the fluidic and biochemical domains from physical processes in the CPSs architecture. Another research (10) proposed an evolvable system architecture for lab-on-a-chip (LOC) devices. That work was extended to define platform-based design for LOC devices (11) and later a model-based system design framework was proposed for life sciences instruments (12). The works (9; 12) motivated model-based system design methodology in bio-analytical and diagnostic devices and modeled the system using SysML. It is possible to model system behavior using SysML; however, as mentioned earlier in this paper, non-functional properties are required for synchronized operation of the system under constraints; they cannot be fully handled with this approach. Furthermore, as the number of interconnected systems increases, so do the variables used to account for this interaction, necessitating a more simplified and reliable modeling approach.

Moreover, neither of the aforementioned works focused on the communication domain of the device in detail. The introduction of wireless control in bio-analytical devices could help enable several features including scalability, robustness, and remote operation of these devices but will also introduce significant challenges. According to the authors' knowledge, despite its many features and advantages, wireless control of bio-analytical devices has not been investigated in depth. This paper seeks to address this research gap by providing a wireless control model for bio-analytical devices. Figure 1 depicts a simplified architecture concept for wireless control of a bio-analytical CPS also known as CBPS (12) and CPBS (9) by introducing the communication domain, in addition to the physical, fluidic and cyber domains. Here, the communication domain connects the cyber domain with the physical and fluidic domain and is assumed to deal with network management and supervision.

So far, the best method for modeling the non-functional properties of CPSs is to use formal techniques. Formal techniques use a mathematical approach to precisely define system behavior (13). Some of the formal methods are Pi-calculus, Petri-net and Hybrid automata. Hybrid automata (14; 15) is the most popular formal technique used in CPSs modeling because of its ability to model both the continuous and discrete behavior of the system. Timed automata, a sub-class of hybrid automata, are widely used for modeling a wide range of real-time systems as they can completely automate the verification and validation process, which is our main motivation.
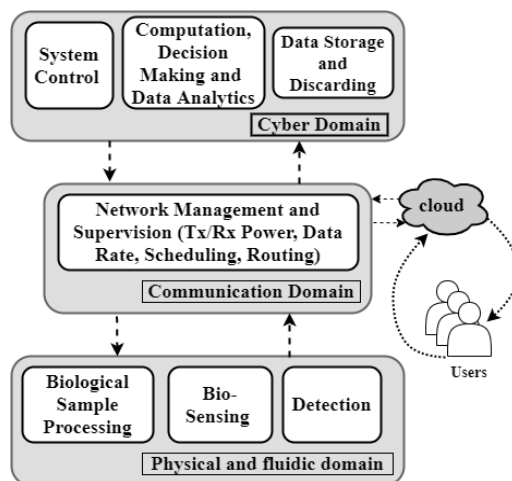

Figure 1. Bio-analytical CPS concept with cyber, communication, physical and fluidic domains

This extended version of the paper (16) provides a more extensive review of the state of the art and proposes additional features and corresponding results related to the modeling of multi-system interaction and analysis of the trade-off between centralized and decentralized information flow strategies. The major contributions of this paper are as below:

- Using extended timed automata, we propose a novel model-based system architecture concept for event-triggered wireless control of bio-analytical CPSs.

- We specify and verify the proposed system concept using extended timed-automata in UPPAAL (17), for a droplet flow cytometer for antibiotic susceptibility testing of bacteria study case.

- To analyze the interaction of several devices, we evaluated the system's trade-off by means of UPPAAL to choose between centralized and decentralized communication architectures under known and unknown traffic patterns.

An investigation of the system's software and hardware requirements for baseline practical implementation of the use-case was made. The event-trigger wireless control approach is employed to make the system resource-efficient. Aside from resource efficiency, the main idea behind modeling the system as event-triggered rather than time-triggered is that biological processes are typically slow and can take minutes to hours to complete, whereas communication occurs in the order of a few milliseconds. The non-functional properties, specifically the time dependent occurrence of different events in terms of synchronization for the whole system, is ensured. Furthermore, using stochastic timed automata, the high-level interaction between two systems for delay and resource constraints is investigated.

To the best of the authors' knowledge, this is the first work that models a bio-analytical system using a formal method, takes wireless network constraints into account and investigates high-level interaction of systems. The rest of the paper is organized as follows: Section 2 highlights related work in this field; Section 3 describes the preliminaries for the modeling framework; Section 4 discusses the problem formulation; Section 5 presents the timed-automata based modeling for the case study; Section 6 discusses the model verification; Section 7 discusses multi-system scenario for optimal system performance under constraints; Section 8 summarizes the software and hardware implementation consideration; and Section 9 concludes the paper and provides some suggestions for future directions.

2. Related Work

CPSs have applications in several disciplines including healthcare, education, smart grid, automotive industry, etc. (18). In (13), a comprehensive survey highlighting different modeling languages and techniques and what aspects each of them lacks has been provided. In addition to highlight modelling requirements, the work discusses the importance of addressing function and non-functional properties of CPS to achieve correct operation of device. The study (19) demonstrated the importance of a simulation-based model for clinical applications when compared to practical tests. The simulated and validated models included component-based models for medical devices as well as regression models for vital sign simulation. Medical CPS design issues and requirements are addressed in the research (20) for the telemonitoring of high-risk pregnancies use-case using a Plug-and-Play architecture (21) for interaction between patients and caregivers. The work (22) provides a comprehensive survey for computation, communication and memory resource efficiency in CPSs. In work (23), a rule-based simulation of bio-chemical process is addressed. In research (24), a service-oriented industrial CPS with cloud infrastructure support is presented. The paper (25) provided an overview of "Safe Cooperating Cyber-Physical Systems Using Wireless Communication (SafeCOP)," which focused on safety-related Cooperating CPSs (CO-CPS) characterized by wireless communication usage and uncertain operating environments. The work (26) provides an in-depth overview of formal methods in specification, design, and verification for software and hardware systems. The paper (27) highlights multi-dimensional hardware design verification using machine learning where intersection of functional and non-functional properties of electronic design is analyzed. The works (28; 29; 30) presents solutions for fault tolerance, safety and reliability in industrial and automotive CPSs.

3. Modeling Framework Basics

Timed automata (31) are a sub-class of hybrid automata with a finite number of real-valued clocks which can be reset. As discussed earlier, the formal approach adopted in this work is based on timed automata; this section provides a few essential preliminary definitions of hybrid and timed automata.

Definition 1 A hybrid automaton is a tuple *H= (L, Var, g, Γ, Edge, Act, Inv, Init)* where:

$L \rightarrow$ *Set of locations, States* $\Sigma = L \times V$, *V: set of all valuations* v, *where* $v : Var \rightarrow \mathbb{R}$

$Var \rightarrow$ *Real-Valued Variables,* $L \rightarrow 2^{Var}$

$g \rightarrow$ *Conditional/Guard function*

$\Gamma \rightarrow$ *Set of Labels*

$Inv \rightarrow$ *Invariant function,* $Inv(l) \subseteq V$, $l \in L$

$Act \rightarrow$ *functions consists of set of activities,* $f : \mathbb{R}_{\geq 0} \rightarrow V$

$Edge \rightarrow$ *Set of transitions, Edge* $\subseteq L \times \Gamma \times g(Var) \times 2^{Var} \times L$

$Init \rightarrow$ *Initial Location, Init* $\subseteq L$

The semantics of hybrid automata are based on two rules, i.e. discrete rule for discrete state transitions and continuous time rule based on continuous time steps. The discrete rule governing transitions between states is written as $(l, v) \xrightarrow{a} (l', v')$ for $(l, a, (v, v'), l') \in Edge$ and invariant $v' \in Inv(l')$ must hold. On the other hand, the time rule governing the time can pass in current location and the variable related to the location can evolve given that $f \in Act$ such that $f(0) = v$, $f(t) = v'$. The continuous time rule is given by $(l, v) \xrightarrow{a} (l, v')$ for $f[(0, t)] \in Inv(l)$ and t is strictly positive.

Definition 2 A timed automaton is a tuple $T = (L, \Gamma, Edge, C, Inv, Init)$ where:

$L \rightarrow$ *Set of locations, States* $\Sigma = L \times V$, *V: set of all valuations* v, *where* $v : Var \rightarrow \mathbb{R}$

$C \rightarrow$ *Set of real-valued clocks*

$\Gamma \rightarrow$ *Set of Labels*

$Inv \rightarrow$ *function that assigns set of invariants to locations based on Clock Constraints (CC),* $L \rightarrow CC(C)$

$Edge \rightarrow$ *Set of transitions, Edge* $\subseteq L \times CC(C) \times \Gamma \times 2^C \times L$

$Init \rightarrow$ *Set of Initial States, Init* $\subseteq L$

The semantics for timed-automata are given for the discrete rule and continuous rule:

Discrete Rule

$$(l, v) \xrightarrow{a} (l', v') : (l, a, (g, C), l') \in Edge$$
$$, v \models g, v' = reset(C) \ v, v' \models Inv(l') \quad (1)$$

where g is the guard.

Continuous Time Rule

$$(l, v) \xrightarrow{t} (l, v') : t \in \mathbb{R}_{\geq 0},$$
$$v' \models Inv(l), v' = v + t \quad (2)$$

Definition 3

Parallel composition The parallel timed automata composition $T_1 \parallel T_2 ... \parallel T_n$ of n systems such that $T_1 = (L_1, \Gamma_1, Edge_1, C_1, Inv_1, Init_1)$, $T_2 = (L_2, \Gamma_2, Edge_2, C_2, Inv_2, Init_2)$, ..., $T_n = (L_n, \Gamma_n, Edge_n, C_n, Inv_n, Init_n)$, and such that clocks and states are pair-wise disjoint, is given by:

- $L = L_1 \times L_2 \times ... \times L_n$

- $C = C_1 \times C_2 ... \times C_n$

- $\Gamma = \Gamma_1 \times \Gamma_2 ... \times \Gamma_n$

- $Inv(l_1, l_2) = Inv_1(l_1) \wedge Inv_2(l_2), ...,$
  $Inv(l_{n-1}, l_n) = Inv_{n-1}(l_{n-1}) \wedge Inv_n(l_n)$ for all $(l_1, l_2, ...l_n) \in L$

- $Init = \{((l_1, l_2, ...l_n), v) \in \Sigma | (l_1, v) \in Init_1 \wedge (l_2, v) \in Init_2, ... \wedge (l_n, v) \in Init_n\}$

For $i = 1, ..., n$ systems, the discrete transitions between the edges for two systems with automata T_i and T_{i+1} is given by *Rule Synchronization* and *Rule Non − Synchronization* i.e.:

Rule Synch :

$$\frac{(l_i, a, (g_i, C_i), l'_i) \in Edge_i, (l_{i+1}, a, (g_{i+1}, C_{i+1}), l'_{i+1}) \in Edge_{i+1}}{((l_i, l_{i+1}), a, (g_i \wedge g_{i+1}, C_i \times C_{i+1}), (l'_i, l'_{i+1})) \in Edge} \quad (3)$$

Rule Non − Synch$_i$:

$$\frac{(l_i, a, (g, C), l'_i) \in Edge_i, a \notin \Gamma_{i+1}}{((l_i, l_{i+1}), a, (g, C), (l'_i, l_{i+1})) \in Edge_i} \quad (4)$$

Rule Non − Synch$_{i+1}$:

$$\frac{(l_{i+1}, a, (g, C), l'_{i+1}) \in Edge_{i+1}, a \notin \Gamma_i}{((l_i, l_{i+1}), a, (g, C), (l_i, l'_{i+1})) \in Edge} \quad (5)$$

4. Problem Formulation

In this section, essential concepts to obtain an event-triggered control for bio-analytical CPSs over a non-deterministic wireless network and the extension of timed-automata is provided.

4.1. Event-Triggered Control system with Non-deterministic Network

Assuming that each bio-analytical system acts as a Linear Time Invariant (LTI) system, we have the following equation:

$$\dot{\zeta}(t) = A\zeta(t) + Bx(t). \quad (6)$$

where $\zeta(t)$ is the current state of the system, $\dot{\zeta}(t)$ is the next state of the system and $x(t)$ is the feedback for the system, depending upon controller gain K. Assuming the network is non-

$$\tau_r^{*min} \leq \tau_r \leq \tau_r^{*max} \qquad \tau_t^{*min} \leq \tau_t \leq \tau_t^{*max}$$
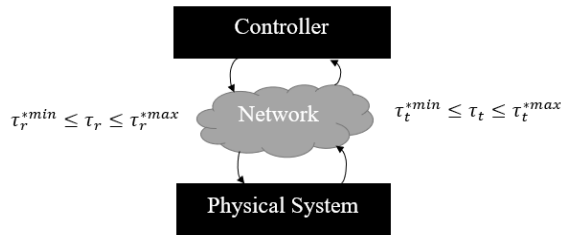
Figure 2. Wireless control over a non-deterministic network

deterministic, i.e. the time taken by each sample to reach its destination is unknown, the delay associated with each sample to be transferred is τ_t and for reception is τ_r. Moreover, there exists minimum times τ_t^{*min}, τ_r^{*min} and maximum times required τ_t^{*max}, τ_r^{*max} for the sample to be transferred and received, respectively as depicted in figure 2. For a sequence of communication events τ_{ti} and τ_{ri} where $i \in \mathbb{N}$, the following assumption can be made:

$$\tau_t^{*min} \leq \tau_{ti+1} - \tau_{ti} \leq \tau_t^{*max}, \quad 0 < \tau_t^{*min} \leq \tau_t^{*max} \quad (7)$$

$$\tau_r^{*min} \leq \tau_{ri+1} - \tau_{ri} \leq \tau_r^{*max}, \quad 0 < \tau_r^{*min} \leq \tau_r^{*max} \quad (8)$$

To account for the network delays in more detail, one can refer to (32). The feedback provided by the system to the controller will suffer delay based on the network delay (33). Equation 9 reflects the controller feedback accounting for network delay.

$$v(t) = K\zeta(t) \quad t \in [t_k + \Delta, t_{k+1} + \Delta] \quad (9)$$

where Δ depends upon τ_r and τ_t. Hence, the difference between the sampled state and the current state is given by equation 10.

$$e(t) = \zeta(t_k) - \zeta(t) \quad t \in [t_k + \Delta, t_{k+1} + \Delta] \quad (10)$$

Employing the event triggered approach based on the same principle as mentioned in (34), the sampled trigger time rule is given by:

$$t_{k+1} = min\left\{t | t > t_k \quad : \quad |e(t)|^2 \geq \sigma|\zeta(t)|^2\right\} \quad (11)$$

For sampled state x the inter-sample time is given by equation 12 based on trigger coefficient σ

$$\tau_\sigma = min\left\{t | |e(t)|^2 \geq \sigma|\zeta(t)|^2 \quad : \quad \zeta(0) = x\right\} \quad (12)$$

4.2. Timed Automata based Model for Non-Deterministic Wireless Communication

For the bio-analytical devices consisting of various subsystems, the proposed approach is to control each sub-unit using an event-triggered mechanism, while the network scheduling is priority based. For a simple use case, let σ_i be the trigger coefficient defined by event-triggered system control over non-deterministic channel for the ith single sub-system in the whole system, where $\sigma_i \in [0, \bar{\sigma}]$. The clock constraints (or guards) related to this sub-system are given by

$$\tau_s^{\sigma_i} \leq c \leq \tau_s^{\bar{\sigma}_i} . \quad (13)$$

Assuming that the subsystem has only two states, i.e. Init and Process, the timed automata model of the sub-system can be written as:

- $L = \{Init, Process\}$

- $C = \{c\}$

- $\Gamma = \{a, b\}$

- $Edge = \{(Init, a, (c \geq \tau_s^{\sigma_i}, \{c\}), Process), (Process, b, (c \geq \tau_s^{\bar{\sigma}_i}, \{c\}), Init)\}$
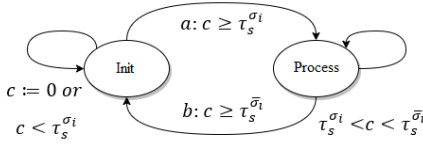
Figure 3. State machine representation of event triggered control

- $Inv = \{Inv(Init) : c \leq \tau_s^{\sigma_i}, Inv(Process) : \tau_s^{\sigma_i} < c < \tau_s^{\bar{\sigma}_i}\}$

- $Init = \{(Init, v_0)$ with $v_0(c) = 0\}$

The graphical representation of the sub-system is given in Figure 3. To include non-clock local and shared variables (channels) and to model stochastic network behavior, we have extended the timed automata as below:

Definition 4 Extended timed automata is a tuple $T = (L,$
$\Gamma, Edge, C, Var, Chan, Inv, Init, P)$ Where
$L \rightarrow$ *Set of locations, States* $\Sigma = Loc \times V$, *V: set of all valuations*
v, where $v : Var \rightarrow \mathbb{R}$
$C \rightarrow$ *Set of real-valued clocks*
$Var \rightarrow$ *Set of non-clock real valued local variables*
$Chan \rightarrow$ *Set of non-clock shared variables*
$\Gamma \rightarrow$ *Set of Labels*
$Inv \rightarrow$ *function that assigns set of invariants to locations based on Clock Constraints (CC), local variables constraints* $\Phi(Var)$ *and set of shared channel variables* $\varphi(Chan)$, $L \rightarrow CC(C) \wedge \Phi(Var)$ $\wedge \varphi(Chan)$
$Edge \rightarrow$ *Set of transitions, Edge* $\subseteq L \times CC(C) \times \Phi(Var) \times$ $\varphi(Chan) \times \Gamma \times 2^C \times 2^{Var} \times 2^{Chan} \times L$
$Init \rightarrow$ *Set of Initial States, Init* $\subseteq L$
$P \rightarrow$ *Assigns user-defined exponential delay rate (e) to each location,* $L \rightarrow e(P)$

where the exponential rate P defines an exponential distribution to leave each state under unbounded delays. The extended model is well-suited to control parameters like volume, flow-rate and synchronization between the bio-analytical devices.

5. Case-Study: Bio-Analytical Devices

The basic working principle of a droplet-based flow cytometer for the analysis of bacterial antibiotic susceptibility is based on droplet generation on a large scale, where each droplet encapsulates a single cell or small population of bacteria, reagents and antibiotics (1). The generated droplets are then incubated to allow bacteria to grow or die depending upon their resilience against the specific concentration of the antibiotic. After the incubation, several images are captured using a high-speed camera. The camera images are then classified using a Machine Learning (ML) algorithm where dead and alive cells are identified. Depending upon the ratio of dead or live cells, the bacterial susceptibility against a specific concentration of the antibiotic can be determined. Figure 4 shows the major sub-blocks of the considered droplet flow cytometer for the analysis of the antibiotic susceptibility of bacteria.
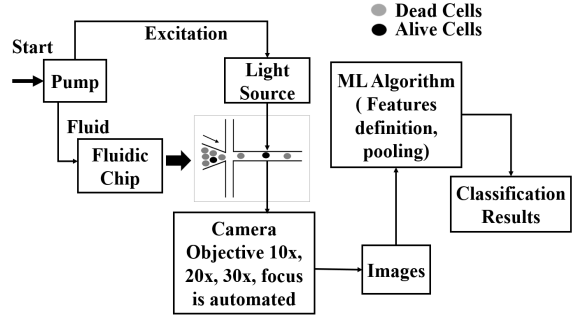

Figure 4. Use case: flow cytometer for antibiotic susceptibility of bacteria

Based on the major building blocks of the droplet flow cytometer, the system can be divided into three major units, i.e. the Droplet Generation Unit, Imaging Unit/Sensing Unit and Detection Unit. Each of the sub-block has a control unit which is connected to the central controller over a wireless communication network. A brief description of each sub-unit and wireless control unit is given below.

5.1. Droplet-Generation Unit

The droplet generation unit consists of a pump for controlling pre-processed (incubated) fluids volume at a specific rate for a specified duration and a microfluidic chip. The droplet generation starts with an initialization command to the pump with a defined flow rate and duration. The central controller communicates over the network for initialization and goes to the sleep mode until it is not triggered by the sub-unit with an acknowledgement about its task completion.

5.2. Imaging Unit

The imaging unit consists of a light source and a high-speed smart camera unit which is capable of capturing images at a variable frame rate (FR). The imaging unit is also able to adjust the resolution and Depth of Field (DoF). The control of the imaging unit activates via central controller at a specified FR, resolution and DoF which is adjustable by the smart camera unit depending on the required image quality.

5.3. Detection Unit

The detection unit consists of a micro-controller able to classify the images using machine learning. The used ML algorithm could be based on deep learning using artificial neural networks where a trained classifier can classify images depending upon their features.

5.4. Wireless Control Unit

Upon instantiating, the central controller activates each sub-unit in a specified order over a wireless communication network and goes to sleep or low power mode unless a trigger command is received to acknowledge the task completion by the sub-units. As mentioned earlier in section 4.2 the network scheduling is priority-based and there is a specified duration for a non-deterministic network to receive and send the commands, both to the controller as well as to the sub-units. The path or run time transitions for the modeled wireless control of these devices are based on Boolean variables/channels, as well as clock variables. They are given as:

Controller Run Time Transitions

$$Initialization \xrightarrow{\text{d1:U1,Chan}} Droplet\_Generation$$
$$\xrightarrow{\text{y:Init2,C}} : Init\_U2 \xrightarrow{\text{d2:U2,Chan}} Imaging, ...$$
$$Detection \xrightarrow{\text{y:finish,C}} Initialization$$

with invariants as below:

$$Inv = \{Inv(Droplet\_Generation) : y{<}tc1\_max,$$
$$Inv(Imaging) : y{<}tc2\_max,$$
$$Inv(Detection) : y{<}tc3\_max\}$$

Network Run Time Transitions

$$Init \xrightarrow{\text{d1:C1,Chan}} DG\_sending$$
$$\xrightarrow{\text{z:S1,C}} : wait\_DG \xrightarrow{\text{End\_1:R1,Chan}} ACK\_DG, ...$$
$$ACK\_DT \xrightarrow{\text{Rx3:end,Chan}} Init$$

with invariants as below:

$$Inv = \{Inv(DG\_sending) : z{<}tx1\_max,$$
$$Inv(wait\_DG) : z{<}rx1\_max, Inv(ACK\_DG) : z{<}$$
$$rx1\_max, Inv(Im\_Sending) : z{<}tx2\_maxInv(wait\_Im) :$$
$$z{<}rx2\_max, Inv(ACK\_Im) : z{<}rx2\_max, Inv(DT\_$$
$$Sending) : z{<}tx3\_maxInv(wait\_DT) : z{<}rx3\_max,$$
$$Inv(ACK\_DT) : z{<}rx3\_max\}$$

The run time transitions for other sub-units and their parallel composition can be formulated based on the same principles as mentioned here and in Section 4.

6. Verification with UPPAAL

Model verification is essential to ensure that the designed system meets all the specifications e.g. time constraints, synchronization and is deadlock-free. For model checking and verification, we used UPPAAL. UPPAAL is a model checking, verification and validation tool (17). During verification, the system was analyzed under bounded, unbounded and probabilistic delay distribution using Stochastic Model Checking (SMC).
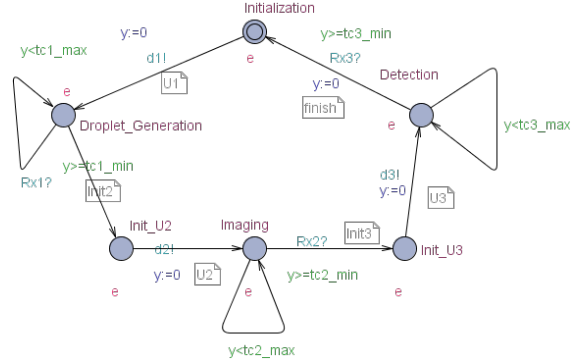

Figure 5. Control unit for droplet flow cytometer

Figures 5 and 6 show the Control and Network models executed in UPPAAL for generic subsystems with no specific functionality defined. Each of the sub-systems was then further modeled in depth. Figure 7 shows the detection unit model; for conciseness, the other sub-system models can be found at url: $https : //github.com/KanwalAshraf/UPPAAL\_Models.git$.
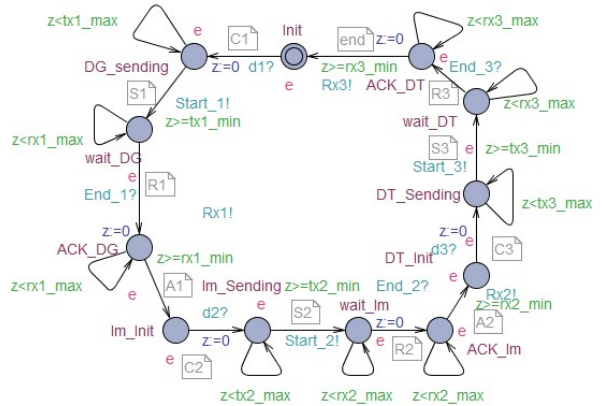

Figure 6. Network unit for droplet flow cytometer

In addition to the use of the UPPAAL simulator, the models have been further verified using different queries based on the language reference guide of UPPAAL. Examples of some of the queries used for system verification is given in Table 1. Using the query-based verification system, state transitions, probability density distribution and probability comparison of states at different intervals could be verified.

Figure 8 shows the state transition within a bounded time interval; here, the synchronization between different states of the controller, network and sub-unit can be visualized. In addition to exponential delay distribution, the network model could also have discrete probabilistic delay defined for different paths in the model.

Figure 9 shows an example of the network model with a discrete probability defined for delayed and non-delayed paths.

Figure 7. Detector unit for droplet flow cytometer

Table 1. Verification Queries

Queries	Properties
E <> *Communication.wait and z $\geq$ tx1_max*	Delay
A[]!*(Communication.Sending&&*	Synchronization
Bio_Chip_control.Rate_Definition)	
A[]*Communication.wait implyz $\geq$* tx1_min	Reset
simulate[< = 300]Network.ACK_DG, Control.	Simulation
Droplet_Generation, Imaging,Process_D2	
Pr[=<100](<> Network.DG_sending) >	Probability Comparison
= *Pr[<= 100](<> Control.Imaging)*	

Figure 10. Probability density distribution for the network unit
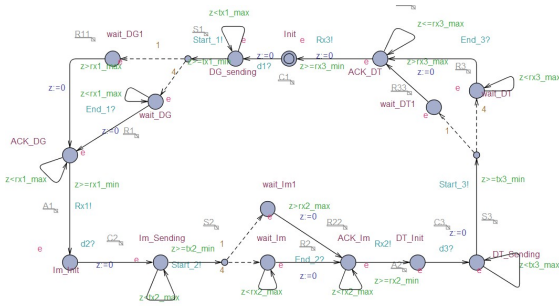
Figure 10 shows the probability density distribution for *ACK_DG* state for time lower than (blue bars) and higher than (orange bars) $rx1\_max$ threshold, with confidence 0.95, for the model depicted in Figure 9. Here the discrete probabilistic choices (1/5, 4/5) associated with the paths increases the probability density associated with $z > rx1\_max$. The discrete probabilistic choice for each path could help in the estimation of the delay in any system. Additionally, the cost and reachability time analysis could also be performed for each path. The formal verification showed that the modeled use case did not violate time constraints and that the device operation was executed in order and synchronized.

7. Multi-System Interaction

In previous sections, we have considered the problem for a single device with sub-units; however, CBPS are real-time distributed systems in nature, with multiple devices interacting with each other in both competitive and cooperative ways (35; 36) to achieve better performance. In this section, the single use case problem is extended to a multi-system problem for optimization of delay and bandwidth consumption.

When dealing with multi-system interaction (37; 38) a centralized CPS control approach (39) might become inefficient as the systems might be highly distributed in space and overall computational complexity could increase drastically. Therefore, a decentralized and distributed network control approach is more suitable. Figure 11 shows the overview of generalized centralized, decentralized, and distributed system architectures. In case of scarce network resources such as limited bandwidth or strict time-delay restrictions, a distributed or decentralized CPS architecture (40) is more desirable. Decentralized and distributed communication and control architectures
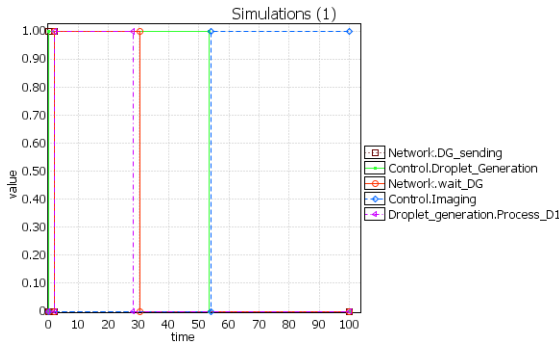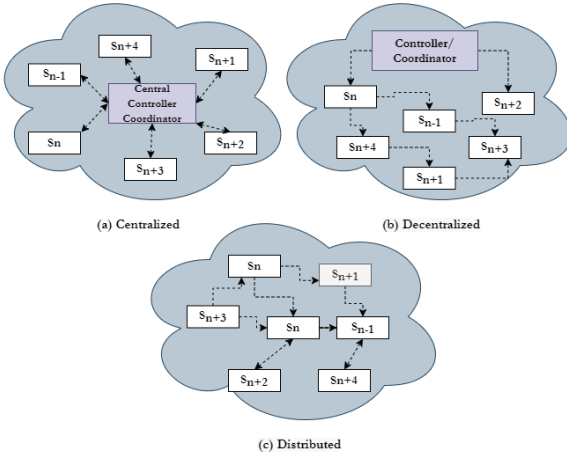

Figure 8. Network control model simulation: state transition within a bounded interval

Figure 9. Network unit with discrete probabilistic delays

Figure 11. (a) Centralized, (b) Decentralized, (c) Distributed System Architecture

Figure 12. Centralized vs decentralized Control

are already present around us for many for applications e.g microgrids (41; 42). However, there is always a trade-off when choosing between a centralized control approach and a decentralized or distributed control approach. If the number of systems interacting with each other is less than the upper bound on network constraints, such as bandwidth and power, a centralized control and communication approach would be preferable to a distributed one, where information flow could suffer from large delays.

We aimed to study the necessary interaction between different devices in combination with their interaction with the subunits of the device. A strategic approach is employed to determine whether to select a centralized or decentralized control approach which eventually effects the overall performance of the system when traffic patterns are known or unknown. To analyze which approach is better suited, a Stochastic Timed Automata (STA) based approach was used where the choice of transferring information between one system to another system is kept random. The definition of stochastic timed automata is given as:

STA:Definition: A stochastic timed automata is a tuple $STA=$ (TA, ρ, ω) where a timed automata TA is equipped with probability measure ρ and positive weights ω. (43)

where the transition between states depends not only upon the probability of transition between states but also on the waiting time or guard on the state. The transition from state s_t to s_{t+1} is dependent on wait time (t_s) and probability p_s and is written as $s_t \overset{t_s, p_s}{\rightarrow} (s_{t+1})$. We used Uppaal Stratego (44), an optimization, modeling, and strategy exploration tool for pricing strategic timed games, to simulate the strategy. For the use-case, we modelled the interaction between two system where sending information flow between the two systems could be centralized, decentralized or could be network traffic aware where system will have the possibility to choose between centralized or de-
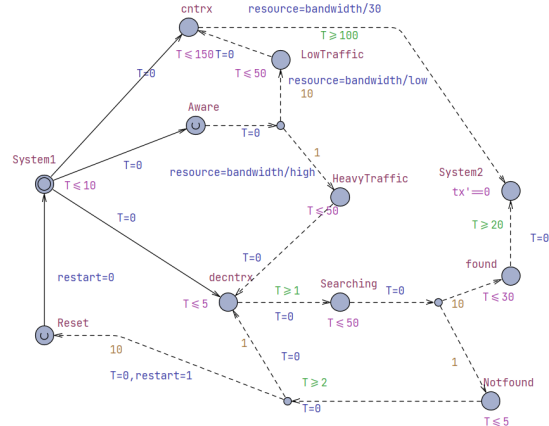
centralized Figure 12.

In both centralized and decentralized control the network traffic is an uncontrollable parameter but by making the system aware of the traffic load we can choose which strategy is best for the information flow for optimal network resource consumption under delay constraint. The strategies computed by UPPAAL Stratego is to send information via centralized, decentralized and traffic aware information flow, as shown in Figure 13.
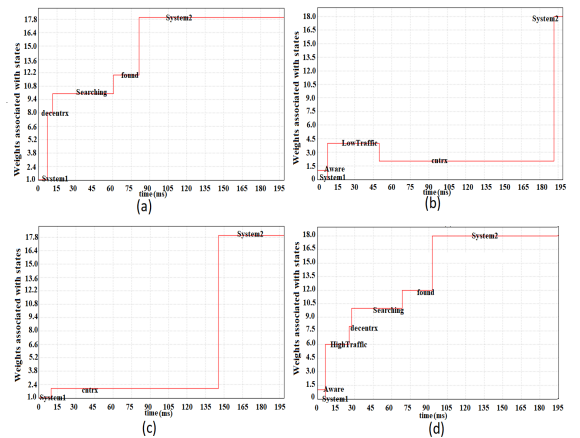

Figure 13. UPPAAL Strategies **(a):** Decentralized Information Flow (System1→decntrx→Searching→found→System2); **(b):** Traffic Aware Information Flow (System1→Aware→LowTraffic→cntrx→System2); **(c):** Centralized Information Flow (System1→cntrx→System2); **(d):** Traffic Aware Information Flow (System1→Aware→HighTraffic→decntrx→Searching→found→System2)

The probability of achieving a delay below 150 ms with all the mentioned approaches is 0.76 with 95% confidence interval, whereas the average delay estimate is 120 ms with probability

0.98 with 95% confidence interval. The mean bandwidth consumption (i.e. achieved throughput) is 1700 kbps with probability 0.68 and 95% confidence interval (see Figure 14).
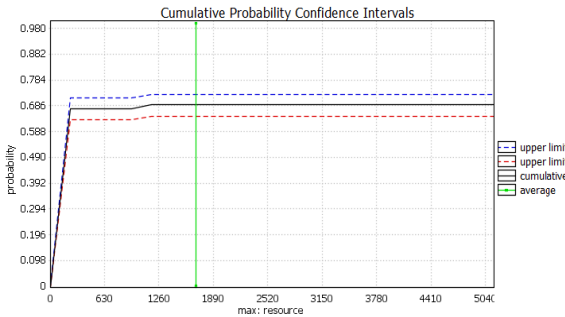

Figure 14. Bandwidth consumption: cumulative probability confidence intervals. . The mean bandwidth consumption is 1700 kbps as denoted by the green line.

Deciding which architecture to choose highly depends upon the delay constraints. For analyzing the strategies to choose from decentralized, centralized, or traffic aware communication, four different strategies were analyzed.
In the first strategy, named **Lenient Delay Strategy**, the requirement is to compromise delay requirement in order to avoid high network traffic scenarios and ensure the information transfer. In the second strategy, named **Stringent Delay Strategy**, the focus is to achieve minimal transmission delay. In the third strategy, named **Opt Strategy**, the middle ground where minimal delay is achieved regardless of communication via a centralized or decentralized architecture avoiding high network traffic scenarios is analyzed. In the fourth strategy, named **network_res Strategy**, the goal is to consume minimum network resources i.e. bandwidth in combination with lowest possible delay regardless of network architecture was analyzed.

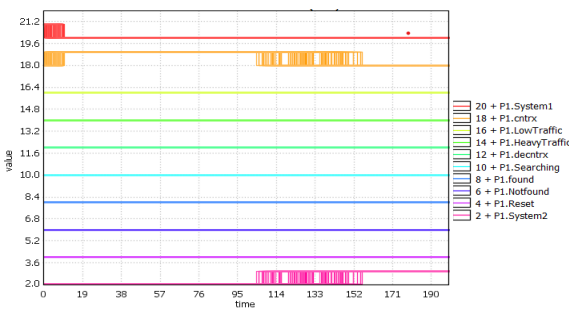The first strategy was analyzed with upper bound on delay as

Figure 15. Simulation execution of the Lenient delay strategy

high as 200 ms with the possibility to avoid large delays due to high network traffic. Figure 15 shows the simulation execution of the Lenient Delay Strategy. The mean delay (Figure 17(a)) value which is then obtained is 129 ms with 95% confidence in-

terval whereas the centralized communication is chosen as the main architecture.
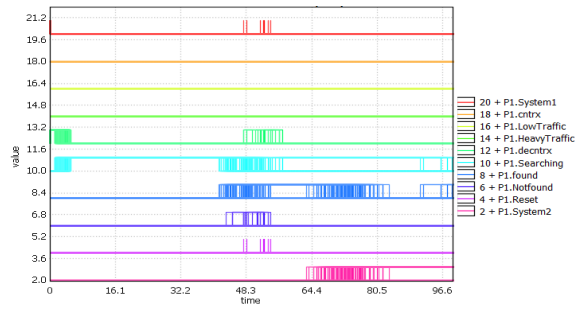

Figure 16. Simulation execution of the Stringent Delay Strategy

To obtain an overview of the strategies employed for a stringent delay requirement (Stringent Delay Strategy), the upper bound is chosen to be 100 ms without caring about network traffic; the simulation execution (Figure 16) indicates that the system tends to select the decentralized communication strategy in this scenario.
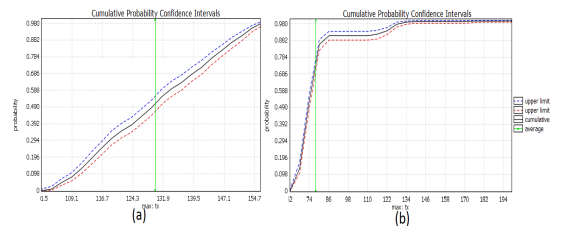

Figure 17. Strategies **(a): Lenient Strategy** Cumulative Probability Interval (Delay). Parameters: $\alpha = 0.05, \epsilon = 0.05$, Bucket Width = 1.6923, Bucket Count = 23. Mean Estimate = 129.9 ms; **(b):Stringent Delay Strategy** Cumulative Probability Interval (Delay). Parameters $\alpha = 0.05, \epsilon = 0.05$, Bucket Width = 1.6923, Bucket Count = 23. Mean Estimate = 77.94 ms

Under Stringent strategy (Figure 17(b)), the mean delay achieved is 78 ms with 95% confidence interval.
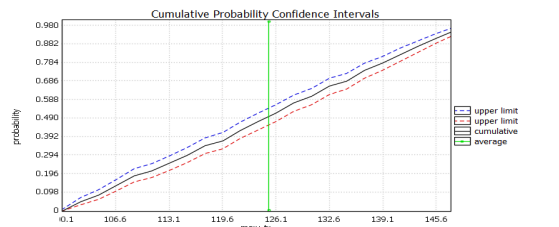

Figure 18. Strategies **Opt Strategy** Cumulative Probability Interval (Delay). Parameters: $\alpha = 0.05, \epsilon = 0.05$, Bucket Width = 1.6923, Bucket Count = 23. Mean Estimate = 125.2 ms

The third strategy (Opt Strategy) was employed to check the middle ground between the lowest delay achieved via decentral-

ized or centralized strategy; the simulation results (Figure 18) show that the best suited method for the employed use-case is to choose a centralized architecture for guaranteed lower delay and reliable communication. The mean estimated delay is 125 ms with 95% confidence interval.

The fourth strategy (network_res Strategy) is employed to minimize the delay under minimum network resource i.e. bandwidth consumption. Figure 19 shows the cumulative probability confidence for bandwidth consumption and minimum delay. The mean estimate for bandwidth consumption is 960 kbps with a mean delay estimate of 109 ms with 95% confidence interval.
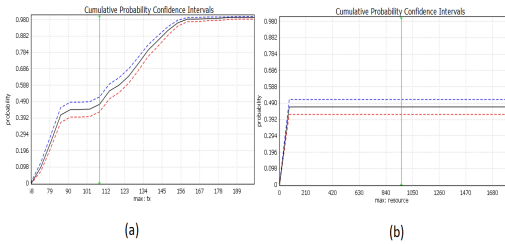

(a)   (b)

Figure 19. network_res (resource-minimization) Strategy **(a):** Cumulative Probability Interval (Delay). Parameters: $\alpha = 0.05, \epsilon = 0.05$, Bucket Width = 1.6923, Bucket Count = 13. Mean Estimate = 109 ms; **(b)** Cumulative Probability Interval (Bandwidth consumption). Parameters: $\alpha = 0.05, \epsilon = 0.05$, Bucket Width = 1.6923, Bucket Count = 13. Mean Estimate = 960 kbps

8. Implementation Considerations

The implementation of Cyber Physical Bio-analytical devices faces critical challenges such as limited data storage and hardware computing capabilities, the need for low energy/power consumption and efficient data communication, as well as interaction with users or the environment. These critical aspects necessitate an examination of both software and hardware design aspects prior to the practical implementation of use-cases.

8.1. Software Design Architecture

Software design of CPBS should be able to bridge the gap to enable the control of both functional and non-functional properties of the devices. While considering the software design for CPBS, the goal is to use a single publisher-subscriber interface software which enables all hardware interactions with humans and other devices to make them easy-to-use. To achieve required operating capabilities in the hardware, it is necessary to take care of the following major requirements of the CPBS software:

- Information communication including remote device connection and information routing including constraint violation, errors and trigger events;

- Data handling including data storage, defining data structure, data flow control and sensing and actuation data processing;
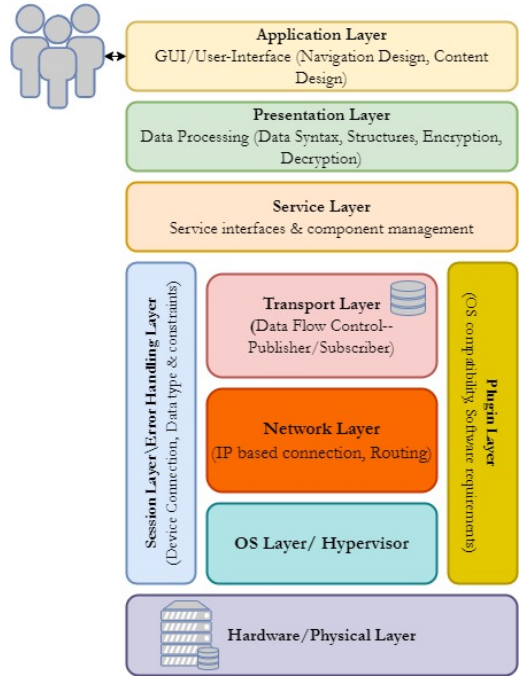

Figure 20. Layered Software Architecture for CPBS

- Process management, scheduling, operating system capabilities, user-interface.

Figure 20 shows the proposed multi-layer software architecture which is design by considering service-oriented software architecture (45; 46; 47), three tier architecture, OSI model (48) and Cisco's OSI model for cloud computing (49). Our aim is to develop the software with capabilities such that each software service capability could be used individually for subsystems. The presentation layer allows the interface to user input's and user-controlled actions via Graphical User Interface (GUI) or Command-line User Interface (CUI) based-interaction. The interface is connected to several back-end processes which include data processing or control actions determination as well as communication with sub-processes and devices. Presentation layer includes data processing and lies on the top of service layer which manages different service components and interfaces.

The plugin layer manages OS compatibility and software requirements. The session layer manages connections between different services, devices and sub-processes. The transport layer in combination with network layer handles data flow control and IP/TCP based connection and information routing. The low-level layers are of the same type as in case of any software design e.g. hardware/physical layer and OS layer or hypervisor for management of hardware resources.

8.2. Hardware Consideration

To achieve an effective control and wireless communication between different devices, the aim is to select cost-effective, reliable and easy-to-use Single Board Computers (SBCs) as well as where needed simple micro-controllers. A comparison of different specifications of SBCs helped to analyze Raspberry Pi as a strong candidate for the implementation of the communication and control algorithms. Raspberry Pi 4 is equipped with ARM cortex and its benchmarking showed significant performance results for image processing as well as for base-line implementation of publish-subscriber based event-triggered wireless communication.

The next step in our work will be to use the above SW/HW considerations to move forward with the practical implementation for the use-case, with a focus on open-source system design availability.

9. Conclusion

In this paper, an extended timed-automation-based formal technique for modeling bio-analytical CPSs with constraints over a wireless network was presented. In addition, an overview of delay and bandwidth constraints was provided using a timed strategic approach. The main goal was to provide a formal model-based architecture for bio-analytical devices in order to encourage the use of formal techniques in bio-analytical devices in the future. To depict the application of the proposed technique, a case study was modeled and verified using UP-PAAL and was extended to multi-system interaction using timed stochastic automata which was evaluated by means of by means of UPPAAL Stratego. The results showed that the minimum delay achieved to reach from system1 to system2 by centralized communication architecture is 129 ms, 87 ms with decentralized architecture, and 125 ms when avoiding high traffic scenarios. The use of this model is promising when dealing with large laboratory setups and diagnostic systems and can be used in Model-based System Engineering Methodology (MBSE) as evident from the multi-system interaction example. The introduction of wireless connectivity will enable the connection of different units in a high-throughput laboratory setup without any physical connection between sub-units and event-triggered control will make the system resource-efficient in terms of computation and communication. The verification of both the model and strategies helped to analyze the system under bounded, unbounded and probabilistic delay distribution. Although we attempted to address several challenges for the CPBS, there are still several issues to consider regarding the system's hardware and software implementation. Some of them include the device's non-deterministic behavior in response to various user inputs, as well as hardware bugs and other network constraints and issues such as network failure. With the achieved current results, we are moving towards the practical implementation of the use-case and trying to analyze the challenges.

References

[1] O. Scheler, K. Makuch, P. Debski, M. Horka, A. Ruszczak, N. Pacocha, K. Sozański, O.-P. Smolander, W. Postek, P. Garstecki, Droplet-based digital antibiotic susceptibility screen reveals single-cell clonal heteroresistance in an isogenic bacterial population, Scientific Reports 10 (2020) 3282. doi:10.1038/s41598-020-60381-z.

[2] W. Li, H. Xi, S. H. Tan, Insights and Advancements in Microfluidics, MDPI, 2017. doi:10.3390/books978-3-03842-517-5.
URL http://www.mdpi.com/books/pdfview/book/360

[3] L. Brümmer, S. Katzenschlager, M. Gaeddert, C. Erdmann, S. Schmitz, M. Bota, M. Grilli, J. Larmann, M. Weigand, N. Pollock, A. Macé, S. Carmona, S. Ongarello, J. Sacks, C. Denkinger, Accuracy of novel antigen rapid diagnostics for sars-cov-2: A living systematic review and meta-analysis, PLOS Medicine 18 (2021) e1003735. doi:10.1371/journal.pmed.1003735.

[4] N. Gyimah, O. Scheler, T. Rang, T. Pardy, Can 3d printing bring droplet microfluidics to every lab?—a systematic review, Micromachines 12 (3) (2021). doi:10.3390/mi12030339.
URL https://www.mdpi.com/2072-666X/12/3/339

[5] K. Pärnamets, T. Pardy, A. Koel, T. Rang, O. Scheler, Y. Le Moullec, F. Afrin, Optical detection methods for high-throughput fluorescent droplet microflow cytometry, Micromachines 12 (3) (2021). doi:10.3390/mi12030345.
URL https://www.mdpi.com/2072-666X/12/3/345

[6] R. Crowder, 11 - cyber physical systems and security, in: R. Crowder (Ed.), Electric Drives and Electromechanical Systems (Second Edition), second edition Edition, Butterworth-Heinemann, 2020, pp. 271–289. doi:https://doi.org/10.1016/B978-0-08-102884-1.00011-X.

[7] K.-D. Kim, P. R. Kumar, Cyber–physical systems: A perspective at the centennial, Proceedings of the IEEE 100 (Special Centennial Issue) (2012) 1287–1308. doi:10.1109/JPROC.2012.2189792.

[8] H. Li, Chapter 1 - introduction to cyber physical systems, in: H. Li (Ed.), Communications for Control in Cyber Physical Systems, Morgan Kaufmann, Boston, 2016, pp. 1–8. doi:https://doi.org/10.1016/B978-0-12-801950-4.00001-9.

[9] E. Evin, Y. Uludağ, Bioanalytical device design with model-based systems engineering tools, IEEE Systems Journal 14 (3) (2020) 3139–3149. doi:10.1109/JSYST.2020.2993377.

[10] F. Patou, M. Dimaki, W. E. Svendsen, K. Kjægaard, J. Madsen, A smart mobile lab-on-chip based medical diagnostics system architecture designed for evolvability, in: 2015 Euromicro Conference on Digital System Design, 2015, pp. 390–398. doi:10.1109/DSD.2015.11.

[11] F. Patou, Evolvable smartphone-based point-of-care systems for in-vitro diagnostics, 2016.

[12] F. Patou, M. Dimaki, A. Maier, W. E. Svendsen, J. Madsen, Model-based systems engineering for life-sciences instrumentation development, Systems Engineering 22 (2) (2019) 98–113. arXiv:https://onlinelibrary.wiley.com/doi/pdf/10.1002/sys.21429, doi:https://doi.org/10.1002/sys.21429.

[13] I. Graja, S. Kallel, N. Guermouche, S. Cheikhrouhou, A. Hadj Kacem, A comprehensive survey on modeling of cyber-physical systems, Concurrency and Computation: Practice and Experience 32 (15) (2020) e4850, e4850 cpe.4850. arXiv:https://onlinelibrary.wiley.com/doi/pdf/10.1002/cpe.4850, doi:https://doi.org/10.1002/cpe.4850.

[14] S. Geng, J. Peng, P. Li, Modeling and verification of cyber-physical systems under uncertainty, in: 2017 13th International Conference on Natural Computation, Fuzzy Systems and Knowledge Discovery (ICNC-FSKD), 2017, pp. 1491–1496. doi:10.1109/FSKD.2017.8392986.

[15] F. Tan, Y. Wang, Q. Wang, L. Bu, R. Zheng, N. Suri, Guaranteeing proper-temporal-embedding safety rules in wireless cps: A hybrid formal modeling approach, in: 2013 43rd Annual IEEE/IFIP International Conference on Dependable Systems and Networks (DSN), 2013, pp. 1–12. doi:10.1109/DSN.2013.6575357.

[16] K. Ashraf, Y. L. Moullec, T. Pardy, T. Rang, Model-based system architecture for event-triggered wireless control of bio-analytical devices, in: 2021 24th Euromicro Conference on Digital System Design (DSD), 2021, pp. 465–471. doi:10.1109/DSD53832.2021.00076.

[17] J. Bengtsson, K. Larsen, F. Larsson, P. Pettersson, W. yi, Uppaal - a tool suite for automatic verification of real-time systems., Vol. 3, 1995, pp. 232–243. doi:10.7146/brics.v3i58.18769.

[18] H. Chen, Applications of cyber-physical system: A literature review, Journal of Industrial Integration and Management 02 (2017) 1750012. doi:10.1142/S2424862217500129.

[19] L. C. Silva, M. Perkusich, F. M. Bublitz, H. O. Almeida, A. Perkusich, A model-based architecture for testing medical cyber-physical systems, in: Proceedings of the 29th Annual ACM Symposium on Applied Computing, SAC '14, Association for Computing Machinery, New York, NY, USA, 2014, p. 25–30. doi:10.1145/2554850.2555028.
URL https://doi.org/10.1145/2554850.2555028

[20] J. Jezewski, A. Pawlak, K. Horoba, J. Wrobel, R. Czabanski, M. Jezewski, Selected design issues of the medical cyber-physical system for telemonitoring pregnancy at home, Microprocessors and Microsystems 46 (2016) 35–43. doi:10.1016/j.micpro.2016.07.005.
URL http://dx.doi.org/10.1016/j.micpro.2016.07.005

[21] T. Li, F. Tan, Q. Wang, L. Bu, J.-N. Cao, X. Liu, From offline toward real-time: A hybrid systems model checking and cps co-design approach for medical device plug-and-play (mdpnp), in: 2012 IEEE/ACM Third International Conference on Cyber-Physical Systems, 2012, pp. 13–22. doi:10.1109/ICCPS.2012.10.

[22] Z. Li, C. Huang, X. Dong, C. Ren, Resource-efficient cyber-physical systems design: A survey, Microprocessors and Microsystems 77 (2020). doi:10.1016/j.micpro.2020.103183.

[23] S. Ehmes, Rule-based Simulation of biochemical Reaction (2018).

[24] X. Yue, H. Cai, H. Yan, C. Zou, K. Zhou, Cloud-assisted industrial cyber-physical systems: An insight, Microprocessors and Microsystems 39 (8) (2015) 1262–1270. doi:10.1016/j.micpro.2015.08.013.
URL http://dx.doi.org/10.1016/j.micpro.2015.08.013

[25] P. Pop, D. Scholle, I. Šljivo, H. Hansson, G. Widforss, M. Rosqvist, Safe cooperating cyber-physical systems using wireless communication: The SafeCOP approach, Microprocessors and Microsystems 53 (2017) (2017) 42–50. doi:10.1016/j.micpro.2017.07.003.
URL http://dx.doi.org/10.1016/j.micpro.2017.07.003

[26] I. Rodhe, M. Karresand, Overview of formal methods in software engineering (December 2015) 6–13.

[27] X. Lai, A. Balakrishnan, T. Lange, M. Jenihhin, T. Ghasempouri, J. Raik, D. Alexandrescu, Understanding multidimensional verification: Where functional meets non-functional, Microprocessors and Microsystems 71 (2019) 102867. doi:10.1016/j.micpro.2019.102867.
URL https://doi.org/10.1016/j.micpro.2019.102867

[28] G. Tertytchny, N. Nicolaou, M. K. Michael, Classifying network abnormalities into faults and attacks in IoT-based cyber physical systems using machine learning, Microprocessors and Microsystems 77 (2020). doi:10.1016/j.micpro.2020.103121.

[29] R. Nouacer, M. Djemal, S. Niar, G. Mouchard, N. Rapin, J. P. Gallois, P. Fiani, F. Chastrette, A. Lapitre, T. Adriano, B. Mac-Eachen, EQUITAS: A tool-chain for functional safety and reliability improvement in automotive systems, Microprocessors and Microsystems 47 (2016) 252–261. doi:10.1016/j.micpro.2016.07.020.
URL http://dx.doi.org/10.1016/j.micpro.2016.07.020

[30] S. Balasubramaniyan, S. Srinivasan, F. Buonopane, B. Subathra, J. Vain, S. Ramaswamy, Design and verification of Cyber-Physical Systems using TrueTime, evolutionary optimization and UPPAAL, Microprocessors and Microsystems 42 (2016) 37–48. doi:10.1016/j.micpro.2015.12.006.
URL http://dx.doi.org/10.1016/j.micpro.2015.12.006

[31] R. Alur, D. L. Dill, A theory of timed automata, Theoretical Computer Science 126 (2) (1994) 183–235. doi:https://doi.org/10.1016/0304-3975(94)90010-8.

[32] M. S. Mahmoud, M. M. Hamdan, Fundamental issues in networked control systems, IEEE/CAA Journal of Automatica Sinica 5 (5) (2018) 902–922. doi:10.1109/JAS.2018.7511162.

[33] R. G. Sanfelice, Networked hybrid dynamical systems: Models, specifications, and tools, 2018.

[34] P. Tallapragada, N. Chopra, Event-triggered dynamic output feedback control of lti systems over sensor-controller-actuator networks, in: 52nd IEEE Conference on Decision and Control, 2013, pp. 4625–4630. doi:10.1109/CDC.2013.6760613.

[35] T. Sanislav, S. Zeadally, G. Mois, H. Fouchal, Multi-agent Architecture for Reliable Cyber-Physical Systems (CPS) (Pediswesa) (2017) 2–7.

[36] Q. Zhu, L. Bushnell, T. Başar, Resilient Distributed Control of Multi-agent Cyber-Physical Systems, Springer International Publishing, Heidelberg, 2013, pp. 301–316. doi:10.1007/978-3-319-01159-2_16.
URL

Kanwal Ashraf is a PhD student at Tallinn University of Technology, Estonia. Kanwal received her Joint-International Master's degree in Smart System Integration from Heriot-Watt University, UK, USN, Norway and BME, Hungary in 2020. She holds a bachelor's degree in electrical engineering from University of the Punjab, Pakistan. Her research topics include application of Wireless communication in CPSs and Co-Design of Wireless Networked Control Systems for bioanalytical applications.

Yannick Le Moullec received the M.Sc. degree in electrical engineering from Université de Rennes I, Rennes, France, in 1999 and the Ph.D. degree in Electrical Engineering from Université de Bretagne Sud, Lorient, France, in 2003. From 2003 to 2013, he successively held Postdoc, Assistant, and Associate Professor positions with Aalborg University, Aalborg, Denmark. He then joined Tallinn University of Technology, Tallinn, Estonia as a Senior Researcher and then on a professorship of Cognitive Electronics. He has supervised eleven Ph.D. theses and nearly 60 M.Sc. theses. He was Co-PI for the H2020 COEL ERA-Chair project. His research interests include HW/SW codesign, embedded systems, reconfigurable systems, and IoT.

Tamas Pardy received the M.Sc. degree in info-bionics engineering from Peter Pazmany Catholic University, Budapest, Hungary, in 2014, and the Ph.D. degree in electronics and telecommunication from Tallinn University of Technology, Tallinn, Estonia, in 2018. He is currently a senior researcher at Tallinn University of Technology, focusing on flow- and temperature-control of Lab-on-a-Chip devices.

Toomas Rang was born on November 10, 1951, in Tallinn, Estonia. He graduated the Tallinn Technical University (TTU), Estonia as an Electronics Engineer in 1975. In 1981 he successfully defended the PhD degree in Electronics at the Hungarian Academy of Sciences. From 1984/1985, he held the Postdoc position at Saarland Uni-

versity, Germany. In 1996 he was elected for the professor position in Electronics Design at TTU. In 1998 he was elected to the head of the Department of Electronics. Since 2020 he is the Professor Emeritus at TTU. He the senior member of IEEE. He has successfully supervised fifteen Ph.D. theses and is author of about 120 scientific publications. His research interests cover the topics from wide bandgap-based semiconductor devices and metallization technologies, till the microfluidics-based Lab-on-Chip devices.

Appendix 3

Publication 3

Joint Optimization via Deep Reinforcement Learning in Wireless Networked Controlled Systems

KANWAL ASHRAF[1], YANNICK LE MOULLEC[1], (SENIOR MEMBER, IEEE), TAMAS PARDY, (MEMBER, IEEE)[2,1], and TOOMAS RANG, (SENIOR MEMBER, IEEE),[1,2]

[1]Thomas Johann Seebeck Department of Electronics, Tallinn University of Technology, Tallinn, 19086 Estonia
[2]Department of Chemistry and Biotechnology, Tallinn University of Technology, Tallinn, 19086 Estonia

Corresponding author: Kanwal Ashraf (e-mail: kanwal.ashraf@taltech.ee).

ABSTRACT This paper proposes a deep Reinforcement Learning (RL) based co-design approach for joint-optimization of wireless networked control systems (WNCS) where the co-design approach can help achieve optimal control performance under network uncertainties e.g. delay and variable throughput. Compared to traditional and modern control methods where the dynamics of the system are important for predicting a system's future response, a model-free approach can adapt to many applications of stochastic behaviour. Our work provides a comparison of how the control performance is affected by network uncertainties such as delays and bandwidth consumption under an unknown number of devices. The control data is transmitted under different network conditions where several applications transmit background traffic data using the same network. The problem contains several sub-optimization problems because the optimal number of devices is non-deterministic under network delay and channel capacity constraints. The proposed approach seeks to minimize control error in wireless network control systems in order to improve Quality of Service and Quality of Control. This proposed approach is used and compared using three model-free RL Q-learning algorithms for high-throughput flow control in a double emulsion droplets formation application. The results show that the allowable number of devices for reliable network communication under bounded network constraints is 10 when using binary search. The control performance of the system without considering network effect in the reward function (Scenario 1) was good with the C51 algorithm; when including OMNet++ based network effect in the reward function (Scenario 2), the best performance was achieved with all three algorithms (C51, DQN, DDQN) with an exponential reward function, and only with C51 in the case of a linear reward function. Finally, under random network conditions (Scenario 3), C51 and DDQN performed well, but DQN did not converge. Comparisons with other machine learning and non-machine learning algorithms also highlight the superior performance of the utilized algorithms.

INDEX TERMS Wireless Networked Control Systems; Co-Design strategies; Reinforcement Learning.

I. INTRODUCTION

The outset of this work in wireless networked control systems (WNCS) stems from a multidisciplinary research effort related to a microfluidics application. Microfluidics has enabled automation in the pharmaceutical and diagnostic fields thanks to the use of small reagent volume, increased particle monodispersity with uniform drug composition and efficient evaluation methods for drug testing [4], [50]. To integrate microfluidic devices in the consumer market, a highly syn-chronized flow rate is a major challenge to be addressed [66]. For example, in the case of liposomal drug delivery [47], [48] which is promising for high-throughput cell screening, double emulsion could help in the better formation of droplets. The formation of double emulsion droplets depends upon the synchronized delivery of the reagents at a specific flow rate [58]. The formation of double emulsion requires at least four pumping units for generating emulsions and additional

pumps for reagents delivery. To achieve a high flow rate, different techniques have been proposed, which include several microfluidic units working in parallel [34], [73]. This raises issues that include not only the control of the devices but also the data communication and storage for achieving efficient control in a high throughput production unit. Our previous research focused on integrating wireless Cyber-Physical System (CPS) concepts [8], [9] with bioanalytical devices which could help with efficient control in a high throughput laboratory setup. Such a Cyber Bioanalytical Physical System (CBPS) integrates the physical and biological processes with the computation and communication domains, enabling an efficient remote operation of the processes which is the future of laboratory automation.

In a CBPS, synchronization between the devices is important to ensure the overall stability and reliability of the system [75]. The fault tolerance and delay requirement restrictions put constraints on the overall performance of the system (as in the case of Ultra-Reliable Low Latency Communications (URLLC)) [18]. These factors are affected by delays introduced by the control systems which include computation and prediction delays, as well as the uncertainties of the wireless networks including queuing delay, transmission delay and backhaul delays [41], [44]. It is thus important to see the design of this sub-domain of CPS, i.e. WNCS, as a co-design problem [12], [43] rather than an interactive design in which one design lies on top of the other. The control and information distribution aspects of the application can be exploited by looking at the co-design of WNCSs. The principle of co-design of networked control system is well established [17] and Figure 1 shows the design framework for networked controlled systems (inspired by the above-mentioned work) which acted as a starting point for our work in WNCS. In this paper, we use reinforcement learning

FIGURE 1. Framework for the co-design of networked controlled systems (inspired by [17])

to compensate for the delays of the systems (both wireless and control) in order to optimize the overall system's error

response reliability. The reason behind using model-free RL rather than model-based approaches is that when dealing with massive systems, the delay models are non-deterministic in nature; additionally the physical dynamics of the system might be unknown.

In addition, over a shared communication network, the traffic pattern [24] could be highly non-deterministic, specifically when dealing with event-triggered control; i.e., developing a traffic model over a shared communication network is also a non-deterministic problem. Because of factors such as data storage capacities and adaptability, simple search algorithms become infeasible when attempting to cope with changes in real-time as the problem complexity increases with network growth. The use of online learning algorithms could help solving these issues at the expense of convergence time as compared to offline algorithms which require a lot of data. The proposed concept could even be extended to Ultra Reliable Low Latency Communication (URLLC) applications in which the system is subject to stringent delay constraints and system-wide optimization is necessary to achieve reliable performance.

A. SUMMARY OF CONTRIBUTIONS
Our contributions are summarized as follows:

1) We present our proposed joint optimization of WNCSs using a co-design approach. The aim is to analyze the benefit of using a model-free RL in stochastic systems as compared to classical and modern control methods.
2) To analyze the problem in-depth, classical optimization theory is used to formulate the problem. The objective of the problem is defined as the minimization of control errors under network constraints as well as errors introduced via the used reinforcement Q-learning technique.
3) The problem is extended for the application of droplet generation using a stepper motor where the flow rate is controlled by motor operation. To estimate the control delays as close as possible to reality, we performed the benchmarking of Raspberry Pi which is used as a central control unit of fluidic pumps in our laboratory setups. The wireless control of the pump is obtained via WiFi and the network uncertainties were mimicked using the OMNet++ simulation tool.

Furthermore, our proposed solution is evaluated under three different network scenarios:

Scenario1: The network uncertainties such as delay and bandwidth consumption were simulated using OMNet++. The optimal number of devices was calculated using binary search methods which satisfied the delay and bandwidth constraints for reliable performance. Finally, RL was performed using different algorithms i.e. DQN, DDQN, C51 and LSTM and a comparison was made based on the convergence of the algorithms.

Scenario2: The delay and network data simulated via OMNET++ was used as a control factor during the RL environment design and was also used as a dynamic parameter
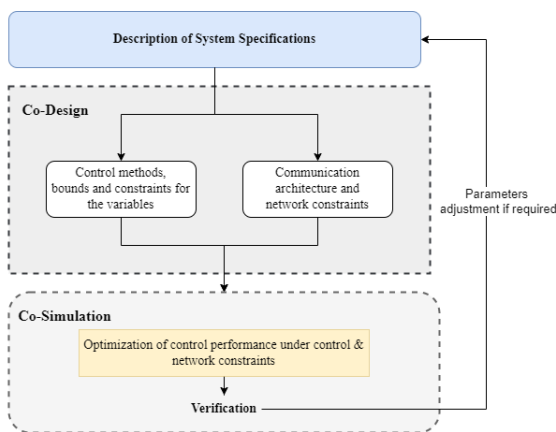
in the reward function to obtain an efficient performance of the algorithm under the network uncertainties.

Scenario3: The network uncertainties were defined as random variables and were introduced in the RL reward function.

To mitigate the overestimation errors, a deep Q-learning algorithm is used instead of Q-learning and the performance of the methods is compared with other model-free RL algorithms including C51. Furthermore, our results show that double-DQN is more efficient to mitigate overestimation errors. These RL algorithms are equipped with an experience replay buffer [5] which acts as a middle ground between the offline and online algorithms; in turn this helps making convergence faster. An experience replay buffer is used to save the trajectory of previous experiences in order to improve the learning process's performance. The size of the previous observation must not be too small nor too large; i.e. updating the policy after each iteration will be extremely time consuming, and updating it after too many observations (which may overlook the pattern of change) will not improve performance.

B. DESCRIPTION OF THE APPLICATION

The formation of single or double emulsion droplets helps in high-throughput screening of the cell's susceptibility for drug formation and testing. There are several other applications of microfluidic droplets in the chemical industry [20] other than drug testing. In microfluidic applications, the formation of a double emulsion requires a synchronized flow of the different reagents. As mentioned earlier, the generation of such droplets requires at least four pumping units for emulsion generation, and more if needed. These pumping units require an efficient control method that guarantees the fluidic flow from each pumping unit at a specified flow rate.

Control of such pumps over wireless networks could add the possibility of cost-effective remote operation. However, if the systems are running in parallel with other high-data-consuming applications, such as video streaming, wireless communication may introduce additional challenges such as delay, packet loss, and channel congestion. Using classic control methods or robust control methods, e.g. Proportional Integral Derivative (PID) or Model Predictive Control (MPC) could be highly inefficient for applications with high synchronization requirements [28]. Indeed, one drawback of PID is that it is ineffective for Multi-Input Multi-Output (MIMO) systems and necessitates the tweaking of several parameters to get the desired response; one drawback of MPC it that it necessitates the modeling of the system's dynamics. The wireless network in a wireless control system is non-deterministic by nature, necessitating the continual adjustment of PID parameters or the development of the MPC model.

However, using a model-free (Black box) [59] or semi-supervised (grey box) implementation could help such a system achieve an optimal response. RL is based on trial and
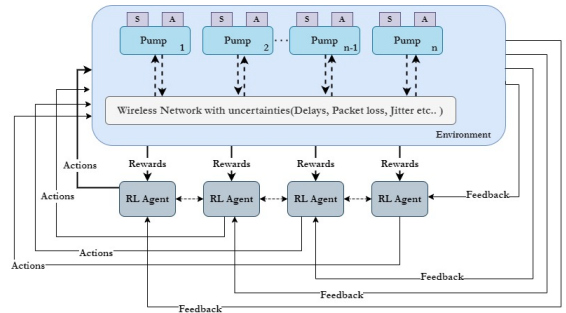

FIGURE 2. Reinforcement Learning Application for Distributed Systems

error methods and is derived from the field of psychology e.g. animal learning [46]; several pumping systems controlled over wireless networks will obtain the actions from the RL agents working in parallel and might learn from each other if necessary, as depicted in Figure 2. The use of the RL algorithms assists in adaptation of the system to a higher level without remodelling the system dynamics. Further details of RL and its comparison with other control methods are provided in the upcoming section II.

C. PREVIOUS WORKS

Existing research in the topic of WNCS focuses on several elements of its design challenge such as stability, reliability, and energy efficiency. On the other hand, the use of deep learning is mostly studied in the case of URLLC [54]. In work [29], a hybrid approach which combines wireless connectivity with wired connectivity for control of Unmanned Aerial Vehicles (UAVs) has been provided. The proposed reliable VANET routing decision scheme is dependent on network conditions and is based on the Manhattan mobility model. In [38], a model-free deep RL based framework is analyzed for URLLC in downlink of OFDMA systems while optimizing the power. A delay sensitive joint optimization control studies has been carried out for networked control systems in [42] for multiloop systems, emphasizing the importance of delay sensitivities in the design of optimal control and network policies. In [36], a clustering-based strategy for efficient energy optimization in embedded processors for wireless sensor networks is investigated in order to increase the lifetime of WSN nodes and enhance better utilization of resources. In the context of communication rivalry, an adaptive learning-based approach for vehicle-to-vehicle and vehicle-to-infrastructure communication has been presented in [53]. The gain settings of the PID controller are explored under the influence of non-linear delay using neural networks and ant colony optimization in study [65], but other critical network parameters such as packet error and channel capacity are not taken into account. The use of RL algorithms has been examined in study [37] to handle the collision problem in vast IoT networks, with encouraging findings; the optimization problem is modelled as a function of access

delay, access success and energy consumption rewards. A similar technique to ours has been investigated in [70] with the goal of optimizing platoon performance by accounting for wireless network delay and control stability. However, the work models the vehicles dynamics, which is a complex task in case the dynamics of the application are unknown or difficult to model. In [35], a framework for prediction and communication co-design has been provided for improving reliability of URLLC systems using optimization technique; however, a limitation of that work is that the implementation requires the information about the state transition of different parameters of the system. In [26], an offline scheduling algorithm has been proposed for machine-to-machine communications; however, as mentioned earlier offline algorithms are less adaptable to real-time changes. A joint optimization method for Quadratic Linear Regulator (LQR) cost and energy consumption is analyzed in [67], providing an energy-to-control efficiency framework for URLLC in IoT systems, but where factors such as channel capacity and number of users have not been taken into account.

II. REINFORCEMENT LEARNING VERSUS PREDICTIVE CONTROL

In reinforcement learning algorithm, an agent learns a strategy to control an environment based on feedback and reward strategy.

The state of the system is determined by valuation function Q(s, a) which is based on the sum of expected rewards R associated with previous states plus the discount factor γ related to next states. The overall reward R_t is given by:

$$R_t = r_t + r_{t+1}, ..., r_n \tag{1}$$

whereas the long-term reward is based on γ discount factor is given by:

$$R_{t+1} = r_{t+1} + \gamma R_t \tag{2}$$

For policy π that defines the probability distribution for any action a for state s, the valuation function is given by:

$$Q^\pi(s, a) = \mathbb{E}[\sum_{i=t}^{T} \gamma^{i-t} r(s_i, a_i)] \tag{3}$$

The valuation function tries to achieve an optimal value $Q^*(s, a)$ [60] where:

$$Q^*(s, a) = max_\pi Q^\pi(s, a) \tag{4}$$

Q-Learning is based on following Bellman update rule [6]:

$$Q_{t+1}(s_t, a_t) = Q_t(s_t, a_t) + \alpha(r_{t+1} + \gamma \max_{a_{t+1} \in A}$$
$$Q(s_{t+1}, a_{t+1}) - Q(s_t, a_t)) \tag{5}$$

where α denotes the learning rate. The reward function plays a significant role in RL; to reach a particular objective. The major challenges while designing a reward function includes positive infinitive loop in the feedback of a reward function as the objective would be achieved sooner while the agent has not still learned all the possible scenarios. Including a

discount factor [39] in the reward function which comprises the factor affecting the overall performance of the system such as bandwidth assigned to each device after a certain device has left the network could help solve the infinite loop. The discount factor used in RL is similar to the quasi-hyperbolic discount as mentioned in Equation 6.

$$f(t) = \beta\rho^t \tag{6}$$

The quasi-hyperbolic discount function gets a value of ρ when $\beta = 1$; the discount factor solves the problem of positive loop in the infinite horizon as well as adds the contribution from the next states.

A. REINFORCEMENT LEARNING AND PREDICTIVE CONTROL

Predictive control of any system is regarded as an optimization problem where the problem is solved over a control horizon based on the system dynamics. Classic and robust control methods revolve around achieving a stable response of the system e.g. PID, LQR, MPC, etc. MPC has been in use for decades for solving networked control system problems thanks to its stable response [10], [69]. On the other hand, RL is based on agent(s) and an environment where the agent tries to learn the policy based on the feedback from the environment to solve an optimization problem through exploration and exploitation [68]. RL deals with how to learn control strategies by acting as an optimization framework for complex problems.

MPC algorithms might not converge in the real world where problems are more complex and non-deterministic in nature. Table 1 shows a brief comparison of RL with MPC and LQR. MPC might perform as close as to the RL algorithms for convex problems [15], but for WNCS where the network problem itself could be non-deterministic or non-convex in nature, MPC control will fail to solve the problem in an efficient manner [55] (see also Table 1).

B. MODEL-FREE REINFORCEMENT LEARNING ALGORITHMS

In RL, an agent learns the policy or valuation function based on dynamics of the system i.e. the model is given or learns the model of the environment with provided data or practical implementation [21], [27], [56]. RL algorithms can be model-based or model-free.. In real-world problem where the system model might not be present or demonstration for a specific action is impossible, model-free algorithms could play an undeniable role. The model-free RL algorithms are divided into policy or valuation based learning techniques [33], [61] and are further classified into different algorithms as shown in Figure 3. In this work, our main focus was to highlight the use of value-based model-free algorithms in wireless networked controlled systems. Although providing only the bounds or rules for the environment should be sufficient for these algorithms, we evaluated the response of the algorithms with deterministic data.

TABLE 1. Reinforcement Learning vs Control Methods

Methods	Complexity	Adaptability	Problem Convexity	Model Requirement	Robustness	Convergence Time	High-dimensional data handling
Reinforcement Learning (Model-based)	Low (Online), High (Offline) [16], [25]	High [32], [52]	Not required [32]	Yes [32]	Low [19], [32]	Low-to-Medium[1][16]	Good [40]
Reinforcement Learning (Model-free)	Low (Online), High (Offline) [16], [25]	High [32], [52]	Not required [32]	No [32]	Low [19], [32]	Low-to-Medium[1][16]	Good [40]
Model Predictive Control	High (Online), Low (Offline) [16], [25]	Low [32]	Required [32]	Yes [32]	High [32]	Medium-to-High[1][16]	Moderate [40]
LQR	Low [23]	Low [30]	Required[2] [49]	Yes	Moderate [30]	Low[3][45]	Moderate

[1] Depends upon dimensional complexity
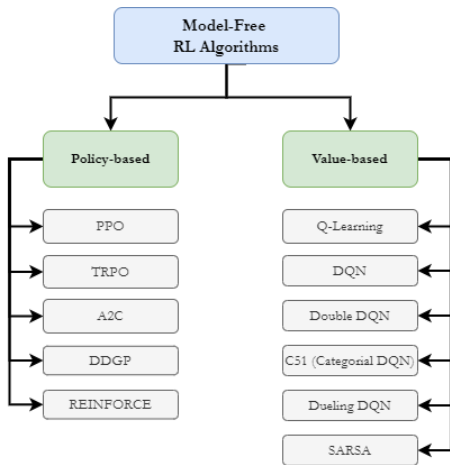[2] RL can help handling model-free cases
[3] Linear Convergence

FIGURE 3. Model-free Reinforcement Learning Algorithms

The algorithms chosen in this work are extensions of simple Q-learning algorithms including DQN, DDQN and C51 also known as categorical DQN. The only difference between Q-learning and DQN [64] is that the agent in DQN is based on neural networks rather than a simple Q-table. In DQN, an overestimation phenomenon is well observed due to the maximization function [7]. To solve this overestimation problem, DDQN uses two identical neural network models where one learns the Q-value and the other is a copy of the model learned from the last stage. Using a second model in combination with the current state model helps the system to evaluate different actions which might be more suitable for some states rather than the one on which the system is trained [1]. As compared to DQN or DDQN, categorical DQN uses a distribution value of the return rather than an expected value [11]. In multi-modal distributed data, where several peaks may be present in the data and a single average cannot truly represent the system's response, categorical DQN can solve the problem by looking at the distribution of the Q-function.

III. PROBLEM FORMULATION

The problem can be considered as a single task being completed by a number of centralized distributed event-triggered systems over a shared communication network where Table 2 provides definitions for necessary variables and symbols. Data from each system is timed stamped, un-synchronized and is transmitted under network imperfections (random delay, variable sampling time, packet drops, packet reordering). The tasks are divided into $p_1, p_2, \ldots, p_n$ systems and are controlled via a series of controllers ($c_1, c_2, \ldots c_n$) with some or no inter dependency. The input of any single system will depend upon the learning parameter of controller i as well as on the output of the same controller and on the output from other controllers.

$$u_i(t) = \lambda_i(y_1(t), y_2(t), \ldots, y_n(t)) \tag{7}$$

Here we are trying to minimize the delay and mean square error of the control system by prediction (model-free), where $u_i(t)$ is the input of the ith system. Consider the ith systems is defined by Equation 8 [51]:

$$x_i(t+1) = f(x_i(t), u_i(t), t) + w(t) \tag{8}$$

$$y_i(t) = g(x_i(t), u_i(t), t) \tag{9}$$

where $w(t)$ is the additive disturbance, $x_i(t)$ is the state of the system, $y_i(t)$ is the output of the ith system and $u_i(t)$ is the input of the system. The control error of the system is given by Equation 10

$$e_c^i = y_r(t) - y_i(t) \tag{10}$$

The learning algorithm is designed to compensate for control errors and additive disturbances in order to follow the reference trajectory for optimum control performance as per Equation 11:

$$\lambda \Delta u^i(t) = e_c^i(t) + w(t) \tag{11}$$

Symbols	Definitions
R_t	Overall Reward
γ, ρ	Discount Factor, reliability parameter
$Q^*(s,a)$	Optimal Value of the Valuation function
$u_i(t)$	Controller Input
λ_i	Controller learning parameter
$y_1(t), \ldots, y_n(t)$	Controller outputs
$x_i(t+1)$	Controller state
$w(t), \zeta_{s'}^a$	Noise, External Noise
$\delta(\sigma)$	Trigger Coefficient
d_t, d_p, d_q, D_{max}	Transmission delay, processing delay, queuing delay, maximum allowable delay
$P_t, h, \sigma^2(B)$	transmission power, channel gain, noise spectral density
ξ_s^i	Synchronization parameter
$\mathbb{E}[\vartheta], e^s$	Upper bound on overestimation errors, synchronization errors
$\varepsilon_{max}, C_{max}, N_{max}$	Maximum allowable errors, maximum channel capacity, Maximum number of devices
K_{ij}	Communication Links

TABLE 2. Symbols & Definitions

A. DECISION VARIABLES | CONSTRAINTS

Several decision variables influence the control performance of the systems, including network and control constraints. The few variables that we included in our problem formulation are as follow:

1) Transmission ACK

The binary valued vector for transmission acknowledgment is defined such that:

$$\delta(\sigma) = \begin{cases} 1 & \text{Transmission happens at } t = \sigma \\ 0 & \text{No transmission is happening} \end{cases} \quad (12)$$

where δ is a function of σ(trigger condition)

2) Delay constraints

The overall delay reduction for the system will ensure the stability of the system. In the case of a wireless networked controlled system with prediction and transmission happening over uncertain/un-reliable networks, the overall delay is the sum of transmission delay d_t, processing delay d_p and queuing delay d_q. The delay of the overall system is random in nature and could be modelled as Markov chains as if the network is under congestion so all the systems over the network will face delay. However, to ensure the stability of any system i, the system should satisfy the following constraint:

$$d_t^i + d_p^i + d_q^i \leq D_{max} \quad (13)$$

where the transmission delay is upper bounded by the maximum channel capacity and is given by:

$$d_t^i = \frac{N_p^i}{T_r} \quad (14)$$

where N_p^i are the bits to be transmitted and T_r is the transmission rate. A complete End-to-End delay model has

been discussed in [44]. There exists an inverse relationship between transmission delay and effective bandwidth of network which eventually puts a bound on queuing delay. However, in the case of non-deterministic network, delay models (where an upper bound on the overall E2E delay and channel capacity is defined by separate tuning of different delay parameters) might not be required. For further details about the relationship between delay and number of devices one can refer to [57], [74].

3) Channel Capacity Constraints

To ensure the efficient utilization of resources and minimum transmission errors as well as packet loss, the information transferred by the cumulative systems should be less than the channel capacity. The channel capacity [13] is a function of bandwidth and Signal-to-Noise Ratio (SNR) and is given by Equation 15, where at any instance t the relation between channel capacity and bandwidth is given by:

$$C = B \ log_2(1 + SNR) \quad (15)$$

where the SNR can be represented as a function of transmission power P_t, channel gain h and noise spectral density σ^2.

$$C = B \ log_2(1 + \frac{P^t||h||^2}{\sigma^2(B)}) \quad (16)$$

To ensure reliability of the overall system when N systems are transmitting, the upper bound on channel capacity is given by:

$$\sum_{i=1}^{N} B_i \ log_2(1 + \frac{P_i^t||h_i||^2}{\sigma_i^2(B_i)}) \leq C_{max} \quad (17)$$

where N is number of devices and the upper bound on the number of devices (N_{max}) is effected by both capacity and delay constraints.

4) Synchronization Errors

The synchronization error [44] between i and j agents is given by:

$$e^s = \mathbb{E}[\sum_{j=1,i\neq j}^{N} K_{ij}(y_j(t) - y_i(t))] \quad (18)$$

where K_{ij} is communication links between the i_{th} and j_{th} agent. For simplicity, we define here a synchronization parameter ξ_s^i which depends upon how much output of agent i_{th} is delayed which will affect eventually output of j_{th} agent.

$$\xi_s^i = y_j(t) - y_i(t)) \quad (19)$$

5) Overestimation Errors

RL is based on learning optimal policies in the Markovian decision process where the objective function $Q(s,a)$ learns incrementally. The state learning depends upon reward r and discount factor γ as in Equation 21. In presence of external noise $\zeta_{s'}^a$, the q-learning overestimation phenomenon occurs [63].

Lemma 2.1: Assuming the Q-learning happens under the stochastic environment with i.i.d variables $X = X_1, X_2, ...X_n$ which introduces a noise $\zeta_{s'}^a$, with zero mean in the evaluated function value, Q-learning overestimates in stochastic environments.

This phenomenon was first reported by Thrun, Anton in 1993. In presence of noises the evaluation function approximates as

$$Q_{t+1}^{approx}(s_t, a_t) = Q_{t+1}^{target}(s_t, a_t) + \zeta_{s_t}^{a_t} \qquad (20)$$

where the target evaluation function is given by

$$Q_{t+1}^{target} = R_{t+1} + \gamma \max_{a_{t+1} \in A} Q(s_{t+1}, a_{t+1}) \qquad (21)$$

The error introduced by the environmental noise in Equation 21 is given by:

$$\vartheta = R_{t+1} + \gamma \max_{a_{t+1} \in A} Q^{approx}(s_{t+1}, a_{t+1}) - R_{t+1}$$
$$- \gamma \max_{a_{t+1} \in A} Q^{target}(s_{t+1}, a_{t+1})$$
$$= \gamma(Q^{approx}(s_{t+1}, a_{t+1}) - Q^{target}(s_{t+1}, a_{t+1})) \qquad (22)$$

The upper bound on this overestimation is given as in equation:

$$\mathbb{E}[\vartheta] \le \gamma c; c = \epsilon \frac{n-1}{n+1} \qquad (23)$$

The upper bound is well proved by Thrun, Anton and is included for the reader's convenience (Lemma 2.2).

Lemma 2.2: [62] While $f(x)$ denoting the density of noise variables $\zeta_{s'}^a$, in interval $[-\varepsilon, \varepsilon]$ i.e., $f(x) = Pr[\zeta_{s'}^a = x] = \frac{1}{2\varepsilon}$

B. OBJECTIVE FUNCTION

The goal is to maximize Quality of Service (QoS) and Quality of Control (QoC), which is achieved by minimizing synchronization and control errors, and is expressed as follows:

$$max(QoS \ and \ QoC)$$

Which is based on minimization of control errors e_c^i and noise $w(t)$ for i^{th} system.

$$minf(e_c^i, w(t))$$

The cost function for Mean-square control error is given by:

$$J_c^e = \mathbb{E}[\sum_{j=1, i \ne j}^{N} (y_r(t) - y_i(t))^T (y_r(t) - y_i(t))] \qquad (24)$$

Where $y_r(t)$ is the reference output. Based on constraints and optimization goal, the overall objective with the constraints is given as below:

$$min(\mathbb{E}[\sum_{\substack{d_q, d_p, d_t \\ C_{max}, j=1 \\ N, i \ne j}}^{N} (y_r(t) - y_i(t))^T (y_r(t) - y_i(t))]) \qquad (25)$$

$$s.t. \ d_t + d_p + d_q \le D_{max} \qquad (25a)$$

$$\sum_{i=1}^{N} B_i \ log_2(1 + \frac{P_t}{B_i \sigma^2} z_t) \le C_{max} \qquad (25b)$$

$$N \le N_{max} \qquad (25c)$$

$$\delta(\sigma_i) \ge 0, \delta(\sigma_i) \in \{0, 1\} \qquad (25d)$$

$$\mathbb{E}[\vartheta] + e^s \le \varepsilon_{max} \qquad (25e)$$

$$\mathbb{E}[\vartheta] \le \gamma c; c = \epsilon \frac{n-1}{n+1} \qquad (25f)$$

$$e^s = \mathbb{E}[\sum_{j=1, i \ne j}^{N} K_{ij}(y_j(t) - y_i(t))] \qquad (25g)$$

The objective is to reduce MSE under reliability constraints (25a, 25b, 25e) where constraint (25c) shows the upper limit on maximum number of devices and constraint (25d) is a feasibility constraint.

C. FORMAL DESCRIPTION

The importance of the use of formal methods in understanding the behaviour of stochastic systems has been discussed in our previous research [8]. Learning automata have been used for decades to solve complex problems like routing in stochastic environments [31]. In this context, RL provides the core of learning automata. A learning automaton based formal description of the problem could help to understand the considered problem in a perspective to replicate the approach for multi-agent systems as shown in Figure 4.
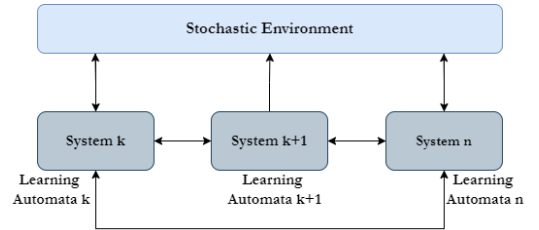

FIGURE 4. Learning Automata for mutli-agent systems

This section provides the necessary definitions for learning automaton.

Definition A learning automaton [3] is a tuple described as $L = (\eta, Act, P, p_t, u_n, \zeta_n, R)$

where:

$\eta \rightarrow$ Set of bounded input

$Act \rightarrow$ Defines the set of action in the action space $(a_1, a_2, ..., a_n)$

$\zeta_n \rightarrow$ Defines the sequence of environmental response. $\zeta_n \subseteq \eta$

$u_n \rightarrow$ Set of outputs/actions

$P \rightarrow$ Probability Space, which depends upon Probability and Sigma-Algebra function (F) of a set for bounded inputs and output sequence

$F_n = \sigma(\zeta_1, p_1, u_1; ...; \zeta_n, p_n, u_n)$

$p_t \rightarrow$ Set of probability distribution

$p_t = [p_n(1), p_n(2), ..., p_n(n)]^T$

$p_n(i)$ is conditional probability for the set of actions occurring under σ algebra function and sum of probabilities equates to 1

$p_n(i) = Pr\{\varsigma : u_n = u(i)|F_{n-1}\}$ where $F_{n-1} \subset F$

$R \rightarrow$ defines the reinforcement scheme where

$R_{t+1} = r_{t+1} + \gamma R_t$ where R_t represents the overall reward for the previous actions and γ is the discount factor

$\zeta_n \rightarrow$ conditional probability of the environment responses

$\zeta_t = [\zeta_n(1), \zeta_n(2), ..., \zeta_n(n)]^T$

IV. PROPOSED SOLUTION

As mentioned in the introduction section, a co-design approach offers a more satisfactory optimal control performance in the presence of wireless network constraints as compared to an interactive design approach. To formulate the problem, conventional optimization theory is used. The problem is formulated in mathematical form as indicated in Equation 25 with network constraints 25a, 25b, 25c, 25d, 25e, 25f and 25g. The problem under consideration is highly non-deterministic subjected that the number of devices (N) communicating is unknown. To solve the problem, the initial step is to calculate the maximum number of devices subject to channel capacity, delays and errors. Here we assumed that the minimum channel capacity required for each device to ensure delay and a small error probability is C^*. The constraint $(23g)$ comes into play for multi-agent interaction; to simplify the problem to a single agent, we have dropped the constraint from $(23g)$. Finding the solution to the problem consists of the following steps:

Learning: As mentioned earlier, to ensure optimal control performance a RL technique is used. Allocating a reward to the output response of the system in a stochastic environment under network constraints will help to achieve the desired performance. In case of error greater than the defined control threshold, the reward will be -1 i.e. a penalty, whereas in case of small error the reward will be +1. Section III-C provides a formal representation of the problem and the proposed algorithm 1 summarizes the approach used to solve the problem.

Reliability: To ensure reliability, the channel capacity constraint must be satisfied, which puts a limit on the maximum number of devices communicating. Thus, delays and errors are co-related with the assigned channel capacity. To make the problem simpler, constraints $23a, 23b, 23e$ are assumed to satisfy a reliability upper bound κ_{opt}. κ_{opt} provides minimum delay and errors under channel capacity constraints.

The maximum number of devices is obtained via a common binary search algorithm. Further discussion and explanation can be obtained from the simulation and results section V.

A. TIME COMPLEXITY ANALYSIS

Time complexity analysis for our approach: For the pro-

Algorithm 1 Proposed Algorithm to solve the co-design problem

Require: End to End Delay, $d^p, d^t, d^q, N, B_{max}$, bit-rate, power, sensitivity, Signal-to-Noise Ratio (SNIR) threshold and trigger coefficient

Ensure: $\min(J_c^e)$

  $N \leftarrow n$

  $Step1$:Determine Channel capacity for each user

  $Step2$:Determine Delay for each user

  $Step3$:Determine maximum number of allowable Users

  while $N \leq N_{max}$ and $C \leq C_{max}$ **do**

    if $y_{ref} - y_i$ is positive **then**

      $r \Leftarrow r + 1$

      $y_{ref} \Leftarrow y_i$ ▷ Dynamic Reference Change

    else if $y_{ref} - y_i$ is negative **then**

      $r \Leftarrow r - 1$

    else if $y_{ref} - y_i$ is zero **then**

      $y_{ref} \Leftarrow y_i$

    end if

  end while

---

posed Algorithm 1, if a RL based approach is used, the computational complexity for $step1$ for determining the channel capacity for each user and $step2$ for the delay estimation for each user is $O(n)$. For $step3$, where the upper bound on the number of maximum allowable users is determined using a common binary search, the computational complexity is $O(logn)$. As for the while loop, the complexity is $O(n^2)$. The complexity of the value iteration algorithm is $O(S^2 \times A \times n)$ [22], where S are the states, A are the actions and n is the number of iterations. Therefore, the total time complexity of the proposed algorithm is given as

$$O(n + n + logn + (S^2 \times A \times n)^2)$$

Thus, the overall time complexity of the proposed algorithm becomes $O((S^2 \times A \times n)^2)$.

In what follows, we also present, for reference, the time complexity of approaches based on MPC and LQR.

Time Complexity for an MPC-based Approach: Assuming that the model of the system is given, the relationship between the input and output variables of the system is known. The complexity of the algorithm remains the same as described above for our approach for $step1$, $step2$ and $step3$. However, for the while loop, the complexity for determining the output depends upon the number of inputs m and the prediction horizon p [72]; thus, the overall time complexity of an MPC-based approach under capacity and number of devices constraint is given as:

$$O(n + n + logn + ((m \times p \times n)^3)^2)$$

Hence, the overall time complexity will be $O(m \times p \times n)^3$ in case of conventional MPC and $O(m_i \times p \times n)^3$ in case of step-based MPC, where i represents the number of steps.

Time Complexity for an LQR-based solution Assuming that the system dynamics are known and $step1 - step3$ remains the same, solving the control problem (least-square) [14], [71] alone gives the time complexity as:

$$O(p \times n^3)$$

The total complexity, including the while loop, would turn out as:

$$O(n + n + logn + (p \times n^3)^2)$$

where p is the control horizon; thus the overall time complexity would be $O(p \times n^3)^2$.

V. SIMULATIONS AND RESULTS

To evaluate the performance as close as possible to a real-life scenario, we obtained the network and control parameters for the pump used in our laboratory as shown in Figure 5. The pump is integrated with a Raspberry Pi (RPi) to
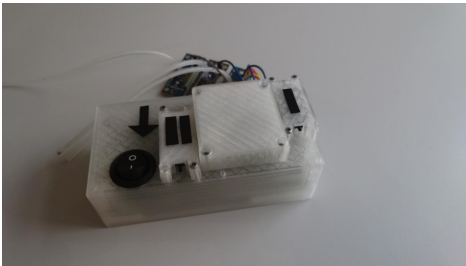
FIGURE 5. Our compact, portable, dual−channel piezoelectric pressure generator (i.e. pump) for droplet microfluidics application

implement a wireless controller over WiFi. The pump unit is a compact, portable, dual-channel piezoelectric pump that uses 2 Bartels mp6 piezo pumps in a closed-loop regulated pressure generator setup. The internal low-level controller is an ESP32 microcontroller, which will be connected to an RPi4 board. RPI4 benchmarking was performed to obtain an overview of its capabilities in terms of computation.

A. NETWORK SIMULATIONS

OMNET++ is a powerful C++ based simulation tool for wireless, wired and many other networks. OMNet++ was used to obtain network parameters such as delay and channel capacity for different numbers of devices. The results of the network simulations were aimed at acquiring End-to-End (E2E) delay, which consists of transmission delay (d_t), processing delay (d_b), propagation delay (d_p), and queuing delay (d_q) for control and background traffic applications. The network was simulated around 802.11e standards with the Quality of Service (QoS) service enabled and disabled [2]. In 802.11e, the MAC uses enhanced distributed channel access (EDCA) by which the video and audio packets sent can have different priorities, which helps achieve minimum

delay in delay-sensitive applications. Using the same services, control commands were sent at the same priority level as video in 802.11e which enforces that control packets will be transmitted before the background traffic. The background traffic model represents unnecessary load over the network while transmitting control data. The network configuration included controllers with static processing delay defined as $5~Sec$, server, configurator, Access Point (AP) and radio medium.

The upper bound on End-to-End (E2E) delay was defined as 200 ms for control applications. The bit rates were defined as 800 kbps and 33.3 Mbps for each control and background application, respectively. The maximum channel capacity was defined as 54 Mbps (2.4 GHz center frequency). The network simulations were performed for different numbers of devices i.e. 1, 5, 10,..., 15. Figure 6 gives an overview of the delay achieved for control devices versus background application when QoS is enabled for a single host. The control application experiences a constant and almost negligible delay whereas background applications experience a huge delay at the start and then tries to stabilizes; this initial delay is due to packet accumulation when the application initializes.
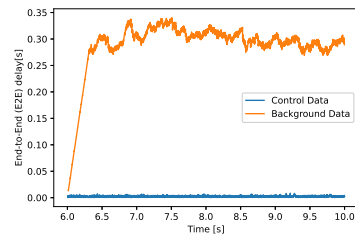

FIGURE 6. End-to-End Delay [s] vs. Time [s] when simultaneously transmitting control data and background data (QoS enabled)
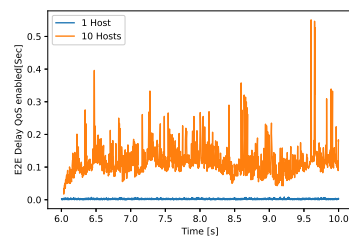

FIGURE 7. End-to-End Delay [s] vs. Time[s] when transmitting control data for 1 and 10 hosts (QoS enabled)

Figure 7 depicts how the delay increases when 10 hosts are communicating control data, versus the case with 1 host due to shared bandwidth. As the number of hosts increases, the delay experienced by the control applications also increases.

Next, when QoS is not enabled, the control applications are not prioritized and the control devices experience severe delay and low throughput. Figure 8 shows the throughput for the control versus background traffic when the QoS is not enabled.
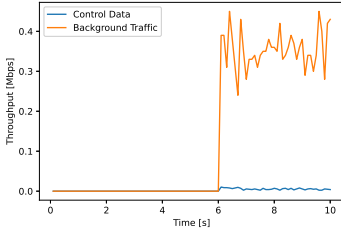

FIGURE 8. Throughput [Mbps] vs Time[s] when simultaneously transmitting control data and background data (Non-QoS)

The simulations were repeated for different numbers of host applications (N=1, 5, 10, 15); Figure 9 gives an overview of the maximum throughput achieved for control applications while QoS service is enabled.
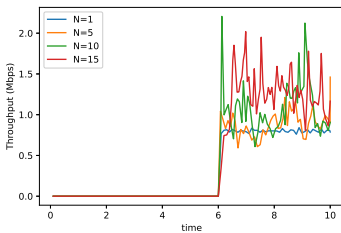
FIGURE 9. Throughput [Mbps] vs Time[s] when transmitting background data for 1, 5, 10, and 15 hosts (QoS enabled)

As compared with the non-QoS case, the throughput of the network changes over time, depending upon the data transmitted by high priority applications. Because of this, the throughput for control applications is comparatively higher than the throughput of the background applications. The average delay and throughput were calculated for control and background applications from the gathered data under QoS-enabled services; Table V-A summarizes the average delay and throughput achieved for a different number of applications.

Summary of the average delay and throughput achieved for different number of applications (hosts) with QoS enabled

Number of Hosts	Avg.Delay [ms]	Avg.Throughput [kbps]
1	2	32.4
5	102	39.2
10	119	52.6
15	245	65.6

B. REINFORCEMENT LEARNING RESULTS

As mentioned in the introduction section, the RL control of the pump was obtained under network uncertainties using three different approaches. To reduce the problem complexity, the agents were assumed to be performing independently from each other and the problem was solved for a single agent interacting with the environment where other agents are present and affecting the same environment. To add the effect of delay and bandwidth consumption parameter in the reward function, a reliability parameter ρ 6 was introduced in the reward function. For accommodating different possibilities where either delay or bandwidth consumed by the application exceeds the upper bound, which in turn leads to packet loss, the reliability parameter ρ was assigned a probability value between 0 and 1.

The ρ factor was introduced in two different ways: as a linear multiplier, as well as an exponential multiplier, to analyze the effect of it in the convergence of the algorithm.

Scenario 1:

In the first scenario, the network effects were not included in the reward function of the RL environment. Three algorithms, namely DQN, DDQN and C51 were used for the learning of the agent. In addition to the state of the system, the difference between allowable upper and lower bound of the flow rate was factored in the reward function. Figures 10, 11, and 12 show the average returns and loss for DDQN, DQN and C51 agents, respectively.
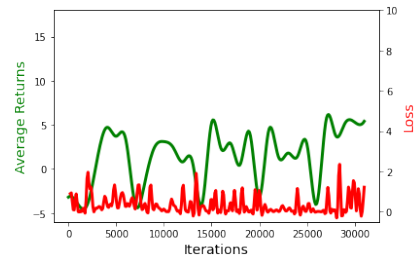

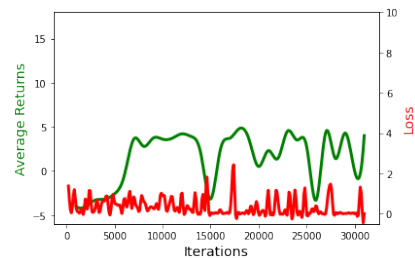**FIGURE 10.** Average returns and loss for DDQN without network

FIGURE 11. Average returns and loss for DQN without network
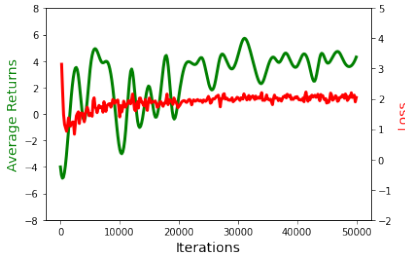
FIGURE 12. Average returns and loss for C51 without network

The performance was best with the C51 algorithm where average returns were more stable; on the other hand, the performance with DDQN and DQN was poor.

Scenario 2: As mentioned earlier, to mimic the real network scenario, OMNET++ simulations were performed. In Scenario 2, the simulation results were included as a learning factor in the reward function either as an exponential or a linear multiplier.

The results with C51 algorithm with either exponential and linear rewards, see Fig. 13, outperformed DDQN and DQN with linear rewards.
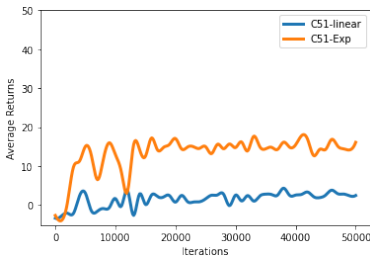

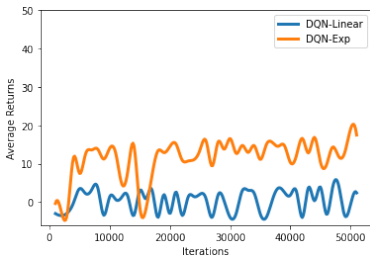**FIGURE 13.** Average returns for C51 with network simulations with Linear and Exponential Rewards

FIGURE 14. Average returns for DQN with network simulations with Linear and Exponential Rewards
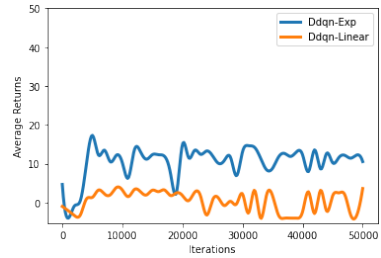

FIGURE 15. Average returns for DDQN with network simulations with Linear and Exponential Rewards

The results with DQN (see Fig.14) and DDQN (see Fig.15) with exponential reward performed well.

Scenario 3: To accommodate more uncertain network scenarios, both bandwidth consumption and delay were introduced in the reward function as random variables.

Under random network conditions, C51 (see Fig.16) and DDQN (see Fig.18) performed well whereas DQN (see Fig.17) did not converged. This implies that although DQN performed satisfactory average reward when the problem was limited to a single agent but taking into account for network congestion or delay caused by other networks showed the unsuitability of the agent in high network traffic scenarios.
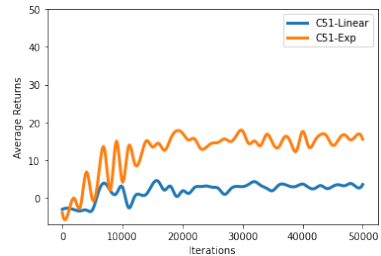

FIGURE 16. Average returns for C51 with random network conditions with Linear and Exponential Rewards
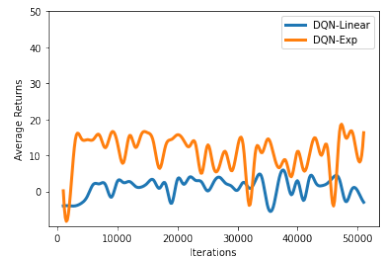

FIGURE 17. Average returns for DQN with random network conditions and Linear Rewards
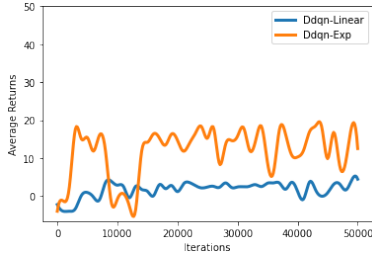
FIGURE 18. Average returns for DDQN with random network conditions and Linear Rewards

FIGURE 20. LSTM Control Error vs Events

Figure 19 shows the variation of flow rate obtained over 30000 iterations where network simulations were included in the reward function. It is evident from figure 19 that the DQN takes a bit longer to reach a stable response for flow rate; however, DDQN and C51 reach stable response comparatively faster.
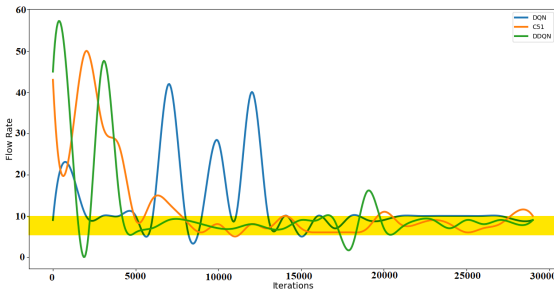

FIGURE 19. Flow Rate Prediction Under Network Constraints using OMNet++ Network Simulation data

In addition to the above discussed scenario, we also analyzed other learning algorithms like LSTM using RNN for scenario 2. A reliability parameter depending upon E2E delay, number of devices and data rate was chosen between 0-1, the Poisson distribution of which was then used as a control error. A Poisson distribution for control error (based on network parameters) is assumed due to the non-deterministic nature of the system leading to no predefined distribution of control error. The total time of computation for 30,000 iterations was recorded as 4m 12 sec. Figure 20 shows the control error for prediction on training and test data for LSTM algorithm using an RNN dense layer. Both of them look back (previous timestamps) and the batch sizes were chosen to be 50, and 333 different events were used as input data. Covariance, Pearson's correlation, and Spearman's correlation between two test flow rate data inputs (lying within the constraints) and flow rate achieved by agents utilizing various RL algorithms were analyzed for further evaluation of the algorithms. Here, the covariance shows a linear relationship between the test data and the actions taken by the agent for achieving the optimal/desired
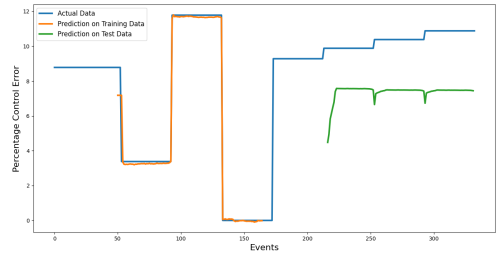
response. The reported value in Table 3 is the covariance between the variables and itself; a positive value indicates a variable change in the same direction whereas a negative value suggests a change in the opposite direction. However, as the covariance is not a best measure to characterize the relationship between data because it is hard to interpret, the Pearson and Spearsman's relationships between variables is also analyzed. The possible value of Pearson's correlation lies between -1 to 1, and values above 0.5 show a strong correlation between data in the same direction, while values below -0.5 show a strong correlation between data in the opposite direction. To account for a non-linear relationship between test data and agent actions, Spearsman's correlation was also calculated, where -1 shows a strong negative correlation and +1 shows a strong positive correlation. As evident from the results summarized in Table 3 for these evaluation metrics, C51 in scenario 1 and scenario 2 outperforms the other algorithms, whereas DDQN shows satisfactory results in some cases.

Another perspective to analyze is the role of the experience replay buffer. As mentioned earlier, C51 is an offline learning algorithm while DQN and DDQN are online learning algorithms; the experience replay buffer provides a middle ground for efficient operation. Based on the evaluation results, the role of the replay buffer in improving the overall performance of the C51 algorithm was further analyzed for Scenario 2. Different batch sizes were used to store the previous observations in the experience replay buffer and the cumulative rewards were calculated. It is evident from Figure 21 that increasing the batch size helps increasing the average rewards in early stages of the learning process and the use of a small batch size leads to less cumulative rewards. However, drawing a conclusion that 'the bigger the batch size the better the performance' is not true as continuous observation and update improves policy. A frequent update of the observations is required, making sure that storing enough past history for the system to learn but not all of the observations. The overall simulation results showed that even if the random network conditions are used still C51 performs well to achieve an optimal control performance in a stochastic

Algorithms	Covariance	Pearson's Correlation	Spearman's Correlation
Test Data Input([10,6,6,10,6,10,6,6,6,6,10,6,6,6,6,10,6,6,6,6,6,6,5,6,6,6,8,6,6,6])			
DQN (Scenario1)	0.39	0.05	0.076
DQN (Scenario2)	-3.69	-0.19	-0.17
DQN (Scenario3)	0.12	0.008	-0.03
DDQN (Scenario1)	0.59	0.02	0.07
DDQN (Scenario2)	-0.57	-0.03	0.43
DDQN (Scenario3)	1.80	0.1	0.04
C51 (Scenario2)	8.49	0.61	0.45
C51 (Scenario1)	1.73	0.26	-0.07
C51 (Scenario3)	-0.4	-0.91	-0.09
Test Data Input([10,6,6,10,6,10,6,6,8,6,10,6,6,6,10,6,6,6,8,9,10,10,8,10,6,10,8,6,10,6])			
DQN (Scenario1)	-0.22	-0.02	0.19
DQN (Scenario2)	-6.5	-0.29	0.03
DQN (Scenario3)	1.47	0.08	0.04
DDQN (Scenario1)	3.07	0.11	0.20
DDQN (Scenario2)	1.32	0.06	0.20
DDQN (Scenario3)	4.38	0.21	0.20
C51 (Scenario1)	-0.8	-0.61	-0.11
C51 (Scenario2)	6.04	0.36	0.39
C51 (Scenario3)	0.11	0.04	0.04
LSTM with RNN with OMNet++ Simulation Data			
LSTM (Prediction on Test Data)	0.031	0.22	-0.35

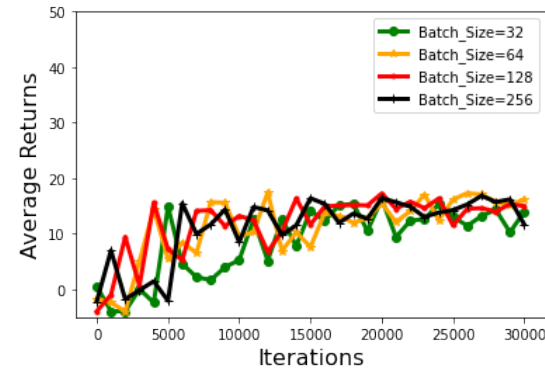**TABLE 3.** Performance Evaluation of Reinforcement Learning Algorithms Results

FIGURE 21. Replay Buffer: Batch Size vs. Average Returns for C51 Algorithm (Scenario 2)

environment. Overall, the results show that reliability can be well achieved using model-free RL approaches. The scalability of the system is restricted by network constraints such as capacity and system requirements, i.e. delay; this sets an upper bound on the number of devices that can be supported under specific network conditions. Event-triggered network control reduces network load but introduces reliability issues which are out of the scope of this work. However, as the problem complicates the method could take more time to converge. Although a binary search can provide an estimate for the optimal number of devices, it is best to include the network effects in the reward function for the system to learn the possible network scenarios for dynamic adaptation to network changes.

VI. CONCLUSION

In this work, we focused on the co-design for joint-optimization of wireless networked controlled systems using model-free RL. The research emphasized the importance of wireless network constraints in addition to the control system constraints to achieve an optimal system performance. The paper focused on many aspects of the problem in terms of optimization theory and argued the presence of various factors which motivated the use of RL as compared with classical and robust control methods. As a use case, the application of the theory was implemented for double emulsion droplet formation unit; DQN, DDQN and C51 algorithms were used to achieve the control performance of the system under bounded constraints. C51 was found to outperform the other algorithms due to its multi-modal problem-solving capabilities. The results also showed that the reward function plays an important role in the agent's learning process and that designing the reward function carefully could help to achieve better performance. Currently, our work does not investigate the reliability issues introduced via event triggered control for better efficiency. In the future, the aim is to explore a middle ground between better performance and reliability under different network scenarios using hybrid control approaches. Also, the power constraints have not been studied and are left for future work.

ACKNOWLEDGMENT

APPENDIX. LEMMAS

Lemma 2.1: Assuming the Q-learning happens under the stochastic environment with i.i.d variables $X = X_1, X_2, ...X_n$ which introduces a noise $\zeta_{s'}^a$ with zero mean in the evaluated function value. Q-learning overestimates in stochastic environments:

With the noise introduced during learning the reward attached with the Q-function is given as below:

$$r(\hat{s}, a) = r(s, a) + \epsilon$$

From probability theory the expectation of any variable X_i is given by its distribution over the N samples and can be formulated as below:

$$\mathbb{E}[X_i] = \frac{1}{|N_i|} \sum_{x_i \in N} x_i$$

At each stage the reward will be higher than expected due to cumulative errors added at each stage. Even if function values are too small at any stage, due to maximum operator in q-learning the function will tend to select the maximum from the estimated distributions ψ_i.

$$\max_{i \in 1,2,...,n} \mathbb{E}[X_i] = \max_{i \in 1,2,...,n} \mathbb{E}[\psi_i]$$

At each stage the estimation is made from the maximized estimates of the previous stages which leads to:

$$\mathbb{E}[\max_{i \in 1,2,...,n} \psi_i] \geq \max_{i \in 1,2,...,n} \mathbb{E}[\psi_i]$$

Under the assumption of ψ_i has non-zero probability the q-learning will tend to overestimate.

Lemma 2.2: [62] While $f(x)$ denoting the density of noise variables $\zeta_{s'}^a$, in interval $[-\varepsilon, \varepsilon]$ i.e., $f(x) = Pr[\zeta_{s'}^a = x] = \frac{1}{2\varepsilon}$

$$\mathbb{E}[\vartheta] = \mathbb{E}[\gamma(Q^{approx}(s_{t+1}, a_{t+1}) - Q^{target}(s_{t+1}, a_{t+1}))]$$
$$= \gamma \mathbb{E}[\max_{a_{t+1} \in A} \zeta_{s'}^a]$$
$$= \gamma \int_{-\infty}^{\infty} x \; n \; f(x) \left(\int_{-\infty}^{\infty} f(z)dz \right)^{n-1} dx$$
$$= \gamma \; n \int_{-\infty}^{\infty} x \frac{1}{2\varepsilon} (\frac{1}{2} + \frac{1}{2\varepsilon})^{n-1} dx$$
$$= \gamma \; n \int_{0}^{1} (2\varepsilon y - \varepsilon) y^{n-1} dy$$
$$= \gamma \; n \; \varepsilon \int_{0}^{1} 2y^n - y^{n-1} dy = \gamma \; n \; \varepsilon (\frac{2}{n+1} - \frac{1}{n})$$
$$\mathbb{E}[\vartheta] \leq \gamma c; c = \epsilon \frac{n-1}{n+1}$$

APPENDIX. OTHER RESULTS

A. COMPARISON TO OTHER NON-MACHINE LEARNING METHODS

To support our argument of using RL instead of simple search algorithms, we analyzed the problem in more depth. For the optimization problem Equation 25, we tried to compute the linear approximation of the control error under constraints based on desired output and input data-set gathered using simulations. For the computation, we used the well-known "*Newton Raphson Method*". However, the method failed to converge already within the first 50 iteration under the subset of the acquired data. The use of "Least Square Minimization" and "Trust Region Constrained" algorithms was also considered, but as discussed earlier, the problem is non-deterministic in nature which did not lead us to any feasible implementation. We also tried using "Binary Search" to solve other constraints of the problem but the algorithm did not find any solution with the provided simulation data-set. The use of a "Brute Force" algorithm was also tested; however, using the whole dataset lead our system to run out of memory, or under best conditions the algorithm was not able to find any solution in a 4-5 hours period. This lead to try the use of smaller subset of the data; however, the algorithm did not manage to find the optimal/desired solution.

B. COMPUTATION TIME

For the simulations we used a Lenovo IdeaPad L340 Gaming Laptop equipped with an Intel (R) Core (TM) i5-9300H CPU @2.4 GHz. Table 4 shows the computation time for the three scenarios for the implemented RL algorithms.

Algorithms	Computation Time (30000 iterations)
DQN (Scenario1)	6 m and 14 s
DQN (Scenario2)	6 m and 38.9 s
DQN (Scenario3)	6 m and 40 s
DDQN (Scenario1)	5 m and 51 s
DDQN (Scenario2)	5 m and 54 s
DDQN (Scenario3)	5 m and 52 s
C51 (Scenario1)	6 m and 14 s
C51 (Scenario2)	6 m and 7.6 s
C51 (Scenario3)	6 m and 21 s

TABLE 4. Computation Time taken by Reinforcement Learning Algorithms

REFERENCES

[1] Deep reinforcement learning: Dqn, double dqn, dueling dqn, noisy dqn and dqn with prioritized experience replay | by parsa heidary moghadam | medium.

[2] IEEE 802.11 Quality of Service — INET 4.3.0 documentation.

[3] Chapter 3 - optimization techniques. In Kaddour Najim, Enso Ikonen, and Ait-Kadi Daoud, editors, Stochastic Processes, pages 167–221. Kogan Page Science, Oxford, 2004.

[4] Insights and Advancements in Microfluidics. MDPI, 9 2017.

[5] Naman Agarwal, Syomantak Chaudhuri, Prateek Jain, Dheeraj Nagaraj, and Praneeth Netrapalli. Online target q-learning with reverse experience replay: Efficiently finding the optimal policy for linear mdps, 2021.

[6] Oron Anschel, Nir Baram, and Nahum Shimkin. Averaged-dqn: Variance reduction and stabilization for deep reinforcement learning. 11 2016.

[7] Oron Anschel, Nir Baram, and Nahum Shimkin. Deep reinforcement learning with averaged target dqn. 11 2016.

[8] Kanwal Ashraf, Yannick Le Moullec, Tamás Pardy, and Toomas Rang. Model-based system architecture for event-triggered wireless control of bio-analytical devices. In 2021 24th Euromicro Conference on Digital System Design (DSD), pages 465–471, 2021.

[9] Kanwal Ashraf, Tamas Pardy, and Yannick Le Moullec. Decentralized distributed data structure for bioanalytical laboratory setups. 06 2021.

[10] Anil Aswani, Neal Master, Jay Taneja, David Culler, and Claire Tomlin. Reducing transient and steady state electricity consumption in hvac using learning-based model-predictive control. Proceedings of the IEEE, 100(1):240–253, 2012.

[11] Marc G. Bellemare, Will Dabney, and Rémi Munos. A distributional perspective on reinforcement learning, 2017.

[12] Héctor Benítez-Pérez, Jorge L Ortega-Arjona, Paul E Méndez-Monroy, Ernesto Rubio-Acosta, and Oscar A Esquivel-Flores. Control Strategies and Co-Design of Networked Control Systems, volume 13. 2019.

[13] Alan Bensky. Chapter 9 - introduction to information theory and coding. In Alan Bensky, editor, Short-range Wireless Communication (Third Edition), pages 211–236. Newnes, third edition edition, 2019.

[14] Professor Stephen Boyd. LQR problem: background, 2008.

[15] Stephen Boyd and Lieven Vandenberghe. Convex Optimization. Cambridge University Press, 2004.

[16] Silvio Brandi, Massimo Fiorentini, and Alfonso Capozzoli. Comparison of online and offline deep reinforcement learning with model predictive control for thermal energy management. Automation in Construction, 135:104128, 03 2022.

[17] M.S. Branicky, V. Liberatore, and S.M. Phillips. Networked control system co-simulation for co-design. In Proceedings of the 2003 American Control Conference, 2003., volume 4, pages 3341–3346 vol.4, 2003.

[18] Bo Chang. URLLC Design for Real-Time Control in Wireless Control Systems. IEEE 5G World Forum, 5GWF 2018 - Conference Proceedings, pages 437–439, 2018.

[19] Shiyu Chen and Yanjie Li. An overview of robust reinforcement learning. 2020 IEEE International Conference on Networking, Sensing and Control (ICNSC), pages 1–6, 2020.

[20] Wei-Lung Chou, Pee-Yew Lee, Cing-Long Yang, Wen-Ying Huang, and Yung-Sheng Lin. Recent advances in applications of droplet microfluidics. Micromachines, 6(9):1249–1271, 2015.

[21] Ignasi Clavera, Jonas Rothfuss, John Schulman, Yasuhiro Fujita, Tamim Asfour, and Pieter Abbeel. Model-based reinforcement learning via meta-policy optimization, 2018.

[22] Dan Klein and Pieter Abbeel. SP14 CS188 Lecture 16 – Bayes Nets.

[23] Sarah Dean, Horia Mania, Nikolai Matni, Benjamin Recht, and Stephen Tu. On the sample complexity of the linear quadratic regulator. Foundations of Computational Mathematics, 20, 10 2017.

[24] Lei Deng, Chih-Chun Wang, Minghua Chen, and Shizhen Zhao. Timely wireless flows with arbitrary traffic patterns: Capacity region and scheduling algorithms. In IEEE INFOCOM 2016 - The 35th Annual IEEE International Conference on Computer Communications, pages 1–9, 2016.

[25] Damien Ernst, Mevludin Glavic, Florin Capitanescu, and Louis Wehenkel. Model predictive control and reinforcement learning as two complementary frameworks. Proceedings of the 13th IFAC Workshop on Control Applications of Optimisation, 01 2006.

[26] Bakhtiyar Farayev and Sinem Coleri Ergen. Towards ultra-reliable m2m communication: Scheduling policies in fading channels. In 2016 23rd International Conference on Telecommunications (ICT), pages 1–6, 2016.

[27] Vladimir Feinberg, Alvin Wan, Ion Stoica, Michael I. Jordan, Joseph E. Gonzalez, and Sergey Levine. Model-based value estimation for efficient model-free reinforcement learning, 2018.

[28] Frank H.P. Fitzek, Eckehard Steinbach, Juan A. Cabrera G., Vincent Latzko, Jiajing Zhang, Yun Lu, Merve Sefunç, Christian Scheunert, René Schilling, Andreas Traßl, Andrés Villamil, Norman Franchi, and Gerhard P. Fettweis. Chapter 11 - communications and control. In Frank H.P. Fitzek, Shu-Chen Li, Stefanie Speidel, Thorsten Strufe, Meryem Simsek, and Martin Reisslein, editors, Tactile Internet, pages 249–275. Academic Press, 2021.

[29] Honghao Gao, Can Liu, Youhuizi Li, and Xiaoxian Yang. V2vr: Reliable hybrid-network-oriented v2v data transmission and routing considering rsus and connectivity probability. IEEE Transactions on Intelligent Transportation Systems, 22(6):3533–3546, 2021.

[30] Alia Abdul Ghaffar and Tom Richardson. Model Reference Adaptive Control and LQR Control for Quadrotor with Parametric Uncertainties. 9(2):244–250, 2015.

[31] R J Gibbens. 5 - teletraffic theory. In Fraidoon Mazda, editor, Telecommunications Engineer's Reference Book, pages 5–1–5–14. Butterworth-Heinemann, 1993.

[32] Daniel Görges. Relations between model predictive control and reinforcement learning. IFAC-PapersOnLine, 50(1):4920–4928, 2017. 20th IFAC World Congress.

[33] Ashton Harvey, Kathryn Laskey, and Kou-Chu Chang. Machine learning applications for sensor tasking with non-linear filtering. 03 2021.

[34] Devon M. Headen, José R. García, and Andrés J. García. Parallel droplet microfluidics for high throughput cell encapsulation and synthetic microgel generation. Microsystems Nanoengineering, 4(1):1–9, 2018.

[35] Zhanwei Hou, Changyang She, Yonghui Li, Li Zhuo, and Branka Vucetic. Prediction and communication co-design for ultra-reliable and low-latency communications. IEEE Transactions on Wireless Communications, 19(2):1196–1209, 2020.

[36] T. Jackulin, M. Ramya, and C. Subashini. Energy optimization for wsn architecture and self test embedded processor. In 2012 International Conference on Emerging Trends in Electrical Engineering and Energy Management (ICETEEEM), pages 253–256, 2012.

[37] Nan Jiang, Yansha Deng, Arumugam Nallanathan, and Jinhong Yuan. A decoupled learning strategy for massive access optimization in cellular iot networks. IEEE Journal on Selected Areas in Communications, 39(3):668–685, 2021.

[38] Ali Taleb Zadeh Kasgari and Walid Saad. Model-free ultra reliable low latency communication (urllc): A deep reinforcement learning framework. In ICC 2019 - 2019 IEEE International Conference on Communications (ICC), pages 1–6, 2019.

[39] W. Bradley Knox and Peter Stone. Reinforcement learning from human reward: Discounting in episodic tasks. Proceedings - IEEE International Workshop on Robot and Human Interactive Communication, pages 878–885, 2012.

[40] Yuan Lin, John McPhee, and Nasser L. Azad. Comparison of deep reinforcement learning and model predictive control for adaptive cruise control. IEEE Transactions on Intelligent Vehicles, 6(2):221–231, 2021.

[41] Mohammad H. Mamduhi, Dipankar Maity, Sandra Hirche, John S. Baras, and Karl H. Johansson. Delay-sensitive Joint Optimal Control and Resource Management in Multi-loop Networked Control Systems. IEEE Transactions on Control of Network Systems, XX(XX):1–12, 2021.

[42] Mohammad H. Mamduhi, Dipankar Maity, Sandra Hirche, John S. Baras, and Karl H. Johansson. Delay-sensitive joint optimal control and resource management in multiloop networked control systems. IEEE Transactions on Control of Network Systems, 8(3):1093–1106, 2021.

[43] Pau Martí, José Yépez, Manel Velasco, Ricard Villà, and Josep M. Fuertes. Managing quality-of-control in network-based control systems by controller and message scheduling co-design. IEEE Transactions on Industrial Electronics, 51(6):1159–1167, 2004.

[44] Sudip K. Mazumder. Wireless networking based control. 2011.

[45] Hesameddin Mohammadi, Mahdi Soltanolkotabi, and Mihailo R. Jovanović. On the linear convergence of random search for discrete-time lqr. IEEE Control Systems Letters, 5(3):989–994, 2021.

[46] Eduardo F. Morales and Julio H. Zaragoza. An introduction to reinforcement learning. Decision Theory Models for Applications in Artificial Intelligence: Concepts and Solutions, pages 63–80, 2011.

[47] Bhushan S. Pattni, Vladimir V. Chupin, and Vladimir P. Torchilin. New developments in liposomal drug delivery. Chemical Reviews, 115(19):10938–10966, 2015. PMID: 26010257.

[48] Mahfoozur Rahman, Sarwar Beg, Amita Verma, Firoz Anwar, Abdus Samad, and Vikas Kumar. Chapter 4 - liposomal-based therapeutic carriers for vaccine and gene delivery. In Vijay Mishra, Prashant Kesharwani, Mohd Cairul Iqbal Mohd Amin, and Arun Iyer, editors, Nanotechnology-Based Approaches for Targeting and Delivery of Drugs and Genes, pages 151–166. Academic Press, 2017.

[49] Anna Scampicchio and Gianluigi Pillonetto. A convex approach to robust lqr. In 2020 59th IEEE Conference on Decision and Control (CDC), pages 3705–3710, 2020.

[50] Ott Scheler, Karol Makuch, Pawel Debski, Michal Horka, Artur Ruszczak, Natalia Pacocha, Krzysztof Sozański, Olli-Pekka Smolander, Witold Postek, and Piotr Garstecki. Droplet-based digital antibiotic susceptibility screen reveals single-cell clonal heteroresistance in an isogenic bacterial population. Scientific Reports, 10:3282, 02 2020.

[51] Computer Scientist. Contributions to Networked and Event-Triggered Control of Linear Systems María Guinaldo Losada. 2013.

[52] Siti Sendari. Study on robustness and adaptability of genetic network programming with reinforcement learning for mobile robot. 2013.

[53] Wei ShangGuan, Bin Shi, Bai-Gen Cai, Jian Wang, and Yu Zang. Multiple v2v communication mode competition method in cooperative vehicle infrastructure system. In 2016 IEEE 19th International Conference on Intelligent Transportation Systems (ITSC), pages 1200–1205, 2016.

[54] Changyang She, Rui Dong, Zhouyou Gu, Zhanwei Hou, Yonghui Li, Wibowo Hardjawana, Chenyang Yang, Lingyang Song, and Branka Vucetic. Deep learning for ultra-reliable and low-latency communications in 6g networks. IEEE Network, 34(5):219–225, 2020.

[55] Changyang She, Rui Dong, Zhouyou Gu, Zhanwei Hou, Yonghui Li, Wibowo Hardjawana, Chenyang Yang, Lingyang Song, and Branka Vucetic. Deep Learning for Ultra-Reliable and Low-Latency Communications in 6G Networks. IEEE Network, 34(5):219–225, 2020.

[56] David Silver, Thomas Hubert, Julian Schrittwieser, Ioannis Antonoglou, Matthew Lai, Arthur Guez, Marc Lanctot, Laurent Sifre, Dharshan Kumaran, Thore Graepel, Timothy Lillicrap, Karen Simonyan, and Demis Hassabis. Mastering chess and shogi by self-play with a general reinforcement learning algorithm, 2017.

[57] Diptanshu Singh. Average Network Delay and Queuing Theory basics - Packet Pushers.

[58] Ariane Stucki, Petra Jusková, Nicola Nuti, Steven Schmitt, and Petra S. Dittrich. Synchronized Reagent Delivery in Double Emulsions for Triggering Chemical Reactions and Gene Expression. Small Methods, 5(8):1–8, 2021.

[59] Freek Stulp and Olivier Sigaud. Policy Improvement Methods: Between Black-Box Optimization and Episodic Reinforcement Learning. 34 pages, October 2012.

[60] Richard S Sutton and Andrew G Barto. Reinforcement Learning: An Introduction Second edition. 2018.

[61] Csaba Szepesvári. Algorithms for Reinforcement Learning, volume 4. 01 2010.

[62] Sebastian Thrun and Anton Schwartz. Issues in using function approximation for reinforcement learning. 1999.

[63] Hado Van Hasselt. Insights in reinforcement learning : formal analysis and empirical evaluation of temporal-difference learning algorithms. 01 2011.

[64] Hado van Hasselt, Arthur Guez, and David Silver. Deep reinforcement learning with double q-learning, 2015.

[65] Qiang Xu and Jia Yang. Wireless networked control systems with neural networks and ant colony optimization algorithm. In 2018 37th Chinese Control Conference (CCC), pages 164–169, 2018.

[66] Sagar Yadavali, Heon-Ho Jeong, Daeyeon Lee, and David Issadore. Silicon and glass very large scale microfluidic droplet integration for terascale generation of polymer microparticles. 9(1):1222.

[67] Haojun Yang, Kuan Zhang, Kan Zheng, and Yi Qian. Leveraging linear quadratic regulator cost and energy consumption for ultrareliable and low-latency iot control systems. IEEE Internet of Things Journal, 7(9):8356–8371, 2020.

[68] Mohan Yogeswaran and S. G. Ponnambalam. Reinforcement learning: Exploration-exploitation dilemma in multi-agent foraging task. Opsearch, 49(3):223–236, 2012.

[69] Jimin Yu, Chunhua Kuang, and Yanan Xie. Model predictive control of ncss with quantization packet dropout and time delays. Proceedings - 2016 8th International Conference on Intelligent Human-Machine Systems and Cybernetics, IHMSC 2016, 1(3):160–163, 2016.

[70] Tengchan Zeng, Omid Semiari, Walid Saad, and Mehdi Bennis. Joint communication and control for wireless autonomous vehicular platoon systems. IEEE Transactions on Communications, 67:7907–7922, 11 2019.

[71] Hong-Yan Zhang, Jia-Zhen Luo, and Yu Zhou. Explicit symplectic-precise iteration algorithms for linear quadratic regulator and matrix differential riccati equation. IEEE Access, 9:105424–105438, 2021.

[72] Langwen Zhang and Jingcheng Wang. A novel multi-step model predictive control for multi-input systems. Asian Journal of Control, 17(2):707–715, 2015.

[73] Qingquan Zhang, Jiaqu Chen, and Hongwei Gai. High-throughput-generating water-in-water droplet for monodisperse biocompatible particle synthesis. Journal of Materials Science, 54(24):14905–14913, 2019.

[74] Ying Jun Zhang, Soung Chang Liew, and Da Rui Chen. Delay analysis for wireless local area networks with multipacket reception under finite load. In IEEE GLOBECOM 2008 - 2008 IEEE Global Telecommunications Conference, pages 1–6, 2008.

[75] Qi Zhu and Alberto Sangiovanni-Vincentelli. Codesign Methodologies and Tools for Cyber-Physical Systems. Proceedings of the IEEE, 106(9):1484–1500, 2018.

TAMAS PARDY received the M.Sc. degree in info-bionics engineering from Peter Pazmany Catholic University, Budapest, Hungary, in 2014, and the Ph.D. degree in electronics and telecommunication from Tallinn University of Technology, Tallinn, Estonia, in 2018. He is currently a senior researcher at Tallinn University of Technology. He has supervised 1 Ph.D thesis and 3 M.Sc. theses and has authored or co-authored 20 scientific publications. His research interests include flow- and temperature-control of Lab-on-a-Chip devices.

KANWAL ASHRAF is a PhD student at Tallinn University of Technology, Estonia. Kanwal received her Joint-International Master's degree in Smart System Integration from Heriot-Watt University, UK, USN, Norway and BME, Hungary in 2020. She holds a bachelor's degree in electrical engineering from University of the Punjab, Pakistan. Her research topics include application of Wireless communication in CPSs and Co-Design of Wireless Networked Control Systems for bioanalytical applications.

TOOMAS RANG was born on November 10, 1951, in Tallinn, Estonia. He graduated the Tallinn Technical University (TTU), Estonia as an Electronics Engineer in 1975. In 1981 he successfully defended the PhD degree in Electronics at the Hungarian Academy of Sciences. From 1984/1985, he held the Postdoc position at Saarland University, Germany. In 1996 he was elected for the professor position in Electronics Design at TTU. In 1998 he was elected to the head of the Department of Electronics. Since 2020 he is the Professor Emeritus at TTU. He the senior member of IEEE. He has successfully supervised fifteen Ph.D. theses and is author of about 120 scientific publications. His research interests cover the topics from wide bandgap-based semiconductor devices and metallization technologies, till the microfluidics-based Lab-on-Chip devices.

• • •

YANNICK LE MOULLEC received the M.Sc. degree in electrical engineering from Université de Rennes I, Rennes, France, in 1999 and the Ph.D. degree in Electrical Engineering from Université de Bretagne Sud, Lorient, France, in 2003. From 2003 to 2013, he successively held Postdoc, Assistant, and Associate Professor positions with Aalborg University, Aalborg, Denmark. He then joined Tallinn University of Technology, Tallinn, Estonia as a Senior Researcher and then on a professorship of Cognitive Electronics. He has supervised eleven Ph.D. theses and nearly 60 M.Sc. thesis. He was Co-PI for the H2020 COEL ERA-Chair project. His research interests include HW/SW codesign, embedded systems, reconfigurable systems, and IoT.

Appendix 4

Future Publication IV
K. Ashraf, Y. Le Moullec, T. Pardy and T. Rang, "Co-Design of a Wireless Networked Control System for Reliability and Resource-Efficiency"

Under revision, to be re-submitted to Baltic Electronics Conference 2024 (BEC2024).

Co-Design of a Wireless Networked Control System for Reliability and Resource-Efficiency

Kanwal Ashraf, Yannick Le Moullec, *Senior Member, IEEE,* Tamás Pardy, *Member, IEEE,* Toomas Rang, *Senior Member, IEEE*

Abstract—We present a co-design method for wireless networked control systems (WNCS) that optimizes both the network and control parameters for optimal performance. The objective is to make the system resource-efficient by introducing the possibility of switching the control policy from reliable control to energy-efficient control, or by optimizing the power consumption using variable inter-packet gap (IPG) in the wireless communication layer. An RL-based approach is used to ensure efficient resource allocation and create effective control performance under moderate to high packet loss. This is achieved by formulating a multi-objective problem that considers both resource efficiency and reliability. Subsequently, the proposed algorithm is used to solve this multi-objective problem. Simulation results show that despite situations where the network experiences packet losses, the proposed co-design reinforcement learning (RL)-based control technique effectively maintains, or in some cases even improves control performance. In contrast to conventional control, where a 15% packet loss in the network causes control performance to completely fail, the proposed RL-based approach is immune to network packet loss and also demonstrates the capability to achieve an average reduction in transmission power of up-to 10%.

Index Terms—Reinforcement Learning (RL), Wireless networked control systems, co-design, latency, inter-packet gap, packet loss, optimal control

I. INTRODUCTION

Applications such as self-driving automobiles, wireless industrial networks, wirelessly remote-controlled surgical robots, and bio-analytical devices [1] are examples of wireless networked control systems (WNCS). Several recent works emphasize the significance of using a co-design methodology for designing such systems. However, the majority of these works either focus on the control aspect of the system ignoring the effect of communication technique and infrastructure on control stability, or vice versa, and thus do not fully exploit the co-design concept. Deep learning-based perception models and optimal control algorithms are used in the joint design framework introduced in the work [2] in which massive datasets were used to train perceptual models for object detection, lane detection, and semantic segmentation for cooperative automatic driving. However, such an effort does not focus on communication infrastructure requirements. In real-world scenarios with network uncertainties such as packet losses and other network degradations, the system's performance is adversely affected; hence the network behavior must be included in the system's design. A recent study [3] emphasizes co-design in the creation of a BotNet simulator

and examines how precise communication models affect multi-agent systems and swarms. However, the paper fails to analyze the previously mentioned network uncertainties and to conduct specific tests to evaluate the BotNet's scalability; hence communication performance benchmarking is crucially missing for evaluating the simulator. The paper [4] talks about control-guided communication co-design for distributed self-triggered control across wireless multi-hop networks. In this design, the control system requests the communication system for resources dynamically, and the communication system either gives them to the control system or turns them off. That study shows that low-powered wireless networks can achieve low latency. However, the work assumes perfect control and communication conditions, and closed-loop control stability is still an open research issue, especially in the presence of message losses. This may affect resource efficiency and strategy efficacy, and it may be prudent to prioritize achieving control stability as the primary objective.

Contribution: In contrast to existing research such as the above [2] for the co-design of wireless networked control systems, our work proposes a joint optimization of control-communication reliability and resource efficiency in both the control and the communication layers, using reinforcement learning (RL). Additionally, contrary to existing works where a purely analytical approach is a common practice [5], we validate the proposed approach on simulation-based scenarios, which is more realistic as this allows modeling e.g. uncertainties. This work is valuable in the field because it helps co-design reliable and resource-efficient WNCS, which also includes incorporating several network parameters that have been ignored so far in existing research. Moreover, the same concepts and design methodology have the potential to be used for several applications, i.e. autonomous vehicles, Ultra Reliable Low Latency Communication (URLLC) systems, etc. In our experiments with a wirelessly controlled pendulum mechanism, we show that compared to conventional control, where a 15% packet loss in the network makes the control completely fail and requires re-tuning of the PID parameters every time a change occurs in the network, our RL-based approach rapidly takes these effects into account and once the training of the RL agent is complete, it is able to compensate for the majority of network fluctuations while achieving an average reduction in transmission power of up-to 10%.

II. ANALYTICAL FORMULATIONS & SIMULATION ASPECTS

To analyze and solve the problem both in theory and simulation, an analytical formulation of the problem was performed as an initial step. Next, this formalized problem is mapped into a simulation environment where the proposed RL-based approach is used to evaluate the effect of the network constraints on the wireless control of an inverted pendulum controlled via tendons for industrial robotics applications (self-balancing robots). The optimization problem formulation, case study, proposed method, and the simulation setup are presented in what follows.

A. Analytical Formulation

The goal is to trade-off control-communication reliability and resource efficiency while maintaining acceptable performance. To do so, we propose to jointly optimize the above system quality attributes. This is a multi-objective optimization problem, and to build up our solution we use the Max-Min optimization strategy because it is well established for optimal control via Model Predictive Control (MPC) [6] in network control systems [7] and also for resource optimization [8]–[10]. Using Max-Min optimization strategies ensures that, even in the worst-case scenario, the system is able to maintain a certain level of acceptable performance or robustness in the face of uncertainty. A multi-objective optimization [11] problem is formulated as a Max-Min problem:

$$Q_{opt_{obj}}(x) = min(Q_1(x)) + max(Q_2(x)), ..., min(Q_n(x))$$
$$\text{s.t.} \quad g_i(x) \leq 0, \qquad i = 1, 2, ..n$$

The optimal system objective is to minimize $Q_1(x)$ and maximize $Q_2(x)$ and so on, among other performance characteristics. Thus, optimal performance is achieved by combining the objectives of several performance metrics that have been minimized or maximized under constraints $g_i(x)$.

Consequently, in our case, the Max-Min problem for joint optimization of reliability (γ_{cc}) and resource efficiency (r_{cons}) for both control and communication is formulated and elaborated below:

$$Q_{opt_{obj}} = max(\gamma_{cc-rel}) + min(r_{cons}) \qquad (2a)$$

$$\text{where } max(\gamma_{cc-rel}) = min \sum_{i=1}^{n}(y_{ref} - yi) + min \sum_{i=1}^{n} p_L^* \qquad (2b)$$

$$\text{and } min(r_{cons}) = min \sum_{i=1}^{n} P_{cons} \qquad (2c)$$

$$\text{s.t.} \quad d_{overall} \leq d_{max} \qquad (2d)$$

$$per \leq per^* \qquad (2e)$$

Eq. (2b) seeks to maximize reliability (γ_{cc-rel}), for which the control error ($y_{ref} - yi$) should be the minimum possible, although this depends on the control method employed. Moreover, in a WNCS, the packet loss (p_L) and packet error rate (per) also significantly affect reliability. Here, we have two goals: the first one is to optimize and achieve higher reliability, and the second one is to make the system resource efficient;
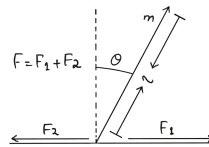

Fig. 1. Illustration of the motion of an inverted pendulum

however, the techniques employed to achieve the second goal will likely negatively affect the first one. To achieve a middle ground, the reliability objective also incorporates a local optimum for packet loss (p_L^*). The control performance is also affected by the delay (d) introduced by the network and the control methodology employed; here, we put an upper bound on the communication delay ($d_{overall} \leq d_{max}$) as the control delay will be decided depending on the strategy used for the system.

On the resource side (Eq. (2c)), the power consumed (P_{cons}) should also be minimized; it is a function of the information transmission frequency (i_{tf}) and transmit power (P_t):

$$P_{cons} = f(i_{tf}, P_t) \qquad (3)$$

$$i_{tf} = f(C_{meth}, IPG, N) \qquad (4)$$

where C_{meth} denotes event-triggered or time-triggered control, IPG the inter-packet gap, and N the devices. A higher IPG can potentially increase energy efficiency, but risks increasing packet losses. Conversely, smaller IPG can congest the network, causing delays and resource access conflicts. Hence, efficient control mechanisms must balance these counteracting factors.

B. Dynamics of Inverted Pendulum

To illustrate the control of a system over a wireless network, we take an inverted pendulum as an example. This control application is a classic example of non-linear control. Despite gravity's nonlinear effect on angle, a simple pendulum model can be linearized for small swings. However, the complex interplay of angular velocity and force prevents linearization of an inverted pendulum model. This makes it ideal for our study, as even minor network uncertainties can significantly impact control performance [12], making control stability exceedingly difficult to achieve if appropriate measures are not taken to minimize the effect of network degradation.

The two equations of motion for the inverted pendulum in Figure 1 can be derived from Lagrange's equation of motion. The reaction force (N) [13] acting on the free body diagram of the inverted pendulum can be derived as:

$$N = m\ddot{x} + ml\ddot{\theta}\cos\theta - ml\dot{\theta}^2 \sin(\theta) \qquad (5)$$

where l is the length of pendulum, m is the mass of pendulum, θ is the vertical angle of pendulum and x is the position of pendulum. To obtain the second equation of motion of this system, it is needed to calculate the sum of forces that are perpendicular to the pendulum. The resolution of the

system along this axis results in a significant reduction in mathematical complexity. The equation obtained should be as:

$$(I + ml^2)\ddot{\theta} + mgl\sin\theta = -ml\ddot{x}\sin\theta \quad (6)$$

where I is the moment of inertia of the pendulum.

C. Proposed Approach

Two distinct algorithms were formulated with the objective of facilitating the training of RL agents. Each technique was specifically designed to tackle the influence of network effects on both actions and states, respectively. This method analyzes the potential impact of network uncertainty on agent actions and states, realizing that network unpredictability can affect many parts of the learning process.

Incorporating uncertainty into the agent's decision-making process has the potential to enhance the learning process's ultimate outcomes. By allowing the agent to adapt to actions that are noisy or lost because of poor or bad network conditions, expected improvements in learning are predicted, see Algorithm 1. This adds a major layer of robustness to the agent's training, allowing it to perform better in a variety of network conditions while pursuing energy optimization goals. However,

---

Algorithm 1 Proposed algorithm to solve the co-design problem with network uncertainties introduced in actions

Require: End to End Delay, d^p, d^t, d^q, N, t (information transmission frequency), power consumption (transmission), action with max reward (a_{rmax}), the minimum required power to transmit P_{min}, previous state $state_{next}$ (velocity, angle), current state $state$, reward as a result of current action $reward_{step}$, agent's action during learning a_{step}, delay introduced due to inter-packet gap (d_{IPG}), state corresponding to action leading to max reward ($state_{a_{max}}$), packet loss (p_L)
Ensure: $max(\gamma_{cc-rel}) + min(r_{cons})$
  $N \leftarrow n$
  while $per \leq per^*$ and $d_{overall} \leq d_{max}$ and $i \leq$ max_iterations **do**
    if $i\%t = 0$ **then**
      $IPG \leftarrow$ True or $P_L \leftarrow$ True
      $P_t \leftarrow P_{min}$
      $state \leftarrow state_{a_{rmax}}$
      $reward \leftarrow reward_{max} \mapsto a_{rmax}$
      $d_{overall} += d_{IPG}$
    else
      $IPG \leftarrow$ False and $P_L \leftarrow$ False
      $P_t \leftarrow P_{max}$
      $state_{next} \leftarrow state$
      $reward \leftarrow reward_{step} \mapsto a_{step}$
    end if
    if p_L or IPG **then**
      $r_{total} += reward_{prev}$
    end if
    if $!p\_L$ and $!IPG$ **then**
      $r_{total} += reward$
      $reward_{prev} \leftarrow reward$
    end if
  end while

---

including network degradation in the agent's state can be helpful in circumstances where environmental disturbances hinder the agent's ability to learn, see Algorithm 2. Using this method has been shown to improve performance by enabling the agent to cultivate a thorough comprehension of the states, thereby mitigating the impact of external interruptions and environmental interference on its learning trajectory.

Algorithm 1 prioritizes the restoration of functionality in the presence of challenging network conditions by returning

---

Algorithm 2 Proposed algorithm to solve the co-design problem with network uncertainties introduced in Agent's state

Require: End to End Delay, d^p, d^t, d^q, N, t (information transmission frequency), power consumption (transmission), action with max reward (a_{rmax}), the minimum required power to transmit P_{min}, previous state $state_{next}$ (velocity, angle), current state $state$, reward as a result of agent's current action $reward_{step}$, agent's action during learning a_{step}, total reward r_{total}, previous reward $reward_{prev}$, packet loss (p_L), delay introduced due to inter-packet gap (d_{IPG})
Ensure: $max(\gamma_{cc-rel}) + min(r_{cons})$
  $N \leftarrow n$
  while $per \leq per^*$ and $d_{overall} \leq d_{max}$ and $i \leq$ max_iterations **do**
    if $i\%t = 0$ **then**
      $IPG \leftarrow$ True or $P_L \leftarrow$ True
      $P_t \leftarrow P_{min}$
      $state \leftarrow state_{prev}$
      $reward \leftarrow -1$
      $d_{overall} += d_{IPG}$
    else
      $IPG \leftarrow$ False and $P_L \leftarrow$ False
      $P_t \leftarrow P_{max}$
      $state_{next} \leftarrow state$
      $reward \leftarrow reward_{step} \mapsto a_{step}$
    end if
    if p_L or IPG **then**
      $r_{total} += reward_{prev}$
    end if
    if $!p\_L$ and $! IPG$ **then**
      $r_{total} += reward$
      $reward_{prev} \leftarrow reward$
    end if
  end while

---

to previously proven effective actions. In contrast, Algorithm 2 adopts a more cautious approach, seeking to prevent the initiation of new choices under unfavorable channel conditions and preserving the existing state in the event of a network loss. It is possible to account for the case of missing or delayed inputs through perturbations in actions by proactively addressing the complexity of wireless communication. The primary objective of this approach is to enhance the agent's capacity to adjust and execute proficiently in scenarios where alterations in network dynamics may pose challenges to maintaining seamless control.

D. Simulation Setup

An inverted pendulum control system with tendons and a wireless network simulates an industrial robotic mechanism (self-balancing robot). The environment was rendered using Pybullet, an open-source physics engine that allows hybrid simulation of neural networks written in C++ [14]. The feedforward neural network is created using PyTorch with two fully connected layers. The state space is box with two dimensions, the action space is a continuous box space, the agent's control input is the torque. The reward is determined by a combination of the cosine of the angle deviation and the velocity deviation. The custom reward function computes a reward by evaluating the difference between the pendulum's joint angle and the desired angle, as well as the difference between the joint velocity and the desired velocity. The control side RL agent accommodates wireless and controls KPIs to ensure dependability. Proximal Policy Optimization (PPO) trains the agent's neural network, which has two fully linked layers separated by ReLU activation. In reinforcement learning

(RL), a policy-based approach, such as the PPO learning technique, is preferred over value-based algorithms due to stability, the ability to handle continuous state spaces, and the overestimation problem. A wireless channel function that simulates packet loss, delay, and IPG was used. The control mechanism, i.e. the RL algorithm, is unaware of packet loss and IPG. Therefore, in both cases of congestion and resource-efficient techniques, the system is able to achieve the desired stability. To simplify the model, we used fixed probabilities for delay and transmission gaps instead of Markov-based probabilities. The GitHub link to the simulation code and networked traces is provided to simulate and verify the proposed approach (*GitHub_Link*).

The control-communication reliability is computed over 100 episodes whereas the reward is calculated over 1000 iterations/steps. As an initial step, the data for control of the pendulum is gathered and a control disturbance is introduced in the data.

E. Time Complexity Analysis

The time complexity for training both algorithms is given by

$$O(S \times n \times (L * b * h^2)^2)$$

where S is the number of maximum episodes and n is the number of iterations. Here, $O(L * b * h^2)^2$ represents neural network forward and backward pass complexity that depends on the total number of input features (n), and the average number of neurons present in the hidden layers (h), the total number of layers in a neural network (L), including both input and output layers, while the variable "b" represents the sample size.

III. RESULTS & DISCUSSION

In this section, the testing and analysis of the proposed approach are performed by simulating the control of an inverted pendulum using tendons (Figure 2a), first with a conventional PID controller, and second with our proposed method. This comparison highlights the capability of RL in achieving optimal performance in terms of control efficiency and power consumption under a wireless network.

A. PID-based Control Baseline Results

Figure 2a shows a snapshot of the rendering of the simulation of the tendon and Figure 2b shows the activation values for 2000 steps, where control input (left Y-axis) versus pendulum angle (right Y-axis) using PID is plotted. To simulate the effect of wireless network uncertainties, a wireless network environment was created, including packet loss, packet error rate, and delay as network uncertainty factors. The control input was passed through the network environment where 15% packet losses were introduced. In this situation, the control of the pendulum did not stabilize when the input was only subjected to packet loss. To improve the control stability, the previous control input was sustained (Figure 3) with the intention that the system could use it in case of loss due to wireless network uncertainties. However, this approach also did not appear to be helpful. Therefore, the proposed RL-based approach was tested, as presented next.
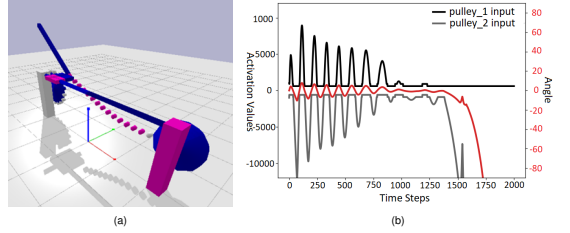

Fig. 2. Inverted pendulum control via tendons using PID, (a) Render Environment, (b) control input (left Y-axis) versus pendulum angle (right Y-axis) variation over time
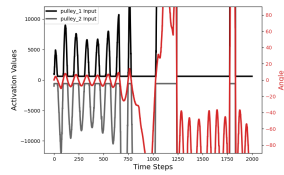

Fig. 3. Inverted pendulum control via tendons using PID under network uncertainties, i.e. 15% packet lossThe PID-based control of the pendulum did not stabilize.

B. RL-based Control over Wireless Network Results

The simulation of the pendulum was then performed using the RL agent; the reward over 100 episodes is plotted in Figure 4a. Each episode consisted of 1000 iterations. The learning factor (α) was set to 0.001.
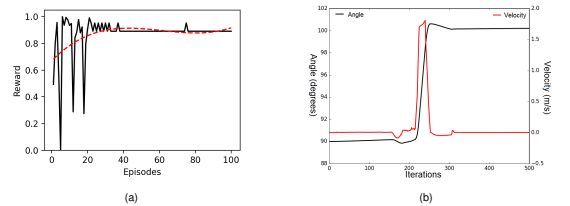

Fig. 4. Inverted pendulum control via tendons using RL control,(a) Reward for RL-based control of a tendon-driven inverted pendulum (b) Inverted pendulum control via tendons using RL control (angle and velocity)

In both cases, the simulation starts in an upright position and the RL agent immediately manages to adjust the position of the pendulum; compared to the PID approach, it shows fewer fluctuations, and control performance becomes stable after training for merely 20-25 episodes. Figure 4b shows the angle and velocity of the tendon over 500 iterations.

Next, disturbances in terms of simple packet loss in the state of the network were introduced during the training of the RL agent. Figure 5 shows fluctuations in the reward of the agent during its training (i.e. noise applied to Figure 4a); nevertheless, the agent is still capable of compensating for them within a similar range of episodes.
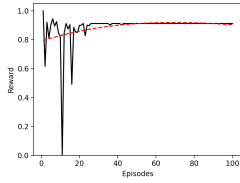
Fig. 5. Reward in the inverted pendulum control via tendons using RL control under the effect of random noise
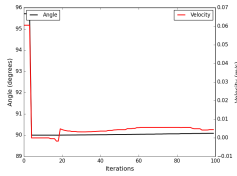

Fig. 6. Inverted pendulum control via tendons using RL control (angle and velocity) under the effect of random noise. Both parameters fluctuate abruptly at first but then stabilize despite random losses.

Figure 6 exhibits angle and velocity stabilization over 100 episodes. As shown in the figure, both parameters fluctuate abruptly at first but then stabilize despite random losses. The agent remembers the prior state in case of packet loss to improve performance. After RL modeling of the control pendulum via tendons, network uncertainties were incorporated to evaluate reliability under different circumstances. We examined network effects on actions and states independently for the RL agent to work under network uncertainties. Introducing uncertainties in actions could improve learning results because the agent will be able to execute if some actions are noisy or lost owing to poor network conditions or as a goal for energy optimization. If the environment is hindering the agent's learning, network degradation may actually improve performance. In order to achieve stability in the presence of various packet losses or IPGs, the performance of the RL algorithm is assessed. In Figure 7, it can be observed that uncertainties in the wireless network impact the state of the system. An IGP is introduced at regular intervals of 10, 100, 500, and 1000 iterations, which has an impact on the system's state by causing packet losses.

As per Figure 7, the results indicate that the stability of the system is enhanced in scenarios where either the state of the system is not subject to any uncertainty (cf. Figure 4a) or where the rate of occurrence of such uncertainty is high (Figure 7a). For some situations, the system is stable but unable to sustain an appropriate performance because it has not experienced the event frequently enough. Note that the system's stability depends on the design of the reward function, specifically its ability to incorporate the immediate previous state of the system. Without such a design, stability cannot be achieved. A buffer with a length of 10 was employed to retain the previous state and the associated reward. This allowed the system to repeat the action with the utmost reward when packet loss or an IGP occurred. The agent can learn the
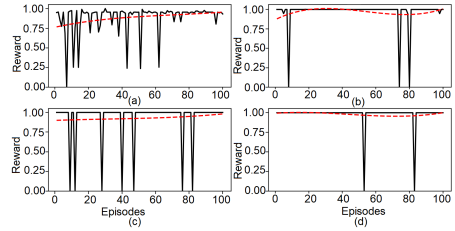

Fig. 7. Rewards in case of network packet loss introduced as a result of an inter-packet gap for every (a) 10, (b) 100, (c) 500, and (d) 1000 iterations in the state
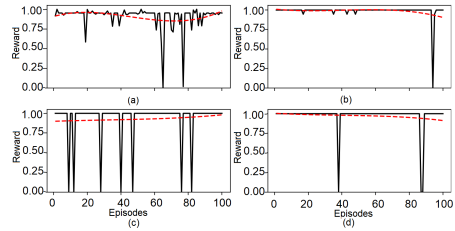

Fig. 8. Rewards in case of network packet loss introduced as a result of inter-packet gap for every (a) 10, (b) 100,(c) 500, and (d) 1000 iteration in the actions

perturbation in control resulting from system-added noise and wireless network interference.

Next, let's focus on the impact on the agent's actions. The impact of change in IPG duration on packet loss is depicted in Figure 8 for 10, 100, 500, and 1000 iterations, under the influence of network uncertainties that affect the agent's actions. Similarly to the preceding scenario, a buffer was used to retain actions and their associated rewards from the last 10 iterations. This buffer was utilized in cases of packet loss and IGP [1]. The system exhibits satisfactory performance in the presence of packet loss or IGP, which are introduced at regular intervals of every 10th (Figure 8a) and 100th (Figure 8b) iterations. In the context of pendulum control using RL, it was observed that the pendulum did not deviate from its intended trajectory, which is a significant improvement compared to the PID-based control presented in the previous section.

According to the data presented in Figure 9, it can be observed that the average power consumption decreased to a range of approximately 19.77 dBm to 19.54 dBm (95 mW to 90 mW) in the discussed scenarios when transitioning from the increased IGP which resulted in packet loss. This is in comparison to the average consumed transmission power of 20 dBm (100 mW) during continuous transmission, indicating a power savings of approximately 5% to 10%. The agent's rewards for the indicated power usage is depicted in Figure 7a. The agent's reward during the learning process demonstrates that despite the implementation of power-saving techniques in the communication layer to enhance resource efficiency, the agent

[1] As the system failed to produce any feasible outcome without the implementation of a buffer, we have omitted these results from this paper
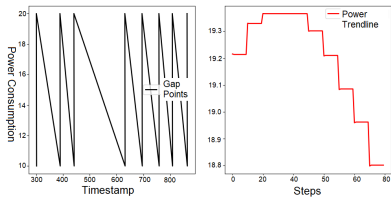
Fig. 9. Power consumption (dBm) vs. IPG for RL-based control of inverted pendulum over wireless network

TABLE I
CPU TIME CONSUMPTION FOR TRAINING CODE (SINGLE EPISODE)

Self CPU %	Self CPU	CPU to-tal %	CPU to-tal	time avg	#of Calls
model_inference	36.55%	575.000us	1.469ms	1.469ms	1
aten::matmul	8.33%	131.000us	385.000us	192.500us	2
aten::mm	7.31%	115.000us	121.000us	60.500us	2
aten::linear	5.47%	86.000us	648.000us	324.000us	2
aten::zeros	4.96%	78.000us	104.000us	104.000us	1
aten::t	4.83%	76.000us	138.000us	69.000us	2
aten::unsqueeze	4.58%	72.000us	81.000us	40.500us	2
aten::_to_copy	3.81%	60.000us	96.000us	96.000us	1
aten::transpose	3.05%	48.000us	62.000us	31.000us	2
aten::squeeze_	2.99%	47.000us	52.000us	26.000us	2

is still capable of maintaining reliable control performance by learning about the environment in few iterations. Finally, Q-learning was also used to study pendulum behavior with fixed and uniform delays and gap probability. Despite network degradation with fixed or uniform probability, the agent failed to learn and the reward remained 0 during training. The agent stabilized by primarily introducing fixed delay probabilities to the system state. For conciseness, the Q-learning test results are omitted; however, the code is on ($GitHub\_link$).

The Pybullet profiler was used to evaluate the CPU time consumed by different functions during the training process, illustrating the training computational resource consumption, see Table I. "Self CPU" indicates CPU time for a specific function, "CPU total" the time for call and execution of the function. # of calls shows how many times a function is called. "model_inference" is the algorithm used for making predictions. Matrices multiplication is done by "matmul" and "mm". "linear" is the linear operation in the neural network. "Zeros" is a tensor that contains only zeros. "t" and "transpose" are for the transpose operation. "Unsqueeze" increases the dimensionality of a tensor. "to_copy" is used for making a copy of a tensor. "Squeeze_" reduces the dimensionality of a tensor. Over 100 episodes the average self CPU % remained highest for the model interference algorithm at almost 40%.

IV. CONCLUSION

Co-designing wireless control systems simultaneously at the network and control layers offers significant advantages over interactive design. To accomplish a reliable and resource-efficient co-design, factors such as packet loss, inter-packet interval, and control strategy must be carefully considered. In contrast to PID performance, where a 15% packet loss in the network causes the control to completely fail and re-tuning of the PID parameters is required for every change in

the network, the proposed RL-based approach is immune to network packet loss. Our proposed RL-based strategy rapidly takes these factors into account; once the training of an RL agent with network parameters is complete, the agent is able to compensate for the majority of network fluctuations. To achieve optimal performance, it is essential to meticulously balance the trade offs between reliability, efficiency, and performance, and to use the appropriate design processes and tools. Thus, a co-design for WNCSs can be fully realized, leading to more efficient and effective wireless control systems for a variety of applications. Although the proposed RL-based approach has many advantages, the training of the agent is still a time-consuming process and sometimes the system does not reach stability.

REFERENCES

[1] K. Ashraf, Y. L. Moullec, T. Pardy, and T. Rang, "Joint optimization via deep reinforcement learning in wireless networked controlled systems," *IEEE Access*, vol. 10, pp. 67 152–67 167, 2022.

[2] G. Giordano, M. Segata, F. Blanchini, and R. L. Cigno, "A joint network/control design for cooperative automatic driving," in *2017 IEEE Vehicular Networking Conference (VNC)*, 2017, pp. 167–174.

[3] M. Selden, J. Zhou, F. Campos, N. Lambert, D. Drew, and K. S. J. Pister, "Botnet: A simulator for studying the effects of accurate communication models on multi-agent and swarm control," in *2021 International Symposium on Multi-Robot and Multi-Agent Systems (MRS)*, 2021, pp. 101–109.

[4] D. Baumann, F. Mager, M. Zimmerling, and S. Trimpe, "Control-guided communication: Efficient resource arbitration and allocation in multi-hop wireless control systems," *IEEE Control Systems Letters*, vol. 4, no. 1, pp. 127–132, 2020.

[5] A. M. Girgis, J. Park, C.-F. Liu, and M. Bennis, "Predictive control and communication co-design: A gaussian process regression approach," in *2020 IEEE 21st International Workshop on Signal Processing Advances in Wireless Communications (SPAWC)*, 2020, pp. 1–5.

[6] A. Bemporad, "Model predictive control design: New trends and tools," in *Proceedings of the 45th IEEE Conference on Decision and Control*, 2006, pp. 6678–6683.

[7] J. Tao, Y. Bai, Z. Chen, H. Li, and F. Wu, "Improved constrained min-max optimization for mpc tracking control in industrial networked process systems," *Measurement and Control*, vol. 56, no. 1-2, pp. 114–123, 2023. [Online]. Available: https://doi.org/10.1177/00202940221083266

[8] A. Jano, R. S. Ganesan, F. Mehmeti, S. Ayvaşik, and W. Kellerer, "Energy-efficient and radio resource control state aware resource allocation with fairness guarantees," in *2022 20th International Symposium on Modeling and Optimization in Mobile, Ad hoc, and Wireless Networks (WiOpt)*, 2022, pp. 185–192.

[9] X. Zhang, T.-H. Chang, Y.-F. Liu, C. Shen, and G. Zhu, "Max-min fairness user scheduling and power allocation in full-duplex ofdma systems," *IEEE Transactions on Wireless Communications*, vol. 18, no. 6, pp. 3078–3092, 2019.

[10] H. Yang, K. Zhang, K. Zheng, and Y. Qian, "Leveraging linear quadratic regulator cost and energy consumption for ultrareliable and low-latency iot control systems," *IEEE Internet of Things Journal*, vol. 7, no. 9, pp. 8356–8371, 2020.

[11] K.-H. Chang, "Chapter 19 - multiobjective optimization and advanced topics," in *e-Design*, K.-H. Chang, Ed. Boston: Academic Press, 2015, pp. 1105–1173. [Online]. Available: https://www.sciencedirect.com/science/article/pii/B9780123820389000193

[12] P. A. Ospina-Henao, D. K. Garcés Bueno, M. J. Peralta Ríos, and C. Gómez-Olejua, "Dynamics, simulation and stabilization of a rotational inverted pendulum using a multivariable predictive controller," in *2022 International Conference on Electrical, Computer, Communications and Mechatronics Engineering (ICECCME)*, 2022, pp. 1–7.

[13] L. B. Prasad, B. Tyagi, and H. O. Gupta, "Optimal control of nonlinear inverted pendulum system using PID controller and LQR: Performance analysis without and with disturbance input," *International Journal of Automation and Computing*, vol. 11, no. 6, pp. 661–670, 2014.

[14] E. Coumans, "Bullet real-time physics simulation," 2015.

Appendix 5

Publication V
K. Ashraf, Y. Le Moullec, T. Pardy and T. Rang, "Decentralized Distributed
Data Structure for Bioanalytical Laboratory Setups," 8th ACM
WomENcourage Conference, 2021,
`https://womencourage.acm.org/2021/wp-content/uploads/202`
`1/07/59_extendedabstract.pdf`

Decentralized distributed data structure for bioanalytical laboratory setups

Kanwal Ashraf
Thomas Johann Seebeck Department
of Electronics, Tallinn University of
Technology
Tallinn, Estonia
kanwal.ashraf@taltech.ee

Yannick Le Moullec
Thomas Johann Seebeck Department
of Electronics, Tallinn University of
Technology
Tallinn, Estonia
yannick.lemoullec@taltech.ee

Tamás Pardy
Department of Chemistry and
Biotechnology & Thomas Johann
Seebeck Department of Electronics,
Tallinn University of Technology
Tallinn, Estonia
tamas.pardy@taltech.ee

ABSTRACT

The integration of information flow and management between different domains within laboratory setups has been under focus for many years. Communication technologies and data distribution play a key role in this integration. In this research, we propose a data distribution structure for bio-analytical laboratories based on a decentralized publish-subscribe model. In particular, we describe the main structure for data communication and the conceptual, logical, and physical data flow models. We believe this research can pave the way for enabling scalable and robust communication between the laboratory units.

CCS CONCEPTS

• **Information systems** → **Data structures**; • **Networks** → *Network architectures*; • **Computer systems organization** → **Distributed architectures**; *Real-time system architecture*.

KEYWORDS

Data distribution structure, scalable communication

1 INTRODUCTION

Scalable and high-performance communication technologies play a key role in real-time automated systems built upon efficient data exchange. The real-time data exchange via a publisher-subscriber architecture is more efficient as compared to a client-server architecture [Mastouri, mohamed anis and Hasnaoui 2007]. Different publish-subscribe middlewares, including MQTT, ROS and DDS, are used for efficient information flow and management for different applications including smart grids, health systems, air-traffic control, process industry and many more [Happ et al. 2017]. However, this concept is still emerging in biochemical and bioanalytical laboratories where client-based architectures [Gibbon 1996] are commonly used for information flow and management [Kang et al. 2018]. This research aims at integrating different domains including computational, communication, fluidic and biochemical domains of a high throughput bioanalytical laboratory setup using a decentralized communication architecture. The proposed structure is data-centric and system models are built around it using SAP PowerDesigner. Moreover, the data structure provides the flexibility to use the same concept for integrating different domains in other types of applications.

2 PROPOSED STRUCTURE/ARCHITECTURE

As mentioned earlier, the proposed data flow structure for bioanalytical laboratory setup is based on the well-known publish-subscribe model. The main elements of the structure include the entities, also known as topics, and different tasks running on the different devices in each unit. Each device in the laboratory will either subscribe or publish to a certain entity with a set of defined Quality of Service (QoS) parameters. These QoS parameters are part of the communication protocol and include delay and packet loss. The data flow between devices is highly decentralized and the same device in any unit could work both as subscriber and publisher for entities.
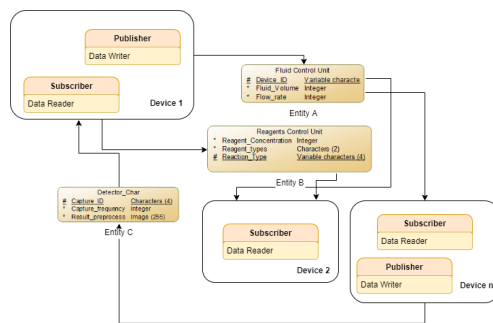

Figure 1: Main Structure for Data Communication. The communication-based data flow structure is decentralized and supports different devices in a bioanalytical laboratory unit.

For the use-case considered in this work, the bio-analytical laboratory setup is divided into three different units [Pärnamets et al. 2021], namely Biological Sample Processing Unit, Computational Unit, and Sensing Unit, with different data types.

Figure 1 shows the main decentralized communication-based data flow structure for different devices in a laboratory unit. SAP PowerDesigner is used to build the conceptual, logical, and physical data flow models for each unit. Figure 2 shows the conceptual model for the system, Figure 3 represents the logical data-flow, while Figure 4 depicts the physical data flow model for the system.

The conceptual model (Figure 2) depicts the information flow relation between different laboratory units which are defined as
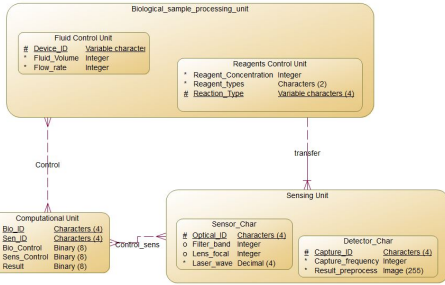
Figure 2: Conceptual Data Flow Model for Bio-analytical Laboratory setup

entities. The attributes for each entity are defined and many-to-many relations are used between different units. Each device is given an identification code and the data is categorized as either mandatory or primary. The logical data flow model is then built upon the conceptual model. Figure 3 shows the logical data flow model for the use-case bio-analytical laboratory setup, exposing the structure of the information flow.
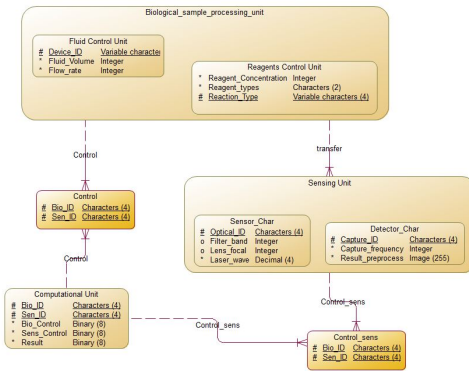

Figure 3: Logical Data Flow Model for Bio-analytical Laboratory setup

Next, by elaborating the logical data model, a more concrete physical data-flow model is generated, as shown in Figure 4. This physical data model includes more details that help analyze different objects and tables in the database and map the model onto the physical elements that will implement and execute the real system. To provide a comparison with centralized data flow structures, the performance evaluation of the purposed model will be performed in high traffic scenarios.

This research work is in progress and the resulting model is further aimed to be implemented in practice on different test units and the performance evaluation of the proposed data flow communication architecture is ongoing.
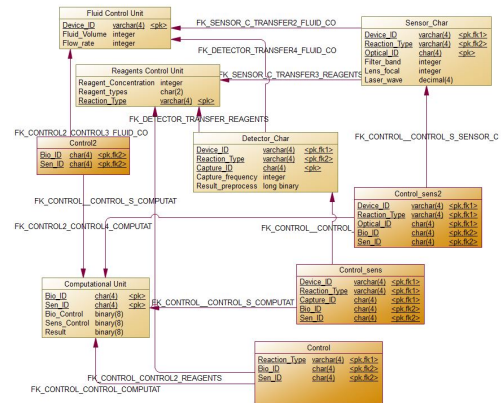

Figure 4: Physical Data Flow Model for Bio-analytical Laboratory setup

3 CONCLUSION

The proposed data flow structure supports the integration of the computational and communication domains with biological and fluidic domains for biochemical and bio-analytical laboratories. By implementing minor changes in entities, the proposed model could help in the robust, scalable, and efficient operation of other types of high throughput laboratory setups.

ACKNOWLEDGMENTS

REFERENCES

Gerst A. Gibbon. 1996. A brief history of LIMS. *Laboratory Automation and Information Management* 32, 1 (1996), 1–5. https://doi.org/10.1016/1381-141X(95)00024-K
Daniel Happ, Niels Karowski, Thomas Menzel, Vlado Handziski, and Adam Wolisz. 2017. Meeting IoT platform requirements with open pub/sub solutions. *Annales des Telecommunications/Annals of Telecommunications* 72, 1-2 (feb 2017), 41–52. https://doi.org/10.1007/s12243-016-0537-4
Wenjun Kang, Sabah Kadri, Rutika Puranik, Michelle N. Wurst, Sushant A. Patil, Ibro Mujacic, Sonia Benhamed, Nifang Niu, Chao Jie Zhen, Bekim Ameti, Bradley C. Long, Filipo Galbo, David Montes, Crystal Iracheta, Venessa L. Gamboa, Daisy Lopez, Michael Yourshaw, Carolyn A. Lawrence, Dara L. Aisner, Carrie Fitzpatrick, Megan E. McNerney, Y. Lynn Wang, Jorge Andrade, Samuel L. Volchenboum, Larissa V. Furtado, Lauren L. Ritterhouse, and Jeremy P. Segal. 2018. System for Informatics in the Molecular Pathology Laboratory: An Open-Source End-to-End Solution for Next-Generation Sequencing Clinical Data Management. *Journal of Molecular Diagnostics* 20, 4 (jul 2018), 522–532. https://doi.org/10.1016/j.jmoldx.2018.03.008
Salem Mastouri, mohamed anis and Hasnaoui. 2007. Performance of a Publish/Subscribe Middleware for the Real Time Distributed Control systems. (2007). https://www.researchgate.net/publication/239555403_Performance_of_a_PublishSubscribe_Middleware_for_the_Real_Time_Distributed_Control_systems
Kaiser Pärnamets, Tamas Pardy, Ants Koel, Toomas Rang, Ott Scheler, Yannick Le Moullec, and Fariha Afrin. 2021. Optical Detection Methods for High-Throughput Fluorescent Droplet Microflow Cytometry. *Micromachines* 12, 3 (2021). https://doi.org/10.3390/mi12030345

Appendix 6

Publication VI
R. Jõemaa, N. Gyimah, K. Ashraf, K. Pärnamets, A. Zaft, O. Scheler, T. Rang and T. Pardy, "CogniFlow-Drop: Integrated modular system for automated generation of droplets in microfluidic applications", IEEE Access, Vol. 11, pp. 104905 - 104929, 2023, DOI: `https://doi.org/10.1109/ACCESS.2023.3316726`.

RESEARCH ARTICLE

CogniFlow-Drop: Integrated Modular System for Automated Generation of Droplets in Microfluidic Applications

RAUNO JÕEMAA[1,2]**, NAFISAT GYIMAH**[1]**, KANWAL ASHRAF**[1]**,**
KAISER PÄRNAMETS[1]**, (Member, IEEE), ALEXANDER ZAFT**[1]**, OTT SCHELER**[2]**,**
TOOMAS RANG[1,2]**, (Senior Member, IEEE), AND TAMÁS PARDY**[1,2]**, (Member, IEEE)**

[1]Thomas Johann Seebeck Department of Electronics, Tallinn University of Technology, 19086 Tallinn, Estonia
[2]Department of Chemistry and Biotechnology, Tallinn University of Technology, 19086 Tallinn, Estonia

Corresponding author: Rauno Jõemaa (rauno.joemaa@taltech.ee)

ABSTRACT Droplet microfluidics enables studying large cell populations in chemical isolation, at a single-cell resolution. Applications include studying cellular response to drugs, cell-to-cell interaction studies. Such applications need a reliable and repeatable droplet generation with high monodispersity. Most systems used in research rely on manual tuning of flow parameters on off-the-shelf instruments. Setups are highly customized, limiting reproduction of experimental results. We propose an integrated, modular system for automated aqueous droplet generation with high monodispersity. The system provides dynamic feedback control of droplet size and input pressure. Input pressure is generated by two piezoelectric micropumps. Droplet sizes are determined via light intensity measurement in an LED-photodiode setup. The system is capable of wireless communication and has a low enough power consumption for battery-powered operation. We report on the assembly and the underlying working principle, as well as an in-depth experimental evaluation of the performance of the proof-of-concept prototype in aqueous droplet generation. Evaluation was performed on a modular as well as on a system level. During module-level evaluations, aqueous droplets were generated in a light mineral oil + Span 80 surfactant carrier medium, using 3 different flow-focusing junction geometries. The presented prototype had a significantly faster pressure stabilization time (10 s) compared to a syringe pump-based reference setup (120 s). During system-level evaluation, deionized water droplets were generated in a carrier medium of HFE7500 + PEG-PFPE triblock surfactant. Resultant droplet sizes were benchmarked with microscopy. The system was able to repeatedly generate mono- and polydisperse droplets on demand, with CVs between 5-10% in the ∼50-200 μm droplet diameter range.

INDEX TERMS Lab-on-a-Chip, microfluidic, automation, pulsatile flow, droplet size control, droplet generation rate control, optical feedback, pressure feedback, closed-loop control, wireless communication.

I. INTRODUCTION

Droplet microfluidics enables studying the response of cell populations to specific chemicals, in isolation, at a very high throughput [1]. Chemical isolation is given by encapsulating

The associate editor coordinating the review of this manuscript and approving it for publication was Zhiwu Li.

cells into aqueous droplets in an immiscible carrier medium, together with the chemicals for their treatment. For example, antibiotics and resistant bacteria, to screen for antimicrobial susceptibility, or circulating multi-drug resistant tumor cells and chemotherapy drugs to screen for drug response among other analysis targets [2], [3]. Working in droplets enables 1) higher throughput than conventional batch processing in

2) a compact, highly integrated, automatic system as well as 3) continued work with individual droplets downstream [4]. Furthermore, it enables analysis of single-cells, or cell-to-cell interactions [5]. Droplet microfluidics has additional applications in chemical analysis and synthesis, as well as bioanalyses other than cytometry (e.g., nucleic acids) [6].

However, imaging droplet flow cytometry necessitates reliable and repeatable droplet generation with high droplet monodispersity (1-5% [4], [7]) at moderate droplet generation rates ($\sim$1-3 kHz [7]). To date, open-loop control and/or manual tuning of flow parameters to achieve desired droplet sizes and stable droplet generation are most common [8], [9]. However, the target parameters are difficult to achieve and maintain with manual tuning. Thus, automated droplet generation with closed-loop control (or in other words, an inline quality control system of droplet generation) is necessary. Zheng et al. [10] demonstrated a reduction of steady-state error to <2% coefficient of variation (CV) across various flow conditions in droplet digital polymerase chain reaction (PCR) applications [11]. Similarly, Duan et al. [12] achieved high monodispersity (<7.6 CV%) by implementing a closed-loop control strategy, which was at least 90% lower than with open-loop control. Additionally, Zeng and Fu [13] addressed the challenge of predicting droplet size by using closed-loop control to account for the nonlinearity of flow-focusing. Moreover, a novel microfluidic system was developed to optimize cell processing conditions using deep learning algorithms for analyzing sensor data and closed-loop control to update a pressure pump and maintain optimal cell flow speed [14]. Several other works have demonstrated closed-loop control of droplet sizes by tuning flow parameters based on an image/video stream of the flowing droplets [15], [16], [17]. Most demonstrated systems (TABLE 1) used droplet imaging for control. However, overall throughput in camera-based tracking is limited by the imaging throughput of the camera (increasing throughput increases cost and heat dissipation). The price/performance ratio of imaging droplets for flow control (in contrast with cell imaging, which is a different application) is also not optimal.

A compact system with a laser-photodiode setup for bubble tracking was demonstrated in [18]. Such an integrated, compact benchtop setup enables portability between labs, which in turn enables transferring experimental workflows with excellent repeatability. It also allows replication of results, thus enabling virtual parallel labs and digital, rather than physical exchange of results and knowledge. However, at present, widely used setups are an ensemble of off-the-shelf instruments, assembled specifically for the experiment on hand, with little to no integration (TABLE 1). The lack of integration means the setup (and results created with it) cannot be easily transferred between labs. It is also notable that while in microfluidics in general, syringe pumps are the most popular choice due to their flow stability, affordability, and ease of use, in droplet microfluidics, pressure pumps are also very common, as they do not need refilling. The need to refill the syringe causes interruptions in experimental workflows,
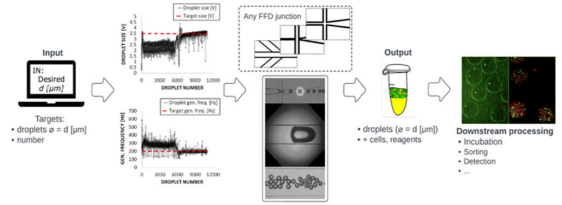

FIGURE 1. CogniFlow-Drop concept: droplets with user-defined process and dimensional parameters are generated automatically from reagents and samples needed by the user, with minimal user interaction, in a compact, standalone device. These can then be collected for further downstream processing, e.g., incubation and detection.

and possibly also the need to recalibrate flow parameters. Finally, in our earlier reviews, we found a pronounced interest towards low-cost instrumentation and the democratization of instruments for droplet microfluidics [4], [19].

As of today, compact, integrated droplet microfluidics instruments, particularly with wireless communication and low-cost hardware, are uncommon. Setups exist that meet some but not all criteria (TABLE 1) for a compact, modular, automated, wirelessly communicating droplet generator.

In this work, we describe a proof-of-concept experimental setup meeting the aforementioned criteria, its underlying methodology, and the evaluation of its performance in droplet generation experiments. The CogniFlow-Drop system concept (Fig. 1) offers the following advantages over the state of the art (TABLE 1):

1. It is integrated and modular (some modules can be swapped out for easy upgrades), improving reliability, and enabling portability. These features ensure that results and workflows are transferable between labs (enabling creation of virtual parallel labs).
2. It is low-cost ($\sim$650€) compared to commonly used experimental setups built from off-the-shelf components. With future development, modularity will enable customization, affordability will open wider collaboration using the platform.
3. Can offer comparable performance to commonly used droplet generation setups through its dual-PID control of droplet size and generation frequency. With future optimizations, can significantly reduce carrier/sample/reagent waste. Furthermore, through automation, can ensure better repeatability without manual recalibration or in-depth knowledge of the technology.
4. Measures droplet generation in real-time via intensity change in a simple LED-photodiode setup (water droplets, passing between, causing a change compared to the carrier medium).
5. Uses tilting mounts to reliably set up chip, light source, and detector alignment, to optimize channel/droplet visibility in a given microfluidic chip. This also increases reproducibility of results.
6. Uses wireless communication, which enables remote control and monitoring of the system.

TABLE 1. Overview of the state-of-the-art feedback-controlled droplet generators compared to our novelty.

Reference	Flow actuation	Flow control algorithm	Continuous phase fluid	Discrete phase fluid	Monodispersity (CV%)	Flow sensor	Integrated & standalone?	Communication
[12]	Programmable pressure pump	PID controller	Silicone oil	Calcium chloride solution	<7.6%	N/A	No	USB
[11]	Pressure pump	PI controller	Silicone oil	Water	2%	Pressure sensor		
[16]	Pressure pump	PID controller	Fluorinated oil	Water	0.32%	N/A		
[13]	Pressure pump	PID controller	Silicone oil	Water	N/A	N/A		
[34]	Microvalves	PI controller	Silicone oil	Water	No steady state errors	N/A		
[35]	Syringe pump, and gas regulator	PI controller	BSA in NaCl	Nitrogen	N/A	N/A		
[36]	Syringe pump	PID controller	Paraffin + 10% Span80	Water	RMSE reduces from 3.4 to 0.48	N/A		
[37]	Pressure pump	Pi controller	Silicone oil	Water	N/A	Pressure sensor		
[18]	Gas-driven	Dual-PID (pressure, bubble size) control	Water + Tween80	C_4F_{10}/CO_2 gas	N/A	Laser-photodiode	**Yes**	
Our work	**Dual piezo pumps**	**Dual -PID (pressure, droplet size/gen. rate) control**	**HFE7500/ mineral oil + tri-block surfactant**	**Water**	**5-10%**	**LED-photodiode**	**Yes**	**WLAN**

7. Has a sufficiently low power consumption ($\sim$8.0 W) that it can be powered from batteries for portable operation (based on the estimated consumption, >4.5h battery life on a 10000 mAh Li-ion power bank).

II. COGNIFLOW-DROP SYSTEM PROTOTYPE

In this section, we present a structural overview of the complete prototype assembly (Section II-A), then in following sections (Section II-B to II-D) overview each system module in detail, including both hardware and software, from a structural as well as functional perspective (working principles).

A. OVERVIEW

The system prototype (Fig. 2/4) was constructed as a compact, modular assembly with an emphasis on ease of use and low hardware cost. In this section, we overview the assembly and subassemblies, and link to sections with further details on

each. The system consisted of three main modules (see also block diagram in Fig. 3) and the enclosure:

1) **Electronics module** (Section II-B and Fig. 2/1): functionally responsible for communication, instrument control and signal processing. Physically was constructed as a stack of stages onto which electronic parts were mounted:

   a) *Power supply unit* (PSU) stage (Fig. 2/1/a): mounted the RJ45 adapter, the power switch, the mains connector, and the PSUs (ECS45US05, XP Power).

   b) *Pump controller and pressure sensor stage* (Fig. 2/1/b): mounted the pump controller interface (with the low-level pump controller running on an ESP32 DevKitC board) and pressure regulation board. The stage was shielded from noise from above and below by copper plates attached
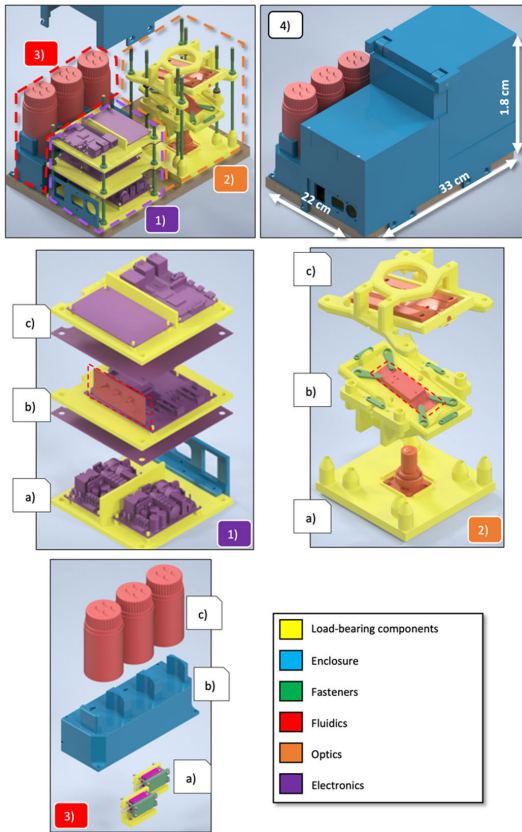
FIGURE 2. Prototype assembly, consisting of modules: (1) electronics module consisting of the power supply stage (a) , the pump driver and pressure sensor stage (b) and the stage that contained the RPi4B as well as the ADC and filtering circuit for the optical sensor (c), plus the corresponding copper shielding plates. (2) The sensorics module, consisting of the base stage with the photodiode and lens (a), the microfluidic chip mount stage (b) and the light source mount stage (c). (3) fluidics module, which included L-mounts for the pumps (a) and a foam-padded enclosure (b), as well as (c) sample, reagent, and product collection containers. (4) The enclosure with 3D printed internal and external walls, as well as a wooden base plate to which all modules were mounted for stability. The M5 bolts mounting the stages of the modules are hidden in the close-up explosion views (1)-(3).

to and grounded through structural conductive threaded rods.

   c) *Communication, control, and signal processing stage* (Fig. 2/1/c): mounted the Raspberry Pi 4B (RPI), responsible for system control and communication, and the filter-amplifier, analog-to-digital conversion (ADC) board for the optical sensor.

2) **Sensorics module** (Section II-C and Fig. 2/2): functionally responsible for optical flow rate measurement. Physically also holds the microfluidic droplet generator chip and consists of the following stack of stages:

   a) *Photodetector stage* (Fig. 2/2/a): the photodetector PCB and the connecting microscope lens were mounted to the bottom plate.

   b) *Chip mount stage* (Fig. 2/2/b): included the chip mount with 3 degrees of freedom (DoF; height, roll, pitch) and a removable microfluidic chip holder.

   c) *Light source mount stage* (Fig. 2/2/c): positioned at the top of the sensorics module was an analogous 3 DoF mount stage for the light source as was for the chip mount stage. The light source was an LED, soldered to a 25 mm × 75 mm sized PCB. A diffuser/lens was attached over the LED. Aluminum or large copper area on the PCB was used for heat dissipation from the LED.

3) **Fluidics module** (Section II-D and Fig. 2/3, Fig. 2/1/b, Fig. 2/2/b): functionally responsible for generating droplets from the carrier medium, reagents, and sample(s). Additionally responsible for dampening secondary vibration and sound produced by piezoelectric micropumps.

   a) *Pump mount* (Fig. 2/3/a): both pumps were mounted on an L-shaped mount. The pumps were fastened to the mount with shock dampening rubber in between.

   b) *Shock- and audibility-dampening piezopump enclosure* (Fig. 2/3/b): 2-part enclosure with rubber padding fitted around the micropumps for additional sound absorption. The top of the enclosure was designed with slots for three 100 ml lab bottles.

   c) *Liquid containers* (Fig. 2/3/c): included the reagent and sample containers, as well as the product collector.

   d) *Pressure sensors* (mounted to electronics module Fig. 2/1/b)

   e) *Fluidic chip* (mounted to sensorics module Fig. 2/2/b)

4) **Enclosure** (Fig. 2/4): held the components together, including the interior walls between compartments, as well as the external enclosure. The base plate was a wooden board of 22 cm × 33 cm × 1.8 cm, selected to provide mechanical support to the assembly. Internal walls were used to route cables and tubing, as well as providing slots for T-junctions that bridged connections between the microfluidic chip, the pumps, and the pressure sensors. All plastic components were 3D printed. Load-bearing components were 3D printed with a Prusa i3 mk3S, the T-junctions [20] with an Anycubic Photon Mono. Electronics and sensorics modules were fastened to the base plate with structural ISO M6 size threaded rods, whose internal components were fastened to load-bearing components with ISO M3 size bolts (metal fasteners are hidden on the explosion views for better clarity). The pump enclosure was fastened to the base plate with ISO M3 size bolts. The chip mount stage was set between spring-loaded knurled nuts (DIN 466 M6) to reduce vibrational sensitivity.
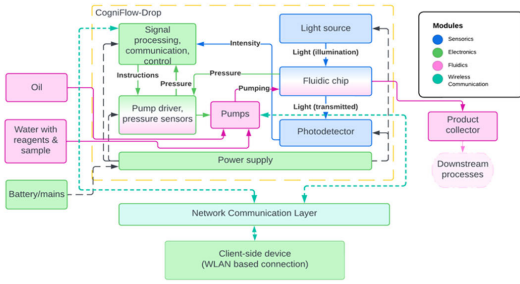
FIGURE 3. CogniFlow-Drop device: in the device, oil-water droplets of a user-defined size are generated, encapsulating cells and reagents of given kinds. The regulation of droplet sizes takes place by means of simultaneous pressure and flow rate control, resulting in a high control precision (in terms of CV% [coefficient of variation] of droplet diameter). The system implements distributed wireless control in an event-triggered manner [25].

B. ELECTRONICS MODULE

1) FLOW CONTROL STRATEGY

For the pressure-driven droplet generator, a dual-PID controller strategy with two feedback loops (inner and outer feedback loops, Fig. 4/a) was designed and implemented:

- The inner feedback loop was used to rapidly reach target pressure levels in the microfluidic chip and to reduce pressure fluctuations, inherently induced by the droplet pinch-off process, the pulsatile nature of the micropumps and the rapid target pressure level approach. The inner loop consisted of PID controllers for each micropump separately.
- The outer feedback loop was used to reach and maintain user defined droplet size and generation rates through discretized light sensor data.

The proposed design of the dual-PID control strategy (depicted on Fig. 4/a) for the CogniFlow-Drop system can be described as follows:

1) The inner PID closed feedback loop used pressure readings from sensors 1 (S_1) and 2 (S_2) of pumps 1 and 2, respectively, as well as pressure readings from sensor 3 (S_3) at the microfluidic chip's output.
2) The PID controller associated with each pump regulated the pressure drop across the chip using the differential pressures (i.e., S_1-S_2, S_1-S_3) as feedback. The accurate and rapid control of pressures produced by the inner feedback loop action improved the stability and precision of the outer feedback loop.
3) The outer PID controller achieved user-defined droplet size and droplet generation frequency set points (d_{set} and f_{set}) by adjusting the pressure of pump 1 and 2 respectively (i.e., disperse and continuous phase flows). The size related pressure target was derived from using the error (e_d) between the set point (d_{set}) and the average measured droplet size (d_m). The generation frequency related pressure target was derived from using the error (e_f) between the set point (f_{set}) and the average measured droplet generation frequency (f_m). By fixing the disperse phase pressure, the

control variable relationships between "droplet size" to "disperse phase pressure" could be made as "droplet size" to "continuous phase pressure", depending on the sensitivity of the target parameter to the fluid phase type [21].

In reference to our earlier work, the PID controller parameters (i.e., proportional gain, integral gain, and derivative gain) were derived using a Genetic Algorithm (GA). The dual-PID control strategy, adapting the framework implemented with MATLAB, Simulink in [22], was modified to include droplet generation frequency control for the presented version of the droplet microfluidics system, using Python.

2) PUMP CONTROLLER AND PRESSURE SENSOR STAGE

The pumping system embedded into CogniFlow-Drop was an updated version of the non-automated dual-channel piezo-electric pumping device demonstrated in our earlier work [23], [24]. Relevant notable modifications to our standalone pump PCBs ([24]) are mentioned in the electronic supporting information (ESI) S1.

While the base design with all its features was carried over, standalone operation (wireless communication and battery power) was not. Wireless communication was not necessary as the pump controller exchanged commands and sensor data, as well as received power, over a USB cable connecting the pump controller (ESP32) to the main controller (RPI). Additional updates were required to be made to the pump controller firmware from the earlier work ([24]) with relevant notable ones mentioned in ESI S1.

3) COMMUNICATION, CONTROL, AND SIGNAL PROCESSING STAGE

RPI was selected as the main controller for the system due to its quad-core processor and extensive interfacing options. It ran Ubuntu desktop (ver. 21.10) with its tasks written in Python 3.9 and C++. With four cores, the RPI was able to dedicate one for each independent task:

1) Communication with the user, over local network, using the methodology described in Section II-B-IV.
2) Communication with the pump hardware described in Section II-B-II.
3) Interpretation of data obtained from the optical sensor, expanded upon in Section II-C.
4) Calculation of pumping pressure targets based on both the measured pressure data (obtained from task 2) and the resolved optical data (obtained from task 3), detailed in Section II-B-I.

The interpretation of links between tasks and their interactions with parts of the system, external from the Raspberry Pi, are shown in Fig. 5, and an explanation with more details about the internal mechanism of each task is described in ESI S2.

4) USER INTERFACE

Data and information flow are critical aspects when considering the design of any bioanalytical device. In our
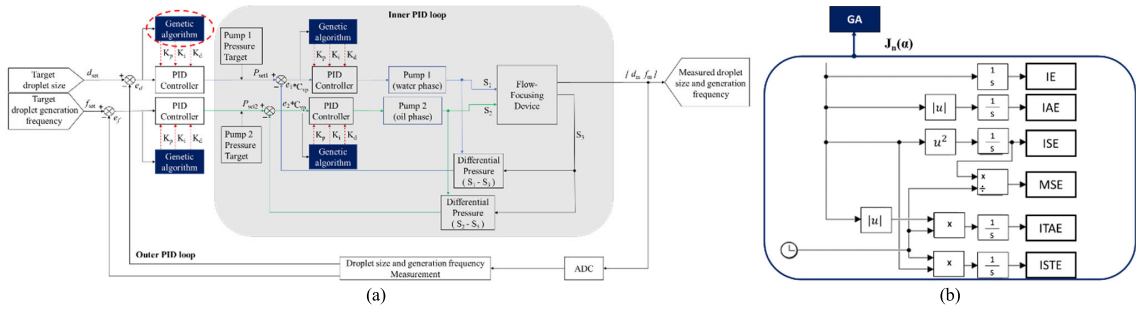
FIGURE 4. a) Structure of dual-loop PID control strategy. The inner feedback loop reduced pressure fluctuations, improved accuracy, and speed of reaching target pressure level. Outer feedback loop adjusted droplet sizes and generation rates based on optical flow rate measurement from module 2 in Fig. 2; b) Structure of PID tuning method with six objective function criteria obtained from using genetic algorithm.
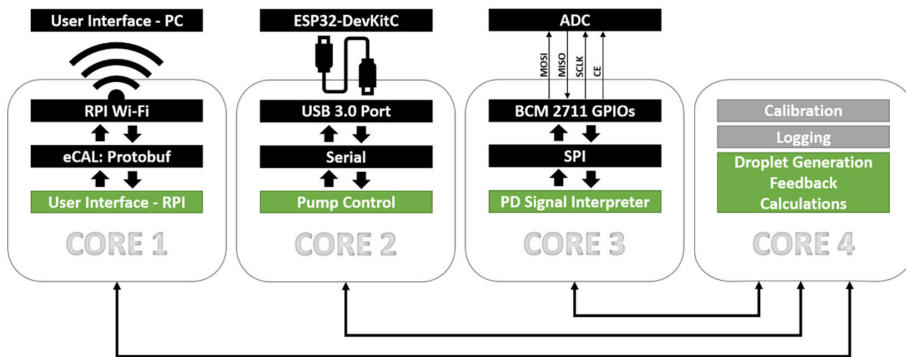

FIGURE 5. Four main tasks (in green) of the system controller were made to run concurrently on separate cores. Core 1 handled user commands received over local network using eCAL API with Protobuf format. Core 2 communicated with the pumping system's control board ESP32-DecKitC via serial protocol. Core 3 received discretized photodiode signal from an ADC in SPI protocol format through Raspberry Pi's BCM 2711 GPIOs and using it to measure running droplet generation parameters. Core 4 managed commands and information from the other three cores to start, stabilize and end droplet generation.

previous work we presented a framework for integrating event-triggered wireless data distribution and information flow into a bioanalytical device [24]. In this work, we focus on structured data serialization (along with metadata) using Google's Protobuf serialization protocol [25]. With this method, the number (and type) of devices in the network could be extended with minor edits to the data structures.

Inter-host communication was performed using an enhanced Communication Abstraction Layer (eCAL, v5.9.5) middleware [27]. The data rate through eCAL was payload dependent, and the employed data-centric communication architecture offered low latency communication with fair reliability.

Data was sent between devices along with a unique device ID and name, chip name, flow rate, transmission/reception status, flag for different process activation, and droplet size (see example in Fig. 6/a) and message ID. On the publisher/sender side, a Protobuf message object (see example in Fig. 6/b), was created based on the data structure defined and serialized using the Protobuf protocol, followed by being broadcast to any listening device. For any device to catch

the broadcast data, an eCAL subscriber/receiver function was cyclically polled. Concurrently, the method was used in reverse to transfer data from the controlled device to the controller. Devices could communicate with each other in an event-triggered wireless or wired manner. The overall data transfer mechanism is shown in Fig. 7.

The CogniFlow-Drop prototype could be controlled via the graphical user interface (GUI, Fig. 8) by defining parameters for droplet generation rate and size and passing them on using the available task specific buttons. If the chosen parameters were not within acceptable limits or of the wrong type, an error was presented, asking for appropriate corrections. The entered parameters were serialized by protocol and sent to the other device in the form of messages. Unless manually halted from the GUI, tasks were halted automatically on the controlled device after completion.

5) OPTICAL FEEDBACK SIGNAL ACQUISITION

The digitization PCB before signal processing on RPI, was made with three stages.

```
1    syntax = "proto3";
2
3    package proto_message;
4
5    message spec
6  ∨ {
7      float  dsize       = 1;
8      uint32 id          = 2;
9      float  drate       = 3;
10     string status      = 4;
11     uint32 command     = 5;
12     string deviceName  = 6;
13     string chipName    = 7;
14
15   }
16
```

```
134    # set message content
135    specific.dsize = dropsize
136    specific.id = message_id
137    specific.drate = input_rate
138    specific.status = status
139    specific.command = command_nr
140    specific.deviceName = device_name
141    specific.chipName = chip_name
142    print("Status is {}".format(specific.status))
143    if command_nr != 1:
144        print("Droplet size {} and rate {}".format(specific.dsize,specific.drate))
145        if chip_name != "None":
146            print("Chip under test: {}".format(specific.chipName))
147        else:
148            print("Chip Name is not defined")
149
150    # send message
151    while ecal_core.ok() and specific.id < repeat_msg:
152        if command_nr != 1:
153            if inputs_in_range is True:
154                pub.send(specific)
155                print("Successful tranmission iteration {}".format(specific.id))
```

(a)   (b)

FIGURE 6. Communication interface implementation. (a) Data Structure for CogniFlow-Drop: droplet size (dsize), message id, droplet generation rate (drate), sender status/role, operational command, sender device name, and saved calibration parameters named with corresponding microfluidic chip. (b) instances of eCAL-based message transmissions.
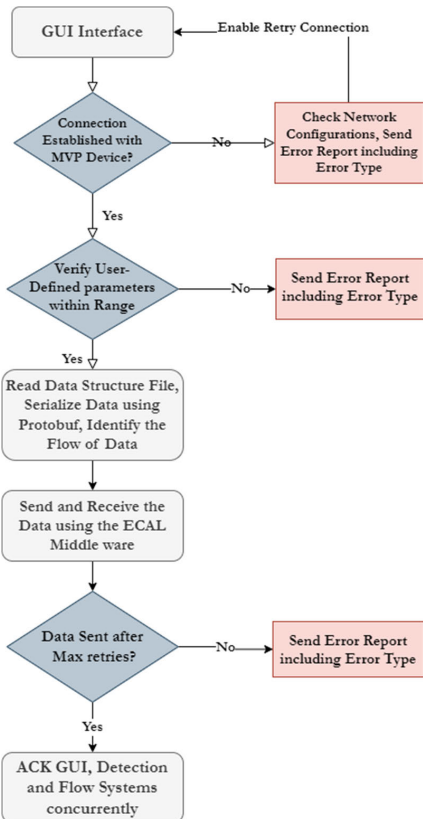

FIGURE 7. Implementation of the communication interface, data transmission, reception, verification, and a Graphical User Interface for accessibility.
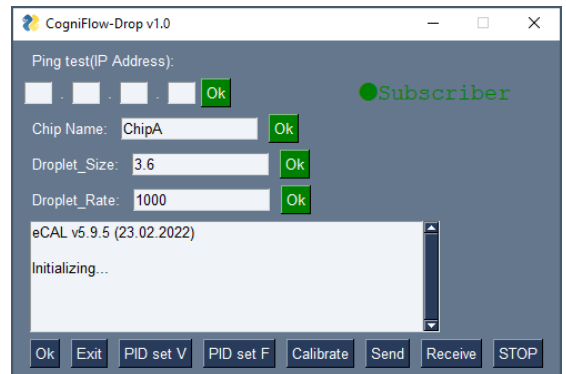

FIGURE 8. ECAL based Graphical User Interface (CogniFlow-Drop v1.0).

distortions, with a cutoff frequency at $\sim$7.26 kHz and a quality factor of $\sim$0.64. Filtering was necessary to reduce noise acquired from the system (in most part from the used switch-mode PSUs).

Before discretization with an ADC, to maximize the information gained from the incoming, filtered optical signal, per bit, an adjustable inverting amplifier stage was used. This enabled scaling of captured waveform to the ADC's analog input limits. Additionally, this filter-amplifier circuit was designed to discard any inherent DC component from the optical signal and bias it instead with 2.5 V, to position it in the middle of the 0 to 5 V ADC measurement window.

The converter used was a 16-bit ADC (ADS8681, Texas Instruments). In the presented version of the system, the PCB on which it was installed was a perforated protoboard, which introduced additional noise to the measured signal due to a non-ideal splitting of digital and analog signals.

C. SENSORICS MODULE
1) DROPLET MEASUREMENT HARDWARE
In our previous works, we demonstrated cost-effective imaging [28] and non-imaging [29] droplet flow sensor

The first stage, receiving the feedback signal directly from the sensorics module described in Section II-C, was a 2nd order Sallen-Key low pass filter. The filter was designed for detection of up to 5000 droplets per second without
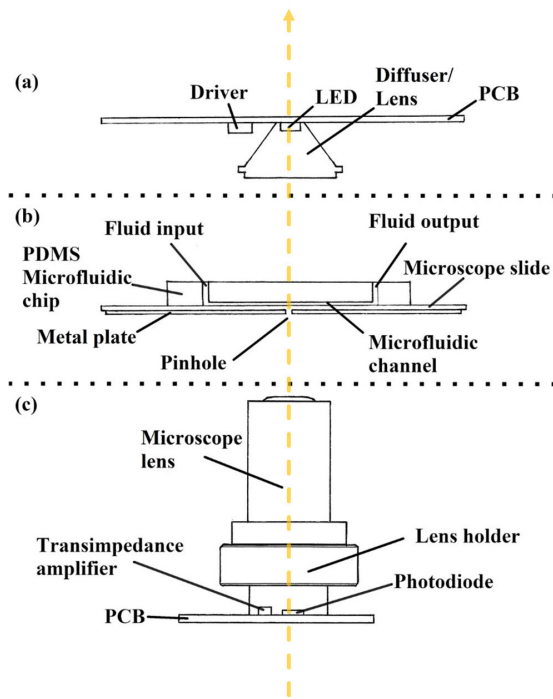
FIGURE 9. Cross-section of the microfluidic droplet measurement system with parts aligned to the axis marked with a dashed yellow line. (a) An LED with an LED driver is soldered to a printed circuit board (PCB) that is used to illuminate the microfluidic chip. In addition, a matted lens is used to diffuse and focus the light. (b) A PDMS-glass microfluidic chip is mounted to the chip holder with a metal plate with a micro-drilled pinhole positioned underneath. (c) A non-imaging photodiode collects light, while a high gain transimpedance amplifier is added nearby. On a custom PCB, components are mounted along with a lens holder and microscope lens.

prototypes with up to 750 frames per second throughput. With cost-effectiveness in mind, a more compact setup with a higher throughput for capturing droplets during generation was constructed as follows (Fig. 9):

- A light source constructed of a cold white 1 W wide-beam LED (Fig. 9/a). Soldered to a PCB with large copper areas for heat dissipation. Current-limited to ∼150 mA using an LED driver.
- The light source was covered with a diffusing lens (Fig. 9/a) to reduce its beam angle and reduce beam intensity variations from smaller misalignments with the sensor axis.
- A PDMS-glass microfluidic chip, further detailed in Section II-D (Fig. 9/b).
- A thin metal plate, with a noise-reducing micro-drilled pinhole (sized proportionally with the chip's junction width), positioned beneath the microfluidic chip to increase the relative dimming impact of a passing droplet (Fig. 9/b).
- Based on Texas instruments application [30], using a 1 MΩ as feedback resistor instead, to obtain a gain of 1 MV/A and a 1.3 pF capacitor for stability at

higher frequencies, a photodiode (PD) sensor (Osram SFH 2240, Fig. 9/c) was connected to a transimpedance amplifier (TIA). A 20x microscope lens was mounted to the PCB, over the sensor, for improved focus of the droplets flowing in the microchannel.

Using the droplet flow sensor setup described above, a theoretical detection throughput was raised above 10000 droplets per second.

2) DETECTION OF DROPLET SHADOWS
The chip mount (Section II-A-II-b and Fig. 2/2/b) was positioned between the light sensing PD and the light source, all of which were vertically aligned to the pinhole under the outlet junction of the microfluidic chip (Fig. 9). As generated droplets were moving over the pinhole, a shadow was cast through it, onto the PD. The changing current through the PD was converted to voltage using a high-gain TIA, passed on to a connected filter-amplifier circuit in the electronics module (Section II-B-V and Fig. 2/1). The filtered signal moved through a DC decoupler into an inverting and level-shifting amplifier circuit. The extra amplification also provided compensation when the height of the light source was adjusted. The inversion of the photodiode voltage meant that any increase in the shadow corresponded to an increase in measured voltage. The filtered and amplified photodiode output was discretized with the ADC and sent over to the main control board using SPI. The RPI dedicated 1 of its 4 cores to communicating with the ADC, enabling photodiode voltage sampling rates of up to ∼440 kHz (without an interpretation algorithm).

D. FLUIDICS MODULE
1) DROPLET GENERATION CHIPS
The microfluidic chip designs used in this work were adapted from the group's earlier works, notably the "Droplet counting chip" in the ESI of [31]. The principle design (Fig. 10/a) was a flow-focusing device (FFD) laid out on an SU8 mask in multiple copies with different junction widths and geometries. In TABLE 2 the chip designs used in experiments in this work are shown. The mask design is openly available on our GitHub [32]. Silanized silicon-SU8 masks were purchased from the BioMEMS group of the Hungarian Academy of Sciences [33]. PDMS-glass chips were fabricated as follows: 1) PDMS was molded off the mask (PDMS was allowed 3 days at room temperature to cure and degas), 2) the PDMS was punched to create ports using a tissue biopsy tool, 3) PDMS and glass surfaces were cleaned from dust, 4) surfaces were activated with oxygen plasma generated by a handheld corona discharge surface treater, 5) surfaces were bonded, 6) chip walls were coated with Novec™1720 Electronic Grade Coating.

2) MOUNTING OF THE DROPLET GENERATION CHIP
The removable chip holder (Section II-A-II-b) in the sensorics module (Fig. 2/2/b) had a 2 by 2 mm square hole at the
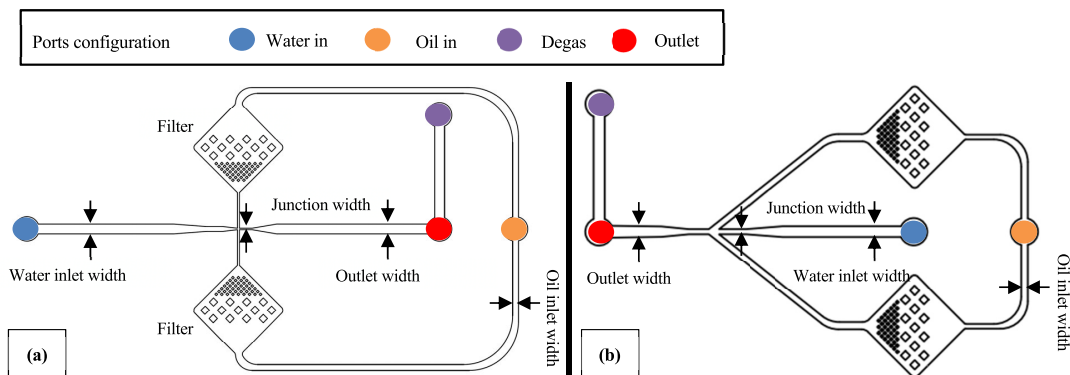
FIGURE 10. Parameterized flow-focusing device for controlled droplet generation. Oil inlet is split equally and filtered through micropillar arrays to prevent impurities on the oil line from clogging the junction. The outlet has a 1 ml gas spring attached to smoothen out flow rate fluctuations coming from the pump. Chip variant A/B (a) had a 90-degree entry in the flow-focusing junction, whereas variant C (b) had a 38.33-degree entry angle and a shorter outlet length. There was no other difference between the 3 chip variants apart from the junction width. Water inlet, outlet and oil line widths were the same.

TABLE 2. Primary/main mould design parameters for microfluidic droplet generator chips.

Chip variant	A	B	C
Junction width [mm]	90	125	280
Junction angle of entry [°]	90	38.33	
Oil inlet width [mm]	360		
Water inlet width [mm]	6		
Outlet width [mm]	0.6		
Number of filters	2		

center, over which the metal plate (Fig. 9/b) with a pinhole was placed. The pinhole was manually centrally aligned with the square hole in the chip holder. Lastly, a droplet generation chip was positioned on the pinhole plate and fastened to the holder. The chip was aligned to have the pinhole beneath the chip's outlet channel, $\sim$300 μm after the cross-junction. For the used chips, this distance mitigated capturing forming droplets and deforming droplets flowing into the wider section of the outlet where capturing distinct droplets could be jeopardized by the loss of gaps between droplets. The assembly was attached to the top of the 3 DoF chip mount (Section II-A-II-b and Fig. 2/2/b).

III. EVALUATION METHODOLOGY

In this section, we present the prototype system evaluation methodology used for characterization and benchmarking on a system as well as on a submodule level.

The first test series (Section III-A) focused on evaluation of system submodules or groups of submodules. Fine-tuning steps were also taken to prepare for the system integration. The second test series (Section III-B) focused on characterizing and benchmarking the integrated system prototype in droplet generation.

In all test setups, droplets were generated using fluids as described in TABLE 3.

In all test setups including a camera, a high-speed camera module (acA640-750uc, Basler) was used. The camera frames were captured in real time on the computer using Basler's pylon Viewer software.

A. SUBMODULE EVALUATION

The test setup used (Fig. 11/a) in this section was an early proof-of-concept implementation of the full experimental setup presented in Section II-A. The setup was derived from components demonstrated in our earlier works ([23], [24]). In the setup, DIW was used as the disperse phase, oil A or B as the continuous phase. Both phases were pumped into the droplet generation chip using our custom pumping system based on Bartels Mikrotechnik micropumps (mp6-liq). Results are presented in Section IV-A.

1) PRESSURE-BASED SYSTEM FEEDBACK MODELLING
Tests done with the following methodology gave results for: characterization of pressure control, definition of voltage to pressure transfer functions and tuned pressure feedback PID gains using the transfer functions.

TABLE 3. Fluid phases used in droplet generation experiments.

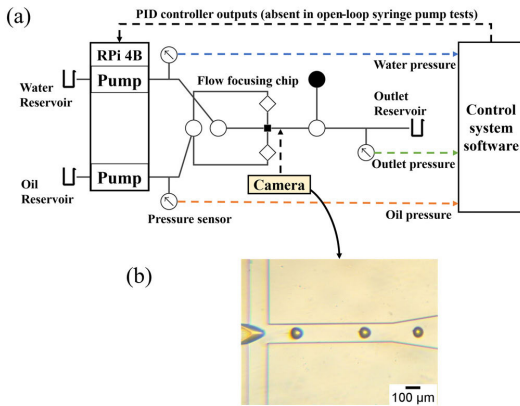|	A	B
Disperse phase	deionized water (DIW)	deionized water (DIW)
Continuous phase	Sigma-Aldrich 33079 mineral oil + 2% w/w surfactant (Span® 80, Sigma-Aldrich)	HFE 7500 fluorocarbon oil + 2% w/w surfactant (perfluoropolyether (PFPE)-poly(ethylene glycol) (PEG)-PFPE triblock)

FIGURE 11. Schematic diagram for the experimental setup of droplet microfluidics system: (a) block diagram of the control system, (b) camera image of the droplet generator junction.

FIGURE 12. Pressure drops vs. peak-to-peak voltages of the piezoelectric micropump for the chip variants with cross-junction widths: 90 μm with DIW (a) and with oil A (b); 125 μm with DIW (c); and 280 μm with DIW (d) and with oil A (e). Driving frequency for water pump was 200 Hz sinewave. The driving voltage waveform was 200 Hz sinewave for the water pump and 50 Hz sinewave for the oil pump.

The pressures at the inlets and outlets of the microchannel were measured using Honeywell pressure sensors MPRLS0015PG0000SA and MPRLF0250MG0000SA, respectively, with a sampling rate of ~166 Hz. To obtain pressure to pump driving voltage relationships, driving voltage tests were conducted. For three chip variants (relevant chip dimensions in TABLE 2), the driving voltage of the piezo pumps ranged from 25 V to 250 V, with a step size of 25 V. Corresponding pressures were recorded for a duration of one minute at each step with the steady state averaged as the resulting pressure value. Measurements were done separately for DIW and oil A. Unwanted transients or spikes in the experimental data were removed using median filtering (performed in MATLAB).

To tune the PID gains, experimental data (from our earlier works [21], [22]) demonstrating the effect of inlet pressure on droplet size were used in MATLAB to derive pumping system component transfer functions. The transfer functions were implemented in Simulink in a setup-derived closed loop feedback model. PID K-values were found among six objective function criteria obtained from using genetic algorithm method: the Integral Squared Error (ISE) criterion; the Integral Time Squared Error (ITSE) criterion; the Integral of Time Absolute Error (ITAE) criteria; the Integral of Absolute Error (IAE) criterion; the Mean Squared Error (MSE) criterion; the Integral Error (IE) criterion.

2) SYRINGE PUMP VS. PRESSURE-DRIVEN PUMP
As laboratories often use syringe pumps for droplet microfluidics, the performance of our pressure-based micropump system against syringe pumps was compared here.
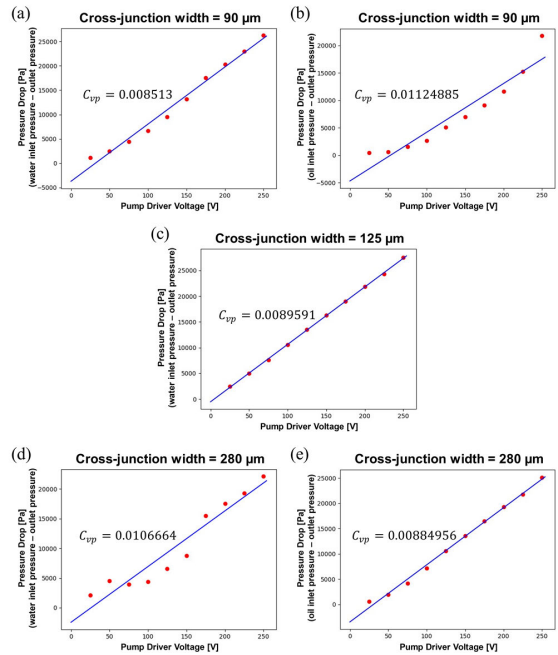
Two syringe pumps (NetPump, SpinSplit LLC, Budapest, Hungary) with plastic syringes were used to pump oil A and DIW into chip variant A. Pressure sensors were set in the established configuration (Fig. 11/a). The syringe pumps were connected to local network via Ethernet and interfaced with SpinStudio (SpinSplit LLC, Budapest, Hungary) on a desktop computer. Droplet formation was observed using a camera, placed beneath the FFD's cross-junction. Syringe pumps were set to run for about four minutes, with fixed flow rates (Fig. 14/a), producing uniform droplets. One minute from the end of the steady state period of the measured oil and water pressure drops over the chip were averaged and used as targets for the pressure pump PIDs corresponding to the matching fluid phase. Followingly, the inlet tubes were disconnected from the syringe pumps and connected to the pressure pumps. For two minutes, pressure pumps were pumping oil and water with closed loop control, with comparable pressure (Fig. 14/b).
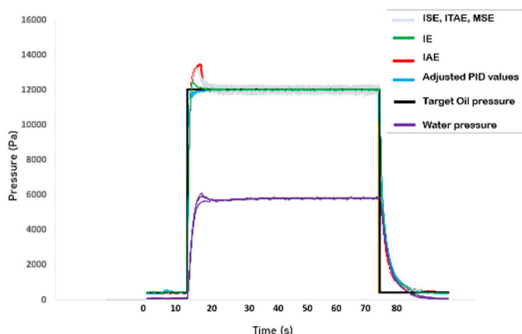
FIGURE 13. Simulation results for pressure feedback PID controller tuning with a genetic algorithm for oil pressure control.
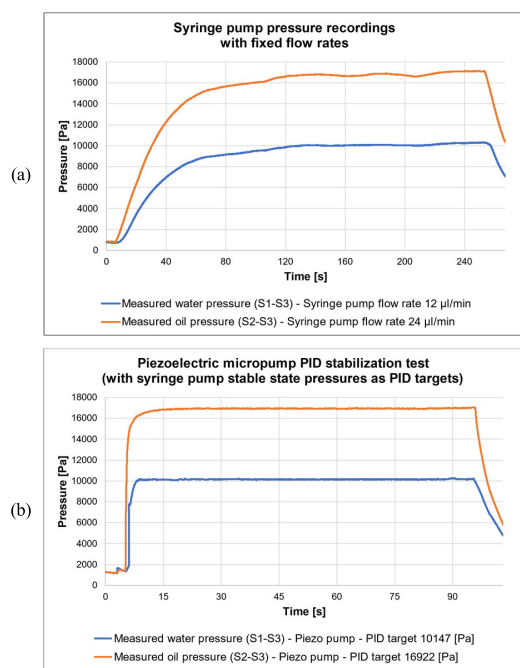

FIGURE 14. Pressure stabilization experiments performed on the setup shown in Fig. 11/a. Syringe pumps were set to pump with 12 μl/min for DIW and 24 μl/min for oil A. One minute period from the end of stable state pressures on (a) were averaged and used as pressure targets for the piezoelectric micropump PIDs. a) Responsiveness of flow-rate driven system (with third-party syringe pumps); b) Responsiveness of our pressure-driven system.

3) SENSORICS, PHOTODIODE VOLTAGE INTERPRETATION

Before droplet observations with a PD, a camera was used to analyze possible scenarios. Droplets were generated with DIW in separate combinations with oil A and B (TABLE 3). Droplets were recorded as image series to a computer and afterwards analyzed visually. Additionally, images of droplets were scanned through a custom pixel color summation program, used to estimate possible collectable wave-

forms from the PD. The custom program had an additional feature to roughly mimic a variable pinhole (determinable by the angle of the droplet generation chip in the chip mount).

4) SYSTEM CONTROLLER BENCHMARKING

The selected controller (RPI) had a quad core processor limiting concurrent tasks to four. Additionally, with RPI running a desktop OS, loop stability of each task, split using multiprocessing Python library, was measured in a one-time operation – finishing with complete termination processes. As this required all connected submodules, the test took place at the final stages of integration. All tasks running in parallel on RPI were timed over a 90 second droplet generation operation using chip variant C with oil B.

Furthermore, three additional 90 second tests were run (2 with chip variant C and 1 with chip variant B). After 45 seconds into the tests, $\sim$3 seconds of ADC data (from task/core 3) was logged in more detail to analyze controller related latency and performance with a custom droplet interpretation algorithm. In the same period, a sample image was taken from the waveform entering the ADC, visualized on a connected oscilloscope (DSO5014A, Keysight).

B. SYSTEM EVALUATION

In system evaluation methodology, unless specified otherwise, oil B (TABLE 3) was used as the continuous phase.

1) DROPLET SIZE AND FREQUENCY CONTROL

For this evaluation process, two sets of target series tests (size and generation rate) were conducted for each of the two chip variants (B and C) – shown on TABLE 4–7. All samples in series were given 15 seconds for stabilization which was discarded from further calculations. The remaining 21 seconds for each sample was used for CV% and error calculations. Due to geometric differences between chip variants, target ranges of named series were limited to combinations more likely to produce droplets.

2) MEASUREMENT OF COEFFICIENT OF VARIABILITY OF GENERATED DROPLETS

To measure the stability of droplet generation with the proposed system, coefficients of variability (CV%) were calculated from "digitized" droplet data (relative droplet size over the photodiode as voltage and droplet generation rate as frequency from droplet-to-droplet period) obtained with specified droplet feedback PID targets after the setup was ran through the calibration algorithm described in ESI S3. CVs were calculated from voltage and frequency series obtained from dual-PID tests, allowing 15 seconds for stabilization at the start of each stage. This left 21 seconds of stabilized data on each target for CV calculation. CVs were also calculated from additional datasets made with longer stabilization (30 s) and stable periods (45 s). As generation frequency did not strictly apply to droplet length, CV of generation frequency was not combined with relative size CVs. However, droplet generation frequency target series were further quantitatively

TABLE 4. Chip B – voltage target series over fixed generation frequency targets.

	Fixed Generation Rate Target	Voltage / Size Target 1	Voltage / Size Target 2	Voltage / Size Target 3
1	200 Hz	2.0 V	2.8 V	3.6 V
2	400 Hz	2.0 V	2.8 V	3.6 V
3	600 Hz	2.0 V	2.8 V	3.6 V
4	800 Hz	2.0 V	2.8 V	3.6 V

TABLE 5. Chip B – frequency target series over fixed voltage (size) targets.

	Fixed Voltage / Size Target	Generation Rate Target 1	Generation Rate Target 2	Generation Rate Target 3	Generation Rate Target 4
1	2.0 V	200 Hz	400 Hz	600 Hz	800 Hz
2	2.8 V	200 Hz	400 Hz	600 Hz	800 Hz
3	3.6 V	200 Hz	400 Hz	600 Hz	800 Hz

TABLE 6. Chip C – voltage target series over fixed generation frequency targets.

	Fixed Generation Rate Target	Voltage / Size Target 1	Voltage / Size Target 2	Voltage / Size Target 3	Voltage / Size Target 4
1	200 Hz	3.2 V	3.4 V	3.6 V	~~3.8 V~~
2	300 Hz	3.2 V	3.4 V	3.6 V	3.8 V
3	400 Hz	3.2 V	~~3.4 V~~	~~3.6 V~~	~~3.8 V~~
4	500 Hz	3.2 V	~~3.4 V~~	~~3.6 V~~	~~3.8 V~~

TABLE 7. Chip C – frequency target series over fixed voltage (size) targets.

	Fixed Voltage / Size Target	Generation Rate Target 1	Generation Rate Target 2	Generation Rate Target 3	Generation Rate Target 4	Generation Rate Target 5
1	3.2 V	200 Hz	300 Hz	400 Hz	500 Hz	600 Hz
2	3.4 V	200 Hz	300 Hz	400 Hz	500 Hz	600 Hz
3	3.6 V	200 Hz	300 Hz	400 Hz	~~500 Hz~~	~~600 Hz~~
4	3.8 V	200 Hz	300 Hz	400 Hz	~~500 Hz~~	~~600 Hz~~

analyzed via standard deviations and CVs (further detailed in ESI S4). Multiple CV sets were required for observing the impact from droplet generation frequency, pumping frequency (as piezo pump driving frequency) and average pressure in the chip to droplet size CV.

In addition, to attest to the meaning and comparability of voltages obtained from the photodiode, claimed as corresponding to droplet size, visual data of droplets was needed. For visual data, droplets, generated with fixed pressure targets, were collected into an Eppendorf Tube® to be measured afterwards. Imaging for measurements was done with a trinocular microscope (BX61, Olympus) using a camera (DP70, Olympus) and a 4x/0.16 lens (UPLSAPO, Olympus). CVs and averaged cross-sectional areas and diameters were calculated using ImageJ software (further described in ESI S5). For better viewing, droplets were pushed into

Countess™ Cell Counting Chamber Slides (ThermoFisher) with a channel height of 100 μm.

IV. EVALUATION RESULTS AND DISCUSSION
In all tests, droplets were generated with liquids following the naming scheme given in Section III.

A. SUBMODULE EVALUATION
1) PRESSURE-BASED SYSTEM FEEDBACK MODELLING
With the ramping pump driving voltage (25 V to 250 V) tests, linear correlation between voltage and pressure generated in tests with all chip variants were observed (Fig. 12). The relationship of pressure drops across the chip to pumping voltages varied for the different chip variants. This was quantified with the voltage-to-pressure coefficient (C_{vp}). Furthermore, while the rising trend of the C_{vp} of water tests was rising

along with the cross-junction width, the ratio of water and oil C_{vp} was different between chips with different oil entry angles (Fig. 12/a-b vs. Fig. 12/d-e). The coefficients obtained with chip A were used in the controller design to account for differences in junction widths.

Based on our earlier works [21], [22], the system components were mathematically represented as transfer functions in eqns. 1-3, using the collected data in MATLAB software.

$$\text{t.f.}_{\text{pwat}} = \frac{-17.42s + 83.92}{s + 0.69} \tag{1}$$

$$\text{t.f.}_{\text{poil}} = \frac{-8.40s + 30.6123}{s + 0.216} \tag{2}$$

$$\text{t.f.}_{\text{chip90}} = \frac{19.04s + 0.339}{s + 0.275} \tag{3}$$

where t.f.$_{\text{pwat}}$ is the transfer function of the water pump, t.f.$_{\text{poil}}$ the transfer function of the oil pump, and t.f.$_{\text{chip90}}$ the transfer function of the chip variant A. From Simulink results the controller parameters with the lowest fitness values (error) were chosen for real-world experiments. PID's K_p, K_i, K_d values for water pump (10.5, 60.77, 1.64e5), obtained from the IE objective function, resulted in good long-term stability, albeit with an overshoot, whereas K_p, K_i, K_d values (6.69, 46.10, 5.81e-5), obtained from the IAE objective function, resulted in a response with negligible overshoot, but instead with oscillations around the target value. Based on the comparison of GA tuning results (Fig. 13), manual adjustments to K_i were made to prevent overshoot and maintain good stability, with new K_p, K_i, K_d values (10.5, 17.5, 5.81e-5) for water. Following the same process, K_p, K_i, K_d values were found for oil (40.0, 18, 4.78e-4).

2) SYRINGE PUMP VS. PRESSURE-DRIVEN PUMP

The pressure stabilization and steady states of the two test scenarios described in Section III-A-II are shown in Fig. 14. Syringe pumps took approximately 120 seconds to reach a reasonable steady state for new pressure targets, with minor oscillations persisting. Slower response time for syringe pumps was attributed to linear operation of the motors' speeds, however, the likely cause for persistent oscillations was attributed to inconsistent friction of the syringe's rubber gasket. In comparison, pressure-driven micropumps showed better responsiveness and stability between changing input pressure targets, taking about 10 seconds to reach the defined inlet and outlet pressure values.

The faster response rate helped significantly reduce experiment runtimes and reagent waste during the system evaluation tests (Section IV-B, e.g., exploring ranges of producible droplet sizes and generation rates).

3) SENSORICS, PHOTODIODE VOLTAGE INTERPRETATION

While generating droplets using oil A, the formed droplets (Fig. 15) indicated that once the droplet's diameter exceeded the larger dimension of the channel (Fig. 15/c), the shadow caused by refractions in the phase transition region would
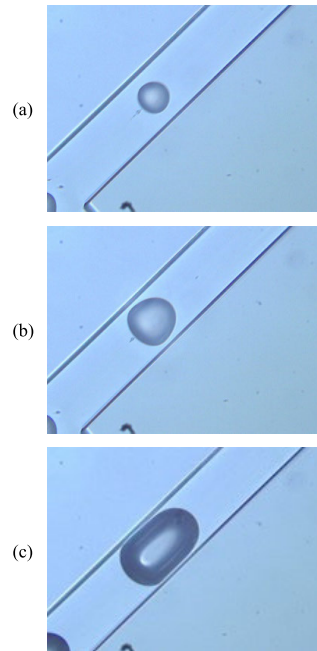

FIGURE 15. Recorded camera images of droplets generated with DIW and oil A in a 125 μm wide microfluidic channel taken at 555 frames per second under brightfield LED. a) ~58.4 μm length droplet, generated with 5.2 kPa and 11.0 kPa for water and oil pressures respectively; b) ~112.7 μm length droplet, generated with 5.2 kPa and 9.5 kPa for DI water and oil A pressures respectively; c) ~182.0 μm length droplet, generated with 5.2 kPa and 7.5 kPa for water and oil pressures respectively.

intensify. Furthermore, a central low refraction region would emerge.

The possible impact of the low refraction region on the captured photodiode light intensity waveform was estimated from the custom pixel color summation program (Fig. 16). Given the fixed size moving window on Fig. 16/a-c, it was noted, that even with a longer than "window size" droplet, whose diameter was less than the larger dimension of the channel (Fig. 16/b), the estimated waveform gained little to no distortions. Mild distortion could be attributed to the bullet-like shape of the droplet. However, a much more noticeable distortion was noted once the low refraction region became significant relative to the window size. The non-phase transition region had the potential to invert the tip of the waveform. The impact of this effect was amplified with a less viscous continuous phase, as that reduced the surface tension of the droplet and the intensity of the droplet's shadow along with it.

Using oil B for the continuous phase, generated droplets showed inherently thinner phase transition regions and gave way for larger low refraction regions (Fig. 17). The images show a case where not only was the phase transition region very thin, but the aligned droplet acted like a lens (Fig. 17/c). To further inspect the impact of such cases, consecutive
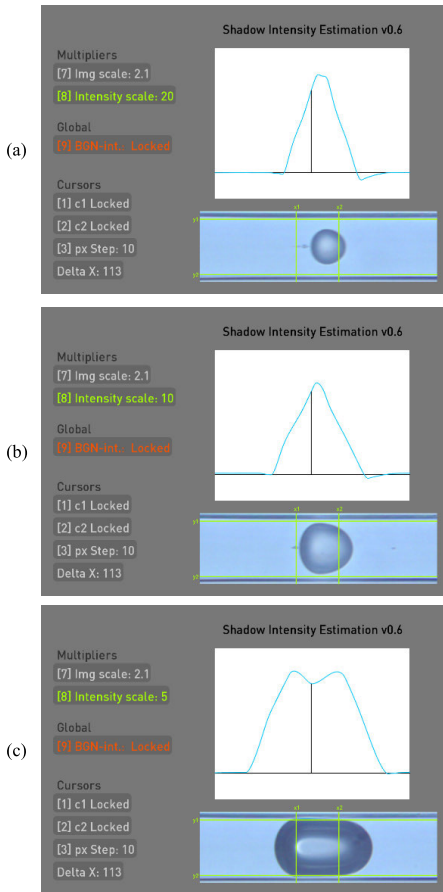
FIGURE 16. Rotated and cropped camera images shown in Fig. 15, respectively, were scanned with a fixed size moving window, indicated by green vertical lines to obtain corresponding intensity graphs (blue waveform above droplet image). a) low-distortion triangular waveform produced by the ~58.4 μm length droplet with a relative intensity multiplier of 20.0; b) low-distortion triangular waveform produced by the ~112.7 μm length droplet with a relative intensity multiplier of 10.0; c) high-distortion trapezoidal (double-peak) waveform produced by the ~182.0 μm length droplet with a relative intensity multiplier of 5.0.

FIGURE 17. Cropped recorded frames of a passing droplet during generation with oil B. Droplet was generated at 5.0 kPa and 5.5 kPa water and oil pressures respectively. Displayed droplet measures ~171.9 μm in length and was recorded at 1810 frames per second. A circular ~190 μm diameter pinhole was used under the microfluidic chip below the recorded region to improve the visibility of the droplet. a) reference frame 1 in series, droplet entering the pinhole aperture; b) reference frame 2 in series, droplet approaching the center of the pinhole aperture; c) reference frame 3 in series, droplet in the middle of the pinhole aperture; d) reference frame 4 in series, droplet leaving from the center of the pinhole aperture; e) reference frame 5 in series, droplet exiting the pinhole aperture.

frames were viewed in the custom pixel color summation program (Fig. 18). Due to the usage of a pinhole, the extra shadows at the edges (background noise) were subtracted from further intensity calculations using the 6th additional frame (Fig. 18/f). Seen from Fig. 18 with a droplet, sized large enough to be squished in the microfluidic channel, flowing in low viscosity oil B, the possible recorded waveform for a single droplet could resemble a much more severe case of Fig. 16/c – instead of a slightly dipping peak, a waveform section representing a single droplet with a possible dip as low as to split into two discernible droplets.

4) SYSTEM CONTROLLER BENCHMARKING

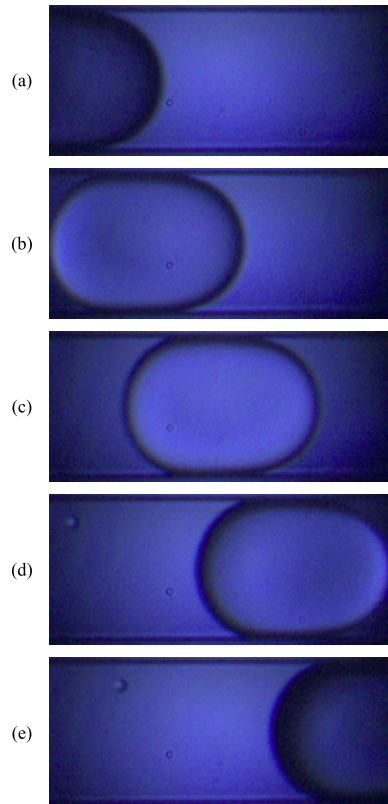Individual task duration details can be seen on TABLE 8. Maximum loop durations of the waveform interpretation and

pumping pressure target calculation tasks (marked with * in TABLE 8) were caused by spikes in OS latency. Noticeably longer than average maximum loop durations for the remaining tasks were caused by delays from communication termination procedures included in the timing of the last loop. Total durations of tasks other than the pumping pressure target calculation task, where the main operation timer was running, were longer due to beginning their termination process after the defined 90 s time limit. Their difference was caused by sequential termination process (some extending for multiple seconds due to large log file generation). For droplet waveform interpretation task, the average loop duration extended to ~6.5 μs, resulting in a mean sampling rate of ~153 kHz. The discrepancy between minimum loop duration of pump communication task (~15 ms) and pump
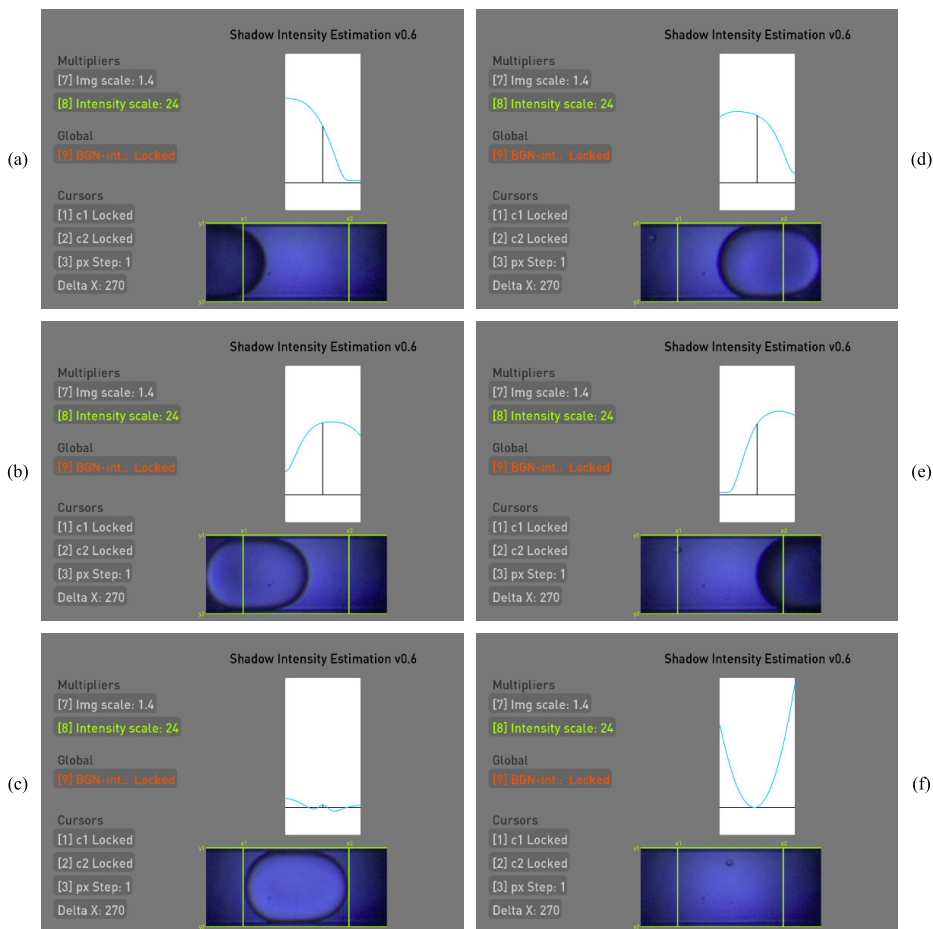
FIGURE 18. Camera images shown in Fig. 17, respectively, and an extra 6th frame were scanned with a fixed size moving window, indicated by green vertical lines to obtain corresponding intensity graphs (blue waveform above droplet image). All intensity graph scaling multipliers were kept at 245.0 for better visualization and comparability. The intensity of the 6th frame, representing the background noise, was recorded first, and locked into memory. Background intensity was subtracted from the following calculations. a) Indicating a rising shadow intensity as the darkest region of the droplet entered the pinhole aperture and the moving window; b) indicating a past-peak shadow intensity as the droplet moved closer to the center of the pinhole aperture and the moving window; c) indicating the lowest shadow intensity while the droplet was positioned at the center of the pinhole aperture; d) indicating an approaching-peak shadow intensity as the droplet was leaving the central region of the pinhole aperture and the moving window; e) indicating a falling shadow intensity as the darkest region of the droplet was exiting the pinhole aperture and the moving window; f) indicating the intensities of the shadows at the edges of the frame, caused by the pinhole.

TABLE 8. Controller software's task loop duration.

	Core 1 – User interface coms. (Section II-B-3-1)	Core 2 – Pumping system coms. (Section II-B-3-2)	Core 3 – Droplet interpretation (Section II-B-3-3)	Core 4 – Droplet PID calculations (Section II-B-3-4)
Maximum [ms]	203.4370	215.0430	20.25914*	21.05400*
Average [ms]	102.0334	18.98948	0.006515	0.169749
Minimum [ms]	100.6310	14.74400	0.002861	0.104000
Loops counted	1005	4 758	14 640 000	530 200
Total [s]	102.54	90.35	95.38	90.00

sensor update rate of ∼166 Hz (6 ms) was attributed to having used asynchronous communication method.

In the OS latency and droplet interpretation algorithm impact analysis, droplet waveform from the first additional
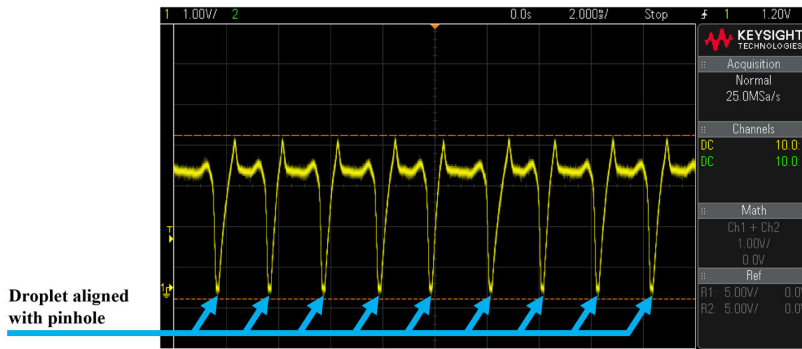
FIGURE 19. Oscilloscope screen capture of recorded amplified, inverted photodiode voltage during droplet generation with chip variant C, at a rate of ∼500 Hz. Droplet alignment with the pinhole noted with blue arrows (at the "troughs"). Instability in the droplet production rate is recognizable by the varying time gaps between the „troughs".

test with chip variant C (Fig. 19) indicated that the pinhole-aligned droplets were seen as an increase in light intensity. Meaning that the droplets functioned as lenses instead of obstacles. In this scenario, the "peak" of the alignment was measured at the "trough". Each "trough" could be imagined as a more severe form of the dip shown in Fig. 16/c. Each "trough" was accompanied by its darker incoming and outgoing edges (Fig. 18/a, 18/e). From the logged ADC data, a sample section (Fig. 20) showed the limits of RPI running code written in Python on a non-real-time OS and specific functions circumstantially interacting poorly with the OS. As the average ADC task loop duration was measured around ∼6.5 μs (TABLE 8), Python's multiprocessing Queue functions empty() and get_nowait(), called after 100 mV above the average line for every other droplet, delayed the loop duration minimally another ∼100 μs producing erroneous droplet size measurements. In comparison, the second test with chip variant C (Fig. 21) showed a waveform with similar sharp peaks, but each with longer duration. Long enough to preserve the peaks captured by the ADC (Fig. 22). In the third additional test, with chip variant B, OS latency was spotted causing the loss of 2-3 consecutive droplets (Fig. 23) with an unexpected delay between two ADC sampling cycles. Albeit being relatively rare, the measurement error of such events was mitigated to prevent destabilizing the flow rates. When time delay between two ADC samples exceeded 30% of the average droplet generation period, the following erroneous droplets were excluded from the logs and use in the droplet feedback PIDs. It improved fluidic stability, but in the case of random OS delays, at the cost of up to 10% of generated droplets not getting logged (losses were lower with lower generation rates). Likewise, in the case of get_nowait() delay, if it exceeded 30% of the average droplet generation period, the irregular droplet measurement would be excluded from the log and PID feedback.

B. SYSTEM EVALUATION

After assembly, programming, and fine-tuning through preliminary testing, connection between a laptop and the

CogniFlow-Drop device was established through a Wi-Fi hotspot to validate the communication interface. After a successful connection, the interface effectively transmitted and received message packets every ∼100 ms, artificially delayed with eCAL message polling delay on the RPI. Other functional tests with the remote control included:

- initiating setup calibration (tied to variables: chip position/angle, chip variant, liquids used),
- initiating droplet generation with desired size and generation rate,
- initiating droplet size (V) target series test,
- initiating droplet generation rate (F) target series test.

Each feature of the GUI (Fig. 8) was proceeded to be used as remote initiator for the following system evaluation steps.

1) RESULTS OF DROPLET SIZE AND FREQUENCY CONTROL TEST SERIES

During experimentation, some target droplet size and generation frequency combinations did not yield droplets regardless of having used selective ranging – highlighted on TABLE 6-7. Overall, chip C showed lower ranges for both sizes and generation rates. Additionally, chip C behaved uniquely between voltage and frequency series, as the combination of (400 Hz; 3.4 V) in voltage series did not yield droplets, but in contrast, was unexpectedly stable in frequency series. This hinted to higher sensitivity to size target alterations during droplet production combined with how current droplet feedback PID handles high instability.

Target series over all four sets, named in Section III-B-I, resulted in averaged droplet size errors, seen on Fig. 24, which indicated higher accuracy for droplet size control with chip B, more specifically with droplet size (V) series when the marked outlier of ChipB-Fseries was taken into account. With an average error of -0.06%, ChipB-Vseries obtained averaged sizing errors between +2.86 to -1.79%. Contrast of accuracy of reaching average target size, can be seen on droplet capture graphs between ChipB-Vseries (row 4 from TABLE 4) and ChipC-Vseries (row 2 from TABLE 6) on Fig. 24/b and Fig 24/c respectively, with target sizes per sample,
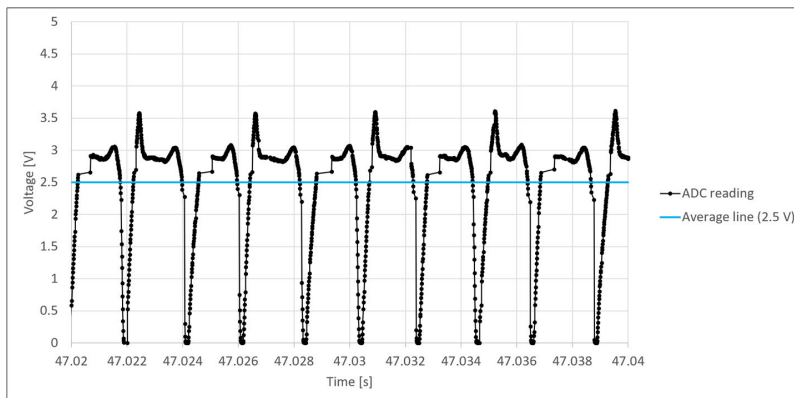
FIGURE 20. Sample frame from ADC measurement log on RPI showing ADC readings and the average line over which droplet detection was handled. Shown graph links with Fig. 19, however, with every other peak cut off due to specific cross-core communication function delays.
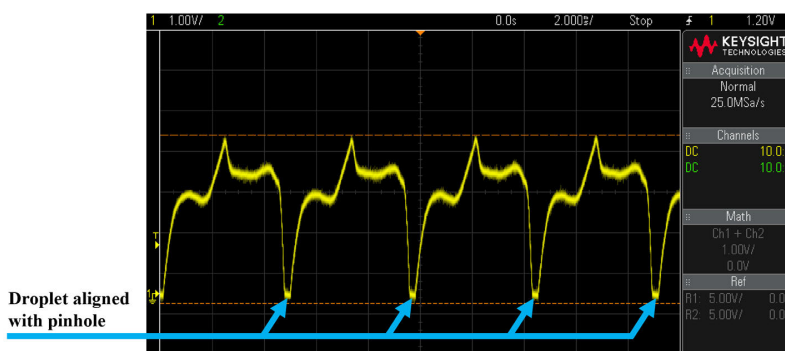

FIGURE 21. Oscilloscope screen capture of recorded amplified, inverted photodiode voltage during droplet generation at a rate of ∼200 Hz. Droplet alignment with the pinhole noted with blue arrows (at the "troughs").
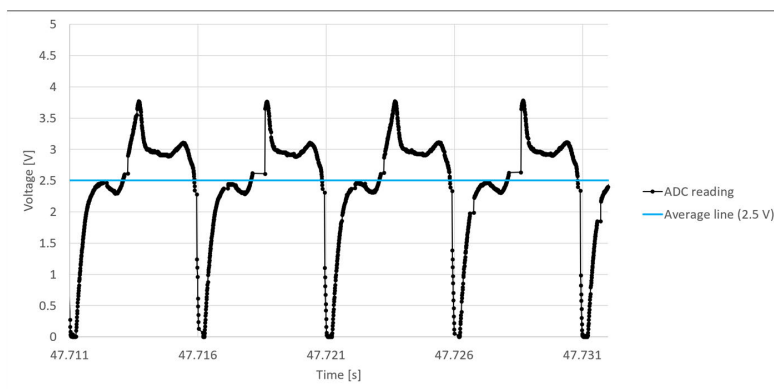

FIGURE 22. Sample frame from ADC measurement log on RPI showing ADC readings and the average line over which droplet detection was handled. Shown graph links with Fig. 21, however, in contrast to Fig. 20, cross-core function delays caused after every other detected droplet, were not long enough to cut off the relevant peaks of the droplet waveform.

segmentally overlayed as orange horizontal lines. Target size errors on Fig. 24/b were [+0.35; -1.79; -1.56] % respectively. Together with the fixed frequency (200 Hz) accompanied

with varying droplet size targets, frequency errors of [+0.88; −2.00; −5.63] %, respectively, showed a decreasing total output volume with the combined error staying further and
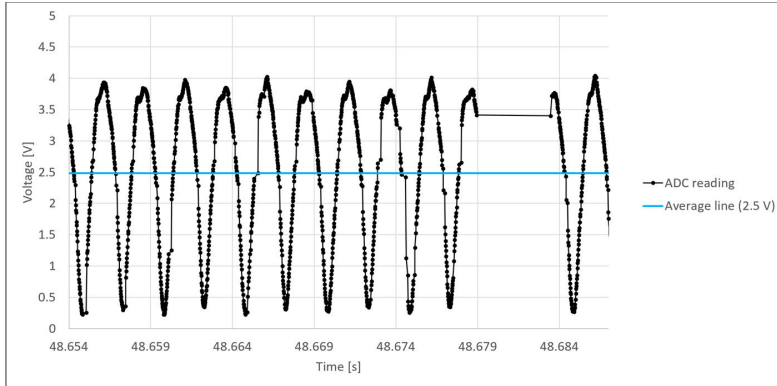
FIGURE 23. Sample frame from ADC measurement log on RPI showing ADC readings and the average line over which droplet detection is handled. In shown example, spontaneous latency delays caused by the operating system running on RPI prevented three consecutive droplets being captured and measured.
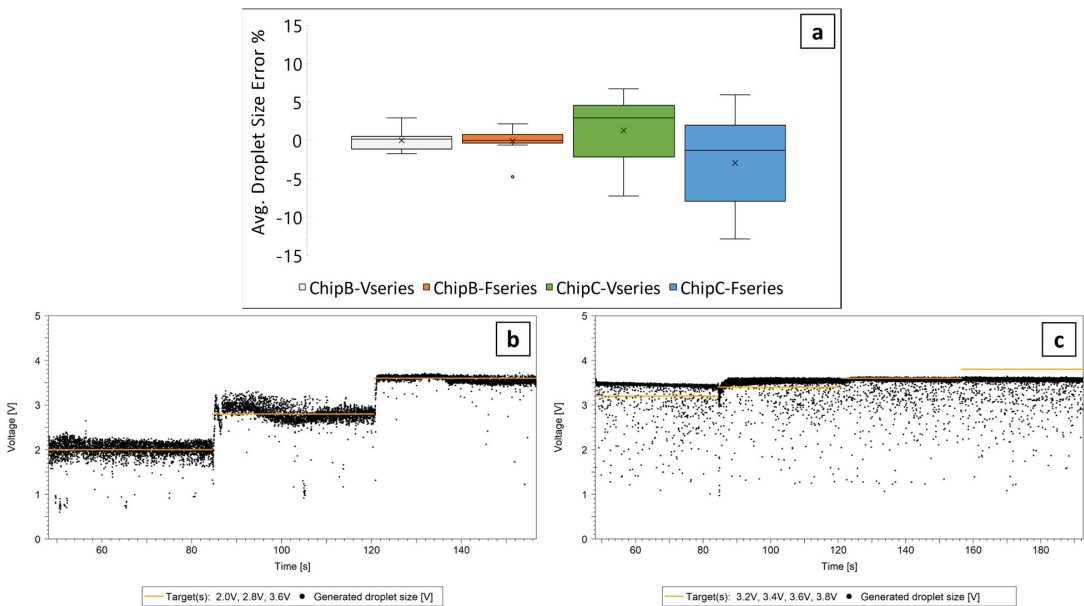

FIGURE 24. Results from Section IV-B-I. a) Averaged droplet size target errors for chips B and C, further split by size and frequency series test sets. Sample sizes for series respectively [12, 12, 9, 16]; b) Droplet size control dataset of row 1 from TABLE 4, from ChipB-Vseries test set. Graph indicating higher accuracy of stabilization around target voltage levels; c) Droplet size control dataset of row 2 from TABLE 6, from ChipC-Vseries test set. Graph indicating lower accuracy of stabilization around target voltage levels, preference to droplet size (influenced by chip geometry).

further below the targets. Target errors on Fig 24/c were [+5.62; +2.88; −2.03; −7.24] % respectively. For the comparably reduced functional size range that channel geometry of chip C offered, target size control did not yield droplets in all requested sizes. This could largely be contributed to inclinations caused by the channel geometry. This was made clear from its accompanied averaged frequency target errors of [−1.99; +2.65; −0.73; −0.30] % respectively, which did not follow the pattern of size errors. The secondary contributor was attributed to the erroneous droplet size averaging caused by what was shown on Fig. 20. Due to alterations in perception of captured droplet sizes, calibration

for chip C test series had been segmentally impacted where droplet waveforms exhibited shapes more predisposed to peak losses.

Additionally, averaged droplet generation rate errors, seen on Fig. 25/a, again indicated higher accuracy for droplet rate control with chip B, more specifically with generation rate (F) series when marked outliers of ChipC-Fseries were taken into account. With an average error of +0.94%, ChipB-Fseries obtained averaged generation rate errors between +3.62 to −1.65%. Contrast of accuracy between the best and the worst captured series of reaching average target generation rate, can be seen on droplet capture graphs between
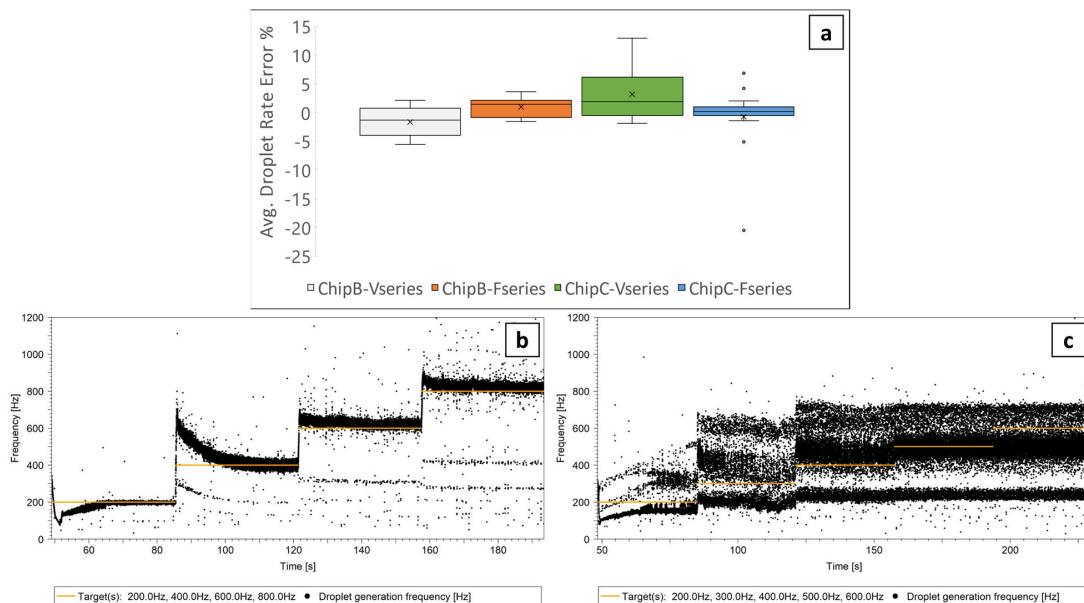
FIGURE 25. Results from Section IV-B-I. a) Averaged droplet rate target errors for chips B and C, further split by size and frequency series test sets. Sample sizes for series respectively [12, 12, 9, 16]; b) Droplet generation rate control dataset of row 2 from TABLE 5, from ChipB-Fseries test set. Graph indicating higher accuracy of stabilization around target frequency levels; c) Droplet generation rate control dataset of row 1 from TABLE 7, from ChipC-Fseries test set. Graph indicating lower accuracy of stabilization around target frequency levels and significant fluctuation in periodicity of droplet production.
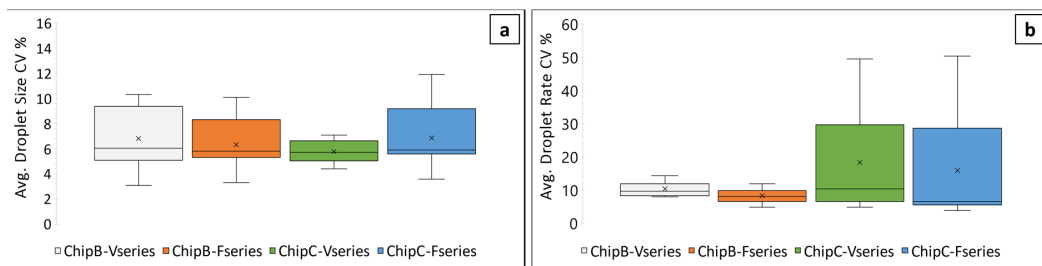

FIGURE 26. Results from Section IV-B-II. a) Averaged droplet size CVs for chips B and C, further split by size (V series) and frequency (F series) series test sets; b) Averaged droplet generation rate CVs for chips B and C, further split by size (V series) and frequency (F series) series test sets. Sample sizes for series respectively [12, 12, 9, 16].

ChipB-Fseries (row 2 from TABLE 5) and ChipC-Fseries (row 1 from TABLE 7) on Fig. 25/b and Fig. 25/c respectively, with target sizes per sample, segmentally overlayed as orange horizontal lines. Target averaged frequency errors, with chip B, on Fig. 25/b were [−1.43; +0.86; +1.83; +1.67] % respectively. Together with the fixed size target (2.8 V) accompanied with the example varying frequency targets, averaged size errors of [+0.50; −0.61; +0.61; +0.14] % respectively, showed no explicit relationship between size and frequency errors. This alluded to lesser impact from frequency alterations during droplet generation, in other words, lesser impact from changes in oil pressure rather than water pressure. Target averaged frequency errors, with chip C, on Fig. 25/c were [+1.93; +4.11; +6.78; −5.11; −20.61] %

with accompanying size target (3.2 V) errors of [+5.91; −0.06; −1.56; −1.09; −1.13] %, respectively, showing little correlation in comparison. This example showed large fluctuations in periodicity, but small droplet size variation (similar to Fig. 24/c from ChipC-Vseries).

2) MEASUREMENT RESULTS FOR COEFFICIENT OF VARIABILITY OF GENERATED DROPLETS
a: DROPLET SIZE DATA (PD VOLTAGE DISCRETIZED WITH THE ADC) FROM CONSECUTIVE DROPLET SIZE AND FREQUENCY TARGET SERIES
V and F series performed in Section IV-B-I resulted in averaged droplet size CVs represented on Fig. 26/a and averaged
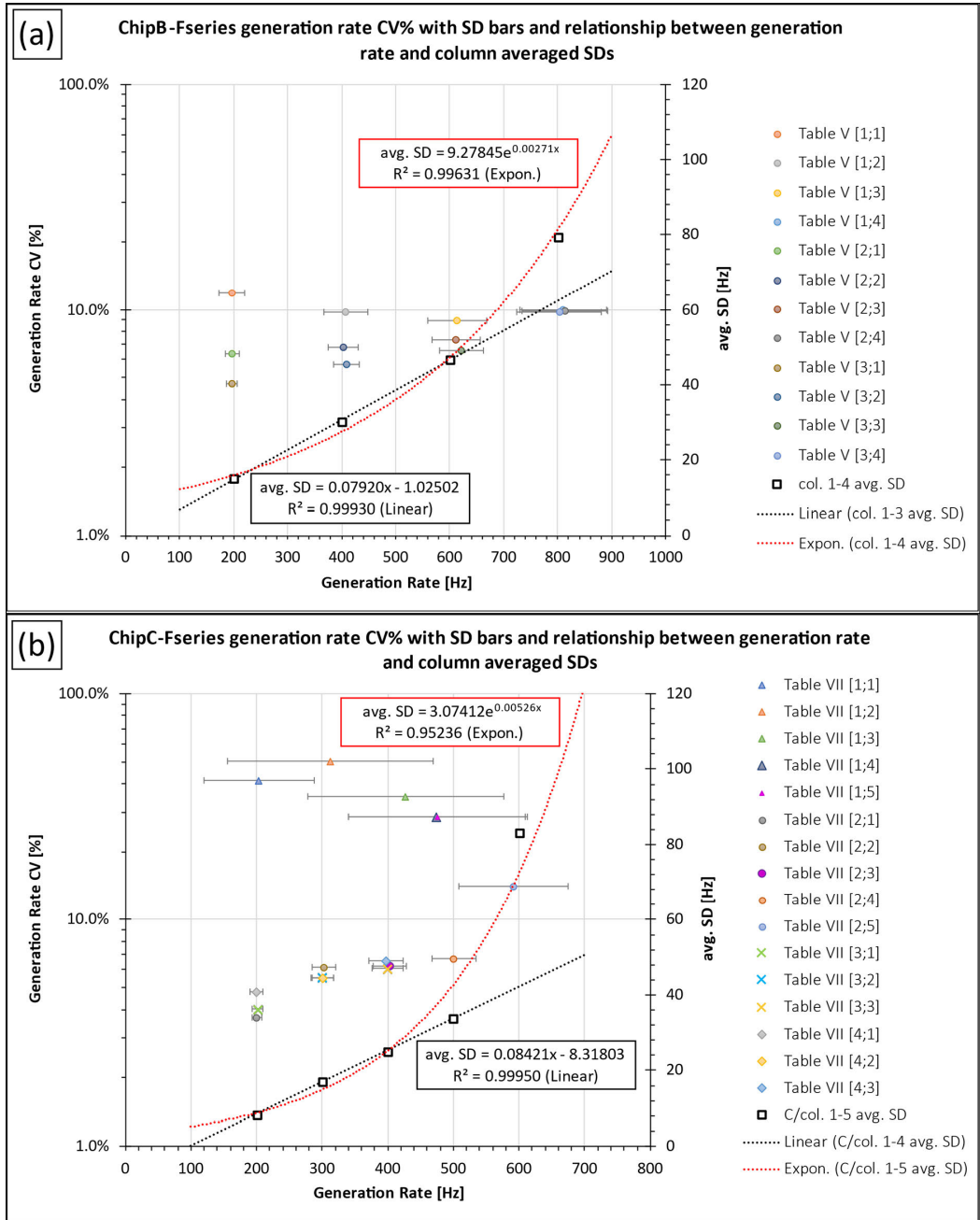
FIGURE 27. Results from Section IV-B-II. Quantitative analysis of F series data. a) Droplet generation rate CV%, from droplet size and rate combinations in TABLE 5, plotted against averaged generation rate, calculated over the stabilized generation period. TABLE 5 column (col.) averaged SDs (from target rate columns 1 to 4 and target size rows 1 to 3) plotted against column target generation rates together with a corresponding exponential regression line. Col. avg. SDs were cropped to columns 1 to 3 to highlight the highly linear correlation region; b) Droplet generation rate CV%, from droplet size and rate combinations in TABLE 7, plotted against averaged generation rate, calculated over the stabilized generation period. TABLE 7 column conditionally (C/col.) averaged SDs (from target rate columns 1 to 5 and target size rows 2 to 4 – row 1 conditionally excluded due to indicating a different mode of operation, see ESI S4 for details) plotted against column target generation rates together with a corresponding exponential regression line. C/col. avg. SDs were cropped to columns 1 to 4 to highlight the highly linear correlation region.
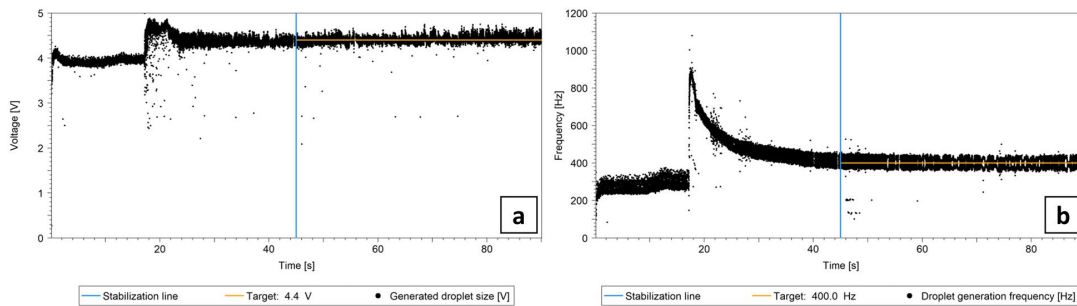
FIGURE 28. Results from Section IV-B-II. a) Droplet size target data set from a combination of [4.4 V; 400 Hz] with chip B. Stabilization period 45 seconds which includes an initial 15 seconds of default initiation period. Stabilization and stable segments are separated by blue vertical line. Target size in voltage is shown with an overlayed horizontal line; b) Droplet generation rate target data set from a combination of [4.4 V; 400 Hz] with chip B. Stabilization period 45 seconds which includes an initial 15 seconds of default initiation period. Stabilization and stable segments are separated by blue vertical line. Target size in voltage is shown with an overlayed horizontal line.
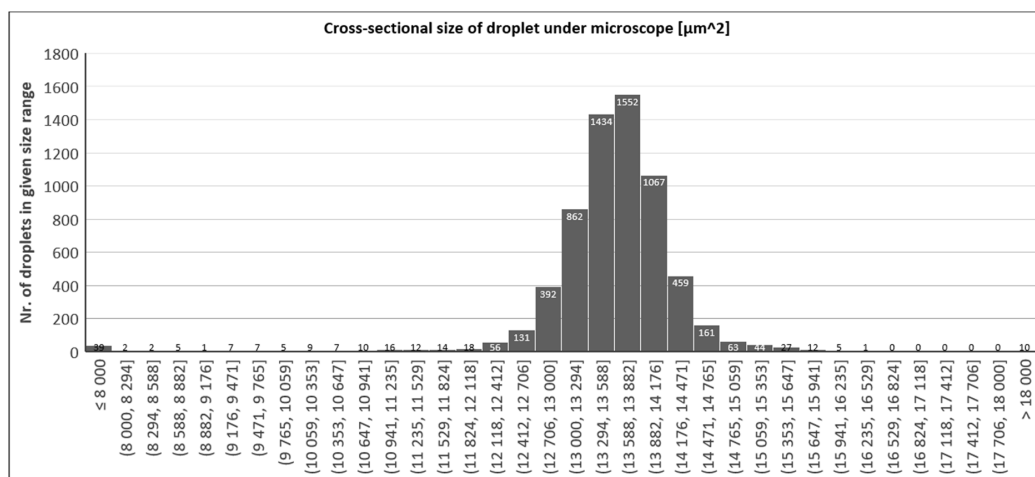

FIGURE 29. Droplet cross-sectional size spread from a droplet generation sample, generated with fixed water and oil pressure of 9 kPa and 12 kPa respectively. 6429 droplets measured over 11 images with ImageJ software.

droplet generation rate CVs represented on Fig. 26/b. Medians of averaged CVs from Fig. 26/a, [6.83; 6.33; 5.78; 6.84] %, respectively, showed that while the measured droplet sizes in tests with chip C were off noticeably more than with chip B, the size stability can be better. However, minimum CVs [3.10; 3.30; 4.40; 3.60] % showed favorability towards chip B. While some maximum CVs reached over 10%, more significant reasons for the larger instabilities stemmed from the chosen pressure combinations working less favorably with chosen chip geometries. From the averaged droplet generation rate results on Fig. 26/b, the difference between chip B and C was hard to mistake. As the CVs between size and rate for chip C, have a noticeable difference in scale, it was evident that the generation frequency of droplets does not inherently link to droplet size in a pulsatile pressure-based pumping system.

Further analysis of target F series provided relationships between the generation rate to generation rate CVs at each obtained average frequency level with standard deviation

(SD) bars and between the target generation rate to column averaged SDs (SD averaging for chip C was done conditionally, further explained in ESI S4), for chips B and C respectively on Fig. 27/a and Fig. 27/b (numeric details in ESI S4, TABLE 1-4). Generation rate CVs for chip C revealed behavioral outliers with target size and rate combinations in row 1 of TABLE 7 (while producing droplets in a stable manner with size CVs < 10%, the frequency CVs were well above 25%). By omitting the TABLE 7 row 1 CVs and SDs from comparison between chip variants, the general rule of increasing SD with increasing generation rate becomes noticeable. By having excluded row 1 SDs also from averaging of SDs, chip B and C generation rate averaged SDs ($\overline{SD}$) showed analogous trends. Both show the highest correlation to exponential relationships. Additionally, for both chip types, cropped $\overline{SD}$s revealed high linear correlation regions up to the second highest tested respective generation rate targets (Fig. 27) which in terms of generation rates would narrow down on the stable frequency region of use for that specific
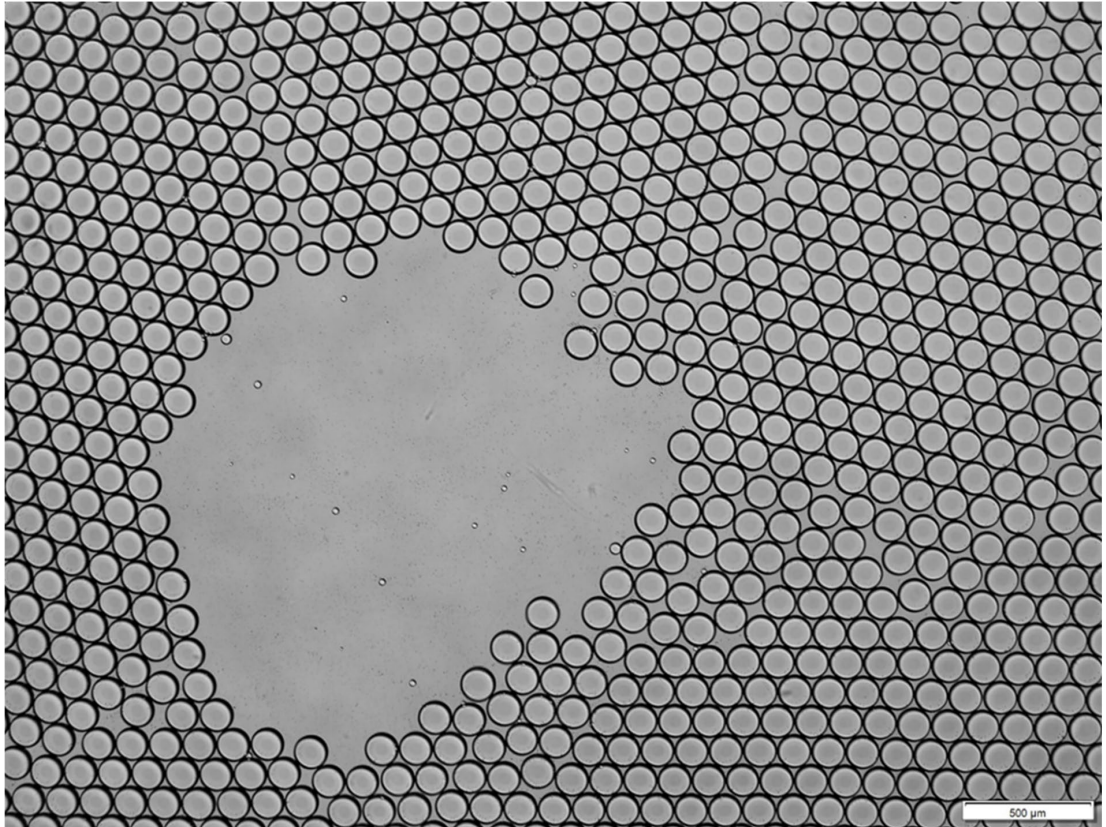
FIGURE 30. Droplets generated with chip design B with fixed water and oil pressures of 9 kPa and 12 kPa respectively, pumped using pressure-based piezoelectric micropumps, viewed under microscope (4x/0.16 lens).

chip geometry and fluidic phase combination. Between the observed initial and cropped data, beyond a certain generation rate, the behavior of frequency stability deteriorates from linear into exponential regime. The possible causes of which could be 1) stability limits, inherited from FFD channel design in combination with pulsatile flow and fluid phase properties, 2) hardware and/or software limits, RPI's droplet interpretation loop delays introducing increasing number of erroneous readings.

b: DROPLET SIZE DATA (PD VOLTAGE DISCRETIZED WITH THE ADC) FROM SINGLE SHOT DROPLET SIZE AND FREQUENCY TARGETS

Using chip B with different calibration (chip position slightly tilted in the light tower), one of the better examples with lowest target error in combination with the lowest droplet size CV (400 Hz, 4.4 V) achieved, can be seen on Fig. 28 with graphed droplet sizes and generation rates respectively. From the size dataset on Fig. 28/a, the CV% was calculated to be 1.77% with a percentage error from target droplet size of +0.27%. From frequency dataset on Fig. 28/b, the CV% was

calculated to be 6.67% with a percentage error from target droplet generation rate of +0.22%.

c: DROPLET SIZE DATA (MICROSCOPE CAMERA ➔ IMAGEJ) FROM SINGLE SHOT PRESSURE TARGETS

Droplets were collected from tests with droplet feedback PIDs disabled to obtain a baseline. Tests were done with fixed water pressure at 9 kPa and several oil pressure targets in the range of 9 kPa – 12 kPa, ran over 90 seconds, where oil pressure at 12 kPa yielded the best results with 7.7% CV, with a spread of cross-sectional areas shown on Fig. 29. Average cross-sectional surface area of recorded droplets was measured 13 558.9 μm^2, translating into an average planar diameter of 131.4 μm when droplets were flattened in the imaging slide. A sample from a series of images taken of droplets in the droplet imaging slide can be seen on Fig. 30.

V. FUTURE PERSPECTIVE
One of the core principles of the CogniFlow-Drop system is modularity. This modularity opens the way to various future upgrades: use-cases enabled by additional modules

(Section V-A), as well as possible upgrades to the core modules (Section V-B).

A. APPLICATION USE CASES

- Inline imaging cytometry: The addition of a high-speed camera/detection module (and ideally a cell incubation module) could enable inline imaging cytometry.
- Cell sorting: The addition of a droplet sorting module, together with the aforementioned imaging cytometry modules, could enable droplet-based cell sorting for further downstream processing of select cells or cell lines. The single-cell resolution and chemical isolation provided by droplets could greatly increase the throughput, while reducing reagent and sample waste compared to current state-of-the-art flow cytometry setups.

B. POSSIBLE UPGRADES TO THE PROTOTYPE SYSTEM

- To improve the droplet capture rate and reliability, an additional ESP32, or a similar low-cost device with an SPI bus and two cores, could be placed between the RPI and ADC to take over task 3 from the RPI. Additionally, the added computational power could enable more complex waveform analysis (e.g., waveform slope measurement and droplet lensing effect detection).
- To improve the droplet size and generation frequency control accuracy and fault tolerance, machine learning models could be implemented on the RPI.
- To improve automation, the following features could contribute: self-priming, self-cleaning, auto-chip-positioner, auto-pinhole-positioner, self-analyzing (e.g., detection of blockages or leaks in the fluidics module), auto-focusing, and auto-calibration-ranging.
- To improve the user interface, the GUI, after calibration, could offer feasible droplet size and generation frequency ranges, with highlighted combinations yielding the best CV% for that specific chip and position. Furthermore, by user request, the GUI could poll captured waveform samples during operation.
- To correlate relatively inexpensively and rapidly measured droplet sizes from their shadows to real droplet volume, a secondary in-line camera setup could be joined in the communication line over eCAL. To image droplets, as proposed in Section V-A, during cytometry.

VI. CONCLUSION

A proof-of-concept prototype of an integrated, modular system for automated aqueous droplet generation with high monodispersity was presented. The system measured droplet sizes and generation rates using a visible spectrum LED-photodiode setup aligned with the cross-junction of the FFD, converting the droplet's shadow to voltage. Resulting peak-to-peak voltages were correlated with relative size of the droplet whereas the time between the beginnings of droplets were used to obtain the generation rate. We reported on the assembly and the underlying working principle, as well as the experimental evaluation of the performance of the prototype,

both on a module level and system level. Module-level evaluation and comparison to reference syringe pumps indicated a 12 times reduction in pressure stabilization times. The system-level evaluation proved that the system was capable of repeatedly generating droplets with stability comparable to other state-of-the-art droplet generation systems. Droplet generation stability was proven over 2 different carrier media and 3 different junction geometries in total. The lowest relative droplet size CV% recorded was 1.77% ($\sim$0.00031 PDI) using Chip B with fluid phase combination B. With droplets controllably generated in tested relative size targets between 2.0 to 4.4 V, polydisperse (PDI > 0.1) droplets with a stable size distribution can also be generated. Unique characteristics from relationships between droplet size/generation rate and chip geometry were made observable through automated calibration and parameter target test series with different chips. Conditional droplet generation rate analysis also revealed high linear correlation regions for the "SD of the generation rate" with the "target rate" for chips B and C, from 200 Hz up to 600 Hz and 500 Hz respectively. In conclusion, the presented prototype system has comparable droplet generation performance metrics to other state-of-the-art droplet generation setups, but offers several advantages: 1) modularity, integration, wireless communication and the option to run from battery power, enabling portability; 2) affordability; 3) automation and ease of use, increasing repeatability of results and allowing transfer of protocols between labs, as well as reducing manual workloads; 4) user-friendly (re-)calibration of chip alignment.

REFERENCES

[1] T. S. Kaminski, O. Scheler, and P. Garstecki, "Droplet microfluidics for microbiology: Techniques, applications and challenges," *Lab Chip*, vol. 16, no. 12, pp. 2168–2187, 2016, doi: 10.1039/C6LC00367B.

[2] W. Postek, P. Gargulinski, O. Scheler, T. S. Kaminski, and P. Garstecki, "Microfluidic screening of antibiotic susceptibility at a single-cell level shows the inoculum effect of cefotaxime on E. coli," *Lab Chip*, vol. 18, no. 23, pp. 3668–3677, 2018, doi: 10.1039/C8LC00916C.

[3] O. Scheler, K. Makuch, P. R. Debski, M. Horka, A. Ruszczak, N. Pacocha, K. Sozański, O.-P. Smolander, W. Postek, and P. Garstecki, "Droplet-based digital antibiotic susceptibility screen reveals single-cell clonal heteroresistance in an isogenic bacterial population," *Sci. Rep.*, vol. 10, no. 1, p. 3282, Feb. 2020, doi: 10.1038/s41598-020-60381-z.

[4] K. Pärnamets, T. Pardy, A. Koel, T. Rang, O. Scheler, Y. Le Moullec, and F. Afrin, "Optical detection methods for high-throughput fluorescent droplet microflow cytometry," *Micromachines*, vol. 12, no. 3, p. 345, Mar. 2021, doi: 10.3390/mi12030345.

[5] M. Li, H. Liu, S. Zhuang, and K. Goda, "Droplet flow cytometry for single-cell analysis," *RSC Adv.*, vol. 11, no. 34, pp. 20944–20960, Jun. 2021, doi: 10.1039/D1RA02636D.

[6] Y. Ding, P. D. Howes, and A. J. Demello, "Recent advances in droplet microfluidics," *Anal. Chem.*, vol. 92, no. 1, pp. 132–149, Jan. 2020, doi: 10.1021/acs.analchem.9b05047.

[7] S. Stavrakis, G. Holzner, J. Choo, and A. de Mello, "High-throughput microfluidic imaging flow cytometry," *Current Opinion Biotechnol.*, vol. 55, pp. 36–43, Feb. 2019, doi: 10.1016/j.copbio.2018.08.002.

[8] C. Cha, J. Oh, K. Kim, Y. Qiu, M. Joh, S. R. Shin, X. Wang, G. Camci-Unal, K.-T. Wan, R. Liao, and A. Khademhosseini, "Microfluidics-assisted fabrication of gelatin-silica core–shell microgels for injectable tissue constructs," *Biomacromolecules*, vol. 15, no. 1, pp. 283–290, Jan. 2014, doi: 10.1021/BM401533Y.

[9] R. Samanipour, Z. Wang, A. Ahmadi, and K. Kim, "Experimental and computational study of microfluidic flow-focusing generation of gelatin methacrylate hydrogel droplets," *J. Appl. Polym. Sci.*, vol. 133, no. 29, pp. 1-10, Aug. 2016, doi: 10.1002/APP.43701.

[10] W. Zeng, H. Fu, and S Li, "Characterization of the pressure-driven flows for droplet microfluidics," in *Proc. CSAA/IET Int. Conf. Aircr. Utility Syst. (AUS)*, Jun. 2018, pp. 309–313, doi: 10.1049/cp.2018.0090.

[11] W. Zeng, S Yang, Y. Liu, T. Yang, Z. Tong, X. Shan, and H. Fu, "Precise monodisperse droplet generation by pressure-driven microfluidic flows," *Chem. Eng. Sci.*, vol. 248, Feb. 2022, Art. no. 117206, doi: 10.1016/J.CES.2021.117206.

[12] X. Duan, Z. Zheng, Y. Luo, and C. Song, "Closed-loop feedback control for droplet-based microfluidics: A characteristic investigation on passive and on-demand droplet generation," *Proc. SPIE*, vol. 12550, pp. 183–188, Jan. 2023, doi: 10.1117/12.2666602.

[13] W. Zeng and H. Fu, "Precise monodisperse droplet production in a flow-focusing microdroplet generator," *Chem. Eng. Res. Des.*, vol. 160, pp. 321–325, Aug. 2020, doi: 10.1016/J.CHERD.2020.06.002.

[14] N. Wang, R. Liu, N. Asmare, C.-H. Chu, O. Civelekoglu, and A. F. Sarioglu, "Closed-loop feedback control of microfluidic cell manipulation via deep-learning integrated sensor networks," *Lab Chip*, vol. 21, no. 10, pp. 1916–1928, 2021, doi: 10.1039/d1lc00076d.

[15] E.-C. Yeh, C.-C. Fu, L. Hu, R. Thakur, J. Feng, and L. P. Lee, "Self-powered integrated microfluidic point-of-care low-cost enabling (SIMPLE) chip," *Sci. Adv.*, vol. 3, no. 3, Mar. 2017, Art. no. e1501645, doi: 10.1126/sciadv.1501645.

[16] D. F. Crawford, C. A. Smith, and G. Whyte, "Image-based closed-loop feedback for highly mono-dispersed microdroplet production," *Sci. Rep.*, vol. 7, no. 1, pp. 1–9, Sep. 2017, doi: 10.1038/s41598-017-11254-5.

[17] B. Miller, "Manipulation of microfluidic droplets," U.S. Patent EP2 411 148 B1, Mar. 23, 2010.

[18] B. van Elburg, G. Collado-Lara, G.-W. Bruggert, T. Segers, M. Versluis, and G. Lajoinie, "Feedback-controlled microbubble generator producing one million monodisperse bubbles per second," *Rev. Sci. Instrum.*, vol. 92, no. 3, Mar. 2021, Art. no. 035110, doi: 10.1063/5.0032140.

[19] N. Gyimah, O. Scheler, T. Rang, and T. Pardy, "Can 3D printing bring droplet microfluidics to every lab?—A systematic review," *Micromachines*, vol. 12, no. 3, p. 339, Mar. 2021, doi: 10.3390/mi12030339.

[20] TalTech-LoC. *HW-Open-Fluidic-Infra*. Accessed: May 16, 2023. [Online]. Available: https://github.com/taltechloc/hw-open-fluidic-infra

[21] N. Gyimah, O. Scheler, T. Rang, and T. Pardy, "Digital twin for controlled generation of water-in-oil microdroplets with required size," in *Proc. 23rd Int. Conf. Thermal, Mech. Multi-Phys. Simul. Experiments Microelectron. Microsystems (EuroSimE)*, Apr. 2022, pp. 1–7, doi: 10.1109/EuroSimE54907.2022.9758876.

[22] N. Gyimah, R. Joemaa, K. Parnamets, O. Scheler, T. Rang, and T. Pardy, "PID controller tuning optimization using genetic algorithm for droplet size control in microfluidics," in *Proc. 18th Biennial Baltic Electron. Conf. (BEC)*, Oct. 2022, pp. 1–6, doi: 10.1109/BEC56180.2022.9935596.

[23] R. Joemaa, M. Grosberg, T. Rang, and T. Pardy, "Low-cost, portable dual-channel pressure pump for droplet microfluidics," in *Proc. 45th Jubilee Int. Conv. Inf., Commun. Electron. Technol. (MIPRO)*, May 2022, pp. 205–211, doi: 10.23919/MIPRO55190.2022.9803371.

[24] M. Grosberg, R. Jõemaa, P. Tamas, and T. Rang. (2022). *Wireless Microfluidic Dual-Channel Pressure Pump*. [Online]. Available: https://www.etis.ee/Portal/IndustrialProperties/Display/353426b9-f02b-44b2-b581-e8f21363157a

[25] K. Ashraf, Y. L. Moullec, T. Pardy, and T. Rang, "Model-based system architecture for event-triggered wireless control of bio-analytical devices," in *Proc. 24th Euromicro Conf. Digit. Syst. Design (DSD)*, Sep. 2021, pp. 465–471, doi: 10.1109/DSD53832.2021.00076.

[26] Alphabet. (2022). *Protocol Buffers | Google Developers*. Accessed: Oct. 31, 2022. [Online]. Available: https://developers.google.com/protocol-buffers/docs/reference/overview

[27] Eclipse. (2022). *Welcome to Eclipse eCALTM—Eclipse eCALTM Documentation*. Accessed: Oct. 31, 2022. [Online]. Available: https://eclipse-ecal.github.io/ecal/

[28] K. Parnamets, A. Koel, T. Pardy, and T. Rang, "Open source hardware cost-effective imaging sensors for high-throughput droplet microfluidic systems," in *Proc. 26th Int. Conf. Electron.*, Jun. 2022, pp. 1–6, doi: 10.1109/IEEECONF55059.2022.9810383.

[29] N. A. Prabatama, R. Joemaa, K. Hegedus, and T. Pardy, "Low-cost open-source flow velocity sensor for droplet generators," in *Proc. 18th Biennial Baltic Electron. Conf. (BEC)*, Oct. 2022, pp. 1–4, doi: 10.1109/BEC56180.2022.9935606.

[30] J. Caldwell. (2014). *An IMPORTANT NOTICE at the End of This TI Reference Design Addresses Authorized Use, Intellectual Property Matters and Other Important Disclaimers and Information*. Accessed: May 12, 2023. [Online]. Available: www.ti.com

[31] O. Scheler, T. S. Kaminski, A. Ruszczak, and P. Garstecki, "Dodecylresorufin (C12R) outperforms resorufin in microdroplet bacterial assays," *ACS Appl. Mater. Interfaces*, vol. 8, no. 18, pp. 11318–11325, May 2016, doi: 10.1021/acsami.6b02360.

[32] TalTech-LoC. (2020). *HW-MVP-Chip*. Accessed: Sep. 21, 2022. [Online]. Available: https://github.com/taltechloc/hw-mvp-chip

[33] (2022). *BioMEMS Group*. Accessed: Oct. 31, 2022. [Online]. Available: https://biomems.hu/

[34] W. Zeng, S. Li, and Z. Wang, "Closed-loop feedback control of droplet formation in a T-junction microdroplet generator," *Sens. Actuators A, Phys.*, vol. 233, pp. 542–547, Sep. 2015, doi: 10.1016/j.sna.2015.08.002.

[35] Y. Xie, A. J. Dixon, J. M. R. Rickel, A. L. Klibanov, and J. A. Hossack, "Closed-loop feedback control of microbubble diameter from a flow-focusing microfluidic device," *Biomicrofluidics*, vol. 14, no. 3, May 2020, Art. no. 034101, doi: 10.1063/5.0005205.

[36] S. Motaghi, M. Nazari, N. Sepehri, and A. Mahdavi, "Control of droplet size in a two-phase microchannel using PID controller: A novel experimental study," *Amirkabir J. Mech. Eng. Amirkabir J. Mech. Eng*, vol. 53, no. 7, pp. 1013–1016, 2021, doi: 10.22060/mej.2020.18250.6783.

[37] H. Fu, W. Zeng, S. Li, and S. Yuan, "Electrical-detection droplet microfluidic closed-loop control system for precise droplet production," *Sens. Actuators A, Phys.*, vol. 267, pp. 142–149, Nov. 2017, doi: 10.1016/j.sna.2017.09.043.
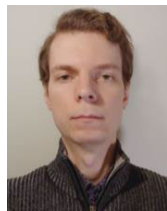
RAUNO JÕEMAA was born in Estonia, in 1991. He received the bachelor's degree in electronics and bionics and the master's degree in communicative electronics from the Tallinn University of Technology, where he is currently pursuing the Ph.D. degree with the Thomas Johann Seebeck Department of Electronics. He is a Junior Researcher with the Department of Chemistry and Biotechnologies, Tallinn University of Technology. His current research interests include electronics and microfluidics.
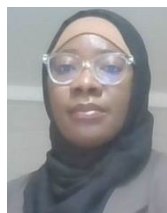
NAFISAT GYIMAH received the B.S. degree in electrical and electronic engineering from the Kwame Nkrumah University of Technology, Kumasi, Ghana, in 2013, and the M.S. degree in communicative electronics from the Tallinn University of Technology, Tallinn, Estonia, in 2020, where she is currently pursuing the Ph.D. degree in high-speed droplet microfluidics sorting and encapsulation. From November 2021 to January 2022, she was with SelfDiagnostics Deutschland GmbH, where she focused on the thermal and electrical characterization of SARS-CoV2 microfluidic multitest kits. She was a Cognitronics Engineer with the Tallinn University of Technology, from June 2020 to December 2020. Her current research interests include lab-on-a-chip, droplet microfluidic system control, and flow control simulations using computational fluid dynamics (CFD).

KANWAL ASHRAF received the bachelor's degree in electrical engineering from the University of the Punjab, Pakistan, and the joint-international master's degree in smart system integration from Heriot-Watt University, U.K., the University of South-Eastern Norway (USN), Norway, and the Budapest University of Technology and Economics (BME), Hungary, in 2020. She is currently pursuing the Ph.D. degree with the Tallinn University of Technology, Estonia. Her current research interests include the application of wireless communication in CPSs and the co-design of wireless networked control systems for bioanalytical applications.
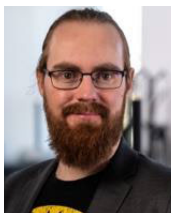
KAISER PÄRNAMETS (Member, IEEE) was born in Tallinn, Estonia, in January 1989. He received the B.Sc. and M.Sc. degrees in engineering from the Tallinn University of Technology, in 2013 and 2016, respectively, where he is currently pursuing the Ph.D. degree. From 2014 to 2017, he was a hardware engineer in the electronics industry and has been an electronics lecturer for bachelor's and master's students, since 2018. His current research interests include lab-on-a-chip and microfluidics.

ALEXANDER ZAFT was born in 1997. He received the bachelor's and master's degrees in computer science from the University of Würzburg, Germany, in 2019 and 2022, respectively. In Summer 2022, he joined the Lab-on-a-Chip Group, Tallinn University of Technology, as an Intern. Since November 2022, he has been a Software Engineer with Heinz-Maier-Leibnitz Zentrum, Garching, Germany.

OTT SCHELER received the Ph.D. degree in biotechnology from the University of Tartu, Estonia, in 2012. He was a Postdoctoral Researcher of microfluidics with the Institute of Physical Chemistry, Polish Academy of Sciences, from 2014 to 2018. After that, he joined the Tallinn University of Technology, where he is currently an Associate Professor of microfluidics with the Department of Chemistry and Biotechnology. His current research interests include microfluidics, microbiology, and biotechnology.

TOOMAS RANG (Senior Member, IEEE) received the Ph.D. degree in semiconductor electronics from the Hungarian Academy of Sciences, in 1981. He is currently a Professor Emeritus with the Thomas Johann Seebeck Department of Electronics and a Senior Research Fellow with the Department of Chemistry and Biotechnologies, Tallinn University of Technology, Estonia. He has supervised 15 Ph.D. students and has fulfilled the PI position in several European and domestic research and industrial projects. His current research interest includes applied microfluidics approaches for lab-on-chip applications. He is the Initiator and today the honor Chairperson of the Baltic Electronics Conference (BEC) Series, in 1987, supported by IEEE, since 1996.

TAMÁS PARDY (Member, IEEE) received the M.Sc. degree in info-bionics engineering from Peter Pazmany Catholic University, Budapest, Hungary, in 2014, and the Ph.D. degree in electronics and telecommunication from the Tallinn University of Technology, Tallinn, Estonia, in 2018. He is currently a Senior Researcher with the Tallinn University of Technology. He has supervised one Ph.D. thesis and five M.Sc. thesis and has authored or coauthored over 20 scientific publications. His current research interest includes flow- and temperature control of lab-on-a-chip devices.

• • •

Supplementary material

Systematic Literature Review on Wireless Communication for Point-of-Care Monitoring and Diagnostic Devices

(Unpublished Work)

Kanwal Ashraf, 2021

Wireless Communication for Point-of-Care Monitoring and Diagnostic Devices

Kanwal Ashraf

IE - Thomas Johann Seebeck Department of Electronics
School Of Information Technologies
Tallinn University of Technology, 12616 Tallinn, Estonia

Abstract:

Objective: In this article, systematic literature review for the application of Wireless Communication in Point-of-Care monitoring and diagnostic Devices is presented. The major aim is to identify the commonly used communication technologies, research gaps associated with different technologies and reasons associated with their implementation in Point-of-Care devices.

Method: The search methodology used for this literature review was based on the Search, Appraisal, Synthesis and Analysis (SALSA) Framework employing a search on IEEEXplore, Google Scholar, Scopus, Web of Science, PubMed, and Cochrane Library.

Results: An initial screening narrowed-down the number of relevant papers to 116; among these, 39 documents were selected, categorized as 23 documents for short-range wireless communication technologies and 16 for long-range wireless communication technologies. Among them, 13 documents showed the use of Wireless communication in Point-of-Care diagnostic devices. However Only 4 papers analyzed the performance and effectiveness of wireless communication specifically applied in Point-of-Care diagnostic devices.

Conclusion: The review showed the limited use of wireless communication in Point-of-Care diagnostic devices despite the benefits associated with it. Although the practice is emerging it is limited to only a few technologies with no significant performance evaluation of the device. Due to lack of research in the field, the possible drawbacks of the applications are in some cases are also being ignored. Thus, given the promising potential of exploiting wireless communication in novel Point-of-Care diagnostic devices, further research in this field is much desired.

Index Terms: Wireless Communication, Point-of-Care Devices, Short-Range Wireless Communication, Long Range Wireless Communication

1. Introduction

With emerging diseases across the world, Point-of-Care (POC) devices have proven to be a robust, cost-effective and efficient monitoring and diagnostic tool [1], [2], [3]. Microfluidics [4] has proven to be a powerful analytical tool in Point-of-Care (POC) devices for molecular diagnostics. Microfluidics helps to reduce the amount of resources required for testing and hence the cost of the test also reduces.

An immense amount of research has been carried out in the past few decades which has transformed the microfluidics field [5] to enable small volume analysis, which led to droplet microfluidics. Droplet microfluidics has enabled the analysis of bacteria on the single-cell level, which has proven to be an extremely useful tool in diagnostics and research e.g. for estimation of bacteria resistance against different drugs and in various concentration [6], [7], [8].

Despite the enormous research carried out to enhance the performance of the POC devices there are a lot of challenges [9] still associated with them, which includes miniaturization and integration of the device, power consumption, accuracy, reliability as well as data acquisition and interpretation using electronic circuitry. Another major challenge is the communication of the exam-

ination results to the central unit for test result interpretation and monitoring. The communication of the examination results to the emergency or health care unit is vital to ensure the viability of POC devices in remote areas or emergencies. This leads to the implementation of wireless communication methods [10], [11], [12], [13], [14], [15], [16], [17], [18], [19], [20], [21] for the data exchange as wired connectivity will severely limit the operation of the devices.

Currently, there are several long-range [16] and short-range [10] wireless communication techniques available which differ based on data rate, range, power consumption, operating frequency range, modulation scheme, security and reliability. Several types of research have focused on the application of communication technologies in the healthcare sector. The survey [22] showed a comprehensive overview of cellular and non-cellular communication technologies for body-oriented applications. However, in body-oriented health care devices, the power consumption, range of connectivity (intra-BAN $\sim$3 m [23]) and data rate required ($\sim$ 1.6 kbps [22]) are different as compared with portable POC diagnostic devices. Another research [24] was focused on short-range wireless communication technologies for Health Information exchange. However, the review lacks a few of the most effective short-range communication technologies like Zigbee and also does not evaluates the use of important long-range communication techniques.

As compared with the mentioned reviews, this systematic literature review paper address the following major research questions:

- **Q1**: Identify the use of some of the major short-range wireless communication techniques including *Zigbee, Bluetooth/BLE, Ultra-Wide-Band (UWB), WiFi, RFID/NFC, ANT/ANT+, WirelessHART, 6LowPAN, Z-wave, DASH7, IrDa* and long-range wireless communication techniques including *SigFoX, LoraWAN, NB-IoT, Wi-SUN* and *LTE-CAT-M1* for POC monitoring and diagnostic devices dated over the last 6 years and provide an overview of different key performance parameters.
- **Q2**: Identify research gaps associated with each mentioned wireless communication technology for its implementation for portable POC diagnostic devices.
- **Q3**: Provide a comparative analysis for selecting the best technique specifically for portable POC diagnostic/Analytical devices based on benefits and research gaps identified through research.

The major key parameters used for the comparative analysis of the selected communication technologies include data-rate, range, power consumption, security, reliability and scalability. The review paper also identifies different key challenges associated with each of the technologies for its deployment in POC diagnostic devices.

The paper is organized as follows. *Section 2* defines the methodology used for this review, Section 3 presents the overview of the wireless technologies and their use in different POC devices in the past 6 years, *Section 4* discusses the use of different wireless communication technologies specifically for POC diagnostic devices and highlights the major challenges associated with each and *Section 5* concludes this paper by proposing the best technique available for POC diagnostic devices and addressing the research gaps present for its deployment in the field.

2. Methodology

As mentioned earlier, this systematic literature review focuses on the research carried out over the past 6 years, the reason behind this is to have updated research methodologies and results. To perform the systematic research, the methodology employed was based on the *Search, Appraisal, Synthesis and Analysis (SALSA)* Framework [25].

2.1. Search

During the search phase, different keywords were created based on the research questions, such as *"Point-of-care", "wireless"* and *"wireless communication"*. Table I gives an overview of some of the search strings used in different search engines and the percentage of results

including wireless communication as keyword. The search engine used included **IEEEXplore, Google Scholar, Cochrane Library, PubMed, Scopus** and **Web of Science** because of the access to enormous resources, advanced search tools and relevance of the resources with the targeted field.

Depending upon the number of results obtained using the initial search string, the total number of documents found on all the search engines related to point-of-care or point-of-care testing devices were around **72000**. Among these documents, the documents stating wireless communication were around **12000**. The major source of these results was **Google scholar** with **9900** articles which included wireless keyword.

TABLE I: Search Strings

Search Engine	Search String	Total Documents found for wireless communication	Percentage (Documents mentioning Wireless communication)
IEEEXplore	*(("All Metadata":point-of-care) AND "All Metadata":wireless), ((("Document Title":point-of-care) AND "Abstract":wireless) AND "Full Text Only":wireless), ("Document Title":point-of-care)*	27	6%
Google Scholar	*point of care testing OR "point-of-care", wireless "point of care testing" OR "point of care"*	~ 9900	$\sim 80\%$
Scopus	*TITLE-ABS-KEY (point-of-care) AND PUBYEAR >2014 , (TITLE-ABS-KEY (point-of-care test) AND TITLE-ABS-KEY (wireless)) AND PUBYEAR >2014*	357	$\sim 0.1\%$
Web of Science	*TS=(point-of-care testing) , TS=((point-of-care testing) AND "wireless") , TS=(Point-of-care testing) AND (AK=(point-of-care) OR KP=(microfluidics OR microfluidic)), TS=(Point-of-care testing) AND (AK=(wireless) OR KP=(wireless))*	8	$\sim 1\%$
PubMed	*(point-of-care test) AND (wireless)*	28	$\sim 2\%$
Cochrane Library	*"point of care test", "point of care test" AND "wireless"*	–	–

2.2. Appraisal

To identify the relevant document for search engines like **IEEEXplore, Scopus** etc. it was possible to look for the keywords in the abstract or other sections of the documents which assisted to further narrow down the results. While for **Google Scholar** different strategies were used. First one was to look for the keywords *"Wireless Communication" and "Point-of-Care" OR "Point-of-Care-testing"* in the title and restricting the search to last 6 years, the results were reduced to **13** but then few major articles were being excluded. A more efficient approach was to perform the search using search string based on the selected wireless communication technology like for Zigbee the search string used was **"Zigbee "point of care testing" OR "point of care""** but still for some technologies like Bluetooth the results were nearly **3000**. So the string was further restricted using AND operator e.g. **Bluetooth ("point of care testing" AND "point of care")**, still, the search results were around **750** which were further narrow-down by excluding reviews and surveys. Finally, a quick overview of the document was performed by going through the abstract and conclusion using inclusion and exclusion criteria.

The inclusion and exclusion criteria used for the screening of documents are as follow:

Inclusion

- Documents including a brief overview of wireless connectivity for discussed Point-of-Care device.
- Document including at least one short-range [10] or long-range wireless [16] communication

technology for point-of-care devices.

- Technical Specification documents defining the architecture or key parameters
- Documents identifying the research gaps for wireless connectivity of Point-of-Care devices and implying methods to improve them
- Documents proposing performance evaluation of wireless connectivity methods for Point-of-Care devices
- Documents (Books, Conference Papers, Journal Articles, view points, technical guide etc.) which are published in any language during 2015-2020

Exclusion

- Patents, reviews, tutorials and presentations were excluded
- Duplicate documents (Same article published in different journals)
- Documents focused on other perspectives of POC devices
- False results which interpreted keywords as different words like showing results for Proof-of-concept instead of Point-of-Care or showing results where Author's name matched the Keyword used for communication technique e.g. LoRa, ANT.

2.3. Synthesis

After this initial screening based on the criteria mentioned in ***Section 2.2*** around 116 relevant documents were obtained. The useful information like key performance parameters were extracted from these documents. The documents were characterized based on the wireless communication technology used.

2.4. Analysis

Based on the data extracted using the synthesis phase the documents were further narrowed down to 39 documents for comparative analysis by discarding the documents not giving in-depth technique implementation or poor quality papers. The final selection of documents included 16 documents for long-range and 23 for short-range wireless communication technologies. The distribution of the documents among different wireless technologies was analyzed which helped to identify which technology is most and least commonly used for POC devices. The research gaps and the most commonly considered parameter was analyzed which helped in formulating the results.

Section 3 gives a brief overview of the wireless communication technologies for creating basic understanding and its use in Point-of-care devices and summarizes the results obtained.

3. Wireless Communication Technologies

In this section, An overview of the use of selected short-range and long-range wireless communication techniques as mentioned in ***Section 1*** for POC devices for the past 6 years is presented. The key findings of this section are summarized in ***Table II*** and ***III*** showing the standard parameters, challenges and citing the selected research papers.

3.1. Short Range Wireless Technologies

3.1.1. Zigbee

Zigbee [10] is a low-power wireless communication technique which has a fairly high range as compared with other short-range wireless communication technologies including Bluetooth, BLE, NFC and RFID. Because of its higher range, it is employed in health care sensing applications [26], [27], [28] where low-data rates are required. The research [29] showed the use of Zigbee for portable surface stress biosensor test system due to its low-cost and low-power. However, the research did not focus on the performance evaluation of the technology for different environment scenarios.

Another work [30] focused on the implementation of the Zigbee communication module for a portable device used for determining the urea concentration to avoid urinary tract problems.

The research compared the power consumption of the module when working in wired configuration mode to wireless configuration mode, but the focus of the research was more towards to demonstrate the overall power consumption of the device. However, the research [31] which aimed to sense and monitor the human pH and glucose level evaluated the stability of the module at different transmission distances and found the range to be 70 m.

3.1.2. Radio-frequency Identification/Near Field Communication

Near Field Communication (NFC) is based on Radio-frequency Identification (RFID) technology which is used to carry out communication in the near field region. The range of NFC is less than 10 cm with a maximum of 426 Kbps data rate. NFC has found to be useful for several health sector applications especially in health management systems for medical data acquisition, disease diagnostics and patient care [32], [33]. Recently a lot of research has been carried out to use NFC in self-diagnostics devices.

The paper [34] discusses a cost-efficient, user-friendly NFC based strip for potassium level measurement in blood for early detection of heart and kidney diseases. The device uses autonomous sensing and identification grain which consists of High-frequency RFID chip to enable near field communication and antenna for transferring the data to the monitoring unit. The strip has no on-board power source and draw its energy from the NFC signal.

Another research [35] shows the use of NFC based Point-of-Care device for micro-nutrients analysis. The developed device uses NFC transceiver with a custom-designed antenna which was used to withdraw power from an NFC enabled phone. The test data was stored in EEPROM and was transmitted to the mobile unit for display. Cloud-based connectivity was provided using a mobile phone.

Most of the POC devices based on NFC are single-use and the data transmitted is simple. In addition to ease of use, the NFC has several issues associated with it the first and foremost is the range which is short as compared with other short-range wireless communication technologies. The data rate is also low, and the devices enabled using NFC usually withdraw a fair amount of power. As most applications using NFC utilizes phone for data acquisition security aspects also come into play with its use.

3.1.3. Bluetooth/BLE

Bluetooth or Low-Energy Bluetooth (BLE) is a powerful short-range wireless communication technology based on data rate and ease-of-use. The typical data rate in Bluetooth 5.0 is 2 Mbps and can be enhanced to 54 Mbps [10] on high-speed operation mode. Whereas BLE is low-energy operation mode for Bluetooth with low power consumption at the expense of data-rate.

Due to higher data rates, the Bluetooth has been beneficial in the transfer of medical data and records in many present health care devices. The paper [36] deliberates the use of Bluetooth as a wireless communication tool for paper-based Point-of-Care testing (POCT) device for the detection of neuron-specific enolase. An ARM-based STM32 microcontroller was used to control the operation of the entire device and was also responsible to save the result data which was later transferred to a cell phone unit via Bluetooth.

Another research [37] showed the use of Bluetooth for microfluidic amperometric analysis. The data processing and acquisition was implemented using an Arduino-based electronic system while the results were transferred via USB or Bluetooth which reduced the cost of the entire device.

A different research [38] is based on use cases of Bluetooth Low Energy (BLE) for health care devices. Regardless of low-cost, low-power consumption and higher data rate, Bluetooth has some major issues including range, high interference and security associated with it. These issues set the limit on the use of Bluetooth in medical devices which require a higher range or better security features.

Communication Technique	Data Rate	Range	Power Consumption	Network Topology	Security	Advantages	Challenges	References
Zigbee	250,40,20 kbps	10-75 m	Low	Star or peer-to-peer	128 bit Advanced Encryption Standard (AES)[39]	Fairly good range, low-cost, Low-power consumption, Network Scalability	less Secure, low data rate	[40], [29], [28], [30], [27], [26], [31], [10]
Bluetooth/BLE	1 Mbps, 54 Mbps (High speed operation)	10 m	Medium/Low	Master-slave, no fixed limit for LE	Enhanced Authentication (Security Mode 1 & 2)[41]	High data rate, low-cost, easy-to-use, low power consumption (BLE)	Short-range, less secure, high interference	[37], [36], [42], [38], [43], [10]
ANT+	60 kbps	30 m	Low	peer-to-peer, star, connected star, tree and fixed mesh topologies	8 byte Network Key,128-bit AES	scalability, Ultra-low power, ease-of-use, efficient	Low data-rate	[44], [45], [10]
UWB	110 Mbps[46]	150 m	Low	peer-to-peer	Extended Security Layer	High-resilience to Interference, High data-rate due to concurrent operation, low-cost, high data-rate	Antenna Design	[47], [48], [49], [10]
RFID\NFC	Proximity-coupling (106 kbps), Vicinity-coupling (27 kbps), 424 kbp(NFC)	max. 5m, <10 cm (NFC)	Low/Ultra-Low	Star or peer-to-peer	PIN controlled data access,Device Validation[50]	Low Power consumption, ease-of-use	Low data-rate, Less Secure, short range	[34], [35], [32], [33], [10]
WiFi	600-1800 Mbps[51]-(WiFi6)	50-150 m	medium	ad-hoc	WPA2-PSK	High data-rate, fairly good range, easy-to-use	High Interference, fairly higher power consumption, less secure	[52], [53], [43]
WirelessHART	250 kbps	100 m	Low	Self-organizing mesh	128-bit AES	Reliable, Secure	Low coverage	[54], [10]
6LoWPAN	250,40,20 kbps	10-200 m	Low	Star or simple 2-point routing	AES	low power consumption	short coverage	[10]
Z-Wave	9.6,40,100 kbps	max. 100 m	Low	peer-to-peer	128-bit AES, 128-bit zero temporary key, Single Network Wide Key	good resilience to interference	Low data-rate, high-power consumption, expensive	[10]
IrDa	2.4 kbps-1 Gbps[46]	10-30 m[46]	Low	peer-to-peer	–	High data rate, low power consumption, secure	not scalable, short-range, No device movement during transmission	[55]
DASH7	13,55,200 kbps	1-2 km	Ultra-Low	Tree or peer-to-peer	128-bit AES private key, crypto public key	low latency, Ultra-Low power consumption, secure & Cost-effective	Low Data Rate	[56], [57], [10]

TABLE II: Short-Range Wireless Communication Technologies for POC Devices

3.1.4. ANT/ANT+

ANT+ [10] is an ultra-low-power, short-range and scalable wireless network protocol used mainly for wearable devices. The maximum data rate achieved by this protocol is around 60 kbps and range is low but better than Bluetooth. The ultra-low-power consumption makes it extremely suitable for the health-care application. The work [44] demonstrated the software architecture design of health care Wireless Body Area Network (WBAN) for health monitoring applications using ANT+ protocol which acquires data from 3 different sensors. The same research was extended in 2016 and proposed architectural design of real-time data acquisition and storage [45] for health care wireless body area networks. To the best of author's knowledge, the ANT+ is not being used in any POC diagnostic device so far. The major benefit of using this technique in POC devices is the ultra-low power consumption but the main issue is the latency associated with ANT+ due to its low data-rate transfer capability which makes it less valuable for high data-rate applications.

3.1.5. Wi-Fi

Wi-Fi [58] is a widely used short-range scalable wireless communication technology because of its 50 folds higher data rate as compared with other Wireless Local Area Networks (WLANs). The higher data rate is due to the combination of Orthogonal Frequency Division Multiple Access (OFDMA) technique with Direct-Sequence Spread Spectrum (DSSS) modulation. Due to higher data rates, Wi-Fi is employed in several medical devices, Abbott's i-STAT POCT analyzer [52] is also based on Wi-Fi connectivity. In the last past few years, several researches [59], [53] showed the use of Wi-Fi as a powerful connectivity tool for e-health applications. The major focus of these researches was to use Wi-Fi as a connectivity tool however performance evaluation of Wi-Fi wasn't performed.

   Wi-Fi direct is the modified version of Wi-Fi with the capability of data-rates up-to 250 Mbps and higher range up to 200 m without the need of access point. However, Wi-Fi direct doesn't support multi-hop communication. The research [60] proposes the introduction of a routing layer to enable device communication in a group and multi-hop communication across the group.

3.1.6. Ultra-Wide Band(UWB)

Ultra-Wide Band (UWB) is a short-range wireless communication technology with minimum interference and lowest power consumption. Because of the multiple UWB [10], [12], [11] channels working concurrently the data rates are expected to exceed 500 Mbps in the future. UWB can co-exist with other wireless communication technologies unlike its competitors with higher data rates like Bluetooth and Wi-Fi which face interference issues.

   The research [47] has given a state-of-art of an overview of UWB use for Wireless Body Area Networks (WBANs) and challenges associated with its implementation in health care devices. The advantages of UWB in terms of power consumption, data-rates, immunity to fading and interference, simple hardware, low cost and time resolution were identified to be the major reasons to adopt this technology in the healthcare sector. The limitations including UWB antenna design and human body effect on the signal are the basic hurdle to adopt this technology in POCT and massive research is going on to overcome these challenges. In paper [49] the authors have elaborated the transmitter design for UWB communication for health care applications. The proposed design was able to achieve the data rate of 3.2 Mbps. Another research [48] focused on performance evaluation of UWB for node locations and density in the network.

3.1.7. WirelessHART, 6LowPAN , Z-wave, DASH7 and IrDa

Other short-range wireless technologies 6LowPAN [10], Z-wave [10], WirelessHART [54], [10], DASH7 [56], [57], [10] and IrDa [10] can also be used in health care devices for patient monitoring applications [46], [61]. However, the research has showed no present use of these technologies in point-of-care medical devices.

3.2. Long Range Wireless Communication Technologies

3.2.1. LoRaWan

LoRaWAN [62] is low-power and long-range communication technology based on asynchronous communication protocol ALOHA. Due to its low-power consumption and long-range, it is considered a suitable option for connected health care applications. The research [19] showed the use of LoRaWAN for e-health applications and evaluate the performance of the communication protocol for different indoor scenarios.

Another work [63] showed the use of LoRaWAN for health-care monitoring applications and the performance of the protocol was tested for different operating range. The research also gave a comparison of LoRaWAN with other short-range wireless technologies which showed that the power consumption of LoRaWAN is extremely less but this comparison should also take into consideration of low data rates of LoRaWAN which makes LoRaWAN almost inapplicable in high data-rate applications. The research [64] also illustrates the comparison of LoRaWAN with other short and long-range wireless technologies and describes the use of LoRaWAN for diagnostic applications (dip test for urinary infection).

3.2.2. NB-IoT

NB-IoT is a low power wide area network (LPWAN) which started under 4G/LTE and continues under 5G with enhanced security features [65], [66]. NB-IoT is suitable for long-range, low-power and low-data rate applications. Due to its long-range and additional security features the technology is being considered to be used for health care applications.

The research [67] showed the use of NB-IoT for drug infusion control, the introduction of an edge computing layer was proposed to reduce the major challenge of NB-IoT which is latency. The research also focused on current challenges present in NB-IoT including data loss, security and interference which are the main restrictions for use of this technology in health-care devices with higher data rate and low latency.

Few other types of research [68], [69] also focused on the use of NB-IoT for patient monitoring applications. However, there is still a lot of room present for research to solve current challenges in the NB-IoT sector before its useful deployment for Point-of-Care (POC) devices.

3.2.3. SigFox

SigFox [73], [18] is an Ultra-Narrow band communication method with data-rate between 100 to 600 kbps. SigFox's major benefits include excellent resilience to interference because of that it is being employed for several health-care applications. The studies [71], [74], [75] proposed the use of SigFox for personalized health-care devices.

3.2.4. LTE-CAT-M1 and Wi-SUN

LTE-CAT-M1 [74] and Wi-SUN [72] are other low-power long-range communication methods considered as a viable wireless communication tool for health care applications. To the author's best knowledge their implementation in rapid diagnostic POCT hasn't been performed yet.

4. Discussion

In this section, the key findings of this literature review have been summarized to answer the research questions. The first two research questions *Q1* and *Q2* are inter-linked as key performance parameters affect the research gaps associated with each technology. So, the suitable approach was to discuss them together whereas the third research question *Q3* was based on the first two research questions and is addressed separately. At the end of this section, the limitations associated with this review are also been discussed.

Communication Technique	Data Rate	Range	Power Consumption	Network Topology	Security Technique	Advantages	Challenges	References
LoRaWAN	0.3 kbps-50 kbps	~ 15-20 km	Low	Star	symmetric cryptography (128-bit network session key & 128-bit (AppSKey))	Low power consumption, good resilience to interference	Low data rate	[70], [64], [63], [19], [57]
Sigfox	~100 bps	~48 km-(rural-areas)	Low	Star	Advanced Encryption Standard (AES)	High range, good resilience to interference, low latency	Low data rate, less secure	[71], [57], [16]
NB-IoT	~50 kbps	<15 km	Low	star	TLS or BEST,L2TP or IPsec, MPLS	low power consumption, good range	Low-data rate, latency, poor mobility	[68], [69], [67], [16], [21]
LTE-CAT-M1	200-400 kbps	<11 m	Low	star	TLS or BEST, L2TP or IPsec, MPLS	low power consumption, low-cost, good coverage	latency, low data-rate	[16], [57]
Wi-SUN	~300 kbps	~ 4 km	Low	mesh	AES	High Range, low latency	Low Data Rate	[57], [72]

TABLE III: Long-Range Wireless Communication Technologies for POC Devices

4.1. Application of the Selected Wireless Technologies, Key Performance Parameters and Research Gaps

The search results showed that among the selected short-range and long-range wireless communication technologies Zigbee, Bluetooth/BLE, RFID/NFC, WiFi and LoRaWAN are the leading candidates based on their use in most of the wireless-enabled POC devices for both diagnostic and monitoring applications while NB-IoT is an emerging technology and its use is found to be considered. The key performance parameters found to be considered in the selected papers included range, power consumption, cost, ease of implementation and data-rate.

Bluetooth [10] was found to be the most commonly used wireless communication technology in wireless-enabled POC and wearable health care devices due to its ease of implementation and range required in applications. But the major problems associated with it included short-range, security and interference which leads to less reliable communication and makes it inadequate for wide health infrastructure. For conventional Bluetooth, power consumption is also an important issue to be considered. The major factors affecting its wide implementation in the devices was found to be the cost and ease of deployment.

RFID/NFC appeared to be used mostly in low-data rate disposable diagnostic devices as well as in some monitoring applications. The key factors noticed to influence the application of RFID/NFC were low-cost, short-range, low data-rate, low-power consumption or energy harvesting and disposal of the device. However, due to fairly low range and data-rate this technology cannot be used for wide health infrastructure or high data-rate applications.

WiFi implementation in POC devices was based on a higher range and higher data-rate which makes it suitable for many health applications [59], [53], [52]. However, the high interference and high-power consumption are the major challenges associated with it which require the performance

enhancement and evaluation of the technology.

Zigbee deployment was also found in both health diagnostic and monitoring applications [29], [28], [30], [27], [26], [31]. The major criteria for its performance evaluation and implementation were considered to be the range and low-power consumption. However, the technology [61] suffers reliability issues as compared with its competitor technology DASH7 which comparatively has better range.

LoRaWAN is used in health-monitoring applications [19], [63] due to its high range, high-resilience to interference and low-power consumption. For low data-rate diagnostic devices [64], its implementation has also found to be useful. The higher range and low-power consumption of LoRaWAN come at the expense of cost and low-data rate. The major performance evaluation criteria found in the literature for this technology is the range and resilience against the interference in different scenarios.

NB-IoT is found to be an emerging technology in the health care sector for low data-rate applications. However, the major challenges of latency are yet to be solved.

The other selected technologies **WirelessHART, UWB, DASH7, IrDa, 6LowPAN, ANT+, Sig-fox, Wi-SUN** and **LTE-CAT-M1** are not found to be commonly used technologies in the health sector. Some of them were found to be used in wearable devices or health monitoring applications but not considered for POC analytical and diagnostic devices. The probable reason could be due to the challenges associated with them as mentioned in **Section 3** or due to the lack of research in the area.

The use of these technologies also varied moving from Point-of-Care diagnostics to Point-of-Care monitoring devices. From the results section, it was found that the use of wireless technologies in diagnostic devices was only limited to the technologies summarized in **Table IV**.

TABLE IV: Wireless Communication Technologies in POC **Diagnostic** Devices

Communication Technique	References
Zigbee	[29], [28], [30]
Bluetooth\BLE	[37], [36], [42]
RFID\NFC	[34], [35]
WiFi	[52], [53], [43]
LoRaWAN	[70], [64]

4.2. Selection of the best Technology

Despite different useful characteristics associated with each of the technology, there are several challenges associated with them. The research showed that the main parameters used for the evaluation of any technology were not its limitation factors but the key features. The use of these technologies in the selected papers was based on the application, depending upon the application the parameters like range, power consumption, data rate and the cost was changing. In addition, there is no right answer to which technology is the best one for all point-of-care devices as the requirements change from application to application and each technology has its limitation.

For short-range and low data-rate applications, RFID/NFC is so far the best technology. For short-range and high data-rate applications both Bluetooth and WiFi can be useful depending upon the range required. Zigbee and DASH7 are useful for low-power consumption, better range and low-data rate applications. LoRaWAN is so far the most suitable long-range wireless communication technology but solving challenges associated with NB-IoT could make it a good candidate as well. As expected with the evolutions of NB-IoT (e.g. already exisiting NB-IoT LTE Cat NB2 in 3GPP Release 14, and next steps.).

4.3. Limitations

This review aimed to depict the broader picture of the wireless communication technologies used or not being considered due to certain research gaps for Point-of-Care devices. However, despite

giving a broader picture as compared with past reviews, this work has certain limitations as mentioned in the exclusion criteria. The future directions could be to improve this review and include other possible wireless communication technology candidates. Furthermore, the addition of patents could help in improving the results found.

5. Conclusion

This review summarizes the use of some major wireless communication technologies including *ZigBee, Bluetooth/BLE, Ultra-Wide-Band (UWB), WiFi, RFID/NFC, ANT/ANT+, WirelessHART, 6LowPAN, Z-wave, DASH7, IrDa, SigFoX, LoraWAN, NB-IoT, Wi-SUN* and *LTE-CAT-M1* for POC devices over the past 6 years. Although for Point-of-Care monitoring devices the use of wireless communication technology is identified as broad whereas, for Point-of-Care diagnostic devices, use is only restricted to few well-known wireless communication technologies (**Table: IV**) due to limited research in the field. The review helped to identify the major research gaps or challenges (**Table: II,III**) associated with each technology which can be used a baseline for its implementation in any application and also promotes further research in the field.

Significant range, low-power consumption, reliability, security, scalability and suitable data-rate are desired wireless communication parameters for the efficient operation of POC diagnostic devices in remote areas. However, there is no single wireless communication technology which can satisfy all the required parameters so either the research gaps related with each technology should be resolved or a trade-off can be made depending upon the application. However, solving research gaps including interference and power consumption associated with WiFi could make it a suitable candidate for Point-of-Care devices. Nevertheless, the review showed that the research should not be limited to only commonly used technologies and there is yet a lot to be revealed in the field.

References

[1] W. Zhang, S. Guo, W. S. Pereira Carvalho, Y. Jiang, and M. J. Serpe, "Portable point-of-care diagnostic devices," pp. 7847–7867, nov 2016. [Online]. Available: www.rsc.org/methods

[2] M. Zarei, "Portable biosensing devices for point-of-care diagnostics: Recent developments and applications," pp. 26–41, jun 2017.

[3] A. St John and C. P. Price, "Existing and Emerging Technologies for Point-of-Care Testing." *The Clinical biochemist. Reviews*, vol. 35, no. 3, pp. 155–67, aug 2014. [Online]. Available: http://www.ncbi.nlm.nih.gov/pubmed/25336761 http://www.pubmedcentral.nih.gov/articlerender.fcgi?artid=PMC4204237

[4] W. C. Tian and E. Finehout, *Microfluidics for biological applications*. Springer US, 2009.

[5] W. Li, H. Xi, and S. H. Tan, *Insights and Advancements in Microfluidics*, 2018.

[6] W. Postek, P. Gargulinski, O. Scheler, T. S. Kaminski, and P. Garstecki, "Microfluidic screening of antibiotic susceptibility at a single-cell level shows the inoculum effect of cefotaxime on: E. coli," *Lab on a Chip*, vol. 18, no. 23, pp. 3668–3677, 2018. [Online]. Available: http://dx.doi.org/10.1039/C8LC00916C

[7] T. S. Kaminski, O. Scheler, and P. Garstecki, "Droplet microfluidics for microbiology: Techniques, applications and challenges," *Lab on a Chip*, vol. 16, no. 12, pp. 2168–2187, 2016. [Online]. Available: http://dx.doi.org/10.1039/C6LC00367B

[8] O. Scheler, K. Makuch, P. R. Debski, M. Horka, A. Ruszczak, N. Pacocha, K. Sozański, O. P. Smolander, W. Postek, and P. Garstecki, "Droplet-based digital antibiotic susceptibility screen reveals single-cell clonal heteroresistance in an isogenic bacterial population," *Scientific Reports*, vol. 10, no. 1, pp. 1–8, 2020.

[9] S. B. Haga, "Challenges of development and implementation of point of care pharma-cogenetic testing," *Expert Review of Molecular Diagnostics*, vol. 16, no. 9, pp. 949–960, sep 2016. [Online]. Available: /pmc/articles/PMC6709578/?report=abstract https://www-ncbi-nlm-nih-gov.ezproxy1.hw.ac.uk/pmc/articles/PMC6709578/

[10] A. Bensky, *Wireless personal area networks*, 2019.

[11] Q. Gu, *RF system design of transceivers for wireless communications*. Springer US, 2005.

[12] I.-r. Sm, K. Ultra-wideband, T. Itu, and R. Assembly, "Characteristics of ultra-wideband technology," no. 2006, 2019.

[13] H. Labiod, H. Afifi, and C. De Santis, *Wi-FiTM, BluetoothTM, ZigBeeTM and WiMaxTM*. Springer Netherlands, 2007.

[14] V. Coskun, B. Ozdenizci, and K. Ok, "The survey on near field communication," *Sensors (Switzerland)*, vol. 15, no. 6, pp. 13 348–13 405, 2015.

[15] A. Souza Oliveira and M. Franco Pereira, "Estudo da tecnologia de identificação por radiofreqüência - RFID," *Gestao e Producao*, vol. 21, no. 3, pp. 133–144, 2015.

[16] B. Foubert and N. Mitton, "Long-Range Wireless Radio Technologies: A Survey," *Future Internet*, vol. 12, no. 1, p. 13, jan 2020. [Online]. Available: https://www.mdpi.com/1999-5903/12/1/13

[17] K. Mekki, E. Bajic, F. Chaxel, and F. Meyer, "Overview of Cellular LPWAN Technologies for IoT Deployment: Sigfox, LoRaWAN, and NB-IoT," in *2018 IEEE International Conference on Pervasive Computing and Communications Workshops, PerCom Workshops 2018*. Institute of Electrical and Electronics Engineers Inc., oct 2018, pp. 197–202.

[18] A. Lavric, A. I. Petrariu, and V. Popa, "Long Range SigFox Communication Protocol Scalability Analysis under Large-Scale, High-Density Conditions," *IEEE Access*, vol. 7, pp. 35 816–35 825, 2019.

[19] M. T. Buyukakkaslar, M. A. Erturk, M. A. Aydin, and L. Vollero, "LoRaWAN as an e-Health Communication Technology," in *Proceedings - International Computer Software and Applications Conference*, vol. 2. IEEE Computer Society, sep 2017, pp. 310–313.

[20] S. K. Park, K. I. Hwang, H. S. Kim, and B. S. Shim, "Challenges and experiment with LoRaWAN," in *Lecture Notes in Electrical Engineering*, vol. 448. Springer Verlag, 2017, pp. 269–276. [Online]. Available: https://link-springer-com.ezproxy1.hw.ac.uk/chapter/10.1007/978-981-10-5041-1_46

[21] P. Masek, M. Stusek, K. Zeman, R. Drapela, A. Ometov, and J. Hosek, "Implementation of 3GPP LTE Cat-M1 Technology in NS-3: System Simulation and Performance," in *International Congress on Ultra Modern Telecommunications and Control Systems and Workshops*, vol. 2019-Octob. IEEE Computer Society, oct 2019.

[22] M. M. Alam, H. Malik, M. I. Khan, T. Pardy, A. Kuusik, and Y. Le Moullec, "A survey on the roles of communication technologies in IoT-Based personalized healthcare applications," *IEEE Access*, vol. 6, pp. 36 611–36 631, 2018.

[23] S. S. Ahmad, S. Camtepe, and D. Jayalath, "Understanding data flow and security requirements in wireless body area networks for healthcare," in *2015 17th International Conference on E-health Networking, Application Services (HealthCom)*, 2015, pp. 621–626.

[24] K. Vidakis, A. Mavrogiorgou, A. Kiourtis, and D. Kyriazis, "A Comparative Study of Short-Range Wireless Communication Technologies for Health Information Exchange," no. June, 2020.

[25] M. J. Grant and A. Booth, "A typology of reviews: An analysis of 14 review types and associated methodologies," pp. 91–108, jun 2009. [Online]. Available: https://onlinelibrary.wiley.com/doi/full/10.1111/j.1471-1842.2009.00848.x https://onlinelibrary.wiley.com/doi/abs/10.1111/j.1471-1842.2009.00848.x https://onlinelibrary.wiley.com/doi/10.1111/j.1471-1842.2009.00848.x

[26] H. Lin, J. Tan, J. Zhu, S. Lin, Y. Zhao, W. Yu, H. Hojaiji, B. Wang, S. Yang, X. Cheng, Z. Wang, E. Tang, C. Yeung, and S. Emaminejad, "system for wearable bio fl uid management and contextual biomarker analysis," *Nature Communications*, no. 2020. [Online]. Available: http://dx.doi.org/10.1038/s41467-020-18238-6

[27] J.-c. Chou, R.-t. Chen, Y.-h. Liao, J.-s. Chen, M.-s. Huang, and H.-t. Chou, "Dynamic and Wireless Sensing Measurements of Potentiometric Glucose Biosensor Based on Graphene and Magnetic Beads," vol. 15, no. 10, pp. 5718–5725, 2015.

[28] M. M. System, Y.-h. Nien, Y.-x. Wu, and T.-y. Lai, "The Analysis of the Urea Biosensors Using Different Sensing Matrices via Wireless Measurement System," pp. 1–12, 2019.

[29] S. Sang, X. Fan, X. Tang, T. Wang, and A. Jian, "Portable surface stress biosensor test system based on ZigBee technology for health care," *Biotechnology & Biotechnological Equipment*, vol. 29, no. 4, pp. 798–804, 2015. [Online]. Available: http://dx.doi.org/10.1080/13102818.2015.1040455

[30] W.-j. Ma, C.-h. Luo, J.-l. Lin, S.-h. Chou, P.-h. Chen, M.-j. Syu, S.-h. Kuo, and S.-c. Lai, "A Portable Low-Power Acquisition System with a Urease Bioelectrochemical Sensor for Potentiometric Detection of Urea Concentrations," pp. 1–15.

[31] J.-c. Chou, J.-t. Chen, Y.-h. Liao, C.-h. Lai, R.-t. Chen, Y.-l. Tsai, C.-y. Lin, J.-s. Chen, M.-s. Huang, and H.-t. Chou, "Wireless Sensing System for Flexible Arrayed Potentiometric Sensor Based on XBee Module," vol. 16, no. 14, pp. 5588–5595, 2016.

[32] P. R. Chopade, P. Deshmukh, K. Kamble, and D. Nazarkar, "NFC Based Health Care System," vol. 3, no. 3, pp. 414–419, 2016.

[33] M. Zulqarnain, S. Stanzione, G. Rathinavel, S. Smout, M. Willegems, K. Myny, and E. Cantatore, "A flexible ECG patch compatible with NFC RF communication," *npj Flexible Electronics*, vol. 4, no. 1, pp. 1–9, 2020. [Online]. Available: http://dx.doi.org/10.1038/s41528-020-0077-x

[34] C. Kollegger, P. Greiner, I. Siegl, C. Steffan, M. Wiessflecker, B. Pekec, M. Hajnsek, F. Sinner, G. Holweg, and B. Deutschmann, "Intelligenter NFC-Kalium-Messstreifen mit Hämolysekontrolle in Kapillarblut," *Elektrotechnik und Informationstechnik*, vol. 135, no. 1, pp. 83–88, 2018. [Online]. Available: http://dx.doi.org/10.1007/s00502-017-0572-5

[35] S. Lee, A. J. Aranyosi, M. D. Wong, J. H. Hong, J. Lowe, C. Chan, D. Garlock, S. Shaw, P. D. Beattie, Z. Kratochvil, N. Kubasti, K. Seagers, R. Ghaffari, and C. D. Swanson, "Flexible opto-electronics enabled microfluidics systems with cloud connectivity for point-of-care micronutrient analysis," *Biosensors and Bioelectronics*, vol. 78, pp. 290–299, 2016.

[36] Y. Fan, J. Liu, Y. Wang, J. Luo, H. Xu, S. Xu, and X. Cai, "A wireless point-of-care testing system for the detection of neuron-specific enolase with microfluidic paper-based analytical devices," *Biosensors and Bioelectronics*, vol. 95, no. April, pp. 60–66, 2017. [Online]. Available: http://dx.doi.org/10.1016/j.bios.2017.04.003

[37] D. Agustini, L. Fedalto, D. Agustini, L. G. de Matos dos Santos, C. E. Banks, M. F. Bergamini, and L. H. Marcolino-Junior, "A low cost, versatile and chromatographic device for microfluidic amperometric analyses," *Sensors and Actuators, B: Chemical*, vol. 304, no. July 2019, p. 127117, 2020. [Online]. Available: https://doi.org/10.1016/j.snb.2019.127117

[38] T. Wu and A. Martin, "Bluetooth Low Energy Used for Memory Acquisition from Smart Health Care Devices," *Proceedings - 17th IEEE International Conference on Trust, Security and Privacy in Computing and Communications and 12th IEEE International Conference on Big Data Science and Engineering, Trustcom/BigDataSE 2018*, pp. 1256–1261, 2018.

[39] B. Fan, "Analysis on the Security Architecture of ZigBee Based on IEEE 802.15.4," *Proceedings - 2017 IEEE 13th International Symposium on Autonomous Decentralized Systems, ISADS 2017*, pp. 241–246, 2017.

[40] A. Menychtas, P. Tsanakas, and I. Maglogiannis, "Automated integration of wireless biosignal collection devices for patient-centred decision-making in point-of-care systems," vol. 3, pp. 34–40, 2016.

[41] J. Padgette, J. Bahr, M. Batra, M. Holtmann, R. Smithbey, L. Chen, and K. Scarfone, "NIST Special Publication 800-121 Revision 2 Guide to Bluetooth Security." [Online]. Available: https://doi.org/10.6028/NIST.SP.800-121r2

[42] A. Furniturewalla, M. Chan, J. Sui, K. Ahuja, and M. Javanmard, "Fully integrated wearable impedance cytometry platform on flexible circuit board with online smartphone readout," *Microsystems and Nanoengineering*, vol. 4, no. 1, pp. 1–10, dec 2018. [Online]. Available: www.nature.com/micronano

[43] C. Mercer, R. Bennett, P. Conghaile, J. F. Rusling, and D. Leech, "Glucose biosensor based on open-source wireless microfluidic potentiostat," *Sensors and Actuators, B: Chemical*, vol. 290, pp. 616–624, jul 2019.

[44] N. Q. Mehmood and R. Culmone, "An ANT+ Protocol Based Health Care System," *Proceedings - IEEE 29th International Conference on Advanced Information Networking and Applications Workshops, WAINA 2015*, pp. 193–198, 2015.

[45] N. Q. Mehmood, R. Culmone, and L. Mostarda, "A Flexible and Scalable Architecture for Real-Time ANT+ Sensor Data Acquisition and NoSQL Storage," *International Journal of Distributed Sensor Networks*, vol. 2016, 2016.

[46] C. A. da Costa, C. F. Pasluosta, B. Eskofier, D. B. da Silva, and R. da Rosa Righi, "Internet of Health Things: Toward intelligent vital signs monitoring in hospital wards," pp. 61–69, jul 2018.

[47] I. Čuljak, Ž. L. Vasić, H. Mihaldinec, and H. Džapo, "Wireless body sensor communication systems based on UWB and IBC technologies: State-of-theart and open challenges," *Sensors (Switzerland)*, vol. 20, no. 12, pp. 1–32, 2020.

[48] A. Chehri and H. T. Mouftah, "Internet of Things - integrated IR-UWB technology for healthcare applications," no. January 2019, pp. 1–10, 2020.

[49] H. Trabelsi, I. Barraj, and M. Masmoudi, "International Journal of Electronics and Communications (AEÜ) A 3 – 5 GHz FSK-UWB transmitter for Wireless Personal Healthcare applications," *AEUE - International Journal of Electronics and Communications*, vol. 69, no. 1, pp. 262–273, 2015. [Online]. Available: http://dx.doi.org/10.1016/j.aeue.2014.09.009

[50] S. Ghosh, J. Goswami, A. Kumar, and A. Majumder, "Issues in NFC as a form of contactless communication: A comprehensive survey," *2015 International Conference on Smart Technologies and Management for Computing, Communication, Controls, Energy and Materials, ICSTM 2015 - Proceedings*, no. May, pp. 245–252, 2015.

[51] T. B. Ahmed, M. S. Krishnan, and A. K. Anil, "A Predictive Analysis on the Influence of WiFi 6 in Fog Computing with OFDMA and MU-MIMO," in *Proceedings of the 4th International Conference on Computing Methodologies and Communication, ICCMC 2020*. Institute of Electrical and Electronics Engineers Inc., mar 2020, pp. 716–719.

[52] S. Synchronization and R.-t. Feedback, "Integrated Control of Microfluidics – Application in Fluid World ' s largest Science , Technology & Medicine Open Access book publisher," no. December, 2016.

[53] C. Zhao and X. Liu, "A portable paper-based microfluidic platform for multiplexed electrochemical detection of human immunodeficiency virus and hepatitis C virus antibodies in serum," *Biomicrofluidics*, vol. 10, no. 2, p. 024119, mar 2016. [Online]. Available: http://aip.scitation.org/doi/10.1063/1.4945311

[54] S. Han, J. Song, X. Zhu, A. K. Mok, D. Chen, M. Nixon, W. Pratt, and V. Gondhalekar, "Wi-HTest: compliance test suite for diagnosing devices in real-time WirelessHART^{TM} mesh networks," *Wireless Networks*, vol. 21, no. 6, pp. 1999–2018, aug 2015. [Online]. Available: https://link.springer.com/article/10.1007/s11276-015-0903-6

[55] "Ieee draft standard for health informatics – point-of-care medical device communications – transport profile – irda based – infrared wireless," *IEEE P1073.3.3/D8, July 2003*, pp. 1–74, 2019.

[56] A. Yearp, D. Newell, P. Davies, R. Wade, and R. Sahandi, "Wireless remote patient monitoring system: Effects of interference," in *2016 10th International Conference on Innovative Mobile and Internet Services in Ubiquitous Computing (IMIS)*, 2016, pp. 367–370.

[57] W. Ayoub, A. E. Samhat, F. Nouvel, M. Mroue, and J. C. Prévotet, "Internet of Mobile Things: Overview of LoRaWAN, DASH7, and NB-IoT in LPWANs Standards and Supported Mobility," *IEEE Communications Surveys and Tutorials*, vol. 21, no. 2, pp. 1561–1581, 2019.

[58] H. Trsek, J. Jasperneite, L. L. Bello, and M. Manic, *Wireless local area networks*, 2016.

[59] L. J. V. Escobar and S. A. Salinas, "E-Health prototype system for cardiac telemonitoring," *Proceedings of the Annual International Conference of the IEEE Engineering in Medicine and Biology Society, EMBS*, vol. 2016-Octob, pp. 4399–4402, 2016.

[60] J. H. Lee, M. S. Park, and S. C. Shah, "Wi-Fi direct based mobile ad hoc network," *2nd International Conference on Computer and Communication Systems, ICCCS 2017*, pp. 116–120, 2017.

[61] A. Yearp, D. Newell, P. Davies, R. Wade, and R. Sahandi, "Wireless remote patient monitoring system: Effects of interference," in *Proceedings - 2016 10th International Conference on Innovative Mobile and Internet Services in Ubiquitous Computing, IMIS 2016*. Institute of Electrical and Electronics Engineers Inc., dec 2016, pp. 367–370.

[62] C. Bouras, V. Kokkinos, and N. Papachristos, "Performance evaluation of LoraWan physical layer integration on IoT devices," *2018 Global Information Infrastructure and Networking Symposium, GIIS 2018*, pp. 2018–2021, 2019.

[63] M. S. Islam, M. T. Islam, A. F. Almutairi, G. K. Beng, N. Misran, and N. Amin, "Monitoring of the human body signal through the Internet of Things (IoT) based LoRa wireless network system," *Applied Sciences (Switzerland)*, vol. 9, no. 9, 2019.

[64] P. A. Catherwood, D. Steele, M. Little, S. McComb, and J. McLaughlin, "A Community-Based IoT Personalized Wireless Healthcare Solution Trial," *IEEE Journal of Translational Engineering in Health and Medicine*, vol. 6, may 2018.

[65] F. Al-turjman, *Trends in Cloud-based IoT*.

[66] W. Ayoub, A. E. Samhat, F. Nouvel, M. Mroue, and J.-c. Prévotet, "Internet of Mobile Things : Overview of LoRaWAN , DASH7 , and NB-IoT in LPWANs Standards and Supported Mobility," vol. 21, no. 2, pp. 1561–1581, 2020.

[67] H. Zhang, J. Li, B. Wen, Y. Xun, J. Liu, and S. Member, "Connecting Intelligent Things in Smart Hospitals Using NB-IoT," vol. 5, no. 3, pp. 1550–1560, 2018.

[68] W. Manatarinat, S. Poomrittigul, and P. Tantatsanawong, "Narrowband-internet of things (NB-IoT) system for elderly healthcare services," *Proceeding - 5th International Conference on Engineering, Applied Sciences and Technology, ICEAST 2019*, 2019.

[69] Z. Wang, F. Wang, H. Liu, Z. Qian, and Z. Bi, "Design of Human Health Monitoring System Based on NB-IoT," *Proceedings of 2019 IEEE 3rd Advanced Information Management, Communicates, Electronic and Automation Control Conference, IMCEC 2019*, no. Imcec, pp. 6–9, 2019.

[70] S. Prabhu, C. Gooneratne, K. A. Hoang, and S. Mukhopadhyay, "IoT-Associated Impedimetric Biosensing for Point-of-Care Monitoring of Kidney Health," *IEEE Sensors Journal*, pp. 1–1, jul 2020.

[71] M. Mayer and A. J. Baeumner, "A Megatrend Challenging Analytical Chemistry: Biosensor and Chemosensor Concepts Ready for the Internet of Things," *Chemical Reviews*, vol. 119, no. 13, pp. 7996–8027, jul 2019. [Online]. Available: https://pubs.acs.org/sharingguidelines

[72] T. Kato, "Standardization and Certification Process for "Wi-SUN" Wireless Communication Technology," vol. 22, no. 1, pp. 22–33, 2016.

[73] K. Mekki, E. Bajic, F. Chaxel, and F. Meyer, "A comparative study of LPWAN technologies for large-scale IoT deployment," *ICT Express*, vol. 5, no. 1, pp. 1–7, mar 2019.

[74] M. M. Alam, H. Malik, M. I. Khan, T. Pardy, A. Kuusik, and Y. Le Moullec, "A survey on the roles of communication technologies in IoT-Based personalized healthcare applications," *IEEE Access*, vol. 6, pp. 36 611–36 631, jul 2018.

[75] A. Ahad, M. Tahir, and K. L. A. Yau, "5G-based smart healthcare network: Architecture, taxonomy, challenges and future research directions," *IEEE Access*, vol. 7, pp. 100 747–100 762, 2019.

Curriculum Vitae

1. Personal data

Name	Kanwal Ashraf
Date and place of birth	23 February 1996, Pakistan
Nationality	Pakistani

2. Contact information

Address	Tallinn University of Technology, School of Information Technologies, Thomas Johann Seebeck Department of Electronics, Ehitajate tee 5, 19086 Tallinn, Estonia
Phone	+372 54590227
E-mail	kanwal.ashraf@taltech.ee

3. Education

2020–…	Tallinn University of Technology, School of Information Technologies, Thomas Johann Seebeck Department of Electronics, Ph.D. studies
2018–2020	Heriot Watt University, Electrical, Electronic and Computer Engineering, Joint International Master's in Smart Systems Integration
2012–2016	University of the Punjab, Faculty of Engineering, BSc (Electrical Engineering)

4. Language competence

Estonian	basic
English	fluent
Urdu	native

5. Computer skills

- Operating systems: Linux, Windows

- Programming skills: C/C++, Java, PHP, JS, Python, Full stack development

6. Honours and awards

- 2021, DSD Best paper award

7. Field of research

- Wireless Networked Control Systems

8. Scientific work
Papers

1. (ETIS 3.1) **K. Ashraf**, Y. Le Moullec, T. Pardy and T. Rang, "Model-based System Architecture for Event-triggered Wireless Control of Bio-analytical Devices," 2021 24th Euromicro Conference on Digital System Design (DSD), 2021, pp. 465-471, DOI: `https://doi.org/10.1109/DSD53832.2021.00076`. [12]

---

[12]This paper received the Euromicro DSD 2021 Special Session Best Paper Award

2. (ETIS 1.1) **K. Ashraf**, Y. Le Moullec, T. Pardy and T. Rang, "Design of Cyber Bio-Analytical Physical Systems: Formal Methods, Architectures, and Multi-System Interaction Strategies," Microprocessors and Microsystems, Vol. 97, Issue C, pp. 104780, 2023, DOI: `https://doi.org/10.1016/j.micpro.2023.104780`.

3. (ETIS 1.1) **K. Ashraf**, Y. Le Moullec, T. Pardy and T. Rang,"Joint Optimization via Deep Reinforcement Learning in Wireless Networked Controlled Systems," IEEE Access, Vol. 10, pp. 67152 - 67167, 2022, DOI: `https://doi.org/10.1109/ACCESS.2022.3185244`

V (ETIS 5.2[13]) **K. Ashraf**, Y. Le Moullec, T. Pardy and T. Rang, "Decentralized Distributed Data Structure for Bioanalytical Laboratory Setups," 8th ACM WomENcourage Conference, 2021, `https://womencourage.acm.org/2021/wp-content/uploads/2021/07/59_extendedabstract.pdf`

VI (ETIS 1.1) R. Jõemaa, N. Gyimah, **K. Ashraf**, K. Pärnamets, A. Zaft, O. Scheler, T. Rang and T. Pardy, "CogniFlow-Drop: Integrated modular system for automated generation of droplets in microfluidic applications", IEEE Access, Vol. 11, pp. 104905 - 104929, 2023, DOI: `https://doi.org/10.1109/ACCESS.2023.3316726`

---

[13]Extended abstract + poster

Elulookirjeldus

1. Isikuandmed

Nimi	Kanwal Ashraf
Sünniaeg ja -koht	23.02.1996, Pakistan
Kodakondsus	Pakistani

2. Kontaktandmed

Aadress	Tallinna Tehnikaülikool, Thomas Johann Seebecki elektroonikainstituut, Ehitajate tee 5, 19086 Tallinn, Estonia
Telefon	+372 54590227
E-post	kanwal.ashraf@taltech.ee

3. Haridus

2020–…	Tallinna Tehnikaülikool, Infotehnoloogia teaduskond, Thomas Johann Seebecki elektroonikainstituut, doktoriõpe
2018–2020	Heriot Watt ülikool, Elektri-, elektroonika- ja arvutitehnika, MSc
2012–2016	Pandžabi ülikool, inseneriteaduskond, BSc

4. Keelteoskus

urdu keel	emakeel
inglise keel	kõrgtase

5. Arvutioskus

- Operatsioonisüsteemid: Linux, Windows
- Programmeerimiskeeled: C/C++, Java, PHP, JS, Python

6. Autasud

- 2021, DSD parima artikli auhind